Rehabilitation of waste materials near lead and zinc mining sites in Galena, Kansas

by

Abdulaziz Ghazi Alghamdi

B.S., King Saud University, 2001
M.S., King Saud University, 2009

AN ABSTRACT OF A DISSERTATION

submitted in partial fulfillment of the requirements for the degree

DOCTOR OF PHILOSOPHY

Department of Agronomy
College of Agriculture

KANSAS STATE UNIVERSITY
Manhattan, Kansas

2016

Abstract

The abandoned lead (Pb) and zinc (Zn) mines in the Tri-State Mining District of Kansas, Missouri, and Oklahoma have left a legacy of environmental contamination. The waste materials are highly polluted, not only with Pb and Zn, but also cadmium (Cd), which often co-occurs geologically with Zn. The District includes Galena, Kansas, where mines operated between 1876 and 1970. Because limited information exists concerning these mines, three studies were done to characterize them and to investigate a way to remediate the mine waste materials.

In the first study, the physical characteristics of the mine waste materials were determined. Plots at Galena that had been established by researchers in May 2006 were sampled in November 2014, 8.5 years after they had received amendments (combinations of compost, lime, and bentonite). Water content, bulk density, infiltration rate, unsaturated hydraulic conductivity, aggregate stability, and particle size distribution were determined. The physical characteristics were highly variable, and the amendments added 8.5 years earlier had no effect on them, except the wind erodible fraction (fraction <0.84 mm in diameter) which was low on treatments that contained bentonite.

Because biosolids had never been applied to the mine waste materials at Galena for remediation, an experiment was done to see their effect on plant growth and availability of heavy metals. In 2014 the plots established in 2006 were sampled and a greenhouse study was set up with sudex [*Sorghum bicolor* (L.) Moench x *S. Sudanese* (P.) Staph]. Plants grew in the mine waste materials with and without biosolids, and 110-111 days after planting the roots, shoots, and heads with grain were harvested and analyzed for heavy metals. At the same time, the mine waste materials were analyzed for heavy metals, organic carbon (C), nitrogen (N), and

phosphorus (P). Plants grew better with biosolids than without biosolids, and only the plants grown with biosolids produced heads . Plants grown without biosolids were stunted and showed severe heavy metal toxicity. Organic C and P were increased in the mine waste materials after the addition of biosolids. Thus, the biosolids increased organic C and P, and they apparently made the heavy metals less available for plant uptake.

Many studies have shown the importance of attic dust in documenting metal pollution from a mine. Attic dust in Galena had never been studied, so in a third experiment, 14 dust samples in Galena were collected from interiors (attics and one basement) of nine different buildings using two methods: sweeping with a brush and vacuuming. Dust samples were analyzed for heavy metals (Cd, Cu, Fe, Mn, Ni, Pb, and Zn), mineralogy using X-ray diffraction (XRD), scanning electron microscopy (SEM) in conjunction with energy dispersive spectroscopy (EDX), and particle size. Concentrations of Cu, Fe, Mn, Ni, and Zn in the dust were higher than in the mine waste materials. The results from XRD agreed with those from the SEM-EDX analysis. About 10% of each dust sample contained particulate matter (PM) with a diameter of less than 10 μm (PM_{10}), which is a health concern.

Rehabilitation of waste materials near lead and zinc mining sites in Galena, Kansas

by

Abdulaziz Ghazi Alghamdi

B.S., King Saud University, 2001
M.S., King Saud University, 2009

A DISSERTATION

submitted in partial fulfillment of the requirements for the degree

DOCTOR OF PHILOSOPHY

Department of Agronomy
College of Agriculture

KANSAS STATE UNIVERSITY
Manhattan, Kansas

2016

Approved by:

Major Professor
Dr. DeAnn Presley

Copyright

Abstract

The abandoned lead (Pb) and zinc (Zn) mines in the Tri-State Mining District of Kansas, Missouri, and Oklahoma have left a legacy of environmental contamination. The waste materials are highly polluted, not only with Pb and Zn, but also cadmium (Cd), which often co-occurs geologically with Zn. The District includes Galena, Kansas, where mines operated between 1876 and 1970. Because limited information exists concerning these mines, three studies were done to characterize them and to investigate a way to remediate the mine waste materials.

In the first study, the physical characteristics of the mine waste materials were determined. Plots at Galena that had been established by researchers in May 2006 were sampled in November 2014, 8.5 years after they had received amendments (combinations of compost, lime, and bentonite). Water content, bulk density, infiltration rate, unsaturated hydraulic conductivity, aggregate stability, and particle size distribution were determined. The physical characteristics were highly variable, and the amendments added 8.5 years earlier had no effect on them, except the wind erodible fraction (fraction <0.84 mm in diameter) which was low on treatments that contained bentonite.

Because biosolids had never been applied to the mine waste materials at Galena for remediation, an experiment was done to see their effect on plant growth and availability of heavy metals. In 2014 the plots established in 2006 were sampled and a greenhouse study was set up with sudex [*Sorghum bicolor* (L.) Moench x *S. Sudanese* (P.) Staph]. Plants grew in the mine waste materials with and without biosolids, and 110-111 days after planting the. roots, shoots, and heads with grain were harvested and analyzed for heavy metals. At the same time, the mine waste materials were analyzed for heavy metals, organic carbon (C), nitrogen (N), and

phosphorus (P). Plants grew better with biosolids than without biosolids, and only the plants grown with biosolids produced heads . Plants grown without biosolids were stunted and showed severe heavy metal toxicity. Organic C and P were increased in the mine waste materials after the addition of biosolids. Thus, the biosolids increased organic C and P, and they apparently made the heavy metals less available for plant uptake.

Many studies have shown the importance of attic dust in documenting metal pollution from a mine. Attic dust in Galena had never been studied, so in a third experiment, 14 dust samples in Galena were collected from interiors (attics and one basement) of nine different buildings using two methods: sweeping with a brush and vacuuming. Dust samples were analyzed for heavy metals (Cd, Cu, Fe, Mn, Ni, Pb, and Zn), mineralogy using X-ray diffraction (XRD), scanning electron microscopy (SEM) in conjunction with energy dispersive spectroscopy (EDX), and particle size. Concentrations of Cu, Fe, Mn, Ni, and Zn in the dust were higher than in the mine waste materials. The results from XRD agreed with those from the SEM-EDX analysis. About 10% of each dust sample contained particulate matter (PM) with a diameter of less than 10 μm (PM_{10}), which is a health concern.

Table of Contents

List of Figures

List of Tables

Acknowledgements

I would like to thank my major advisor Dr. DeAnn Presley for her excellent guidance and help. It was my pleasure to be one of her student. Especial thanks and appreciation to Dr. Marry Beth Kirkham for all her help, guidance, and support. It was a great opportunity to work with her and I have learned a lot from her. I am also thankful my helpful committee members, Dr. Ganga Hettiarachchi and Dr. Bimal Paul for their guidance and support. I appreciate all of their help.

I would like to thank King Saud University in Riyadh, Saudi Arabia, and Saudi Arabian Cultural Mission for their funded the research assistantship of the senior author. We thank the following people: Dr. Yuxin (Jack) He and Ms. Cathryn Davis for helping to get the mine waste materials and dust samples; Mr. Mosaed A. Majrashi for help throughout the experiment and to get dust samples; Ms. Terri L. Branden, Facilities Maintenance Supervisor, Plant Sciences Greenhouse Complex, for help in the greenhouse during the experiment; Mr. Arthur Selman for constructing the temperature and humidity sensors used in the greenhouse; Dr. Kendra McLauchlan in the Department of Geography; Dr. John Tatarko formerly of the Wind Erosion Research Unit, USDA, Agricultural Research Service (ARS), Manhattan, KS, and Mr. Matt Kucharski of the USDA, ARS, Manhattan, KS; Mr. Jebril Jebril for statistical help; Mr. Ian Andree, graduate student in the Department of Geology for help with the XRD; Mr. Ravi Thakkar in the Nanotechnology Innovation Center in the Veterinary College for the SEM analyses; Mr. Jay Yaege, Laboratory Manager, Manhattan, KS, Wastewater Treatment Plant, for supplying the biosolids; Dr. Abdu Durar, Environmental Compliance Manager, City of Manhattan, Public Works Department, Water and Wastewater Division, Manhattan, KS, for information on the N and P in the biosolids; Ms. Zhining Ou, statistical consultant in the

Statistics Laboratory, Kansas State University, for help with the statistical analyses; and Ms. Kathleen M. Lowe and Mr. Jacob (Jake) A. Thomas in the Soil Testing Laboratory at Kansas State University for doing the analyses, which were paid for by two awards to M.B. Kirkham (Dr. Ron and Rae Iman Outstanding Faculty Award and the Higuchi-University of Kansas Endowment Research Achievement Award) and by Hatch Grant No. 371047 to M.B. Kirkham.

Dedication

To My Parents

Ghazi S Alghamdi “God bless his soul and makes the resting place of paradise”

Azzah H Alghamdi

My Wife

Nurah M Alghamdi

My Children

Sadeem A Alghamdi

Ghazi A Alghamdi

Mohammed A Alghamdi

To my Brothers and sisters

Saleh G Alghamdi

Hamdah G Alghamdi

Abdullah G Alghamdi

Badreah G Alghamdi

Ahmed G Alghamdi

Nadia G Alghamdi

Maha G Alghamdi

To all of my nephews and nieces

To Prof. Ali M Al-Turki

Chapter 1 - Introduction

Abandoned mines are sites where mining activities once occurred, but mining no longer takes place. They are abandoned usually due to economic or environmental reasons (Jung, 2008). They present a serious risk to human health and the environment and occur around the world. For example, there are more than 50,000 abandoned mines in Australia (Unger et al., 2012), and Canada has about 10,000 abandoned mines (Mackasey, 2000). In the USA in August, 2015, a toxic spill from an abandoned gold mine in Colorado contaminated the Animas River and its watershed with 3 million gallons (11,400,000 L) of waste. It affected the drinking water of 200,000 people in Colorado, New Mexico, and Utah. The water was contaminated with lead and arsenic. After the accident, an estimated 880,000 pounds (400,000 kg) of heavy metals spilled into the Animas River, and it is believed that more have been leaking into the river for years from abandoned mines (Carlton, 2016). The lead is of special concern because it can cause behavioral and learning problems in children. Abandoned lead (Pb) and zinc (Zn) mines are common around the world (Gutiérrez et al., 2016), and they occur in Kansas.

The abandoned Pb and Zn mine in the Tri-State Mining District of southeast Kansas, southwest Missouri, and northeast Oklahoma have left a legacy of contamination. The wastes from these mines have polluted groundwater, rivers, lakes, sediments, and soils. The District includes Galena, Kansas, where mines began to operate in 1876. The mines lasted to 1970. The century of mining operations in Galena has left Pb and Zn contamination throughout the city. The waste materials around the mines are highly polluted, not only with Pb and Zn, but also with cadmium (Cd), which often co-occurs geologically with Zn. The miners and local population have endured health problems from the beginning of the mining. Residents of Galena have a high incidence of diseases, including cancer, which suggests that the mine waste materials are

causing these illnesses. Studies are urgently needed to characterize the mine waste materials and to develop methods to rehabilitate them.

The overall goal of this dissertation is to characterize and remediate mine waste materials in Galena, Kansas. Gaps in the knowledge about mine wastes and their legacy effects justified three different studies, which are presented in three chapters in this dissertation. Determining as much information as possible about the risks and properties of the mine waste materials will add to scientific knowledge and understanding.

Because the physical characteristics of the mine waste materials had not been determined, particularly after several years since the wastes had been amended, in the first chapter, they were measured. The chapter reports the hydraulic conductivity, bulk density, water content, aggregate stability, and particle size distribution, including the wind-erodible fraction (fraction of less than 0.84 mm in diameter), of the mine waste materials that had been treated 8.5 years earlier with amendments of compost, lime, and bentonite.

Because no studies had been done to see if biosolids could be used to remediate the mine waste materials, the second chapter describes a greenhouse experiment in which biosolids from the Manhattan, Kansas, Wastewater Treatment Plant were applied to pots with the mine waste materials. Sudex, a sorghum-sudan grass hybrid, was planted in the pots to determine the effect of biosolids on the growth of the sudex and transfer of heavy metals from roots to shoots and then to heads.

Dust from mine waste materials potentially poses a health problem. Not only can the dust can have fine enough particles to be breathed into the lungs, but it also likely contains the same heavy metals present in the mine waste materials. The size of dust that is of medical concern has particulate matter (PM) called PM_{10}. Particles of this size are less than 10 microns

(10 μm) in diameter. PM_{10} is a major component of air pollution that threatens health and the environment. Dust from attics provides a means of reconstructing air pollution. Many studies have shown the importance of attic dust in documenting metal pollution from a mine. Because no one had studied dust in attics in Galena, Kansas, the third chapter documents the sampling and analyses of attic dust from churches, shops, houses, and a school in the town. It was analyzed for heavy metals, mineralogy using X-ray diffraction, scanning electron microscopy, and particle size.

Major conclusions were as follows:

Chapter 1. The physical characteristics of the mine waste materials were highly variable, and the amendments added 8.5 years earlier had no effect on the physical measurements, except the wind erodible fraction (fraction <0.84 mm in diameter) was lesser for treatments that contained bentonite. The results suggested that bentonite (a clay) was able to reduce the wind erodible fraction.

Chapter 2. Only the sudex grown with biosolids produced heads with grain. The plants grown without biosolids showed severe heavy-metal toxicity and were stunted. Biosolids reduced the uptake of Pb, Zn, and Cd from the mine waste materials. Even though large amounts of Pb, Zn, and Cd accumulated in the roots, their transfer to the heads was limited. Concentrations of Pb and Zn in the heads were normal. The use of biosolids may be a promising method to reduce availability of metals at mine sites.

Chapter 3. The attic dust was contaminated with heavy metals, and the concentrations of Cu, Fe, Mn, Ni, and Zn were higher in the dust than in the mine waste materials. The mineralogical analyses showed that the dust contained two minerals with Pb (galena and anglesite) and one mineral with Zn (sphalerite). The dust samples had diameters smaller than 10

μm, the size of medical concern. A dust sample falling within the definition of PM_{10}, which was found in the school, is of major concern, because this means that many children will be exposed to, not only dangerously small dust particles, but also the heavy metals associated with them.

1.1 References

Carlton, J. 2016. Toxic-spill fears haunt southwest. The Wall Street Journal, April 8, 2016, p. A3.

Gutiérrez, M., Mickus, K., and Camacho, L. M. 2016. Abandoned Pb Zn mining wastes and their mobility as proxy to toxicity: A review. *Science of the Total Environment*, *565*, 392-400.

Jung, M. C. 2008. Contamination by Cd, Cu, Pb, and Zn in mine wastes from abandoned metal mines classified as mineralization types in Korea. *Environmental Geochemistry and Health*, *30*(3), 205-217.

Mackasey, W. O. 2000. Abandoned mines in Canada. WOM Geological Associates Inc. Ontario, Canada.

Unger, C., Lechner, A. M., Glenn, V., Edraki, M., and Mulligan, D. R. 2012. Mapping and prioritising rehabilitation of abandoned mines in Australia. *Proceedings Life-of-Mine Conference*. Brisbane, QLD, 10-12 July. p259-266.

Chapter 2 - Physical Properties of Mine Waste Materials at an Abandoned Mine in Central USA

2.1 Abstract

Relatively little information exists for soil physical characteristics of mine wastes in the central USA. The Tri-State Mining District of southeast Kansas, southwest Missouri, and northeast Oklahoma produced lead and zinc from 1871to the 1970s. In May 2006 an experiment was established to determine if soil amendments could decrease the bioavailability of heavy metals in the mine waste. Seven treatments on two different sites near the town of Galena KS, called Site A and Site B, were established, as follows: (1) CO, non-amended control; (2) LC, low compost (45 Mg ha^{-1}); (3) HC, high compost (269 Mg ha^{-1}); (4) LCL, low compost (45 Mg ha^{-1}) + lime as $Ca(OH)_2$ (11.2 Mg ha^{-1}); (5) HCL, high compost (269 Mg ha^{-1}) + lime as $Ca(OH)_2$ (11.2 Mg ha^{-1}); (6) LCLB, low compost (45 Mg ha^{-1}) + lime as $Ca(OH)_2$ (11.2 Mg ha^{-1}) + bentonite (50 g bentonite kg^{-1} compost); and (7) HCLB, high compost (269 Mg ha^{-1}) + lime applied as $Ca(OH)_2$ (11.2 Mg ha^{-1}) + bentonite (50 g bentonite kg^{-1} compost). The treatments were replicated three times per site in a randomized complete block. The soil physical properties were not studied in 2006. In November, 2014, 8.5 years after the addition of the amendments, the plots were sampled and water content (WC), bulk density (BD), unsaturated hydraulic conductivity (k) were measured. Wet-aggregate stability was tested, and geometric mean diameter (GMD) and mean weight diameter (MWD) indexes were calculated. Dry-aggregates were collected and GMD and GSD (geometric standard deviation) were calculated. Significant treatment effects were observed 8.5 years after treatment establishment, especially at Site B. The WC, BD, and k parameters had significant treatment differences at Site B, but no one treatment consistently improved soil physical properties. For the dry-aggregate size distribution test, the

CO and HC treatments at Site B had the highest fraction of <0.84 mm dry aggregates, called the wind erodible fraction (WEF), and the LCLB and HCLB treatments had the lowest WEF. The results showed that the WEF of these mine waste materials can be reduced for over 8 years by adding a combination of compost, lime, and bentonite.

2.2 Introduction

Mines abandoned during previous decades when environmental regulations were lax are sources of contamination that require remediation. They include the closed mines in the central part of the U.S.A. in the Tri-State Mining District of southeast Kansas, southwest Missouri, and northeast Oklahoma.

Prior to the Civil War, trappers and explorers were mining surface deposits of lead to make bullets. Commercial mining of lead did not begin in the area until about 1850, near Joplin, Missouri (Pope, 2005, p. 5). Mining operations before the Civil War were limited because of a lack of adequate transportation and heavy machinery. After the Civil War, the infrastructure was built for deep-mine operations in the Tri-State District (Pope, 2005, p. 5, 7). From 1850 to 1970, the District was the world's leading source of lead and zinc ore. The last mines closed in the District in 1970 (Pope, 2005, p. 2).

Commercial mining in the Kansas part of the Tri-State Mining District, Cherokee County, began in the mid-1870s and lasted until 1970. In 1983, the Environmental Protection Agency listed Cherokee County as a superfund hazardous waste site (Pope, 2005, p. 1; Johnson et al., 2016). The U.S. Geological Survey, the U.S. Fish and Wildlife Service, and the Kansas Department of Health and Environment conducted a study on the appearance and distribution of contaminated streambed sediments in two watersheds in Kansas (Pope, 2005, p. 1). They found much higher concentrations of cadmium, lead, and zinc than their pre-mining estimates of those

elements. However, the concentrations of these elements may have been affected by wind distribution as well as water flow. During the mining process, the wind may have carried dust contaminated with these elements into these watersheds.

The unusable rocks remaining after the valuable minerals are removed in the mining process are called mill tailings or chat. Since only about four percent of the ore processed in the District was lead and zinc, milling produced a large volume of tailings (Pope, 2005, p. 8). The milling process did not remove 100 percent of the lead and zinc, thus residual traces were left in the tailings or chat. The size ranged of chat is about 0.041 to 0.95 cm. These milling remnants were not considered hazardous until more recently, so they were not stored in a way to protect the environment. Therefore, the lead and zinc residuals were a potential source of environmental contamination through either water or wind distribution (Pope, 2005, p. 8).

Adding amendments to allow plant growth has been suggested as one way to remediate mine wastes (Forján et al., 2014; Johnson et al., 2016). Amendments have been applied to the waste materials at Galena, Cherokee County, Kansas. Pierzynski et al. (2002) added cattle manure as a soil amendment to the mine tailings at Galena, to see if tall fescue (*Festuca arundinacea* Schreb.) would grow. After the first growing season, vegetative cover reached 71% but then steadily declined to 29% over the next two growing seasons. They attributed the poor growth to zinc toxicity. In May, 2006, Baker et al. (2011) established plots with amendments of compost, lime, and bentonite on chat at Galena and then planted switchgrass (*Panicum virgatum* L.). The initial seeding of switchgrass (fall, 2006) was not successful in establishing a vegetative cover. After winter ryegrass (*Lolium perenne* L.) establishment and termination with herbicide, switchgrass establishment was again attempted in the spring of 2007 with success, because plots were covered with living grass. However, they concluded that large amounts of compost (e.g,

269 Mg ha^{-1}) may be needed to sustain biomass production. Baker et al. (2011) did not evaluate the physical characteristics of the mine waste materials, except to note that the available water in them was increased by adding compost.

Many studies measure the chemical properties of mine waste materials (e.g., Forján et al., 2014; Perlatti et al., 2015; Zhang et al., 2015), but few characterize the physical properties. Several studies report the physical properties of coal mine soils (Skukla et al., 2004; Shrestha and Lal, 2008, 2011; Yao et al., 2010; Thomas, 2012; DeLong et al., 2012; Krümmelbein et al., 2010; Krümmelbein and Raab, 2012; Sadhu et al., 2012; Jitesh Kumar and Amiya Kumar, 2013; Bi et al., 2014; Zhang et al., 2015). A common issue with coal mine soils is high bulk density. The bulk density of overburden dumps can be as high as 1.91 Mg m^{-3} (Sheoran et al., 2010). Soil compaction limits plant growth, because most species are unable to extend roots through high bulk-density mine soils. Severely compacted (bulk density greater than 1.7 Mg m^{-3}) mine soils, particularly those with in areas that are shallow to bedrock and/or have the presence of large boulders in the soil cannot hold enough plant-available water to sustain plants (Sheoran et al., 2010). However, in contrast to many studies showing that the bulk density of mine spoils are high, in West Bengal, India, Sadhu et al. (2012) found that the bulk density of an open cast mining spoil was less than that of native soil. They did find that the water holding capacity and moisture content of the spoil were less than those of the soil, a common observation. Bulk density is also increased during reclamation. Since the late 1970s and the passage of the Surface Mining Control and Reclamation Act in the U.S.A., mined lands have commonly been reclaimed using smooth grading, which heavily compacts the soil (DeLong et al., 2012).

Shukla et al. (2004) reviewed the effects of coal mining on soil physical properties. Soil structure and water storage and transmission characteristics are influenced by morphological and

physical properties of soil. Compacted reclaimed soil and spoil lack a continuous macropore network, which impedes root development and aeration and decreases water retention and transmission (Indorante et al., 1981). A slow water infiltration rate is reported from newly reclaimed mine soils mainly due to compaction during the reclamation process. Shukla et al. (2004) compared physical properties of reclaimed coal mine soils in eastern Ohio with nearby undisturbed (unmined) sites. The comparison showed that water-stable aggregation and mean weight diameter of aggregates were greater from the unmined soils than the reclaimed mine soils. No significant differences were observed for saturated hydraulic conductivity and water infiltration for the 0-10 cm depth in the reclaimed mine soils and the unmined soils.

Shrestha and Lal (2008) reported the physical characteristics of reclaimed mine soils. These soils have higher bulk density (1.55 to 1.86 Mg m^{-3}), higher rock content (33-45%), poor structure, lower porosity (26-38%), lower water holding capacity, lower infiltration rates, and slower hydraulic conductivities than undisturbed soils. The higher bulk density of reclaimed mine soils is due to compaction by heavy equipment used during the reclamation process. A low water-holding capacity is due to high rock and gravel fragments and low soil organic carbon concentration in mine soils. Shrestha and Lal (2008) collected soil samples from the 0-5, 5-15, and 15-30 cm depths of reclaimed mine soil and undisturbed forest and agricultural soils. The soil was reclaimed by adding 30 cm topsoil in 1977. They found that, after 28 years of reclamation, bulk density in the surface layer of all land uses (forest, hay, and pasture) was similar to that of undisturbed forest (1.1 Mg m^{-3}), but lower than that of agricultural soils (1.3 Mg m^{-3}). However, soil bulk density at lower depths was not affected. The mean-weight diameter (0-30 cm) of aggregates under the reclaimed mine soil with forest and reclaimed mine soil with hay were higher than those under undisturbed forest soil by 41% and 27%, respectively.

The initial infiltration rates at 5 min using a double ring infiltrometer in the reclaimed mine soil under forest, hay, and pasture were less by 20%, 53%, and 85%, respectively, than those under the undisturbed soil with forest which had an infiltration rate of (19.3 cm min^{-1}). The reclamation of the mine soils with forest and hay improved the surface soil bulk density and enhanced water infiltration and water-stable aggregates at the lower depths.

Shrestha and Lal (2011) measured the physical properties of newly reclaimed mine sites (less than 1 year since reclamation). Reclaiming comprised of backfilling using the spoil material, grading to the original contour, applying 20 to 30 cm of topsoil, planting a grass-legume mixture, and mulching with crop residues. They sampled the soil at the 0-15, 15-30, and 30-45 cm depths. The bulk density of the reclaimed mine soil (1.11 to 1.69 Mg m^{-3}) increased by up to 54% compared to that of the undisturbed sites (0.98 to 1.41 Mg m^{-3}) at the 0-15 cm depth but not at the lower depths. They concluded that topsoil required better handling during application, than was done, to preserve soil structure.

In the studies where physical properties of mine soils have been measured (e.g., hydraulic conductivity, bulk density), it is noted that they are highly variable (Skousen et al., 1998; Krüummelbein et al., 2010; Krümmelbein and Raab, 2012).

Phospholipids and fatty acids (PLFA) are used to analyze microbial community structure. Baker et al. (2011) found that, at Site A, the highest total value of PLFA was in high compost treatment, and it was 80.3 μmol kg^{-1}. The control had a value of 30.2 μmol kg^{-1}. At Site B were 84.9 and 23.1 μmol kg^{-1} soil, respectively for the high compost treatment and control, respectively.

No study has been done of the physical characteristics of the waste materials at the Tri-State Mining District. The waste materials pose problems for the welfare of the people living in

the District, because blowing of the materials results in the dust with high lead and zinc concentrations that compromise the health of the citizens. Knowledge of the physical properties, including the wind-blown fraction, is essential to understand the risk that the citizens are experiencing. Therefore, the objective of this research was to determine the physical characteristics and the PLFA content of the waste materials in the plots that Baker et al. (2011) established in 2006. We measured hydraulic conductivity, bulk density, water content, aggregate stability, and particle size distribution, including the wind-erodible fraction, and PLFA.

2.3 Materials and Methods

The abandoned mine was located at Galena, KS (37º 9' 16" N; 94º 50' 2" W; 275 m above sea level). The soil mapped in this area is not a soil at all, and in the soil survey is currently mapped as map unit 9975, called "dumps, mine" (USDA, 2013). In 2006, Baker et al. (2011) established plots at two sites, called Site A and Site B, where mine waste materials had been collected and deposited on the surface for 100 years. The material, called chat, was a by-product in the initial processing of Pb and Zn -containing ores. Site A was established on 8 May 2006 and Site B on 12 May 2006. The sites were on level ground. Each experimental plot was 1 m x 2 m in size with three replications of seven different treatments, for a total of 21 plots at each site (Figure 2.1 and 2.2). Each plot had a galvanized steel border, 1 m x 2 m in size, to limit inter-plot contamination (Baker, 2008, p. 138). The treatments were (1), CO, non-amended control plot; (2) LC, a low compost treatment of 45 Mg ha^{-1}; (3) HC, a high compost treatment of 269 Mg ha^{-1}; (4) LCL, low compost (45 Mg ha^{-1}) + lime as $Ca(OH)_2$ (11.2 Mg ha^{-1}); (5) HCL, high compost (269 Mg ha^{-1}) + lime as $Ca(OH)_2$ (11.2 Mg ha^{-1}); (6) LCLB, low compost (45 Mg ha^{-1}) + lime as $Ca(OH)_2$ (11.2 Mg ha^{-1}) + bentonite applied at 50 g bentonite per kg compost; and (7) HCLB, high compost (269 Mg ha^{-1}) + lime applied as $Ca(OH)_2$ (11.2 Mg ha^{-1}) + bentonite

applied at 50 g bentonite per kg compost. The compost was composted beef (*Bos taurus*) manure, and the bentonite was a Wyoming bentonite obtained from Enviroplug Grout (Wyo-Ben, Inc., Billings, MT) (Baker, 2008, p. 138). Treatments were applied and mixed to a depth of 30 cm (Baker, 2008, p. 138). Switchgrass (*Panicum virgatum* L.) was seeded on the plots on 26 May 2006. Switchgrass did not grow on the plots in 2006 due to the high salinity of the compost and lack of rainfall. In the fall of 2006, plots were seeded to annual ryegrass (*Lolium multiflorum* Lam.) as a winter cover crop, and the ryegrass was killed with Glyphosate in the spring of 2007, when the plots were re-seeded with switchgrass on 19 April 2007 (Baker, 2008, p. 138-139). The plots were sampled for biomass 535 and 841 days after Day 0, which Baker (2008, p. 139) designated as 26 May 2006. These days were 12 Nov. 2007 and 14 Aug. 2008.

Soil was sampled for physical measurements in November, 2014. At this time, although there was great variability in the vegetation on the plots, the control plots generally had no vegetation on them and the plots with high compost and lime generally had switchgrass growing. Most plots with bentonite had no vegetation. Some plots with no vegetation had lichens growing on the waste materials.

On 18 Nov. and 19 Nov. 2014, measurements of physical properties of the waste materials in the plots at Site A and Site B were started. The following measurements were taken: infiltration rate to determine hydraulic conductivity; bulk density; water content; dry aggregate size distribution; and wet aggregate stability. These measurements are important to evaluate or predict soil erosion by wind and water. The available water holding capacity was not measured because of the coarse nature of the mine waste materials. Baker (2008) determined that 74.1% and 75.6% of the mine waste materials at Site A and B, respectively, were coarse fragments. It was impossible to determine available water with such coarse material. Baker (2008) sieved the

mine waste materials through a 2 mm sieve and determined available water using pressure plate extractors. He determined available water on only five of the seven treatments (CO, LC, HC, LCLB, and HCLB). He found for CO, LC, HC, LCLB, and HCLB that the available water was 0.09, 0.1, 0.11, 0.15, and 0.15 g g^{-1}, respectively. On 18 Nov. 2014, measurements were done at Site B, and, on 19 Nov. 2014, measurements were done at Site A. Each method now will be described.

To determine infiltration rate, a standard method such as the ring infiltrometer method could not be used. This was for two reasons. First, the dimensions of the plots of Baker (2008) were determined to be too small to put larger ring infiltrometers on, and still maintain some distance from the edge of the plot. Second, water will not pond on the coarse fragments. Therefore, it was decided that the infiltration rate would be determined using a disk infiltrometer of diameter 3.1 cm, which holds 100 cm^3 of water that infiltrates at a tension of 2.0 cm (Model M1, Mini-disk Infiltrometer, Decagon Devices, Inc., Pullman, WA). Any vegetation on a plot was removed, and contact sand (No. 1 white quartz sand, AGSCO Corp., Wheeling, IL) was applied to the surface on which the infiltrometer was placed. Three measurements of infiltration were done on each plot. Hydraulic conductivity was determined from the infiltration measurements using the procedure described in the instruction manual that came with the infiltrometer (Decagon Devices, Pullman, WA, 1997), which used the method of Zhang (1997). After infiltration rate was determined in a plot, the waste material was sampled for bulk density.

The standard core method to determine bulk density could not be used, because of the coarse nature of the mine waste materials. Therefore, bulk density was determined using method of Bashour and Sayegh (2007). The waste material from the surface 5 cm of the soil was scooped up with a flat shovel and put in a stainless steel container (10 cm diameter; 5 cm height)

and covered with a lid that fit the container. Each container had been numbered and weighed before going to the field site. Three samples (containers) per plot were obtained. On 19 Nov. 2014, the containers were brought back to Manhattan, KS, where both water content and bulk density were determined. The containers were weighed on 19 Nov. 2014 to get wet weight of the soil. They were dried at 105 ^{o}C for two days and weighed again to get dry weight. Gravimetric water content (g g^{-1}) was determined as follows: (wet weight – dry weight)/(dry weight). The values were multiplied by 100 to get values on a percentage basis. Bulk density (g cm^{-3}) was determined as follows: (wet weight – dry weight)/volume of the container.

On 18 Nov. and 19 Nov. 2014, approximately 3 kg of waste materials from each plot at Site A and Site B were put in grey, bakelite rectangular trays (60 cm long; 40 cm wide; 20 cm deep), one plot per tray, to obtain materials for analyses of wet and dry aggregates. The top 5 cm (2 in) were scooped up with a flat shovel. The trays were transported to Manhattan, KS, on 19 Nov. 2014, and a subsample from each tray was put in a plastic bag for determination of wet aggregate analysis. The trays with the remaining waste materials were put in a drying oven at 60 ^{o}C for three days.

Dry aggregate size distribution is discussed by Nimmo and Perkins (2002). After the samples had dried, they were placed on a rotary sieve owned by the USDA and located at the former headquarters of the Wind Erosion Research Unit (Agricultural Research Service, USDA, 1515 College Ave., Manhattan, KS; personnel in the unit were transferred to Fort Collins, CO, in 2014). The rotary sieve, as described by Chepil (1962) and modified by Lyles et al. (1970), divided the waste materials into the seven following diameter ranges: <0.42, 0.42-0.84, 0.84-2.00, 2.00-6.35, 6.35-14.05, 14.05-44.45, and >44.45 mm (Lyles et al., 1970; note that Lyles et al. use 19.05 mm instead of 14.05 mm; we used 14.05 mm).

Aggregates smaller than 0.84 mm are the wind erodible fraction (WEF) (Chepil, 1953; Zobeck, 1991), and it was calculated as follows:

$WEF = (M_a/M_t) \times 100,$ [1]

where WEF is the wind erodible fraction in percentage, M_a is the mass of aggregates (g) with diameter less than 0.84 mm, and M_t is the total mass (g) of the sample.

Geometric mean diameter (GMD) of the wet aggregates was determined using the equation given by Tatarko (2001), who got the equation from Gardner (1956):

$$GMD = \exp[\sum_{i=1}^{n} m_i \ln d_i] \quad [2]$$

where m_i is the mass (g) of soil aggregates in one of the seven collection pans, and d_i is the mean diameter (mm) of each of the seven size fractions.

Geometric standard deviation (GSD) was determined using the formula given by Tatarko (2001) and Gardner (1956):

$GSD = \exp[\sum_{i=1}^{n} m_i (\ln d_i)^2 - (\ln GMD)^2]^{0.5}$ [3]

where m_i and d_i are defined in Equation [2].

Wet aggregate stability (WAS) was determined using the method of Nimmo and Perkins (2002), which is the same method as described by Kemper and Rosenau (1986). About 1 kg of soil was sampled at Sites A and B from each plots at the surface to a depth of 5.0 cm. Soil samples were air dried to collect aggregates between 4.75 and 8.0 mm in size. A quantity of 40 g of >4.75 mm aggregates was oven dried for 24 hrs at 105°C to determine gravimetric water content. Size distribution of WAS, mean weight diameter (MWD), and geometric mean diameter (GMD) were obtained using a 50 g of air-dry aggregates was placed on the top sieve of a column

of nested sieves with mesh openings of 4750, 2000, 1000, 500, and 250 microns, saturated by capillarity with water for 10 min, and then mechanically sieved in water for 10 min sieved in water through a vertical displacement of 35 mm at 30 oscillations min^{-1}. The soil remaining on each sieve was washed into pre-weighed beakers and oven dried at 105 °C for 48 h to obtain soil mass. The oven-dry soil was soaked in a 13.9 g l^{-1} sodium hexametaphosphate solution for 24 h to disperse soil aggregates and then washed for sand correction.

The mean weight diameter (MWD) was calculated as follows (Kemper and Chepil, 1965)

$$MWD = \sum_{i=1}^{n} \bar{x}_i \, w_i \qquad [4]$$

where MWD is equal to the sum of products of (1) the mean diameter, $\bar{x}_i$ (in mm), of each size fraction and (2) the proportion of the total sample mass, w_i (in g), occurring in the corresponding size fraction, where the summation is carried out over all *n* size fractions, including the one that passes through the finest sieve.

Geometric mean diameter (GMD) of the wet aggregates was determined using the equation given by Kemper and Rosenau (1986):

$$GMD = \exp\left[\sum_{i=1}^{n} w_i \log \bar{x}_i \; / \; \sum_{i=1}^{n} w_i\right], \qquad [5]$$

where

w_i is the mass (g) of aggregates in a size class with an average diameter (mm) $\bar{x}_i$ and $\sum_{i=1}^{n} w_i$.

Note that GMD of the wet aggregates was determined using a common logarithmic term, while GMD of the dry aggregates was determined using a natural logarithmic term.

The experimental design of Baker et al. (2011) was a complete block with treatment as the main factor at each site. They separated the sites (Site A and Site B) due to a significant site by treatment interaction ($p \leq 0.05$) for all measurements. We also analyzed the sites separately. All statistical analyses were performed using PROCGLM of Statistical Analysis Software (SAS) program Version 9.3 (Statistical Analysis System, 2001). Means were separated at the 0.10 level of significance. Because bulk density and hydraulic conductivity data were not normally distributed, data were log transformation to transform a not normal distribution to a normal distribution.

2.4 Results

Table 2.1 shows water content, bulk density, and hydraulic conductivity at Sites A and B. Table 2.2 shows the same data but log transformed. In general, the data show in both tables that, at Site A, in general, there were no differences in water content, bulk density, and hydraulic conductivity. At Site B water content, bulk density, and hydraulic conductivity varied, but there were no consistent differences among treatments. For example, the hydraulic conductivity was highest in the low compost plus lime treatment and lowest in high compost plus lime treatment (Table 2.1). For both the non-log transformed data (Table 2.1) and the log-transformed data (Table 2.2), the high compost plus lime treatment had the same hydraulic conductivity as the hydraulic conductivities for the control and low compost treatment. The appendix shows the hydraulic conductivities for Site A (Figure A.1 Appendix) and for Site B (Figure A.2 Appendix) in bar graphs. Note each treatment had great variability in hydraulic conductivities.

Figures 2.3 and 2.4 show cumulative infiltration versus time for the different treatments at Site A and Site B, respectively. Three readings were taken for each replication. The three readings have been averaged together to give an average for each replication, and, consequently,

three curves in each part of the figure. Figures 2.5 and 2.6 show the three replications averaged together along with the standard error. Cumulative infiltration showed great variability. No one treatment always had the highest or lowest infiltration rate. The Appendix show the individual infiltration rates obtained during each measurement on each plot for Site A (Figures A.3-A.9 Appendix) and for Site B (Figures A.10- A.16 Appendix) for Site B.

Table 2.3 shows wet aggregate stability at Sites A and B. At Site A, geometric mean diameter and mean weight diameter did not differ among treatments. At Site B, mean weight diameter did not differ among treatments. At Site B, low compost plus lime plus bentonite had the largest geometric mean diameter, and high compost and high compost plus lime plus bentonite had the smallest geometric mean diameter.

Table 2.4 shows dry aggregate size distribution at Sites A and B. At site A, the <0.84 mm fraction did not vary, but geometric mean diameter and geometric standard deviation did vary with no consistency among treatments. The largest geometric mean diameter was with low compost plus lime and the largest geometric standard deviation was with high compost plus lime. At Site B, the greatest value for the <0.84 mm fraction occurred with the control and high compost. The two treatments with bentonite at Site B were consistent in that they both had the smallest <0.84 mm fraction. At Site B, the control and the low compost plus lime treatment had the smallest geometric mean diameter. The control at Site B had the largest geometric standard deviation and the low compost plus lime plus bentonite treatment had the smaller geometric standard deviation.

Table 2.5 shows total bacteria, Gram positive bacteria, and actinomycetes at Site A and Site B. At Site A there were no differences among total bacteria and Gram positive bacteria due to treatment; low compost plus lime plus bentonite had the most actinomycetes. For site B the

control had the most total bacteria, Gram positive bacteria, and actinomycetes and the high compost plus lime plus bentonite treatment had the fewest total bacteria, Gram positive bacteria, and actinomycetes.

Table 2.6 shows Gram negative bacteria and rhizobia at Sites A and B. At Site A there were no differences among gram negative bacteria, and high compost had the highest number of rhizobia. For Site B the control had the most gram negative bacteria and the number of rhizobia did not differ due to treatment.

Table 2.7 shows total fungi, arbuscular mycorrhizae, and saprophytes at Sites A and B. At Site A there was no difference among total fungi and arbuscular mycorrhizae due to treatment. However, at site A there were more saprophytes in the control plots than in the plots with high compost plus lime plus bentonite. At Site B there were more total fungi, arbuscular mycorrhizae, and saprophytes in the control plots than in the plots with high compost plus lime plus bentonite.

Table 2.8 shows protozoa and undifferentiated microbes at Sites A and B. At Site A there were no differences among protozoa due to treatment; low compost plus lime had the most undifferentiated microbes and high compost plus lime plus bentonite had the lowest number of undifferentiated microbes. For Site B there were no differences among protozoa due to treatment; the control had the most undifferentiated microbes.

Table 2.9 shows total living microbial biomass. At Site A, there was no difference among the treatments. At Site B, it was highest for the control treatment. The rating for total biomass at Site B for the control treatment was average, and the ratings for other treatments ranged from slightly-below-average to poor (information from Ward Laboratories, Inc., Kearney, NE,

November 25, 2014). The slightly-below-average to poor ratings showed that there were few microbes in these treatments.

2.5 Discussion

Physical properties of the mine waste material at Galena, KS, which had received amendments of compost, lime, and bentonite 8.5 years earlier, were not different due to treatment. In general, the water contents, bulk densities, and hydraulic conductivities did not differ due to treatment. Water contents varied from 0.079 to 0.155 g g^{-1}, and bulk densities varied from 0.97 to 1.63 Mg m^{-3} (Table 2.1). Non-contaminated, fine-textured surface field soils have bulk densities that range from 1.0 to 1.3 Mg m^{-3}, and coarse-textured surface field soils have bulk densities that range from 1.3 to 1.8 Mg m^{-3} (Millar et al., 1965, p. 50-51). The rocky, chat material at Galena, KS, essentially covered this entire range of bulk densities, showing their great variability. Hydraulic conductivities varied from 0.000254 to 0.00101 cm s^{-1} (Table 2.1) or 0.219 to 0.873 m day^{-1}. These values are on the low side for hydraulic conductivities of either natural or disturbed soils. The hydraulic conductivity of natural soils in place varies from about 30 m/day for a silty clay loam to 0.05 m day^{-1} for a clay (Kirkham, 2014, p. 89). The hydraulic conductivity for disturbed soil materials varies from about 600 m day^{-1} for gravel to 0.02 m day^{-1} for silt and clay (Kirkham, 2014, p. 89). A soil is said to be drainable if the hydraulic conductivity is 1 m day^{-1}. The hydraulic conductivities of the waste material were less than 1 m day^{-1}, so they materials could be considered to be not drainable.

Infiltration rates are the slopes for the lines shown in Figures 2.5 and 2.6. At Site A (Fig. 2.5), they varied from 0.0087 to 0.0119 cm s^{-1}. At Site B (Fig. 2.6), they varied from 0.0083 to 0.0127 cm s^{-1}. Shukla et al. (2004) give infiltration rates after 5 minutes for un-reclaimed coal mine soil and reclaimed coal mine soil in Jackson County, Ohio (see their Table 2.1). The

surface mine site had been reclaimed in 1975-1976 by applying topsoil, 10 to 36 cm deep, over the graded area and seeded to grass and legumes. Shukla et al. (2004) measured infiltration rates in October 2001 using a double-ring infiltrometer. Five minutes after the start of infiltration, there was no difference in infiltration rates for the un-reclaimed mine soil and reclaimed mine soil. The 5-minute infiltration rates varied from 0.21 to 0.67 cm min^{-1}. Our values, when converted to cm min^{-1}, varied from 0.522 to 0.714 cm min^{-1} at Site A and from 0.498 to 0.762 cm min^{-1} at Site B. The range in our values was similar to those of Shukla et al. (2004).

The values that Shukla et al. (2004) got for infiltration are low compared to the values that Shrestha and Lal (2008) got for reclaimed coal mine soils in Morgan County, Ohio, which were reclaimed in 1977 with 30 cm of topsoil planted to forest, hay, or pasture. Twenty-eight years later, Shrestha and Lal (2008) made measurements of infiltration rates using a double-ring infiltrometer. They compared infiltration rates of the reclaimed mine soil to infiltration rates of undisturbed forest soil and agricultural soil, which had never been mined. Five minutes after the start of infiltration, the infiltration rates of the undisturbed forest soil and agricultural soil were 20 and 3 cm min^{-1}, respectively. The reclaimed mine soils planted to forest, hay, or pasture had 5-minute infiltration rates of 16, 9, and 3 cm min^{-1}, respectively. These values are about an order of magnitude greater than the values we measured, which indicated that our infiltration rates were low compared to unmined soils.

In general, wet aggregate stability, as shown by geometric mean diameter and mean weight diameter, did not differ among treatments (Table 2.3). Effects of the treatments were no longer evident after 8.5 years.

Dry aggregate stability was documented by geometric mean diameter, geometric standard deviation, and the fraction less than 0.84 mm. Geometric mean diameter and geometric standard

deviation varied slightly among treatments, but there was no consistent result. At Site A, geometric mean diameter for the low compost plus lime treatment was the largest, but at Site B, it was the lowest, and had a value similar to that of the control. At Site A, geometric standard deviation was highest for the high compost plus lime treatment, but at Site B, the control had the highest geometric standard deviation.

The fraction of less than 0.84 mm (wind erodible fraction) did not vary at Site A, but it did at Site B. The control and the treatment with high compost had the highest values for the wind erodible fraction, and the treatments with low compost plus lime plus bentonite and high compost plus lime plus bentonite had the lowest values. The results suggest that bentonite (the clay) was able to reduce the wind erodible fraction.

At Site A, populations of bacteria (Tables 2.5 and 2.6) showed no differences among treatments, except actinomycetes were highest in low compost plus lime treatment and the low compost plus lime plus bentonite treatment, and rhizobia were highest in the high compost treatment. At Site A, populations of fungi (Table 2.7) did not vary among treatments, except saprophytes were highest in the control and lowest in the high compost plus lime plus bentonite treatment. At Site B, total bacteria, Gram positive bacteria, actinomycetes and Gram negative bacteria were were highest in the control plots (Tables 2.5 and 2.6). Also at Site B, total fungi, arbuscular mycorrhize, and saprophytes were highest in the control treatment (Table 2.7), and undifferentiated microbes were highest in this treatment, too (Table 2.8). At Site B, the total biomass of microbes was highest in the control treatment (Table 2.9). This is a surprising result and difficult to explain. In May, 2014, Hettiarachchi and colleagues collected samples from the plots established by Baker et al. (2011). Their experimental results showed that over a period of 8 years the high compost treatment had higher microbial biomass and enzyme activities than the

control, while, in general, all low compost treatments did not differ from the control (Wijesekara et al., 2016). Therefore, in the time from May 2014 to November 2014, when we sampled the plots, the high compost treatment no longer had the highest microbial populations. The control soil had no amendments added to it, like compost, which could have increased the microbial population. Baker et al. (2011) concluded that large amounts of organic matter would be needed to support and sustain microbial activity in mine waste materials. This conclusion was valid, because 8.5 years after application of the compost additions, microbial activity in the high compost treatment was less than that of the control. The reason that the control plots at Site B had the highest microbial populations needs to be determined. It is highly possible that the biological properties vary with time of year sampled, and with the microclimate at the time of the sampling (air and soil temperature, soil moisture, etc).

2.6 Conclusion

There was great variability in the measurements taken in the physical characteristics. This agrees with data in the literature showing that the physical properties of mine waste materials are highly variable. However, the results did show that eight and a half years after amendments were added to the mine waste material at Galena, KS, the plots with clay (bentonite) had the smallest wind erodible fraction. Differences in other physical properties due to treatment were not consistent. For an unknown reason, microbial populations were highest in the control plots with no amendments.

2.7 References

Baker, L.R. 2008. In situ remediation of Pb/Zn contaminated materials: Field- and molecular-scale investigations. Ph.D. diss. Kansas State University, Manhattan. xxxi + 357 p.

Baker, L.R., P.M. White, and G.M. Pierzynski. 2011. Changes in microbial properties after manure, lime, and bentonite application to a heavy metal-contaminated mine waste. Applied Soil Ecology 48:1-10.

Bashour, I. I., and Sayegh, A. H. 2007. Methods of analysis for soils of arid and semi-arid regions. FAO, Rome.

Bi, Y., H. Zou, and C. Zhu. 2014. Dynamic monitoring of soil bulk density and infiltration rate during coal mining in sandy land with different vegetation. Int. J. Coal Sci. Technol. 1: 198-206.

Carroll, S.A., P.A. O'Day, and M. Piechowski. 1998. Rock-water interactions controlling zinc, cadmium, and lead concentration in surface waters and sediments, U.S. Tri-State Mining District. 2. Geochemical interpretation. Environ. Sci. Technol. 32: 956-965.

Chepil, W.S. 1953. Field structure of cultivated soils with special reference to erodibility by wind. Soil Sci. Soc. Am. Proc. 17:185-190.

Chepil, W.S. 1962. A compact rotary sieve and the importance of dry sieving in physical soil analysis. Soil Sci. Soc. Am. Proc. 26:4-6.

Decagon Devices, Inc. 1997. Measuring soil hydraulic conductivity with a disk infiltrometer. Application Note. Soil Physics Instruments, Decagon Devices, Inc., Pullman, WA. 4 pages.

DeLong, C., J. Skousen, and E. Pena-Yewtukhiw. 2012. Bulk density of rocky mine soils in forestry reclamation. Soil Sci. Soc. Amer. J. 76: 1810-1815.

Forján, R., V. Asensio, A. Rodríguez-Vila, and E.F. Covelo. 2014. Effect of amendments made of waste materials in the physical and chemical recovery of mine soil. J. Geochmical Exploration 147: 91-97.

Gardner, W.R. 1956. Representation of a soil aggregate-size distribution by a logarithmic-normal distribution. Soil Sci. Soc. Am. Proc. 40: 151-153.

Gibson, A.M. 1972. Wilderness bonanza-the Tri-State District of Missouri, Kansas, and Oklahoma. University of Oklahoma Press, Norman, Oklahoma. 362 p.

Indorante, S.J., I.J. Jansen, and C.W. Boast. 1981. Surface mining and reclamation: Initial changes in soil character. J. Soil Water Conserv. 36: 347-351.

Jitesh Kumar, M., and P. Amiya Kumar. 2013. Physico-chemical characterization and mine soil genesis in age series coal mine overburden spoil in chronosequence in a dry tropical environment. J. Phylogenetics Evolution Biol. 1(1): 1-7. (doi:10.4172/2329-9002.1000101).

Johnson, A.W., M. Gutiérrez, D. Gouzie, and L.R. McAliley. 2016. State of remediation and metal toxicity in the Tri-State Mining District, USA. Chemosphere 144: 1132-1141.

Juracek, K.E. 2008. Sediment storage and severity of contamination in a shallow reservoir affected by historical lead and zinc mining. Environ. Geol. 54: 1447-1463.

Kemper, W.D., and R.C. Rosenau. 1986. Aggregate stability and size distribution, p. 425-442. *In* A. Klute (ed.) Methods of Soil Analysis. Part 1. Physical and Mineralogical Methods. Second Edition. American Society of Agronomy and Soil Science Society of America, Madison, WI.

Kemper, W.D., and W.S. Chepil. 1965. Size distribution of aggregates, p. 499-510. *In* C.A. Black, D.D. Evans, J.L. White, L.E. Ensminger, and F.E. Clark (ed.). Methods of Soil Analysis. Part 1. Physical and Mineraological Properties, Including Statistics of Measurement and Sampling. American Society of Agronomy, Madison, WI.

Kirkham, M.B. 2014. Principles of Soil and Plant Water Relations. Second ed. Elsevier, Academic Press, Amsterdam. 579 p.

Krümmelbein, J., and T. Raab. 2012. Development of soil physical parameters in agricultural reclamation after brown coal mining within the first four years. Soil Tillage Res. 125: 109-115.

Krümmelbein, J., R. Horn, T. Raab, O. Bens, and R.F. Hüttl. 2010. Soil physical parameters of a recently established agricultural recultivation site after brown coal mining in Eastern Germany. Soil Tillage Res. 111: 19-25.

Lyles, L., J.D. Dickerson, and L.A. Disrud. 1970. Modified rotary sieve for improved accuracy. Soil Sci. 109:207-210.

Millar, C.E., L.M. Turk, and H.D. Foth. 1965. Fundamentals of Soil Science. Fourth ed. Wiley, New York. 491 p.

Nimmo, J.R., and K.S. Perkins. 2002. Aggregate stability and size distribution, p. 317-328. *In* J.H. Dane and G.C. Topp (ed.) Methods of Soil Analysis. Part 4. Physical Methods. Soil Science Society of America, Madison, WI.

Perlatti, F., T. Osóorio Ferreira, R. Espíndola Romero, M.C. Gomes Costa, and X.L. Otero. 2015. Copper accumulation and changes in soil physical-chemical properties promoted by native plants in an abandoned mine site in northeastern Brazil: Implications for restoration of mine sites. Ecological Eng. 82: 103-111.

Pierzynski, G.M., M. Lambert, B.A.D. Hettrick, D.W. Sweeney, and L.E. Erickson. 2002. Phytostabilization of metal mine tailings using tall fescue. Practice Periodical Hazardous Toxic Radioact. Waste Manage. 6: 212-217.

Pope, L.M. 2005. Assessment of contaminated streambed sediment in the Kansas part of the historic Tri-State Lead and Zinc Mining District, Cherokee County, 2004. U.S. Geological Survey Scientific Investigations Report 2005-5251. U.S. Department of the Interior, U.S. Geological Survey, Reston, Virginia. 61 p.

Sadhu, K., K. Adhikari, and A. Gangopadhyay. 2012. Effect of mine spoil on native soil of Lower Gondwana coal fields: Raniganj coal mines areas, India. Int. J. Environmental Sci. 2: 1675-1687.

Sheoran, V., A.S. Sheoran, and P. Poonia. 2010. Soil reclamation of abandoned mine land by revegetation: A review. Int. J. Soil, Sediment Water, Vol. 3, Issue 2, Article 13 (21 pages).

Shrestha, R.K., and R. Lal. 2008. Land use impacts on physical properties of 28 years old reclaimed mine soils in Ohio. Plant Soil 306: 249-260.

Shrestha, R.K., and R. Lal. 2011. Changes in physical and chemical properties of soil after surface mining and reclamation. Geoderma 161: 168-176.

Shukla, M.K., R. Lal, J. Underwood, and M. Ebinger. 2004. Physical and hydrological characteristics of reclaimed minesoils in Southeastern Ohio. Soil Sci. Soc. Amer. J. 68: 1352-1359.

Skousen, J., J. Sencindiver, K. Owens, and S. Hoover. 1998. Physical properties of minesoils in West Virginia and their influence on wastewater treatment. J. Environmental Quality 27: 633-639.

Statistical Analysis System. 2001. SAS Institute, Cary, NC.

Tatarko, J. 2001. Soil aggregation and wind erosion: Processes and measurements. Ann. Arid Zone 40:251-263.

Thomas, C.B. 2012. Evaluation of tree growth and chemical, physical, and biochemical soil properties of two reclaimed surface mines in West Virginia. M.S. Thesis. West Virginia Univ., Morgantown.

United States Department of Agriculture. 2013. Custom Soil Resource Report for Cherokee County, Kansas, Soil Survey Staff, Natural Resource Conservation Service, United States Department of Agriculture, Web Soil Survey. Last modified 12/06/2013. Available online at http://websoilsurvey.nrcs.usda.gov/. Accessed 10/20/2016.

Wijesekara, H., Bolan, N. S., Vithanage, M., Xu, Y., Mandal, S., Brown, S. L., and Kirkham, M. B. 2016. Chapter Two-Utilization of Biowaste for Mine Spoil Rehabilitation. Advances in Agronomy, 138, 97-173.

Yao, F. C. Lin, J. Ma, and T. Zhu. 2010. Effects of plant types on physico-chemical properties of reclaimed mining soil in Inner Mongolia, China. Chin. Geogr. Sci. 20: 309-317.

Zhang, L., J. Wang, Z. Bai, and C. Lv. 2015. Effects of vegetation on runoff and soil erosion on reclaimed land in an opencast coal-mine dump in a loess area. Catena 128: 44-53.

Zhang, R. 1997. Determination of soil sorptivity and hydraulic conductivity from the disk infiltrometer. Soil Sci. Soc. Am. J. 61:1024-1030.

Zobeck, T.M. 1991. Soil properties affecting wind erosion. J. Soil Water Conservation 46:112-118.

Figure 2.1 Randomly treatment for Site A.

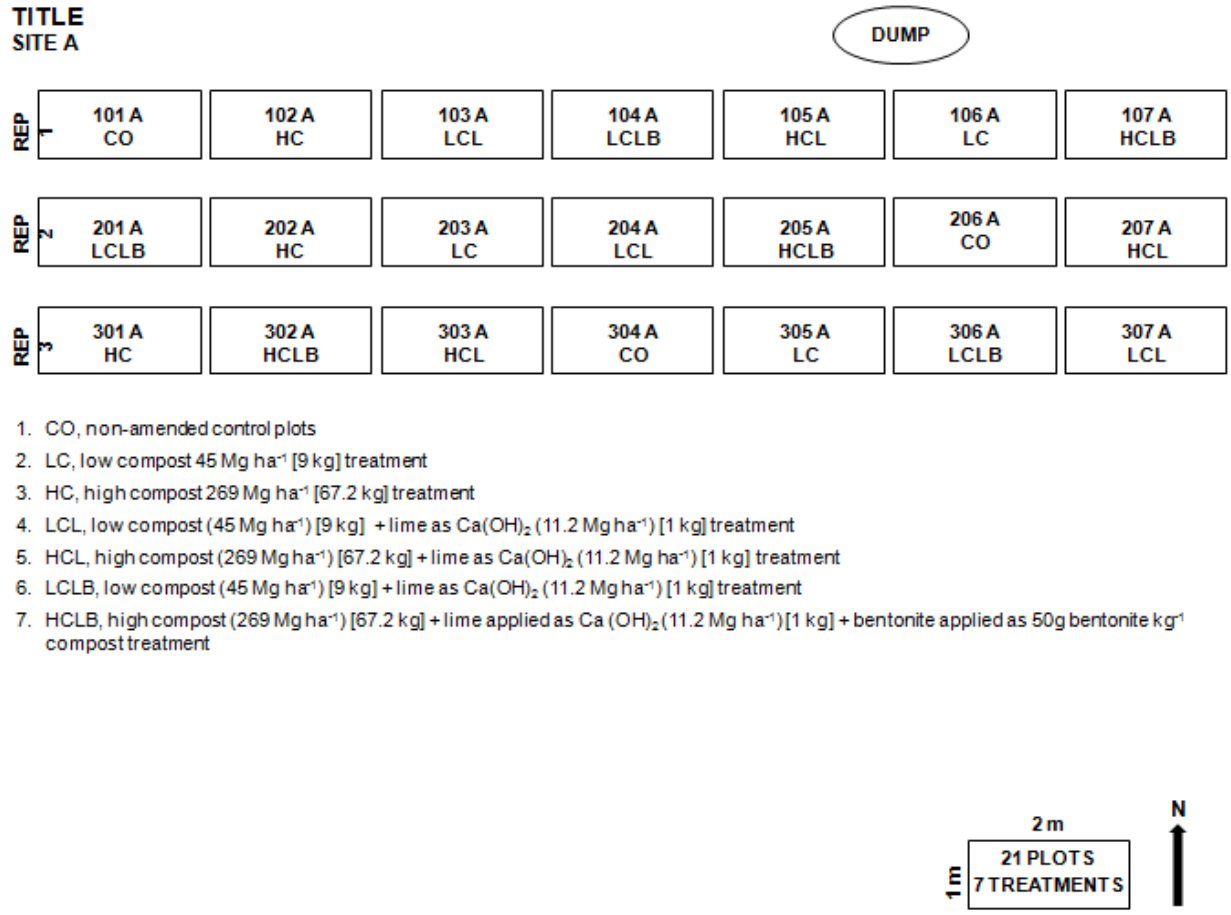

1. CO, non-amended control plots
2. LC, low compost 45 Mg ha^{-1} [9 kg] treatment
3. HC, high compost 269 Mg ha^{-1} [67.2 kg] treatment
4. LCL, low compost (45 Mg ha^{-1}) [9 kg] + lime as $Ca(OH)_2$ (11.2 Mg ha^{-1}) [1 kg] treatment
5. HCL, high compost (269 Mg ha^{-1}) [67.2 kg] + lime as $Ca(OH)_2$ (11.2 Mg ha^{-1}) [1 kg] treatment
6. LCLB, low compost (45 Mg ha^{-1}) [9 kg] + lime as $Ca(OH)_2$ (11.2 Mg ha^{-1}) [1 kg] treatment
7. HCLB, high compost (269 Mg ha^{-1}) [67.2 kg] + lime applied as $Ca(OH)_2$ (11.2 Mg ha^{-1}) [1 kg] + bentonite applied as 50g bentonite kg^{-1} compost treatment

Figure 2.2 Randomly treatments for site B.

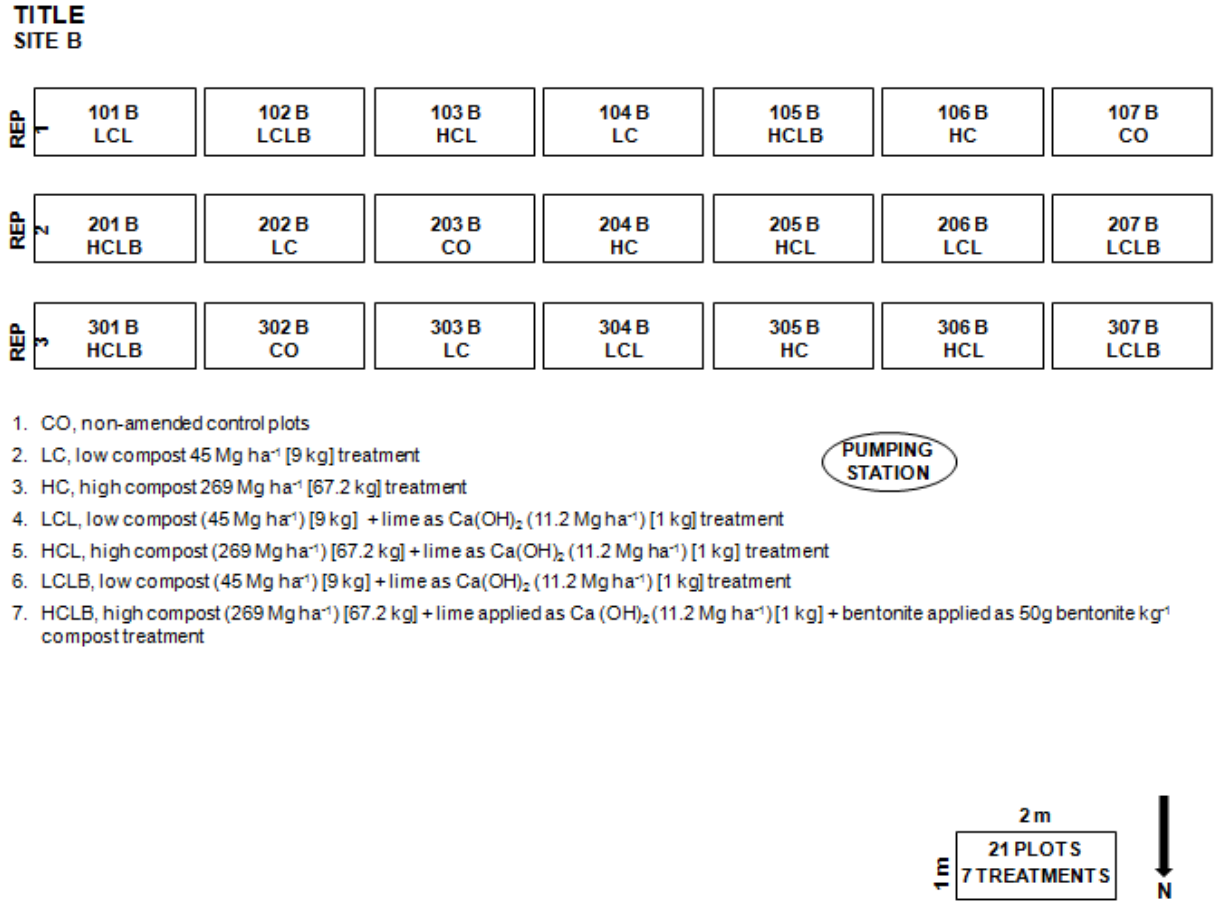

Figure 2.3 Average cumulative infiltration versus time for each treatment at Site A. (a) control, (b) low compost, (c) high compost, (d)low compost plus lime, (e) high compost plus lime, (f) low compost plus lime plus bentonite, (g) high compost plus lime plus bentonite. Triangles show average three readings from first replicate; squares show average three readings from second replicate; circles show average three readings from third replicate. (n = 3 for each symbol)

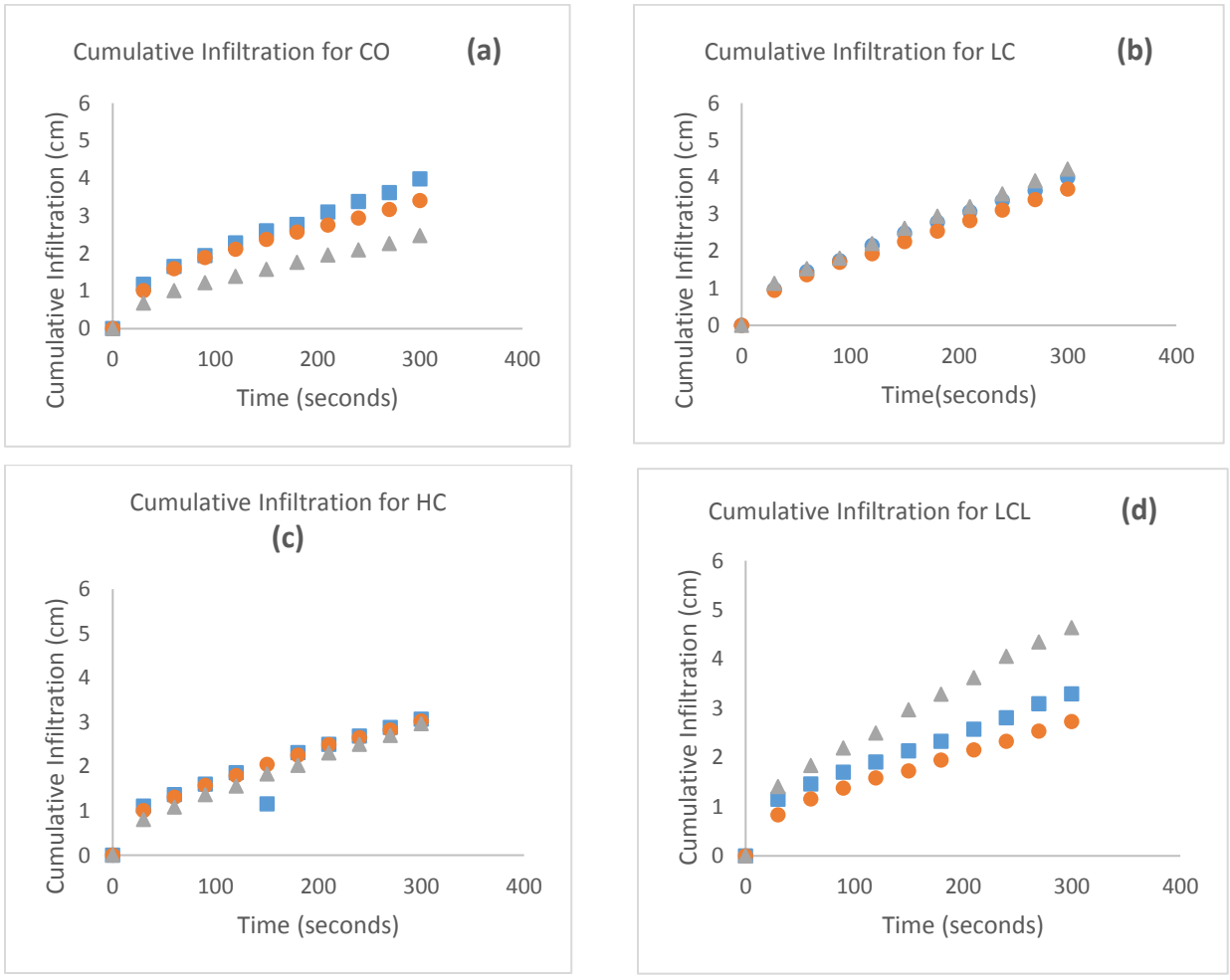

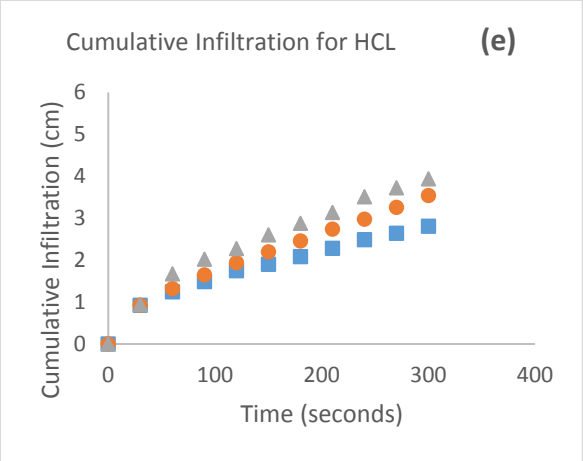
Cumulative Infiltration for HCL
(e)
Cumulative Infiltration (cm)
0
1
2
3
4
5
6
0
100
200
300
400
Time (seconds)

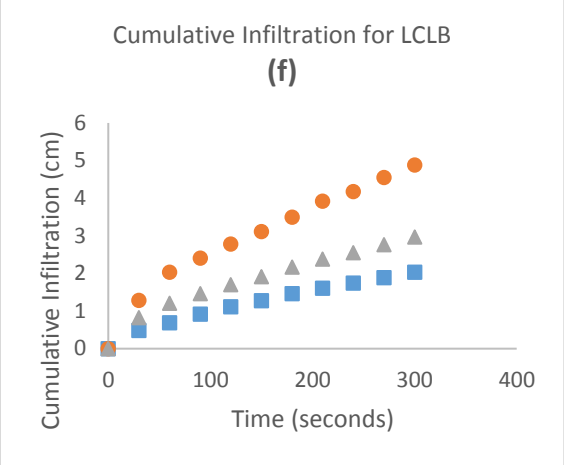
Cumulative Infiltration for LCLB
(f)
Cumulative Infiltration (cm)
0
1
2
3
4
5
6
0
100
200
300
400
Time (seconds)

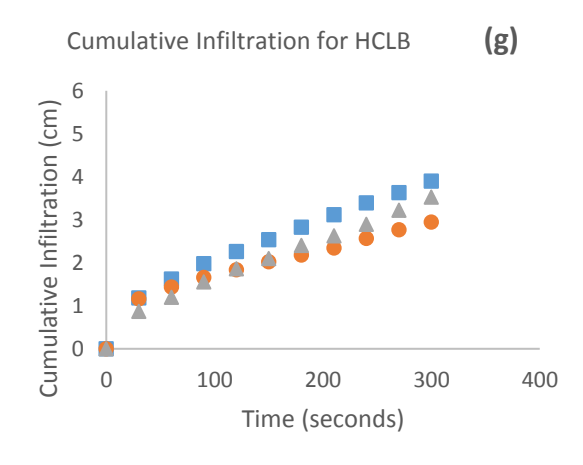
Cumulative Infiltration for HCLB
(g)
Cumulative Infiltration (cm)
0
1
2
3
4
5
6
0
100
200
300
400
Time (seconds)

Figure 2.4 Average cumulative infiltration versus time for each treatment at Site B. (a) control, (b) low compost, (c) high compost, (d) low compost plus lime, (e) high compost plus lime, (f) low compost plus lime plus bentonite, (g) high compost plus lime plus bentonite. Triangles show average three readings from first replicate; squares show average three readings from second replicate; circles show average three readings from third replicate. (n = 3 for each symbol)

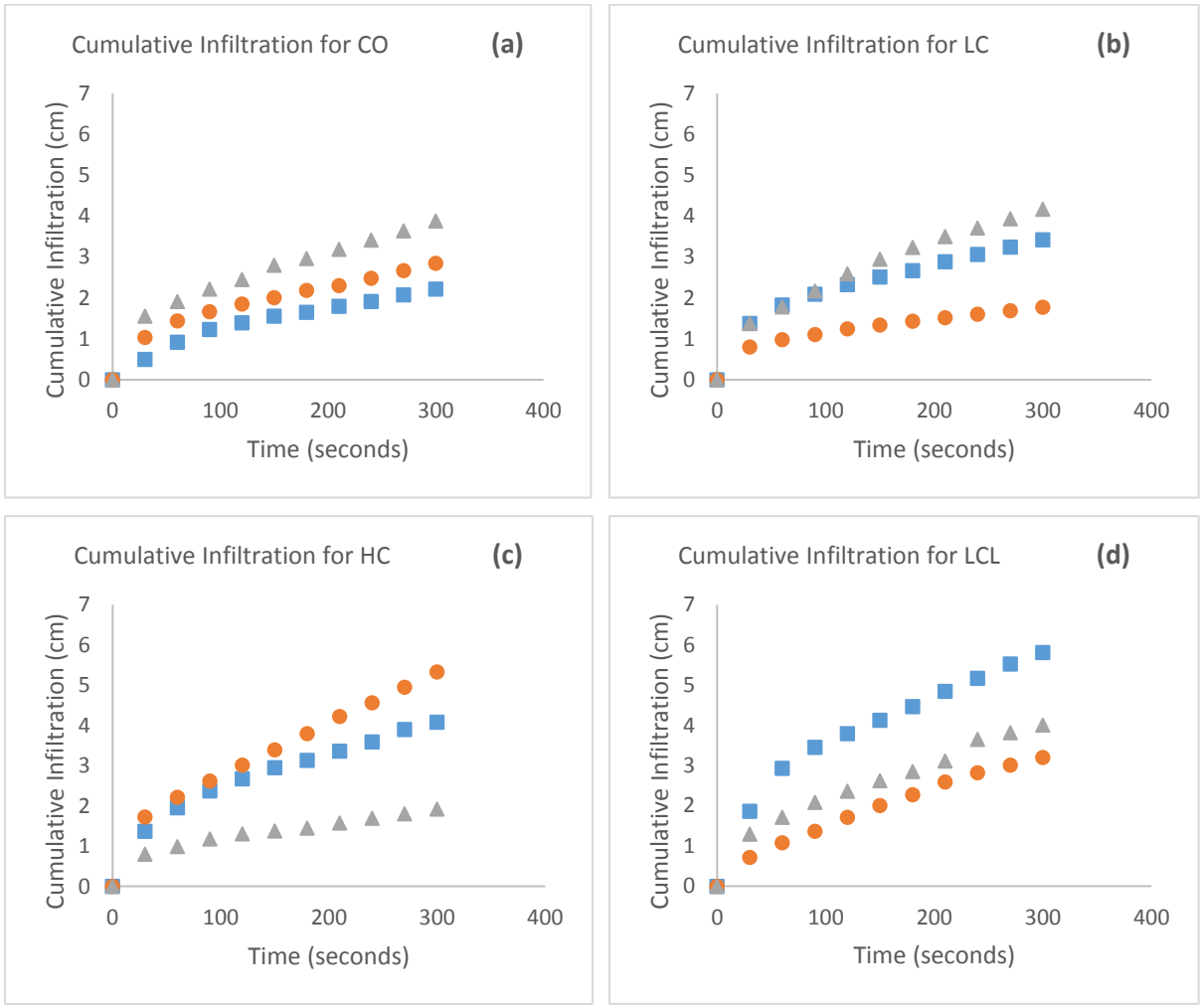

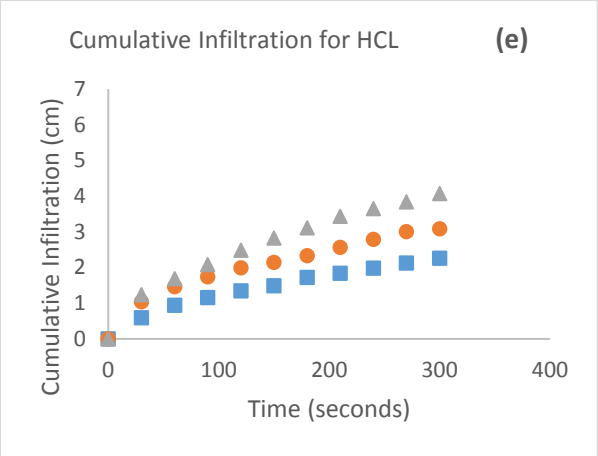
Cumulative Infiltration for HCL
(e)
Cumulative Infiltration (cm)
0
1
2
3
4
5
6
7
0
100
200
300
400
Time (seconds)

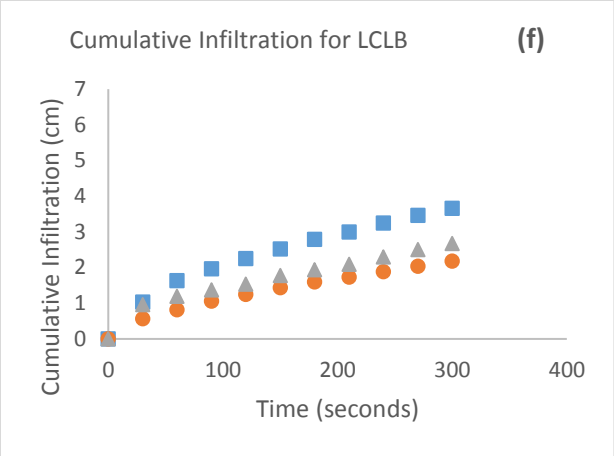
Cumulative Infiltration for LCLB
(f)
Cumulative Infiltration (cm)
0
1
2
3
4
5
6
7
0
100
200
300
400
Time (seconds)

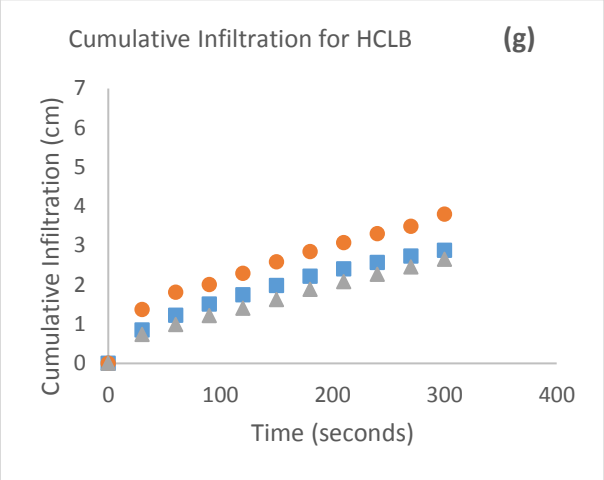
Cumulative Infiltration for HCLB
(g)
Cumulative Infiltration (cm)
0
1
2
3
4
5
6
7
0
100
200
300
400
Time (seconds)

Figure 2.5 Average cumulative infiltration versus time for each treatment after all replications have been combined at Site A. (a) control, (b) low compost, (c) high compost, (d) low compost plus lime, (e) high compost plus lime, (f) low compost plus bentonite, (g) high compost plus bentonite. Average of three replications. Vertical bars show the standard error. (n = 9 for each symbol)

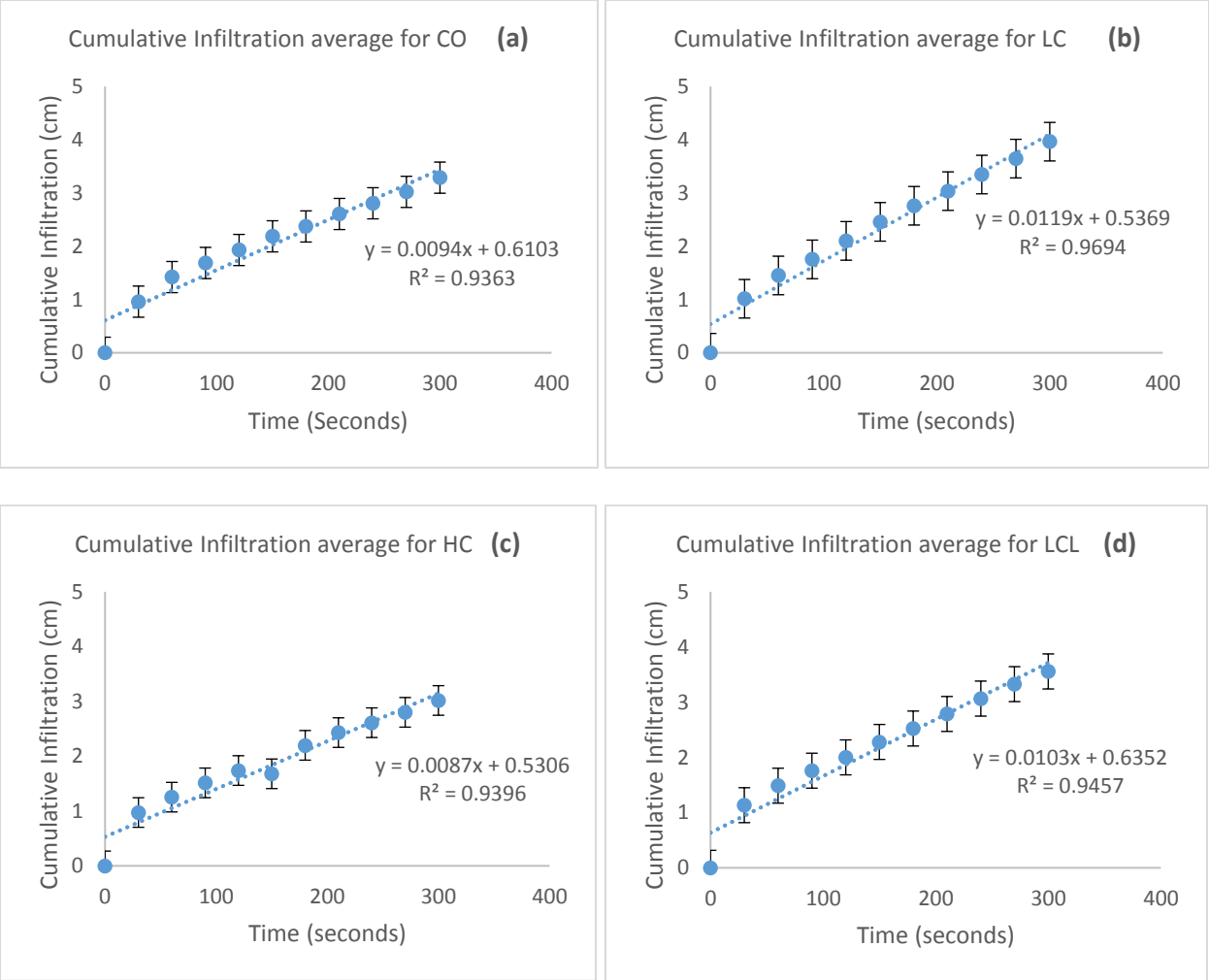

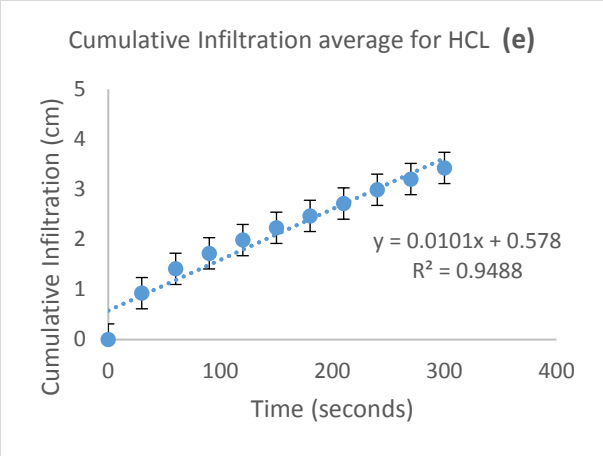
Cumulative Infiltration average for HCL (e)
Cumulative Infiltration (cm)
Time (seconds)
y = 0.0101x + 0.578
R² = 0.9488
0
1
2
3
4
5
0
100
200
300
400

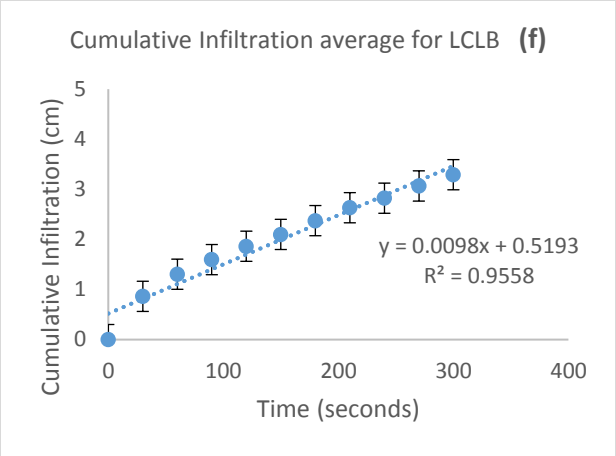
Cumulative Infiltration average for LCLB (f)
Cumulative Infiltration (cm)
Time (seconds)
y = 0.0098x + 0.5193
R² = 0.9558
0
1
2
3
4
5
0
100
200
300
400

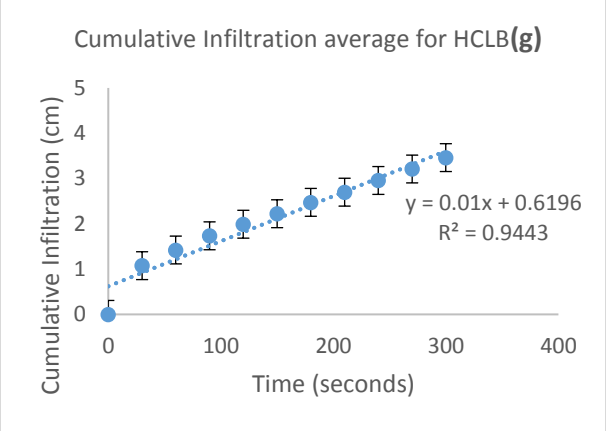
Cumulative Infiltration average for HCLB(g)
Cumulative Infiltration (cm)
Time (seconds)
y = 0.01x + 0.6196
R² = 0.9443
0
1
2
3
4
5
0
100
200
300
400

Figure 2.6 The average cumulative infiltration versus time for each treatment after all replications have been combined at Site B. (a) control, (b) low compost, (c) high compost, (d) low compost plus lime, (e) high compost plus lime, (f) low compost plus lime plus bentonite, (g) high compost plus lime plus bentonite. Average of three replications. Vertical bars show the standard error. (n = 9 for each symbol).

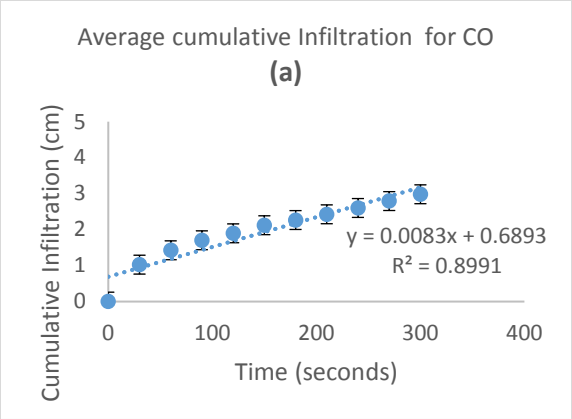

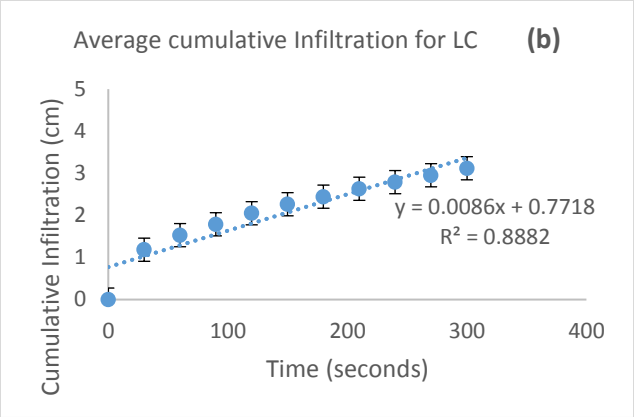

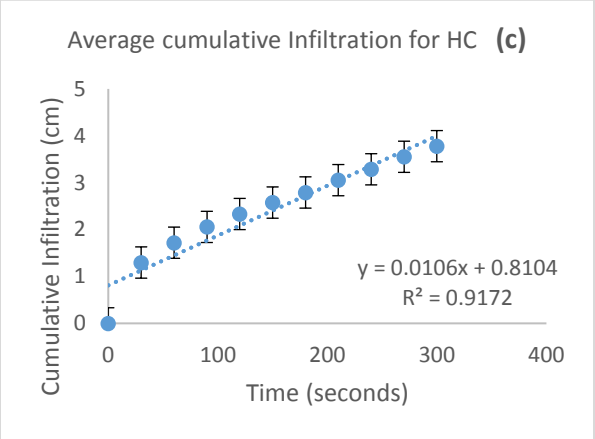

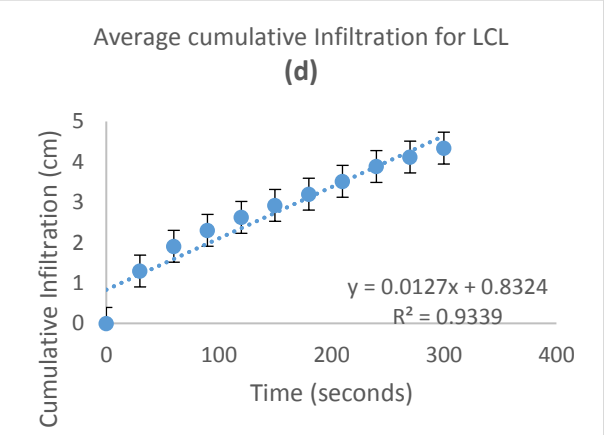

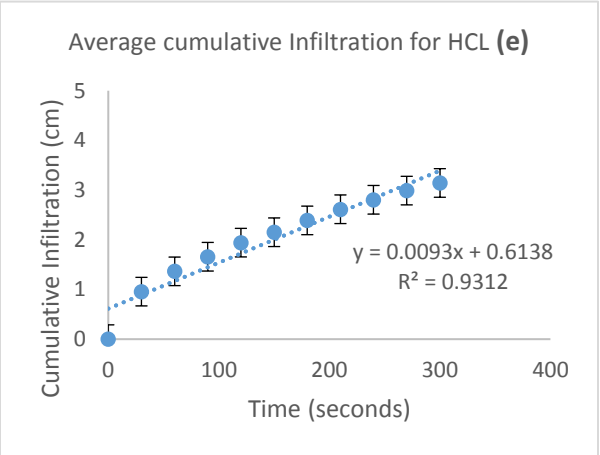

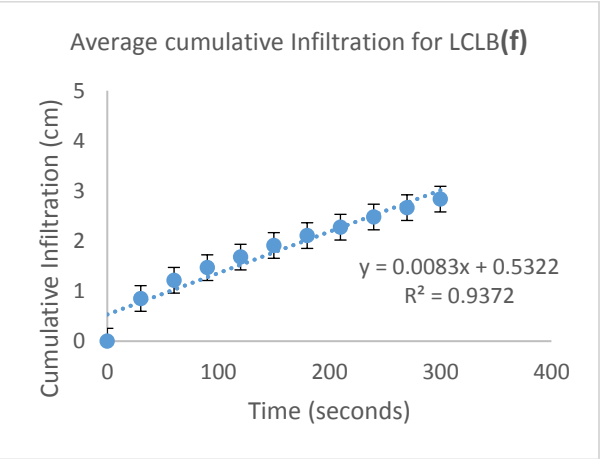

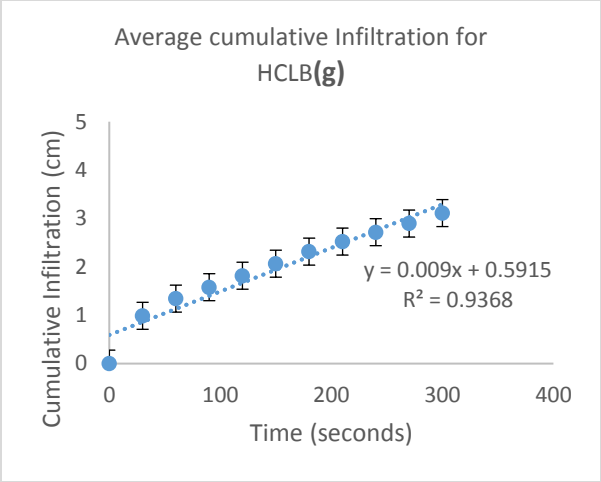
Average cumulative Infiltration for HCLB(g)
Cumulative Infiltration (cm)
0
1
2
3
4
5
0
100
200
300
400
Time (seconds)
y = 0.009x + 0.5915
R² = 0.9368

Table 2.1 Water content, bulk density, and hydraulic conductivity at Sites A and B. Means followed by the same letter are not statistically different at 0.10.

Treatment	Water Content $g\ g^{-1}$		Bulk Density $Mg\ m^{-3}$		Hydraulic conductivity $cm\ s^{-1} \times 10^{4}$	
	Site A	Site B	Site A	Site B	Site A	Site B
Control	0.099 a	0.098 ab	1.14 a	1.12 bc	5.00 b	3.23 b
Low compost	0.132 a	0.099 ab	0.97 a	1.27 a	9.98 a	2.54 b
High compost	0.093 a	0.155 a	1.63 a	1.11 c	4.79 b	5.43 ab
Low compost + lime	0.089 a	0.083 b	1.14 a	1.19 abc	4.39 b	10.13 a
High compost + lime	0.137 a	0.085 b	0.99 a	1.18 abc	4.92 b	4.19 b
Low compost + lime + bentonite	0.137 a	0.084 b	1.02 a	1.27 a	6.51 ab	7.46 ab
High compost + lime + bentonite	0.114 a	0.079 b	1.04 a	1.25 ab	5.51 b	4.73 ab

Table 2.2 Log bulk density and log hydraulic conductivity at Sites A and B. Means followed by the same letter are not statistically different at 0.10.

Treatment	Log Water Content g g^{-1}		Log Bulk Density Mg m^{-3}		Log Hydraulic Conductivity cm s^{-1} x 10^4	
	Site A	**Site B**	**Site A**	**Site B**	**Site A**	**Site B**
Control	1.02 a	1.01 ab	0.052 a	0.051 ab	3.60 b	3.84 ab
Low compost	0.893 a	1.00 ab	0.014 a	0.103 a	3.00 a	4.05 b
High compost	1.04 a	0.867 a	0.064 a	0.044 b	3.39 ab	3.78 ab
Low compost + lime	1.05 a	1.09 b	0.058 a	0.074 ab	3.48 ab	3.14 a
High compost + lime	0.873 a	1.07 b	0.005 a	0.072 ab	3.49 ab	3.53 ab
Low compost + lime + bentonite	0.916 a	1.08 b	0.002 a	0.105 a	3.25 ab	3.31 ab
High compost + lime + bentonite	0.970 a	1.10 b	0.016 a	0.097 ab	3.61 b	3.46 ab

Table 2.3 Wet aggregate stability at Sites A and B, sand free. Means followed by the same letter are not statistically different at 0.10.

Treatment	GMD† mm		MWD‡ mm	
	Site A	Site B	Site A	Site B
Control	2.04 a	1.98 ab	5.28 a	4.01 a
Low compost	1.96 a	1.90 ab	4.81 a	3.80 a
High compost	2.02 a	1.85 b	4.65 a	3.46 a
Low compost + lime	2.01 a	1.97 ab	4.51 a	4.06 a
High compost + lime	2.02 a	1.95 ab	4.65 a	3.44 a
Low compost + lime + bentonite	1.96 a	2.05 a	4.16 a	4.13 a
High compost + lime + bentonite	2.04 a	1.83 b	4.78 a	3.04 a

†**GMD=** Geometric Mean Diameter

‡ **MWD=** Mean Weight Diameter

Table 2.4 Dry aggregate size distribution at Sites A and B. Means followed by the same letter are not statistically different at 0.10.

Treatment	%<0.84 mm		GMD†		GSD‡	
	Site A	Site B	Site A	Site B	Site A	Site B
Control	10.37 a	8.00 a	57.54 b	63.59 b	49.02 ab	33.07 a
Low compost	10.30 a	6.76 ab	59.27 ab	68.34 a	46.14 ab	27.85 abc
High compost	9.71 a	8.04 a	60.94 ab	70.01 a	43.00 ab	28.88 ab
Low compost + lime	9.59 a	7.25 ab	65.73 a	63.88 b	37.12 b	27.79 abc
High compost + lime	11.99 a	7.06 ab	58.35 ab	69.95 a	51.19 a	26.87 abc
Low compost + lime + bentonite	11.08 a	5.4 b	60.14 ab	69.36 a	47.31 ab	21.98 c
High compost + lime + bentonite	10.34 a	4.93 b	61.91 ab	68.87 a	43.42 ab	24.26 bc

†**GMD=** geometric mean diameter

‡**GSD=** geometric standard deviation

Table 2.5 Total bacteria, Gram positive bacteria, and actinomycetes at Sites A and B. Means followed by the same letter are not statistically different at 0.10.

Treatment	Total Bacteria		Gram (+)		Actinomycetes	
	……..…….…….ng/g……..					
	Site A	Site B	Site A	Site B	Site A	Site B
Control	814.9 a	808.9 a	409.1 a	447.14 a	119.65 ab	129.77 a
Low compost	730.3 a	576.6 ab	363.5 a	361.97 ab	112.50 ab	104.99 ab
High compost	686.9 a	384.4 bcd	352.0 a	231.15 bcd	113.0 ab	60.21 bcd
Low compost + lime	908.8 a	235.6 cd	434.9 a	140.39 cd	141.66 a	39.36 cd
High compost + lime	792.1 a	468.6 bcd	397.0 a	274.21 bc	120.84 ab	83.48 abc
Low compost + lime + bentonite	840.3 a	501.9 bcd	432.7 a	255.11 bcd	145.24 a	87.99 abc
High compost + lime + bentonite	346.7 a	177.5 d	180.0 a	111.48 d	56.62 b	28.19 d

Table 2.6 Gram negative and rhizobia at Site A and B. Means followed by the same letter are not statistically different at 0.10.

Treatment	Gram (-)		Rhizobia	
	……..……..ng/g…….……..			
	Site A	**Site B**	**Site A**	**Site B**
Control	405.8 a	361.75 a	13.3 b	32.14 a
Low compost	366.9 a	214.65 abc	10.74 b	8.75 a
High compost	334.9 a	153.22 bc	64.63 a	---†
Low compost + lime	473.9 a	95.18 bc	7.22 b	19.59 a
High compost + lime	395.1 a	194.42 bc	23.76 b	12.11 a
Low compost + lime + bentonite	407.6 a	246.75 ab	16.42 b	27.39 a
High compost + lime + bentonite	166.7 a	66.06 c	2.58 b	---

† No data

Table 2.7 Total fungi, arbuscular mycorrhizae, and saprophytes at Sites A and B. Means followed by the same letter are not statistically different at 0.10.

Treatment	Total Fungi		Arbuscular Mycorrhizae		Saprophytes	
	……..…..ng/g…….…..					
	Site A	Site B	Site A	Site B	Site A	Site B
Control	275.9 a	239.95 a	80.16 a	61.5 a	195.75 a	178.45 a
Low compost	221.2 a	111.84 abc	57.15 a	51.04 ab	164.03 ab	60.78 ab
High compost	184.1 a	76.98 bc	63.96 a	21.27 bc	120.17 ab	55.71 b
Low compost + lime	242.8 a	72.60 bc	74.27 a	5.81 c	168.49 ab	66.79 ab
High compost + lime	226.5 a	108.68 abc	67.57 a	28.05 abc	158.90 ab	80.63 ab
Low compost + lime + bentonite	251.0 a	181.50 ab	70.60 a	53.63 ab	180.38 ab	127.87 ab
High compost + lime + bentonite	84.4 a	17.12 c	18.53 a	0.00 c	65.85 b	17.12 b

Table 2.8 Protozoa and undifferentiated at Site A and B. Means followed by the same letter are not statistically different at 0.10.

Treatment	Protozoa		Undifferentiated	
	……..……..…ng/g…….…….			
	Site A	Site B	Site A	Site B
Control (CO)	48.03 a	28.06 a	657.5 ab	785.8 a
Low compost (LC)	26.32 a	8.24 a	706.6 ab	647.2 ab
High compost (HC)	33.23 a	3.86 a	563.1 ab	509.2 bc
Low compost + lime (LCL)	13.93 a	2.09 a	951.9 a	360.5 c
High compost + lime (HCL)	26.11 a	1.66 a	689.4 ab	542.1 abc
Low compost + lime + bentonite (LCLB)	32.51 a	33.51 a	753.3 ab	444.6 bc
High compost + lime + bentonite (HCLB)	17.57 a	--†	424.3 b	456.8 bc

† No data

Table 2.9 Total Biomass at Site A and B. Means followed by the same letter are not statistically different at 0.10.

Treatment	Total Biomass ng/g	
	Site A	**Site B**
Control	1780.4 a	1853.3 a
Low compost	1684.5 a	1341.1 ab
High compost	1456.3 a	971.8 b
Low compost + lime	2117.4 a	669.3 b
High compost + lime	1734.1 a	1120.4 b
Low compost + lime + bentonite	1877.1 a	1150.3 b
High compost + lime + bentonite	861.2 a	651.5 b

Chapter 3 - Rehabilitation of an Abandoned Mine Site with Biosolids

3.1 Abstract

The abandoned lead (Pb) and zinc (Zn) mines in the Tri-State Mining District of Kansas, Missouri, and Oklahoma have left a legacy of environmental contamination. The waste materials are highly polluted, not only with Pb and Zn, but also cadmium (Cd), which often co-occurs geologically with Zn. In 2006, researchers at Kansas State University added amendments (compost, lime, and bentonite) to two sites at Galena, KS, part of the District, to see if they would change microbial properties. One site, called Site A, was on the outskirts of Galena, and the other site, Site B, was near the center of the town. Biosolids have never been applied to the mine waste materials at Galena to see if they would reduce availability of heavy metals. Therefore, in 2014 the plots established in 2006 were sampled and a greenhouse study was set up with sudex [*Sorghum bicolor* (L.) Moench x *S. Sudanese* (P.) Staph] to determine the effect of biosolids on heavy metal availability. Plants grew with and without biosolids in plastic pots (22 cm diam.; 22 cm height) and were watered with tap water during the experiment. Plant height was measured weekly. On days 110 and 111 after planting, roots, shoots, and heads with grain were harvested and analyzed for heavy metals. At the same time, the mine waste materials were analyzed for heavy metals, organic matter, nitrogen (N), and phosphorus (P). Because differences in concentrations of heavy metals due to the original treatments established in 2006 were not evident, concentrations were averaged together. However, Sites A and B were different. Site A had higher concentrations of the heavy metals than Site B. Plants grew better with biosolids than without biosolids, and they grew better on mine waste materials from Site B than Site A. Only the plants grown with biosolids produced heads. Plants grown without

biosolids were chlorotic and showed purple coloration, symptoms of Pb and Cd toxicity. The roots were highly polluted with Pb, Zn, and Cd, and the shoots less so. But the concentrations of Pb and Zn in the heads were within normal concentration ranges. Cadmium in the heads (0.7 mg kg^{-1}) was slightly elevated above normal levels (maximum normal, 0.2 mg kg^{-1}). Therefore, transfer of the heavy metals from the roots to heads was limited by the plant. At the end of the experiment, heavy metals, organic matter, and N in the mine waste materials with biosolids were similar to those without biosolids, but P was increased in the mine waste materials after the addition of biosolids. Thus, the biosolids increased P, an essential element for plant growth. In addition to promoting growth, the P seemed to be the element in the biosolids that reduced the availability of the heavy metals. The P apparently formed metal compounds that immobilized the heavy metals in the contaminated waste materials, so the sudex could not readily take them up. The results showed that the use of biosolids appears to be a promising method for rehabilitation of mine sites.

3.2 Introduction

Abandoned mine sites have left a legacy of contamination worldwide. The environmental problems associated with them are serious and global (Dybowska et al. 2006). The lead (Pb) and zinc (Zn) mines in the Tri-State Mining District of southeast Kansas, southwest Missouri, and northeast Oklahoma are such mines. The wastes from these mines have polluted groundwater, rivers, lakes, sediments, and soils (Abdel-Saheb et al. 1994; Carroll et al. 1998; Brown et al. 2004; Pierzynski and Gehl 2004; Schaider et al. 2007; Schwab et al. 2007; Juracek 2008; Pierzynski et al. 2010), as well as fish and mussels (Brumbaugh et al. 2005; Schmitt et al. 2005; Angelo et al. 2007). Methods to remediate the mine wastes are urgently needed (Johnson et al. 2016).

The Tri-State Mining District has a history of mining that goes back to the early 1800s, when Pb was mined by trappers and explorers for bullets (Pope 2005, p. 5; Baker 2008, p. 12-13). Commercial mining in this region began about 1850 (Gibson 1972, p. 14) and rapidly expanded after the Civil War (Gibson 1972, p. 26). Mining operations were first limited, because of the lack of adequate transportation (Gibson 1972, p. 24) and heavy machinery. However, after the Civil War, around 1870, railroads extended lines into the Tri-State District. In the late 1800s, small, individually owned surface mines were bought out by larger mining companies (Gibson 1972, p. 68), which further improved opportunities for development. From 1850 to 1950, the District was the world's leading producer of Pb and Zn concentrates, accounting for 50 per cent of the U.S.A.'s Zn production and 10 per cent of its Pb production (Gibson 1972, p. 266). The mines in the District equipped the United States so it could fight four major wars (Civil War, World War I, World War II, and the Korean War). Industry in the United States and abroad used the Pb and Zn concentrates from the District to produce munitions, bearings, castings, pipe, galvanized metals, batteries, chains, nails, and numerous other products (Gibson 1972, p. 266-267). The mines in the Tri-State Mining District lasted until 1970 (Pope 2005, p. 1; U.S. Environmental Protection Agency 2007). The District includes Galena, Kansas, where mines began to operate in 1876 (Pope 2005, p. 7). The century of mining operations in Galena has left Pb and Zn contamination throughout the city. The waste materials around the mines are highly polluted, not only with Pb and Zn, but also with cadmium (Cd), which often co-occurs geologically with Zn.

Despite the high standard of living brought to Americans by the products from the Tri-State mines (Gibson 1972, p. 266), the miners and local population endured health problems from the beginning of the mining. The miners succumbed to silicosis, or miners' consumption,

caused by breathing the flint dust produced by drilling and blasting (Gibson 1972, p. 182). It predisposed the miners and townspeople to tuberculosis. In 1940, Cherokee County in Kansas, where Galena is located, recorded more cases of tuberculosis than any other county in Kansas, and, in 1951, the county's death rate from tuberculosis was six times greater than for the rest of the state (Gibson 1972, p. 194). Residents of Galena have a higher incidence of kidney disease, heart disease, skin cancer, and anemia compared to residents in control towns (Neuberger et al. 1990). These results suggest that environmental agents in Galena are associated with the causation of several chronic diseases in the residents.

Adding amendments to allow plant growth has been suggested as one way to remediate mine wastes. Amendments have been applied to the waste materials in the Tri-State Mining District, and Pierzynski et al. (1994) review the early literature about them. Pierzynski et al. (2002) added cattle manure as a soil amendment to the mine tailings at Galena, to see if tall fescue (*Festuca arundinacea* Schreb.) would grow. After the first growing season, vegetative cover reached 71% but then steadily declined to 29% over the next two growing seasons. They attributed the poor growth to Zn toxicity.

Biosolids (sewage sludge) have often been used to remediate mine sites (Haering et al. 2000; Brown et al. 2005; Karathanasis et al. 2007; Stuczynski et al. 2007; Santibáñez et al. 2008; Sheoran et al. 2010; Madejón et al. 2012; Pepper et al. 2013; Mahar et al. 2015; Wijesekara et al. 2016). Biosolids are recommended for amelioration of degraded land, because they add nutrients, especially nitrogen and phosphorus, and organic matter to the soil for plant growth (Kirkham 1974; Lu et al. 2012). Recycling of biosolids to reclaim and revegetate areas disturbed by mining has long been promoted by the U.S. Environmental Protection Agency (U.S. Environmental Protection Agency 1989).

However, little work has been done using biosolids to remediate the mine waste materials in the Tri-State Mining District. Brown et al. (2007) added amendments, including lime-stabilized biosolids and composted biosolids, on tailings from the Tar Creek National Priorities List Superfund Site in Oklahoma to see if they would restore vegetation and reduce availability of heavy metals that contaminate the tailings (Pb, Zn, and Cd). Plots were seeded with Bermuda grass (*Cynodon dactylon* Pers.). Bioaccessible Pb in the tailings was measured using a physiologically based extraction test. The biosolids did not reduce bioaccessible Pb in the tailings. When diammonium phosphate fertilizer was added with the biosolids, bioaccessible Pb was reduced. In general, six months after the amendments were added, growth was poor due, in large part, to the high electrical conductivity of the tailings (9.0 dS m^{-1}). But 18 months after they were added, all plots supported plant growth. Brown et al. (2007) reported plant Cd and Zn in the Bermuda grass, they did not measure plant Pb.

Between 1998 and 2001, Brown et al. (2014) added biosolids plus lime to plots in Jasper County in southwestern Missouri, part of the Tri-State Mining District. They planted different grasses on the plots. They found that in 2012, 11-14 years after the amendments were added, dry matter of orchard grass (*Dactylis glomerata* L.), big bluestem (*Andropogon gerardii* Vitman), little bluestem (*Andropogon scoparius* Michx.), turkey foot (scientific name not given by Brown et al. 2014), Indian grass (*Sorghastrum nutans* L.), sideoats grama (*Bouteloua curtipendula* Michx.), and fescue (*Festuca* sp.) were increased due to the biosolids with lime. In 2012, the average plant dry weight with biosolids (336 Mg ha^{-1}) and lime (48 Mg ha^{-1}) was 46 g m^{-2}, while minimal or no plant growth occurred at the control sites with non-amended mine waste materials. Brown et al. (2014) reported Pb, Zn, and Cd in the grass leaves, but did not report the concentrations of heavy metals in roots or in heads with grain.

In 2006, researchers at Kansas State University (Baker et al. 2011) added amendments (compost, lime, and bentonite) to mine waste materials at Galena, to see if they would change their microbial properties. They found that only high levels of compost increased microbial activity. Biosolids have never been applied to the mine waste materials at Galena, to see if they would reduce availability of the heavy metals to plants. Therefore, we sampled the waste materials in the plots established by Baker et al. (2011) and set up a greenhouse study with sudex, a sorghum-sudan grass hybrid, to determine the effect of biosolids on the growth of the sudex and transfer of heavy metals from roots to shoots and then to heads.

3.3 Materials and Methods

The experiment was carried out between January and May, 2015, in a greenhouse at Kansas State University in Manhattan, KS (39º12'N, 96º35'W, 325 m above sea level) using mine waste materials from abandoned mines located at Galena, KS (37º5'N; 94º38'W; 275 m above sea level). On the soil survey map, the mapunit at the site location is 9975, labelled as dumps, mine (USDA, 2013). In 2006, Baker et al. (2011) established plots at two sites, called Site A and Site B, where mine waste materials had been collected and deposited on the surface for 100 years. The mine waste materials were a by-product in the initial processing of Zn- and Pb-containing ores. Both Site A and Site B were in the town of Galena and were 2 km apart (Fig. 3.1). Site B was near the center of the town and houses were around it, and Site A was on the outskirts of town and it had no buildings around it. Site A was established on 8 May 2006 and Site B on 12 May 2006. The sites were on level ground. Each experimental plot was 1 m x 2 m in size with three replications of seven different treatments, for a total of 21 plots at each site, or a total of 42 plots. Each plot had a galvanized steel border, 1 m x 2 m in size, to limit inter-plot contamination (Baker 2008, p. 138).

The seven treatments were (1) non-amended control plot; (2) a low compost treatment of 45 Mg ha^{-1}; (3) a high compost treatment of 269 Mg ha^{-1}; (4) low compost (45 Mg ha^{-1}) + lime as $Ca(OH)_2$ (11.2 Mg ha^{-1}); (5) high compost (269 Mg ha^{-1}) + lime as $Ca(OH)_2$ (11.2 Mg ha^{-1}); (6) low compost (45 Mg ha^{-1}) + lime as $Ca(OH)_2$ (11.2 Mg ha^{-1}) + bentonite applied at 50 g bentonite per kg compost; and (7) high compost (269 Mg ha^{-1}) + lime applied as $Ca(OH)_2$ (11.2 Mg ha^{-1}) + bentonite applied at 50 g bentonite per kg compost. The compost was composted beef (*Bos taurus*) manure, and the bentonite was a Wyoming bentonite obtained from Enviroplug Grout (Wyo-Ben, Inc., Billings, MT) (Baker, 2008, p. 138). Treatments were applied and mixed to a depth of 30 cm (Baker 2008, p. 138). Switchgrass (*Panicum virgatum* L.) was seeded on the plots on 26 May 2006. Switchgrass did not grow on the plots in 2006 due to the high salinity of the compost and lack of rainfall. In the fall of 2006, plots were seeded to annual ryegrass (*Lolium multiflorum* Lam.) as a winter cover crop, and the ryegrass was killed with Glyphosate in the spring of 2007, when the plots were re-seeded with switchgrass on 19 April 2007 (Baker 2008, p. 138-139). The plots were sampled for biomass 535 and 841 days after Day 0, which Baker (2008, p. 139) designated as 26 May 2006. These days were 12 Nov. 2007 and 14 Aug. 2008.

No more amendments were added to the plots between May, 2006, when the plots were established by Baker et al. (2011), and 18-19 Nov. 2014, when we sampled the plots 8.5 years after the amendments had been added. At that time in 2014, we scooped up the top 13 cm (5 in) of mine waste materials from each plot at Site A and Site B with a flat shovel and put them into 42 5-gallon (19-L) buckets with lids (Product Code 0 84305 3559 1, Home Depot, Atlanta, GA), one bucket for each plot. On 19 Nov. 2014, we brought the buckets back to Manhattan, KS, where the mine waste materials were laid out on brown paper in the greenhouse to dry. On 1

Jan. 2015, the mine waste materials were sieved using a sieve with 4 mm openings. On 13 Jan., 84 plastic pots (each 22 cm diam.; 22 cm height) were filled with the mine waste materials. On 13 Jan., liquid, aerobically digested biosolids from the Manhattan, Kansas, Wastewater Treatment Plant were obtained. On 14 Jan., 1000 mL tap water were added to each pot and each pot drained. On 21 Jan. and 22 Jan., 500 mL of the liquid biosolids were applied each day to the surface of 42 pots (half of the pots). The 1000 mL of biosolids that were added made a layer about 1 cm thick. The percent of dry solids of the biosolids was measured to be 2.35% following method described in New York State Department of Environmental Conservation (c. 1965, p. 218). On 26 Jan. and 27 Jan., 500 mL tap water were added each day to each pot that did not have biosolids, and the pots drained each day, because of the coarse nature of the mine waste materials, even though they had been sieved to 4 mm. I did not study the heavy metal content of the leachate. The purpose of the study was to monitor growth in the mine waste materials with and without biosolids. However, Wahla and Kirkham (2008) did study leachate from columns containing a Haynie very fine sandy loam soil treated with biosolids. The heavy metals in the biosolids only leached if the soil was saline. They did not leach from control columns.

On 28 Jan., 20 seeds of the forage crop sudex [*Sorghum bicolor* (L.) Moench x *S. sudanese* (Piper) Staph] (Chu and Kerr 1977; Summers et al. 2009) were planted in each of the 84 pots. We chose sudex because it is recommended for erosion control and to improve soil structure (Summers et al. 2009). On 17 Feb., the plants in each pot were thinned to 10 plants per pot. All pots had 10 plants except for nine pots. No plants germinated in two pots (both pots with mine waste material from the control plots, and one had biosolids and one did not have biosolids), and seven pots had between four and nine plants.

Between 30 Jan. and 15 May, the plants were kept pots capacity. The water content in the mine waste materials was monitored using inexpensive soil moisture meters (Faber et al. 1993). Due to the roughness of the mine waste materials, the rod on the meters broke, so two different types were used: Mini Moisture Tester (Luster Leaf Products, Inc., Woodstock, IL; Product Code 0 35307 01810 6) and HoldAll Moisture Meter (Panacea Products Corp., Columbus, OH; Product Code 0 70686 26002 9). Based on the measurements with the moisture meters, 500 mL tap water were usually added two times a week to each pot. Watering did not cause mine waste material splashed up on the plants. The water moved immediately into the mine waste materials due to their coarse nature.

During the experiment, the temperature and relative humidity were measured hourly between 9 Feb. and 21 April with a sensor for each in four boxes located in the southeast, southwest, northwest, and northeast corners of the greenhouse. The sensors were part of the Throckmorton Greenhouse Temperature Tracking System, an in-house built system. The sensors were hand-assembled by Arthur Selman, Network Specialist and Instructor at Kansas State University. Table 3.1 shows the average monthly day and night temperature and the average day and night relative humidity during the experiment at the four locations in the greenhouse. Pan evaporation rate between 28 Jan. and 15 May averaged 0.30 cm day^{-1}. Natural daylight was used during the experiment.

Throughout the experiment, the height of shoots was measured once a week by choosing at random 5 plants per pot. The height was measured from the surface of the mine waste materials to the tip of an extended leaf.

Plants were harvested on 18-19 May (110 and 111 days after planting) by cutting the culms just above the surface of the mine waste materials. Roots were thoroughly cleaned by

water. Heads with grain were removed, if a plant produced a head. Leaves and culms were combined and labelled "shoots," and they were put into paper bags. Fresh weight of the shoots was measured. Dry weights of the shoots were determined by drying them to constant weight at 70 ^{o}C. For the two pots that had no plants, their fresh and dry weights were recorded as zero. Roots were extracted by washing them in water to remove adhered mine waste materials. Because not all the roots were extracted, fresh and dry weights of the roots were not determined. The plant tissues were submitted to the Soil Testing Laboratory at Kansas State University for analyses.

The roots, shoots, and heads were digested using a nitric-perchloric acid digest (Kirkham 2000) and analyzed for P, K, Ca, Mg, Cd, Cu, Fe, Mn, Ni, Pb, and Zn using inductively coupled plasma-atomic emission spectroscopy (ICP-AES), also referred to as inductively coupled plasma-optical emission spectrometry (ICP-OES). Detection limits in mg L^{-1} for the ICP-AES were: Cd, 0.005; Cu, 0.003; Fe, 0.05, Mn, 0.003; Ni, 0.007, Pb, 0.003, and Zn, 0.003. These are the detection limits given by manufacturer for optimal conditions. The detection limits for the elements in mg kg^{-1} of the plant sample were calculated as follows. Each plant sample had about 0.25 g, and the sample volume was 50 mL; 50 mL/0.25 g = 200. Each detection limit given by the manufacturer was multiplied by 200. This gave detection limits for the plant samples in mg kg^{-1} as follows: Cd, 1.0; Cu, 0.6; Fe, 10.0, Mn, 0.6; Ni, 1.4, Pb, 0.6, and Zn, 0.6. For the major elements, the practical quantitation limit of the ICP-AES is 1 mg kg^{-1}. Quality assurance/quality control were done by duplicating 10% of the samples, and the standard came from the National Institute of Standards and Technology (NIST, SRM 1515, apple leaves).

For determination of total nitrogen in plant tissues, a salicylic-sulfuric acid digestion was used (Bremner and Mulvaney 1982, p. 621), and then the digest was analyzed for N by a

colorimetric procedure using the Rapid Flow Analyzer (Model RFA-300) and RFA Methodology No. A303-S072 from Alpkem Corporation, Clackamas, OR.

The mine waste materials were analyzed for chemical constituents when they were brought back from Galena, KS, in November, 2014, and at the end of the greenhouse experiment. When the mine waste materials were sampled at the end of the experiment, the contents of each pot were dumped onto brown paper and then all the contents of each pot were mixed up. For the pots with biosolids, the crust was mixed up into the mine waste materials. The samples were placed in brown bags, which were submitted to the Soil Testing Laboratory for analyses.

The mine waste materials were analyzed for total concentrations of the heavy metals using a nitric acid digest (Wahla and Kirkham 2008). Heavy metals in the mine waste materials were extracted using diethylenetriaminepentaacetic acid (DTPA) (Lindsay and Norvell 1978), and extractable concentrations were determined using the ICP-AES. Total P in the mine waste materials was determined in the same way as total N was determined for the plant samples (see above). Extractable P in the mine waste materials was determined using the Mehlich 3 test (Frank et al. 1998). The pH, electrical conductivity, and cation exchange capacity of the mine waste materials were determined using the methods described by Watson and Brown (1998), Whitney (1998), and Warncke and Brown (1998), respectively. Organic matter in the mine waste materials was determined using the loss of weight on ignition method described by Combs and Nathan (1998). Total nitrogen and total carbon in the mine waste materials, as well as total carbon in the heads, were determined using a LECO TruSpec CN Carbon/Nitrogen combustion analyzer, which reports total levels (inorganic and organic) of C and N on a weight percent basis, according to, for the mine waste materials, the TruSpec CN instrument method "Carbon and Nitrogen in Soil and Sediment," and, for plant tissue, the TruSpec CN instrument method

"Carbon, Hydrogen, and Nitrogen in Flour and Plant Tissue," both published by LECO Corporation, St. Joseph, MI, in 2005. After determination of total C and N in the mine waste materials, total organic carbon was determined, as follows. By pretreatment of a second LECO combustion sample with dilute phosphoric acid, carbon dioxide is released from calcium and magnesium carbonates in the mine waste materials, leaving only the total organic carbon present, which is then calculated.

The tap water used for watering the plants during the experiment was analyzed for pH, electrical conductivity, and elemental composition using the methods described above. The tap water had the following chemical characteristics: pH, 8.72; electrical conductivity, 0.40 dS m^{-1}; Ca, 23.51 mg kg^{-1}; K, 7.53 mg kg^{-1}; Mg, 14.54 mg kg^{-1}; Na, 45.02 mg kg^{-1}; and Cu, 0.01 mg kg^{-1}. Cadmium, Fe, Mn, Ni, Pb, and Zn were below detection levels (less than 0.01 mg kg^{-1}) in the tap water.

The biosolids were analyzed after they were collected on 13 Jan. 2015. They were oven dried at 105 ^{o}C for 24hr, and the sample was submitted to the Soil Testing Laboratory. It was analyzed for total concentrations of the heavy metals, pH, organic matter, and total P using the same methods that were used for the mine waste materials. The biosolids sample had the following chemical characteristics: pH, 4.65; organic matter, 59.90%; total P, 3.40%; Cd, 9.1 mg kg^{-1}; Cu, 361.3 mg kg^{-1}; Fe, 3850.4 mg kg^{-1}; Mn, 90.1 mg kg^{-1}; Ni, 1.6 mg kg^{-1}; Pb, 13.1 mg kg^{-1}, and Zn, 577.0 mg kg^{-1}. United States EPA limits for heavy metals in biosolids in mg kg^{-1} are as follows: Cd, 39; Cu, 1500; Ni, 420; Pb, 300; Zn, 2800. The EPA sets no limits for Fe and Mn.

Another sample of the biosolids from the Manhattan, Kansas, Wastewater Treatment Plant was obtained on 20 June 2016, and a wet sample was submitted to the Soil Testing

Laboratory for analysis of pH (Watson and Brown 1998), electrical conductivity (Whitney 1998), total suspended solids, total N, and total P. Total suspended solids were determined by filtering the biosolids through a 0.45 micron filter using a vacuum. The dry weight of the filter member was measured before and after filtration. The total suspended solids were calculated as mg L^{-1} (Csuros 1997). The total N and P in the liquid sample were determined by taking a 10 mL sample, which was then digested with a potassium persulfate reagent (Nelson 1987) in an autoclave and then analyzed according to Hosomi and Sudu (1986). The 2016 analyses showed that the wet biosolids had a pH of 6.10, an electrical conductivity of 1.75 dS m^{-1}, 18,200 mg L^{-1} total suspended solids, total N of 825.11 mg kg^{-1}, and total P of 685.52 mg kg^{-1}. An electrical conductivity less than 2 dS m^{-1} has negligible effects on crop growth (Bernstein, 1964). Suspended solids refer to small solid particles that remain in suspension in the liquid biosolids. The smaller the number the better the biosolids are digested. Nitrogen and P as documented in the literature are given in the next paragraph. The sample obtained 20 June 2016 was dried and extractable and total concentrations of the heavy metals were determined using the methods used on the mine waste materials. Extractable concentrations in mg kg^{-1} were: Cd, 1.2; Cu, 96.5; Fe, 536.7; Mn, 79.7; Ni, 10.8; Pb, 7.4; and Zn, 406.6. Total concentrations in mg kg^{-1} were: Cd, 1.1; Cu, 314.6; Fe, 6072.3; Mn, 165.1; Ni, 13.2; Pb, 14.0; and Zn, 442.5.

On a long-term basis (1995-2014), the Manhattan biosolids have 2.5% by weight total solids; 1053.9 mg kg^{-1} Kjeldahl N on a wet-weight basis; 44,143.4 mg kg^{-1} total Kjeldahl N on a dry-weight basis; and 25,153.9 mg kg^{-1} total P on a dry-weight basis. In 2015, the Manhattan biosolids were analyzed by the city four times (March, May, Oct., and Nov.), and the average of the four analyses showed that the biosolids had 3.8% by weight total solids; 1814.1 mg kg^{-1} Kjeldhal N on a wet-weight basis; 48,575.0 mg kg^{-1} total Kjeldhal N on a dry-weight basis; and

30,800.0 mg kg^{-1} total P on a dry-weight basis (Dr. Abdu Durar, Water and Wastewater Division, Manhattan, KS, personal communication, 22 June 2016). The concentrations of N and P in the biosolids are similar to those reported in the literature (Peterson et al. 1972; Dean and Smith 1973; Vesilind 1975, p. 23). On a dry weight basis, biosolids have between 1.8 and 6.4% N and 0.8 and 3.9% P.

The greenhouse had three benches oriented in the east-west direction. The door to the greenhouse, located on an interior hallway, was on the north wall of the greenhouse, which had a cooling pad. The south wall of the greenhouse had two fans and windows that faced outside. Near the ceiling of the greenhouse was a large plastic tube, about 80 cm in diameter, with holes through which air was pushed out to ventilate the greenhouse. The tube ran from the north wall to the south wall of the greenhouse. At the beginning of the experiment, the pots with the mine waste materials from the two sites and the three replications established by Baker et al. (2011) were placed on the greenhouse benches as follows:

Bench near north wall of greenhouse:

West side of bench: Site A, Replication 2

East side of bench: Site B, Replication 1

Bench in middle of greenhouse:

West side of bench: Site B, Replication 3

East side of bench, Site A, Replication 1

Bench near south wall of greenhouse:

West side of bench: Site A, Replication 3

East side of bench: Site B, Replication 2

Pots with the seven original treatments of Baker et al. (2011) were placed randomly in a row. Pots with biosolids were lined up on the north side of each bench and the pots without biosolids were lined up on the south side of each bench. Therefore, on each half of a bench, there were two rows of seven pots.

On Mondays, Wednesdays, and Fridays of each week during the experiment, the pots were rotated. In each row of seven pots of a replication, either with or without biosolids, the pot at the eastern side was put in the location of the pot at the western side. Then each pot in a row was moved one pot toward the east. Consequently, each pot had a new position in the greenhouse three times a week.

The experimental design of Baker et al. (2011) was a complete block with treatment as the main factor at each site. They separated the sites (Site A and Site B) due to a significant site by treatment interaction ($p \leq 0.05$) for all measurements. We also analyzed the sites separately. The experiment was a randomized complete block with a split-plot design, in which site was the fixed blocking factor (whole plot treatment factor) for locations within sites (whole plot experimental units) and biosolids' methods was the fixed split plot treatment factor. There were a total of 84 pots (2 sites; 7 original treatments; 3 sample locations within a site; and 2 biosolids' methods, i.e. with and without biosolids). Because differences in measurements taken from plots from the seven original treatments established by Baker et al. (2011) generally were not significant at 0.05, the seven treatments were averaged together. Appendix B shows the statistical analyses for the seven individual treatments. After averaging the 7 original treatments, the observations were reduced to 12 records. Statistical analyses were performed using PROC GLIMMIX of SAS Version 9.4 (Statistical Analysis System 2013). Least Square Means of

biosolids' methods (with or without biosolids) were compared at the 0.05 level of significance within each site.

3.4 Results and Discussion

As noted in the description of the statistical analysis (previous paragraph), differences in measurements taken from plots from the seven original treatments established by Baker et al. (2011) generally were not significant. This was true both for the measurements taken on the mine waste materials and on the plants. If differences did occur among treatments, they were not consistent. The measurements taken on plots with the amendments did not always have a lower or higher value than those from the control plots. Therefore, 8.5 years after the amendments were added, their effects were no longer evident, based on our measurements. Baker et al. (2011) concluded that large amounts of organic matter were needed to support biomass in the mine waste materials over the two-year period that they studied. Their results implied that their amendments would have to be added year after year to sustain growth on the mine waste materials. Gudichuttu (2014) suggested that high amounts of compost would be needed to maintain long term sustainability of plants on the plots of Baker et al. (2011). In contrast to these results, differences among the treatments have been observed even eight years after Baker et al. (2011) added their treatments. Hettiarachchi et al. reported in Wijesekara et al. (2016) that eight years after the amendments were added, the high compost treatment had higher microbial activity than the other treatments.

The mine waste materials at both Site A and Site B were highly contaminated with Pb, Zn, and Cd (Table 3.2). They had at least 10 times more Pb, Zn, and Cd than non-contaminated soils. Total concentrations of these heavy metals in non-contaminated soils range from 2 to 200 mg kg^{-1} for Pb, 10 to 300 mg kg^{-1} for Zn, and 0.01 to 0.7 mg kg^{-1} for Cd (Kirkham 2008). In

non-contaminated soils, extractable concentrations range from 0.05-46 mg kg^{-1} for Pb, 0.01 to 200 for Zn, and 0.01 to 0.5 mg kg^{-1} for Cd (Kirkham 2008). Total and extractable concentrations of Cu, Mn, and Ni in the mine waste materials were within normal concentration ranges. Total concentrations of Cu, Mn, and Ni in soils range from 2 to 200 mg kg^{-1}, 100 to 4000 mg kg^{-1}, and 5 to 5000 mg kg^{-1}, respectively (Kirkham 2008). Extractable concentrations of Cu, Mn, and Ni in soils range from 0.002-19.2 mg kg^{-1}, 0.001 to 4.8 mg kg^{-1}, and 0.01 to 403 mg kg^{-1}, respectively. The element Fe is abundant in soils, the amount ranging from 200 mg kg^{-1} to at least 10% (Sauchelli 1969, p. 40). Norrish (1975) gives an average concentration of Fe in soils, based on data from many different references, as 30,000 mg kg^{-1}. Therefore, the Fe in the mine waste materials was within normal ranges. The electrical conductivities of the mine waste materials at both Site A (0.21 dS m^{-1}) and Site B (0.32 dS m^{-1}) were low. At 0 to 2 dS m^{-1} (or 0 to 2 mmhos cm^{-1}), salinity effects are mostly negligible on crops (Bernstein 1964).

Plants grown with biosolids grew taller than plants grown without biosolids (Fig. 3.2). Plants grown on mine waste materials from Site B grew taller than plants grown on mine waste materials from Site A. At Site A and Site B, the shoots of the plants that grew with biosolids produced 5 and 8 times more fresh weight, and 7 and 13 times more dry weight, respectively, than shoots of plants without biosolids (Table 3.3). Roots in pots with biosolids grew to the bottom of the pots and penetrated the entire volume of the pots. Roots in pots without biosolids were short and were only in the surface of the pots. Only plants grown with biosolids produced heads with grain.

In addition to being stunted, the plants grown without biosolids were chlorotic and showed purple coloration. The symptoms were similar to photographs of toxicities caused by Pb and Cd (Dr. Douglas J. Jardine, Professor, Department of Plant Pathology, Kansas State

University, personal communication, 13 May 2015). Hassett et al. (1976) found that radicle elongation of soil-grown corn (*Zea mays* L.) seedlings was depressed by concentrations of 25 mg Cd kg^{-1} of soil or 250 mg Pb kg^{-1} of soil when the metals were added singly. But when Pb and Cd were added in combination, inhibition of radicle elongation occurred at lower concentrations. The effect of the metals when added in combination was greater than the sum of the effects when the metals were added singly. This shows that growth is more reduced when two toxic heavy metals are present compared to one. The fact that Pb, Zn, and Cd were all elevated in the mine waste materials was a reason why they had an extremely deleterious effect on growth of the sudex without biosolids. As will be discussed later, the phosphorus in the biosolids appeared to immobilize the heavy metals, which allowed the plants with biosolids to grow tall and to maturity.

Roots at both Site A and Site B were highly contaminated with Pb, Zn, and Cd, but the contamination was less at Site A than at Site B (Table 3.4). Concentrations of these heavy metals far exceeded normal concentrations. The maximum concentrations of Pb, Zn, and Cd in plants grown under non-contaminated conditions are 5.0, 150, and 0.20 mg kg^{-1}, respectively (Liphadzi and Kirkham 2006). Except for Mn in roots with and without biosolids at Site A, Cu, Fe, Mn, and Ni were elevated above normal levels in the roots. Normal maximum concentrations of Cu, Fe, Mn, and Ni in plants are 15, 300, 100, and 1.0 mg kg^{-1}, respectively (Liphadzi and Kirkham 2006).

Concentrations of the heavy metals in the shoots were less than in the roots (Table 3.4). Concentrations of Cu and Mn in all shoots were within normal ranges. Concentrations of Cd, Fe, Ni, Pb, and Zn in the shoots were higher than those normally found in plants.

Except for Ni at Site A and Cd at both Sites A and B, concentrations of the heavy metals in the heads of plants were within normal concentration ranges (Table 3.4). Ni was only slightly elevated above normal levels in the heads at Site A (1.4 mg kg^{-1} versus 1.0 mg kg^{-1} for the normal maximum concentration). Even though the roots and shoots were highly contaminated with Pb and Zn, the concentrations of these heavy metals were within normal concentration ranges in the heads.

Other studies have shown that limited movement of heavy metals through plants offers a method to reduce their toxicity. Kirkham (1975) found that roots of corn grown in plots that had been treated for 35 years with biosolids contained high concentration of heavy metals, but only Cd and Cu were elevated in the leaves, and the grain had normal concentrations of heavy metals.

Cadmium was the heavy metal that was elevated above normal levels in the heads, especially at Site A. Site A and B had 2.2 and 0.7 mg kg^{-1} Cd in heads, respectively, and the normal limit for Cd in plants is 0.2 mg kg^{-1}. Unlike Pb, which is highly immobile in plants (Liphadzi and Kirkham 2006), Cd is known to be mobile in plants and move in the transpiration stream (Jaakkola and Yläranta 1976). Both the sudex leaves and heads could not be used for forage, because of the elevated Cd. Other studies have shown that Cd is the heavy metal of most concern in plants that are eaten (Kirkham 1974; Liphadzi and Kirkham 2006; Clemens and Ma 2016).

Concentrations of N, P, K, and Mg in the roots, shoots, and heads were within normal concentration ranges (Table 3.5). Normal concentration ranges for N and K are 0.5 to 5%, and for P and Mg they are 0.1 to 1% (Liphadzi and Kirkham 2006). Normal concentration ranges for Ca in plants range from 0.5 to 5%. Calcium was low in the roots grown with and without biosolids at both Sites A and B.

In general, at the end of the experiment total concentrations of the heavy metals in the mine waste materials both with and without biosolids (Table 3.6) were similar to those at the beginning of the experiment (Table 3.2). Also, at the end of the experiment extractable concentrations of the heavy metals in the mine waste materials both with and without biosolids were similar to those at the beginning of the experiment. The Fe and Mn in biosolids affects the availability of heavy metals like Cd (Hettiarachchi et al., 2003; Hettiarachchi et al., 2006). However, in my experiment I saw no differences in total concentration of Fe and Mn in mine waste materials with and without biosolids except at Site B, where, the mine waste materials with biosolids had a lower concentration of Mn than those without biosolids.

At both Sites A and B with and without biosolids, the electrical conductivities of the mine waste materials at the end of the experiment (Table 3.7) were greater than at the beginning of the experiment (Table 3.2). At both Site A and Site B, the waste materials with biosolids had a higher electrical conductivity than those without biosolids (Table 3.7). However, the electrical conductivity of the mine waste materials with biosolids was still low (c. 1 dS m^{-1}) and below the threshold when electrical conductivity begins to decrease growth of salt-sensitive crops (2 dS m^{-1}) (Bernstein 1964).

Both with and without biosolids, soil organic matter at the end of the experiment (Table 3.7) was greater than that at the beginning of the experiment (Table 3.2). The increase may be due to the roots that were present in the soil at the end of the experiment. Total N was not changed during the experiment (compare Tables 3.2 and 3.7). At Site A, total N was slightly increased by the addition of biosolids, but it was not increased at Site B (Table 3.7). Usually, biosolids add N to soil (Kirkham 1974), but this was evident only at Site A. Therefore, the

increase in growth of the plants grown with biosolids was probably not due to differences in N between the pots with biosolids and the pots without biosolids.

At the end of the experiment, total C and total organic C at both Site A and Site B were increased due to the presence of biosolids (Table 3.7). Digested biosolids are outstanding in their ability to increase the organic content of soils (Kirkham 1974), and this was evident in our experiment. Except for total organic C at Site B, total C and total organic C were higher at the end of the experiment than the beginning of the experiment (Tables 3.2 and 3.7). Karna. (2014) found that OC immobilized Pb and Zn. The C also increases aggregation, which makes the mine waste materials a better medium for plant growth. For both Sites A and B without biosolids, total P and total extractable P in the mine waste materials were slightly higher at the end of the experiment than at the beginning of the experiment (Tables 3.2 and 3.7). At both Site A and Site B, total P and extractable P were increased after the addition of biosolids (Table 3.7), thus, the biosolids increased P which was needed for plant growth. The P added by the biosolids also may have reduced the availability of the heavy metals. It has been known for a long time that P is effective in reducing heavy metal availability in soils (Chaney 1973; Kirkham 1977). Many studies have shown that P can stabilize heavy metals like Pb in soil (Hettiarachchi et al. 2001; Hettiarachchi and Pierzynski 2002; Hettiarachchi et al. 2003; Baker et al. 2014). A patented method for immobilization of metal availability in contaminated soils depends upon the addition of P (Pierzynski and Hettiarachchi 2002). The method is particularly useful for reducing the bioavailability of Pb and Group IIB metals (e.g., Zn, and Cd) and Group VIII metals (e.g., Fe and Ni). Phosphorus can be added to waste materials, to decrease the bioavailability of a metal contaminant. It forms irreversibly adsorbed metals. Phosphorus reacts with the heavy metals to form insoluble metal phosphates. It makes the metal contaminant non-bioavailable. Our results

agree with those of Brown et al. (2007), who found that diammonium phosphate fertilizer reduced bioaccessible Pb in tailings on a site in Oklahoma in the Tri-State Mining District.

3.5 Conclusion

In conclusion, the increased growth of the plants grown with biosolids appeared to be due to the total C, total organic C, and P that they added to the mine waste materials. The OC apparently immobilized the Pb and Zn. The P not only was an essential nutrient, but it also may have bound the heavy metals and made them less available for uptake. The results suggest that biosolids, which are readily available from any town and continually produced, should be added to mine waste materials to revegetate the degraded land.

3.6 Acknowledgments

King Saud University in Riyadh, Saudi Arabia, funded the research assistantship of the senior author. We thank the following people: Dr. Yuxin (Jack) He and Ms. Cathryn Davis for helping to get the mine waste materials; Mr. Mosaed A. Majrashi for help throughout the experiment; Ms. Terri L. Branden, Facilities Maintenance Supervisor, Plant Sciences Greenhouse Complex, for help in the greenhouse during the experiment; Mr. Arthur Selman for constructing the temperature and humidity sensors used in the greenhouse; Mr. Jay Yaege, Laboratory Manager, Manhattan, KS, Wastewater Treatment Plant, for supplying the biosolids; Dr. Abdu Durar, Environmental Compliance Manager, City of Manhattan, Public Works Department, Water and Wastewater Division, Manhattan, KS, for information on the N and P in the biosolids; Ms. Zhining Ou, statistical consultant in the Statistics Laboratory, Kansas State University, for help with the statistical analyses; and Ms. Kathleen M. Lowe and Mr. Jacob (Jake) A. Thomas in the Soil Testing Laboratory at Kansas State University for doing the analyses, which were paid for by two awards to M.B. Kirkham (Dr. Ron and Rae Iman

Outstanding Faculty Award and the Higuchi-University of Kansas Endowment Research Achievement Award) and by Hatch Grant No. 371047 to M.B. Kirkham.

3.6 References

Abdel-Saheb, I., A.P. Schwab, M.K. Banks, and B.A. Hetrick. 1994. Chemical characterization of heavy-metal contaminated soil in southeast Kansas. *Water, Air, Soil Pollution* 78:73-82.

Angelo, R.T., M.S. Cringan, D.L. Chamberlain, A.J. Stahl, S.G. Haslouer, and C.A. Goodrich. 2007. Residual effects of lead and zinc mining on freshwater mussels in the Spring River Basin (Kansas, Missouri, and Oklahoma, USA). *Sci. Total Environ.* 384: 467-496.

Baker, L.R. 2008. *In situ* remediation of Pb/Zn contaminated materials: Field- and molecular-scale investigations. PhD Diss., Kansas State University, Manhattan. xxxvi + 357pp.

Baker, L.R., P.M. White, and G.M. Pierzynski. 2011. Changes in microbial properties after manure, lime, and bentonite application to a heavy metal-contaminated mine waste. *Appl. Soil Ecology* 48: 1-10.

Baker, L.R., G.M. Pierzynski, G.M. Hettiarachchi, K.G. Scheckel, and M. Newville. 2014. Micro-X-ray fluorescence, micro-X-ray absorption spectroscopy, and micro-X-ray diffraction investigation of lead speciation after the addition of different phosphorus amendments to a smelter-contaminated soil. *J. Environ. Quality* 43: 488-497.

Bernstein, L. 1964. *Salt Tolerance of Plants.* Agriculture Information Bulletin No. 283. U.S. Department of Agriculture, Washington, DC, 23pp.

Bremner, J.M., and C.S. Mulvaney. 1982. Nitrogen-total, pp. 595-624. In Page, A.L., Miller, R.H., and Keeney, D.R., Eds., *Methods of Soil Analysis. Part 2. Chemical and*

Microbiological Properties. Madison, 2nd edn. Madison, WI: American Society of Agronomy and Soil Science Society of America, pp. 595-624.

Brown, S., R. Chaney, J. Hallfrisch, J.A. Ryan, and W.R. Berti. 2004. In situ soil treatments to reduce the phyto- and bioavailability of lead, zinc, and cadmium. *J. Environ. Quality* 33: 522-531.

Brown, S., M. Sprenger, A. Maxemchuk, and H. Compton. 2005. Ecosystem function in alluvial tailings after biosolids and lime addition. *J. Environ. Quality* 34: 139-148.

Brown, S.L., H. Compton, and N.T. Basta. 2007. Field test of in situ soil amendments at the Tar Creek National Priorities List Superfund Site. *J. Environ. Quality* 36: 1627-1634.

Brown. S., Mahoney, M., Sprenger, M. 2014. A comparison of the efficacy and ecosystem impact of residual-based and topsoil-based amendments for restoring historic mine tailings in the Tri-State mining district. *Sci. Total Environ.* 485-486: 624-632.

Brumbaugh, W.G., C.J. Schmitt, and T.W. May. 2005. Concentrations of cadmium, lead, and zinc in fish from mining-influenced waters of northeastern Oklahoma: Sampling of blood, carcass, and liver for aquatic biomonitoring. *Arch. Environ. Contam. Toxicol.* 49: 76-88.

Carroll, S.A., P.A. O'Day, and M. Piechowski. 1998. Rock-water interactions controlling zinc, cadmium, and lead concentration in surface waters and sediments, U.S. Tri-State Mining District. 2. Geochemical interpretation. *Environ. Sci. Technol.* 32: 956-965.

Chaney, R.L. 1973. Crop and food chain effects of toxic elements in sludges and effluents. In *Proceedings of the Joint Conference on Recycling Municipal Sludges and Effluents on Land*. Washington, DC: National Association of State Universities and Land-Grant Colleges, pp. 129-141.

Chu, A.C.P., and J.P. Kerr. 1977. Leaf water potential and leaf extension in a sudax crop. *New Zeal. J. Agric. Res.* 20: 467-470.

Clemens, S., and J.F. Ma. 2016. Toxic heavy metal and metalloid accumulation in crop plants and foods. *Annu. Rev. Plant Biol.* 67: 489-512.

Combs, S.M., and M.V. Nathan. 1998. Soil organic matter. In Brown, J.R., Ed., *Recommended Chemical Soil Test Procedures for the North Central Region*. SB 1001. Columbia, MO: Missouri Agricultural Experiment Station, pp. 53-58.

Csuros, M. 1997. *Environmental Sampling and Analysis Lab Manual*. Boca Raton, FL: Lewis Publishers, CRC Press.

Dean, R.B., and J.E. Smith, Jr. 1973. The properties of sludges. In *Proceedings of the Joint Conference on Recycling Municipal Sludges and Effluents on Land*. Washington, DC: National Association of State Universities and Land-Grant Colleges, pp. 39-47.

Dybowska, A., M. Farago, E. Valsami-Jones, and I. Thornton. 2006. Remediation strategies for historical mining and smelting sites. *Sci. Progress* 89: 71-138.

Faber, B., J. Downer, and L. Yates. 1993. Portable soil moisture meters. *HortTechnology* 3: 195-197.

Frank, K., D. Beegle, and J. Denning. 1998. Phosphorus. In J.R. Brown, J.R., Ed., *Recommended Chemical Soil Test Procedures for the North Central Region*. SB 1001. Columbia, MO: Missouri Agricultural Experiment Station, pp. 21-26.

Gibson, A.M. 1972. *Wilderness Bonanza-The Tri-State District of Missouri, Kansas, and Oklahoma*. Norman, OK: University of Oklahoma Press, 362pp.

Gudichuttu, V. 2014. Phytostabilization of multi-metal contaminated mine waste materials: long-term monitoring of influence of soil amendments on soil properties, plants, and

biota and the avoidance response of earthworms. MS Thesis., Kansas State University, Manhattan. v + 173 pp.

Haering, K.C., W.L. Daniels, and S.E. Feagley. 2000. Reclaiming mined lands with biosolids, manures, and papermill sludges. In Barnhisel, R.I., Darmody, R.G., and Daniels, W.L., Eds., *Reclamation of Drastically Disturbed Lands*. Madison, WI: American Society of Agronomy, Crop Science Society of America, and Soil Science Society of America, pp. 615-644.

Hassett, J.J., J.E. Miller, and D.E. Koeppe. 1976. Interaction of lead and cadmium on maize root growth and uptake of lead and cadmium by roots. *Environ. Pollution* 11: 297-302.

Hettiarachchi, G.M., and G.M. Pierzynski. 2002. In situ stabilization of soil lead using phosphours and manganese oxide: Influence of plant growth. *J. Environ. Quality* 31: 564-572.

Hettiarachchi, G.M., G.M. Pierzynski, and M.D. Ransom. 2001. In situ stabilization of soil lead using phosphorus. *J. Environ. Quality* 30: 1214-1221.

Hettiarachchi, G.M., G.M. Pierzynski, F.W. Oehme, O. Sonmez, and J.A. Ryan. 2003. Treatment of contaminated soil with phosphorus and manganese oxide reduces lead absorption by Sprague-Dawley rats. *J. Environ. Quality* 32: 1335-1345.

Hettiarachchi, G.M., J.A. Ryan, R.L. Chaney, and C.M. La Fleur. 2003. Sorption and desorption of cadmium by different fractions of biosolids-amended soils. *Journal of Environmental Quality* 32:1684-1693.

Hettiarachchi, G. M., Scheckel, K. G., Ryan, J. A., Sutton, S. R., and M. Newville. 2006. μ-XANES and μ-XRF investigations of metal binding mechanisms in biosolids. *Journal of environmental quality*, *35*(1), 342-351.

Hosomi, M., and R. Sudu. 1986. Simultaneous determination of total nitrogen and total phosphorus in freshwater samples using persulfate digestion. *Int. J. Environ. Studies* 27: 267-275.

Jaakkola, A., and T. Yläranta. 1976. The role of the quality of soil organic matter in cadmium accumulation in plants. *J. Sci. Agric. Soc. Finland* 48: 415-425.

Johnson, A.W., M. Gutiérrez, D. Gouzie, and L.R. McAliley. 2016. State of remediation and metal toxicity in the Tri-State Mining District, USA. *Chemosphere* 144: 1132-1141.

Juracek, K.E. 2008. Sediment storage and severity of contamination in a shallow reservoir affected by historical lead and zinc mining. *Environ. Geol.* 54: 1447-1463.

Karna, R. R. 2014. Mechanistic understanding of biogeochemical transformations of trace elements in contaminated minewaste materials under reduced conditions (Doctoral dissertation, Kansas State University).

Karathanasis, A., C. Johnson, and C. Matocha. 2007. Subsurface transport of heavy metals mediated by biosolid colloids in waste-amended soils. In Frimmel, F.H., von der Kammer, F., and Flemming, H.-C., Eds., *Colloidal Transport in Porous Media*. Berlin: Springer Verlag, pp. 175-201.

Kirkham, M.B. 1974. Disposal of sludge on land: Effect on soils, plants, and ground water. *Compost Sci.* 15(2):6-10.

Kirkham, M.B. 1975. Trace elements in corn grown on long-term sludge disposal site. Environ. Sci. Technol. 9: 765-768.

Kirkham, M.B. 1977. Trace elements in sludge on land: Effect on plants, soils, and ground water. In Loehr, R.C., Ed., *Land as a Waste Management Alternative*. Ann Arbor, MI: Ann Arbor Science, pp. 209-247.

Kirkham, M.B. 2000. EDTA-facilitated phytoremediation of soil with heavy metals from sewage sludge. *Int. J. Phytoremediation* 2: 159-172.

Kirkham, M.B. 2008. Trace elements. In Chesworth, W., Ed., *Encyclopedia of Soil Science*. Encyclopedia of Earth Sciences Series, Dordrecht, the Netherlands: Springer, pp. 786-790.

Lindsay, W.L., and W.A. Norvell. 1978. Development of a DTPA soil test for zinc, iron, manganese, and copper. *Soil Sci. Soc. Amer. J.* 42: 421-428.

Liphadzi, M.S., and M.B. Kirkham. 2006. Physiological effects of heavy metals on plant growth and function. In Huang, B., Ed., *Plant-Environment Interactions*. 3rd edn. Boca Raton, FL: CRC Press, Taylor and Francis Group, pp. 243-269.

Lu, Q., Z. L. He, and P.J. Stoffella. 2012. Land application of biosolids in the USA: A review. *Appl. Environ. Soil Sci.* Vol. 2012, Article ID 201462, 11 pp., doi: 10.1155/2012/201462.

Madejón, E., A.I. Doronila, P. Madejón, A.J.M. Baker, and I.E. Woodrow. 2012. Biosolids, mycorrhizal fungi and eucalypts for phytostabilization of arsenical sulphidic mine tailings. *Agroforestry Syst.* 84: 389-399. doi: 10.1007/s10457-012-9484-x.

Mahar, A., P. Wang, R. Li, and Z. Zhang. 2015. Immobilization of land and cadmium in contaminated soil using amendments: A review. *Pedosphere* 25: 555-568.

Nelson, N.S. 1987. An acid-persulfate digestion procedure for determination of phosphorus in sediments. *Commun. Soil Sci. Plant Anal.* 18: 359-369.

New York State Department of Environmental Conservation, c. 1965. *Manual of Instruction for Sewage Treatment Plant Operators*. Albany, NY: New York State Department of Environmental Conservation, 247pp.

Neuberger, J.S., Mulhall, M., Pomatto, M.C., Sheverbush, J., Hassanein, R.S. (1990). Health problems in Galena, Kansas: A heavy metal mining superfund site. *Sci. Total Environ.* 94: 261-272.

Norrish, K. 1975. Geochemistry and mineralogy of trace elements. In Nicholas, D.J.D. and Egan, A.R., Eds., *Trace Elements in Soil-Plant-Animal Systems.* New York: Academic Press, pp. 55-81.

Pepper, I.L., H.G. Zerzghi, S.A. Bengson, and E.P. Glenn. 2013. Revegetation of copper mine tailings through land application of biosolids: Long-term monitoring. *Arid Land Res. Manage.* 27: 245-256. doi: 10.1080/15324982.2012.719578.

Peterson, J.R., C. Lue-Hing, and D.R. Zenz. 1973. Chemical and biological quality of municipal sludge. In W.E. Sopper, W.E. and Kardos, L.T., Eds., *Recycling Treated Municipal Wastewater and Sludge through Forest and Croplands*. University Park, PA: The Pennsylvania State University Press, pp. 26-37.

Pierzynski, G.M., and G.M. Hettiarachchi. 2002. Method of in-situ immobilization and reduction of metal bioavailability in contaminated soils, sediments, and wastes. *United States Patent No. 6,383,128*. Alexandria, VA: U.S. Patent and Trademark Office.

Pierzynski, G.M., and K.A. Gehl. 2004. An alternative method for remediating lead-contaminated soils in residential areas: A decision case study. *J. Natural Resourc. Life Sci. Educ.* 33: 63-69.

Pierzynski, G.M., J.L. Schnoor, M.K. Banks, J.C. Tracy, L.A. Licht, and L.E. Erickson. 1994. Vegetative remediation at Superfund Sites. In Hester, R.E. and Harrison, R.M., Eds., *Mining and Its Environmental Impact. Issues in Environmental Science and Technology 1*, Cambridge: Royal Society of Chemistry, pp. 49-69.

Pierzynski, G.M., Lambert, M., Hettrick, B.A.D., Sweeney, D.W., Erickson, L.E. 2002. Phytostabilization of metal mine tailings using tall fescue. *Practice Periodical Hazardous Toxic Radioact. Waste Manage.* 6: 212-217.

Pierzynski, G.M., L.R. Baker, G.M. Hettiarachchi, K.G. Scheckel, V. Gudichuttu, and R. Pannu. 2010. The Tri-State Mining Region USA: Twenty years of trace element research. In *19th World Congress of Soil Science, Soil Solutions for a Changing World*, 1-6 August 2010, Brisbane, Australia: International Union of Soil Science, pp. 254-256. (Published on DVD).

Pope, L.M. 2005. *Assessment of Contaminated Streambed Sediment in the Kansas Part of the Historic Tri-State Lead and Zinc Mining District, Cherokee County, 2004*. USGS Scientific Investigations Report 2005-5251. Reston, VA: U.S. Geological Survey, 61pp.

Santibáñez, C., C. Verdugo, and R. Ginocchio. 2008. Phytostabilization of copper mine tailings with biosolids: Implications for metal uptake and productivity of *Lolium perenne*. *Sci. Total Environ.* 395: 1-10.

Sauchelli, V. 1969. *Trace Elements in Agriculture*. New York: Van Nostrand Reinhold, 248 pp.

Schaider, L.A., D.B. Senn, D.J Brabander, K.D. McCarthy, and J.P. Shine. 2007. Characterization of zinc, lead, and cadmium in mine waste: Implications for transport, exposure, and bioavailability. *Environ. Sci. Technol*. 41: 4164-4171.

Schmitt, C.J., J.J. Whyte, W.G. Brumbaugh, and D.E. Tillitt. 2005. Biochemical effects of lead, zinc, and cadmium from mining on fish in the Tri-States District of northeastern Oklahoma, USA. *Environ. Toxicol. Chem*. 24: 1483-1495.

Schwab, P., D. Zhu, and M.K. Banks. 2007. Heavy metal leaching from mine tailings as affected by organic amendments. *Bioresource Technol*. 98: 2935-2941.

Sheoran, V., A.S. Sheoran, and P. Poonia. 2010. Soil reclamation of abandoned mine land by revegetation: A review. *Int. J. Soil, Sediment Water*, Vol. 3, Iss. 2, Article 13. http://scholarworks.umass.edu/intljssw/vol3/iss2/13.

Statistical Analysis System. 2013. *SAS Version 9.4*. Cary, NC: SAS Institute.

Steel, R.G.D., and J.H. Torrie. 1980. *Principles and Procedures of Statistics. A Biometrical Approach*. 2nd edn. New York: McGraw-Hill.

Stuczynski, T., G. Siebielec, W.L. Daniels, G. McCarty, and R.L. Chaney. 2007. Biological aspects of metal waste reclamation with biosolids. *J. Environ. Quality* 36: 1154-1162.

Summers, C.G., J.P. Mitchell, T.S. Prather, and J.J. Stapleton. 2009. Sudex cover crops can kill and stunt subsequent tomato, lettuce and broccoli transplants through allelopathy. *California Agric*. 63(1): 35-40.

Stuczynski, T., G. Siebielec, W.L. Daniels, G. McCarty, and R.L. Chaney. 2007. Biological aspects of metal waste reclamation with biosolids. *J. Environ. Quality* 36: 1154-1162.

United States Department of Agriculture. 2013. Custom Soil Resource Report for Cherokee County, Kansas, Soil Survey Staff, Natural Resource Conservation Service, United States Department of Agriculture, Web Soil Survey. Last modified 12/06/2013. Available online at http://websoilsurvey.nrcs.usda.gov/. Accessed 10/20/2016.

United States Environmental Protection Agency. 1989. *EPA's Policy Promoting the Beneficial Use of Sewage Sludge and the New Proposed Technical Sludge Regulations*. Office of Water, Office of Municipal Pollution Control, WH-595. Washington, DC: United States Environmental Protection Agency, 24pp.

United States Environmental Protection Agency. 2007. *Tri-State Mining District – Chat Mining Waste*. EPA530-F-07-016B. Washington, DC: United States Environmental Protection Agency. (National Environmental Publications Information System, Online Database, US EPA, http://nepis.epa.gov/Exe/ZyPDF.cgi/P1003J3X.PDF?Dockey=P1003J3X.PDF)

Vesilind, P.A. 1975. *Treatment and Disposal of Wastewater Sludges*. Ann Arbor, MI: Ann Arbor Science, 236pp.

Wahla, I.H., and M.B. Kirkham. 2008. Heavy metal displacement in salt-water-irrigated soil during phytoremediation. *Environ. Pollution* 155: 271-283.

Warncke, D., and J.R. Brown. 1998. Potassium and other basic cations. In Brown, J.R., Ed., *Recommended Chemical Soil Test Procedures for the North Central Region*. SB 1001. Columbia, MO: Missouri Agricultural Experiment Station, pp. 31-33.

Watson, M.E., and J.R. Brown. 1998. pH and lime requirement. In. Brown, J.R., Ed., *Recommended Chemical Soil Test Procedures for the North Central Region*. SB 1001. Columbia, MO: Missouri Agricultural Experiment Station, pp. 13-16.

Whitney, D.A. 1998. Soil salinity. In Brown, J.R., Ed., *Recommended Chemical Soil Test Procedures for the North Central Region*. SB 1001. Columbia, MO: Missouri Agricultural Experiment Station, pp. 59-60.

Wijesekara, H., N.S. Bolan, M. Vithanage, Y. Xu, S. Mandal, S.L. Brown, G.M. Hettiarachchi, G.M. Pierzynski, L. Huang, Y.S. Ok, M.B. Kirkham, C.P. Saint, and A. Surapaneni. 2016. Utilization of biowaste for mine spoil rehabilitation. *Advance. Agronomy* 138: 97-173.

Figure 3.1 Map of Galena, Kansas, showing the location of Site A and Site B, where the mine waste materials were sampled. A map of Kansas is in the lower left-hand corner, and Cherokee County, in southeastern Kansas, is highlighted. Cherokee County is enlarged above the map for Kansas. Labette County is west of Cherokee County, and Crawford County is north of it. The state of Missouri is east of Cherokee County, and the state of Oklahoma is south of it. Galena is in the southeastern part of Cherokee County, and it is highlighted in the map of Cherokee County. In the map for Galena, the gray striations delineate the boundary of the town, and the areas in red show where the lead and zinc mines were located.

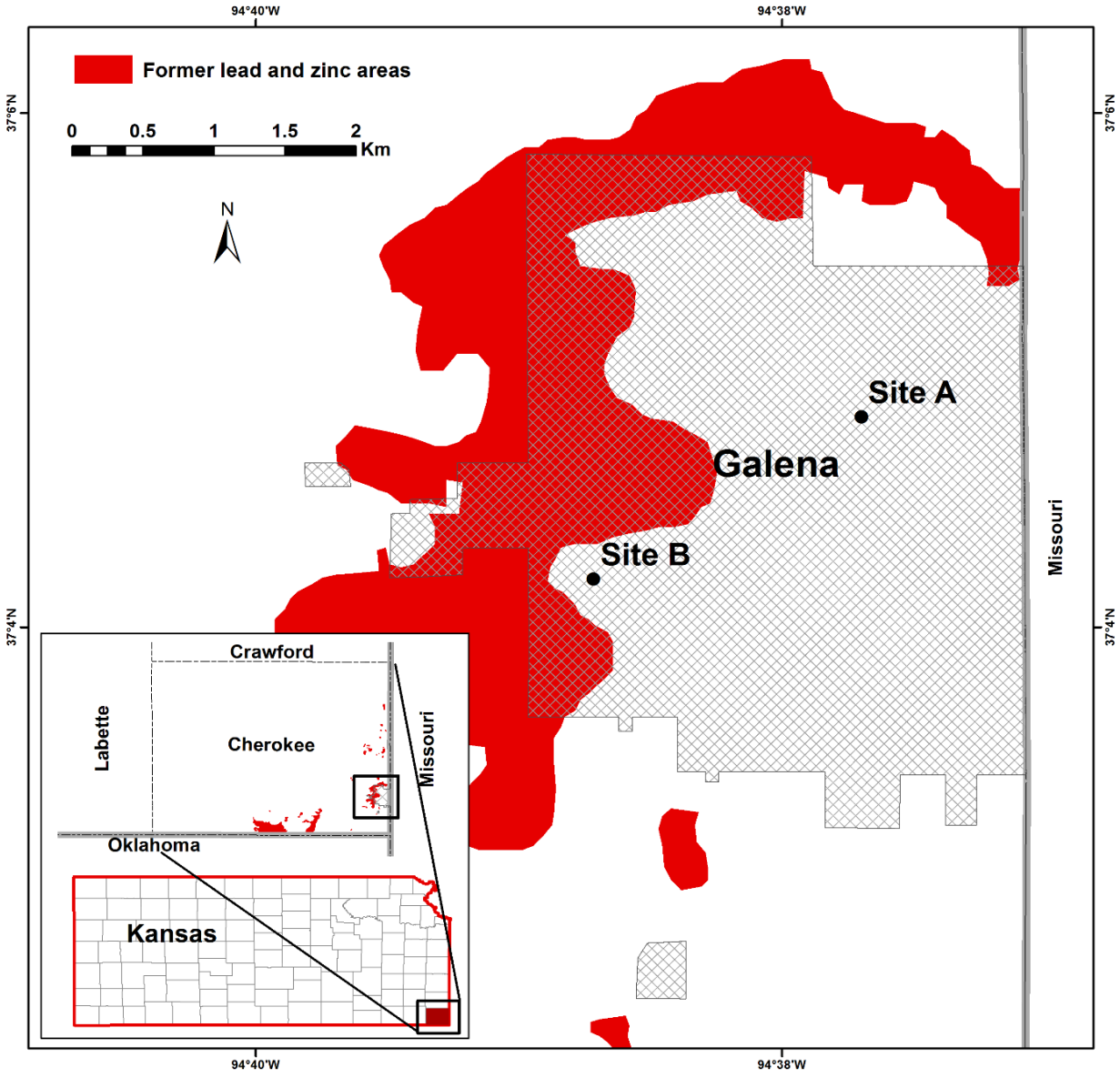

Source: U.S. Geological Survey and Cherokee County

Figure 3.2 Height of sudex grown with and without biosolids in mine waste materials from two different sites in Galena, Kansas. Site A was on the outskirts of town, and Site B was near the center of town. The day of planting was 28 Jan. 2015. Mean and standard deviations are shown for each data point (n = 105). If no standard deviation bars show, they fell within the data point.

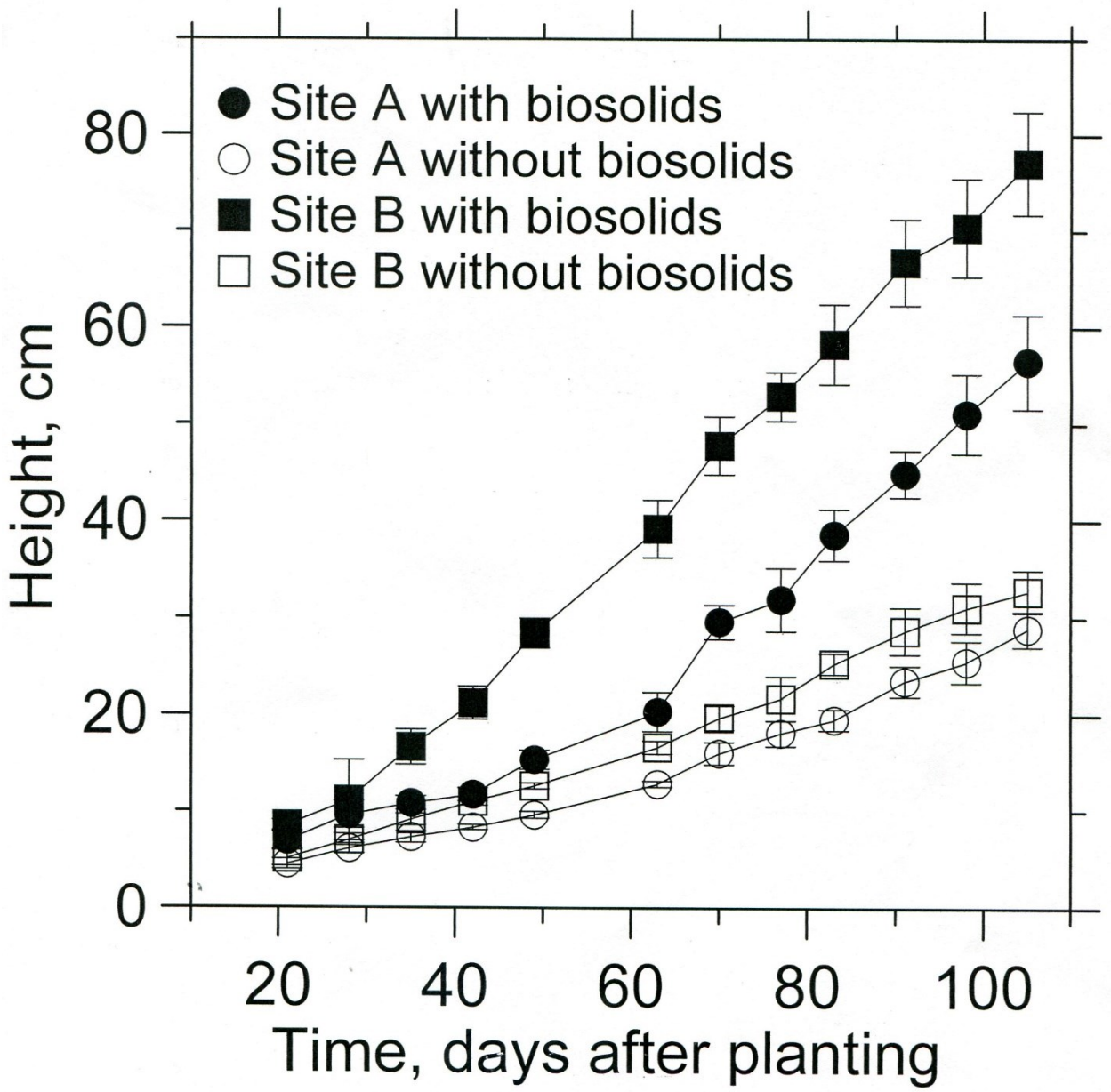

Table 3.1 Monthly average of day and night temperature (oC) and day and night humidity (%) at four locations in the greenhouse during the experiment.

Month (2015)	Temperature		Humidity	
	Day	Night	Day	Night
	Northeast			
February	18.9	16.2	31.3	40.2
March	20.7	20.4	36.5	37.8
April	21.6	21.1	46.7	44.7
	Southeast			
February	18.5	15.6	32.9	41.4
March	20.4	20.1	36.9	38.2
April	21.6	21.3	46.5	44.8
	Northwest			
February	18.8	15.7	31.6	41.2
March	20.7	20.4	36.2	37.2
April	21.4	21.4	46.3	44.3
	Southwest			
February	17.5	14.7	34.5	43.8
March	20.3	20.1	37.2	38.4
April	21.7	21.6	46.3	44.6

Table 3.2 Total and extractable concentrations (mg kg-1) of seven heavy metals in mine waste materials sampled on 18-19 Nov. 2014 at two different sites in Galena, Kansas. Site A was on the outskirts of town, and Site B was near the center of town. Also given are the pH, electrical conductivity (EC), cation exchange capacity (CEC), organic matter, total nitrogen, total carbon, total organic carbon, total phosphorus, and extractable phosphorus of the mine waste materials at the two sites. Within each row, values with the same letter do not differ significantly at 0.05. Each value is the average of 21 measurements. See text for description of statistical analyses.

Measurement	Location	
	Site A	Site B
Cd, total	31.3a	40.6a
Cu, total	44.1a	40.9a
Fe, total	3618.9b	9057.0a
Mn, total	62.0b	212.4a
Ni, total	2.9b	3.6a
Pb, total	2643.0a	1126.6b
Zn, total	3480.3a	3070.5b
Cd, extractable	6.6a	1.5b
Cu, extractable	3.3b	8.1a
Fe, extractable	2.3b	33.5a
Mn, extractable	0.2b	2.4a
Ni, extractable	0.2a	0.1b
Pb, extractable	162.8a	67.2b
Zn, extractable	309.4a	143.2b
pH	7.16a	6.44b
EC, dS m^{-1}	0.21b	0.32a
CEC, meq 100 g^{-1}	4.75a	5.71a
Organic matter, %	1.73a	1.56a
Total N, %	0.13a	0.11a
Total C, %	1.19a	1.03a
Total organic C, %	1.08a	0.98a
Total P, mg kg^{-1}	687a	717a
Extractable P, mg kg^{-1}	253a	175a

Table 3.3 Fresh and dry weights (g pot^{-1}) of shoots and heads of sudex grown with and without biosolids in mine waste materials from two different sites in Galena, Kansas. Site A was on the outskirts of town, and Site B was near the center of town. Within each row, values with the same lower case letter do not differ significantly at 0.05 and values with the same capital letter do not differ significantly at 0.05. Each value is the average of 21 pots. See text for description of statistical analyses.

Site A		Site B	
With biosolids	Without biosolids	With biosolids	Without biosolids
Fresh weight			
Shoots			
41.1a	8.4b	72.6A	9.2B
Heads			
0.8	…[†]	2.0	…
Dry weight			
Shoots			
9.6a	1.3b	17.1A	1.3B
Heads			
0.2	…	0.4	…

[†] Plants grown without biosolids did not produce heads.

Table 3.4 Concentration (mg kg^{-1}) of heavy metals in roots, shoots, and heads of sudex grown with and without biosolids in mine waste materials from two different sites in Galena, Kansas. Site A was on the outskirts of town, and Site B was near the center of town. Within each row, values with the same lower case letter do not differ significantly at 0.05 and values with the same capital letter do not differ at 0.05. Each value is the average of 21 measurements. See text for description of statistical analyses.

	Site A		Site B	
Heavy metal	With biosolids	Without biosolids	With biosolids	Without biosolids
	Roots			
Cd	42.6b	56.4a	18.7B	42.0A
Cu	61.4a	41.3b	49.7A	60.6A
Fe	4842.7a	6465.9a	6465.9B	13,067.1A
Mn	72.2a	52.4a	116.3A	131.6A
Ni	8.0a	7.7a	6.9B	12.4A
Pb	1196.8b	1504.7a	585.0B	715.1A
Zn	7771.7a	6174.8b	3054.0A	5045.6A
	Shoots			
Cd	12.1b	22.1a	6.6B	10.5A
Cu	5.5a	6.3a	8.9B	15.0A
Fe	443.1a	554.9a	186.9B	1966.8A
Mn	50.6a	25.2b	57.3A	65.5A
Ni	1.6a	1.4a	1.1B	2.4A
Pb	59.7b	163.0a	22.2B	121.0A
Zn	2307.3a	1791.9a	711.5A	1117.9A
	Heads			
Cd	2.2	…[†]	0.7	…
Cu	5.9	…	11.0	…
Fe	316.7	…	159.9	…
Mn	17.2	…	21.4	…
Ni	1.4	…	0.7	…
Pb	3.8	…	1.8	…
Zn	116.4	…	57.0	…

[†] Plants grown without biosolids did not produce heads.

Table 3.5 Concentration (%) of N, P, K, Mg, and Ca in roots, shoots, and heads of sudex grown with and without biosolids in mine waste materials from two different sites in Galena, Kansas. Site A was on the outskirts of town, and Site B was near the center of town. Total carbon was determined only in the heads. Within each row, values with the same lower case letter do not differ significantly at 0.05 and values with the same capital letter do not differ at 0.05. Each value is the average of 21 measurements. See text for description of statistical analyses.

	Site A		Site B	
Heavy metal	With biosolids	Without biosolids	With biosolids	Without biosolids
	Roots			
N	1.15a	0.82b	0.78A	0.59B
P	0.30a	0.14b	0.17A	0.14B
K	0.78a	0.88a	0.57B	0.84A
Ca	0.50a	0.41b	0.27B	0.36A
Mg	0.29a	0.27a	0.19B	0.26A
	Shoots			
N	1.57a	1.05b	1.31A	0.93B
P	0.326a	0.21b	0.332A	0.26A
K	1.19a	1.31a	1.31B	1.75A
Ca	0.94b	1.42a	0.59B	0.86A
Mg	0.32a	0.36a	0.40A	0.31B
	Heads			
N	1.45	…[†]	1.40	…
P	0.252	…	0.249	…
K	0.780	…	0.768	…
Ca	0.160	…	0.133	…
Mg	0.217	…	0.256	…
C	44.21	…	45.27	…

[†] Plants grown without biosolids did not produce heads.

Table 3.6 Total and extractable concentrations (mg kg^{-1}) of heavy metals in mine waste materials with and without biosolids. The mine waste materials came from two different sites in Galena, Kansas. Site A was on the outskirts of town, and Site B was near the center of town. Within each row, values with the same lower case letter do not differ significantly at 0.05 and values with the same capital letter do not differ significantly at 0.05. Each value is the average of 21 measurements. See text for description of statistical analyses.

	Site A		Site B	
Heavy metal	With biosolids	Without biosolids	With biosolids	Without biosolids
	Total concentration			
Cd	34.9a	33.4a	36.9A	34.3A
Cu	58.1a	48.0b	47.8A	46.3A
Fe	3931.2a	3764.2a	8914.3A	8095.5A
Mn	82.9a	78.8a	197.9B	220.9A
Ni	3.8a	3.5a	2.9A	3.0A
Pb	3406.5a	2499.5a	1288.7A	1228.9A
Zn	4041.0a	3981.3a	4558.1A	5365.3A
	Extractable concentration			
Cd	6.6a	6.9a	1.1A	1.3A
Cu	3.4a	2.7a	8.6A	8.4A
Fe	3.5a	2.9a	37.4A	31.4B
Mn	0.66a	0.68a	3.9A	2.5B
Ni	0.36a	0.23b	0.08A	0.10A
Pb	113.1b	164.9a	60.0A	60.9A
Zn	319.4a	311.0a	118.6A	117.2A

Table 3.7 The pH, electrical conductivity (EC), cation exchange capacity (CEC), organic matter, total nitrogen, total carbon, total organic carbon, total phosphorus, and extractable phosphorus in mine waste materials with and without biosolids. The mine waste materials came from two different sites in Galena, Kansas. Site A was on the outskirts of town, and Site B was near the center of town. Within each row, values with the same lower case letter do not differ significantly at 0.05 and values with the same capital letter do not differ significantly at 0.05. Each value is the average of 21 measurements. See text for description of statistical analyses.

	Site A		Site B	
Measurement	With biosolids	Without biosolids	With biosolids	Without biosolids
pH	6.7b	7.5a	6.3B	6.7A
EC, dS m^{-1}	1.07a	0.89b	1.25A	0.97B
CEC, meq 100 g^{-1}	6.9a	6.0a	7.6a	7.7a
Organic matter, %	2.73a	2.26b	2.24A	2.00B
Total N, %	0.15a	0.13b	0.11A	0.10A
Total C, %	1.71a	1.36b	1.11A	1.01B
Total organic C, %	1.44a	1.24b	1.08A	0.96B
Total P, ppm	1106a	777b	887A	705B
Extractable P, ppm	551a	349b	311A	208B

Chapter 4 - Characterization of Interior Building Dust Near an Abandoned Lead and Zinc Mining Area

4.1 Abstract

Little information exists for characteristics of attic dust from mining sites in the central USA. The lead (Pb) and zinc (Zn) mines in the Tri-State Mining District of southeast Kansas, southwest Missouri, and northeast Oklahoma have left a legacy of pollution. The mines produced Pb and Zn from 1876 to the 1970s. Galena, KS, is a city located within the Tri-State Mining District. Fourteen dust samples were collected from the interior of buildings (attics and a basement) where little or no human activity had occurred. Samples were obtained from nine different buildings including stores, houses, the Galena Waterworks, a school, and a church, using two methods: sweeping with a brush and vacuuming with a small hand-held vacuum. The dust samples were analyzed for total concentration of heavy metals (Cd, Cu, Fe, Mn, Ni, Pb, and Zn) using inductively coupled plasma-atomic emission spectroscopy (ICP-AES). A Malvern Mastersizer 3000 instrument was used for particle size analysis of the dust samples. Mineral and chemical compositions of the dust samples were obtained using X-ray diffraction (XRD) and scanning electron microscopy-energy dispersive spectroscopy (SEM-EDX). The concentrations of the heavy metals in the 14 dust samples were highly variable. However, the dust samples were enriched with Pb and Zn, as well as Cd, compared to average values found in non-contaminated soils based on the information on non-contaminated soil from the literature. Approximately 10% of each dust sample contain PM_{10}, which might be a heath concern. The XRD showed that galena, sphalerite, anglesite, quartz, calcite, aragonite, pyrite, and cerussite minerals were present in most of the dust samples. The XRD data agreed with the results of SEM-EDX in dust samples.

4.2 Introduction

Dust is displaced soil that is fine enough to be easily suspended in air. It can have both natural and anthropogenic sources. Dust storms are wind storms that sweep up clouds of dust when passing over an arid region, and they have occurred for eons. They were severe in the semi-arid Great Plains of the USA during the Dust Bowl years of the 1930s (Grill, 2009). People died from breathing the dust. The dust due to man's industrial activities can be even more dangerous, not only because it accumulates in the lungs but also because it carries the contaminants associated with the industry. In particular, it has long been known that dust near metalliferous mines is contaminated with the metal mined at that site. Csavina et al. (2012) review the literature and point out that, although there are numerous natural and anthropogenic sources of atmospheric particulates, mining operations pose the greatest potential risk to human health and the environment.

Ancient mining sites are especially polluted. The Rio Tinto mines in Spain are some of the oldest mines on the Iberian Peninsula (Castillo et al., 2013). They have been mined since pre-Roman times for copper (Cu), gold (Au), and silver (Ag). Even though the mines were abandoned in the middle of the 20th century, the mining activities generated large amounts of hazardous mine wastes that are deposited over extensive areas. The dust from them is enriched with toxic metals, including Cu, zinc (Zn), lead (Pb), and cadmium (Cd). These heavy–metals particles can have adverse effects on surrounding soils, plants, and humans.

Dust from attics provides a means of reconstructing air pollution (Ilacqua et al. 2003). Attic dust is derived predominantly from external sources, such as aerosol deposits and soil dusting, and less from household activities (Bačeva Andonovska et al., 2015). Therefore, attic

dust is accepted as a tracer of aerosol pollution. Many studies have shown the importance of attic dust in documenting metal pollution from a mine.

Baceva et al. (2011) studied attic dust in the Kavadarci region in the Tikveš Valley of Macedonia, which is known for its ferronickel industrial activity. Samples of attic dust were collected in 2008 at 31 sites in Kavadarci and its environs. The median value of nickel (Ni) in samples of attic dust taken from the entire Kavadarci region was 220 mg kg^{-1}. However, the Ni concentration in the samples taken from the vicinity of the ferronickel smelter plant was as high as 1,200 mg kg^{-1}.

Balabanova et al. (2011) examined attic dust to study emissions from a Cu mine in the central part of eastern Macedonia that has functioned since 1980. They sampled attic dust from old, rural houses, built between 1920 and 1970, which were located in 29 settlements in the vicinity of the mine. They found geogenic and anthropogenic sources of individual chemical elements in the dust. The dust due to anthropogenic sources contained arsenic (As), Cu, and Pb and mirrored dust fallout from the mining operations. I have no information about the dust fallout in southeastern Kansas.

In another study from the Tikveš Valley in Macedonia, attic dust from 27 rural houses in 13 settlements was sampled in 2008 to see the effect of a Ni smelter plant (Boev et al., 2013). The plant had been built in the valley in 1980 and started production in 1982. The houses sampled were of similar age (constructed after 1982). The minerals in the dust were analyzed, and they were not common constituents of urban dust, but came from the Ni smelter plant.

Since 1668, the Meza Valley in the northern part of Slovenia, close to the Austrian border, has had mines where Zn, Pb, and iron (Fe) have been mined (Šajn, 2006). The valley is strongly polluted as a result of these mining activities. Šajn (2006) sampled attic dust from

houses in the valley that were at least 100 years old. He also sampled topsoil (0-5 cm) in the region. Factorial analysis of chemical elements in the samples was performed and found natural and man-made geochemical associations. The natural geochemical association was mainly influenced by weathering of metamorphic rocks, while the anthropogenic association was a result of Pb and Fe production.

Attic dust was sampled around a mercury (Hg) mine in Slovenia (Gosar et al., 2006). The concentration of Hg in the attic dust was many times higher than in the surrounding soils, and the attic dust/soil ratio changed with distance from the mine. The highest ratios occurred at the greatest distance from the source of the pollution, and the lowest ratios were close to the source. This suggested that the small particles carried by the wind were more enriched than the larger particles. At the greatest distance from the mine, the median Hg concentration of attic dust exceeded the one in soils by more than six times. The lowest ratio, closest to the mine, had a median Hg concentration in attic dust that exceeded the median in soils by less than three times.

Völgyesi et al. (2014) sampled attic dust in 27 houses in the industrial town of Ajka, Hungary. Attics in houses intact for at least 30-40 years were chosen to represent long-term industrial pollution. They analyzed the dust samples for As, Cd, Cu, Ni, Pb, Zn, and Hg. They found Pb, Hg, Zn, and Cd distribution was dominated by anthropogenic sources, and it was characterized by extreme high values, such as high Hg concentrations around a lignite-fired power plant. They concluded that attic dust was an efficient and cheap sampling medium to study long-term airborne contamination and its associated human health risks.

Even though the Pb deposited in soils poses a low risk, because plant uptake of Pb is usually very low (Brown et al., 2015), Pb in dust is of major medical concern. Lead in garden

soil and house dust was studied in the village of Stratoni in northern Greece, an industrial area where sulphide ore is mined (Argyraki, 2014). Total Pb was enriched in house dust samples by a factor of two on average. Total Pb concentration in soil samples had a maximum value of 2,040 mg kg^{-1}, but house dust samples had a maximum value of 7,000 mg kg^{-1} Pb. Lead-enriched Fe and manganese (Mn) oxides predominated in the soil samples, while fine grains of the mineral galena (PbS) (<10-20 μm in diameter) were the major Pb-bearing phase in dust samples. Using an integrated exposure uptake biokinetic model to predict the risk of elevated blood lead levels, there was a 61% probability that the children of Stratoni would have elevated levels of Pb in their blood, when the reference blood Pb level was the one used prior to 2012 (>10 μg dL^{-1}). The results emphasized the importance of house dust as the cause of elevated Pb in blood of children. Health risks of house dust in the vicinity of phosphorus mines in Guizhou, People's Republic of China, showed that As and Pb are of concern (Yang et al., 2015).

Not only is the presence of heavy metals in the dust a health problem, but also the size of the dust is of medical concern, in particular for particles referred to as PM_{10}. Particles of this size are less than 10 μm in diameter. PM_{10} is a major component of air pollution that threatens health and the environment. Particle size analysis of attic dust has been carried out by researchers who study wind erosion in the Dust Belt of the USA where the Dust Bowl occurred (Van Pelt and Zobeck, 2007). Dust from wind erosion is called "fugitive dust," which is a relatively new name for dust. It is dust that comes from a nonpoint source of air pollution and cannot be traced to a specific point of origin. Due to the semi-arid conditions of the region, fugitive dust has been a major environmental management issue from the Dust Bowl years to the present (Gill et al., 2000; Van Pelt et al., 2002). Attic dust has proved to be an important way to document differences between natural and man-made sources of dust in the region. Van Pelt and Zobeck

(2007) did chemical analyses of dust samples collected from attics 4 km from the nearest source of cropped fields. Their results indicated that anthropogenic sources of several important nutrients and trace elements were much larger contributors, by up to nearly two orders of magnitude, to atmospheric loading than fugitive dust from eroding soils. Heurtas et al. (2012) found that PM_{10} particles from a coal mine in northern Colombia exhibited a log normal type distribution, and they observed that the pollution from the PM_{10} particles would be harmful to human health. There is a need to measure the transport of airborne particulates from mining operations, specifically the finer particle fraction (Csavina et al., 2012).

X-ray diffraction (XRD) has been used to assay the mineralogy of materials in dust samples (Querol et al., 2000; Gill et al., 2000; D' Amore et al., 2005; Csavina et al., 2012; Argyraki, 2014). X-ray diffraction is the instrumentation used to provide an atomic structure of crystalline materials (Moore and Reynolds., 1989). X-ray diffraction is a useful method to detect minor materials in soil samples (Lombi and Susini, 2009). The main disadvantage of this technique is that it analyzes only crystalline substances (D' Amore et al., 2005). For example, the crystalline chemical compounds in dust analyzed by Gill et al. (2000) were quartz and calcite.

Morphological and elemental composition of dust particles can be determined by scanning electron microcopy (SEM) equipped with energy dispersive X-ray (EDX) (D' Amore et al., 2005). The method has been used to assay the microscopic structures of dust particles (Reynolds et al., 2003; Csavina et al., 2011, Csavina et al., 2012; Huertas et al., 2012). Size, and elemental composition were determined by (Huertas et al., 2012). Secondary electron (SE) or back scattered electron (BSE) images were used to obtain images of the morphology of dust particles. Scanning electron microcopy – EDX is the tool used to gain indirect evidence of metal

formations (Moral et al., 2009). Back scattered electron images and energy dispersive X-ray scan the surface of dust samples by an electron beam between 2 – 50 KeV, but the disadvantages of BSE and EDX are the moderate resolution and elemental interferences (D' Amore et al., 2005).

The Pb and Zn mines in the Tri-State Mining District of southeast Kansas, southwest Missouri, and northeast Oklahoma have left a legacy of pollution. The district has a history of mining that goes back to the early 1800s, when Pb was mined by trappers and explorers for bullets (Pope, 2005, p. 5). The mines lasted until 1970 (Pope, 2005, p. 1). Galena, Kansas, is a town in the Tri-State Mining District named after the mineral, where mines began to operate in 1876 (Pope, 2005, p. 7). The century of mining operations in Galena has left Pb and Zn contamination throughout the city. The waste materials around the mines are highly polluted, not only with Pb and Zn, but also with Cd, which often co-occurs geologically with Zn.

For this study, the buildings in the town of Galena were chosen because of its rich history, proximity to the mining district, and the possible risks it has imposed to people nearby. Studies have shown health risks in the region. In 1940, Cherokee County in Kansas, where Galena is located, recorded more cases of tuberculosis than any other county in Kansas, and, in 1951, the county's death rate from tuberculosis was six times greater than for the rest of the state (Gibson 1972, p. 194). Residents of Galena have a higher incidence of kidney disease, heart disease, skin cancer, and anemia compared to residents in control towns (Neuberger et al. 1990). These results suggest that environmental agents in Galena are associated with the causation of several chronic diseases in the residents. There has been limited research on the concentration of heavy metals or particle size of attic dust from area with known soil contamination.

The main objective of this research was to obtain and characterize attic dust collected from buildings in Galena, Kansas. Like previous studies from other mining regions, the dust was characterized for chemical and physical properties. Attics were specifically chosen to determine the particle size distribution, chemical composition, mineralogy and morphology of all dust samples.

4.3 Materials and Methods

The dust samples were collected on 20 Aug. 2015, 7 April 2016, and 8 April 2016 in Galena, Kansas (37°5'N; 94°38'W; 275 m above sea level) from attics where little or no human activity had occurred. The attics had been kept dark day and night. Samples were obtained from nine different buildings including stores, houses, the Galena Waterworks, a school, and a church, using two methods: sweeping with a brush and vacuuming with a Shop-Vac® Brand (Williamsport, PA) vacuum. Even though much has been written about the proper procedure for sampling dust, no standard method has yet been established (Wu et al., 2008; U.S. EPA, 1995). Table 4.1 shows the samples obtained, the date of sampling, the method of sampling, the building sampled, the floor of the attic, the age of the building, and the construction material of the building. In Table 4.1, the "first floor" means that the attic was immediately above the floor on the ground level and the "second floor" means that there was a floor between the ground floor and the attic. In Table 4.1, the samples are labeled Nos. 1-15, but only 14 samples were obtained. Sample 8 is missing because when the sample brought out of the attic into bright light, it was found that it was sawdust and not dust. Figure 4.1 shows the location in Galena of the samples taken. The dust samples were sealed in black plastic to avoid bleaching. The thickness of the black plastic was 2.625 MIL. An area was marked out in each attic and samples were

collected from the top of that area, even if it had wood, ducts, pipes, and insulation. The samples were collected using a flash light with a red light to prevent light contamination.

Dust samples were brought back to Manhattan, KS, for all analyses. Once the dust samples were in a dark room (red light), samples were separated into two groups: one group of samples was for the optically stimulated luminescence measurements and it remained in a dark laboratory. (This data is not presented in this dissertation as the research is ongoing). The second group of dust samples was prepared for the other measurements. For all measurements, dust samples were sieved through a 150 μm mesh screen to remove building debris and macrobiological materials including rodent droppings (Van Pelt and Zobeck, 2007).

The four analyses that the dust samples were subjected to were: total concentration of heavy metals; X-ray diffraction; scanning electron microscopy; and particle size analysis.

The dust samples were analyzed for total concentration of seven heavy metals (Cd, Cu, Fe, Mn, Ni, Pb, and Zn) using a method similar to that of Sposito et al. (1982). We used 1 g of dust samples and added 20 mL of 4 M HNO_3 and heated the mixture for 4 hours at 90^{o} C in a water bath. The extract was analyzed using inductively coupled plasma-atomic emission spectroscopy (ICP-AES).

Total concentration of heavy metals in dust samples were compared to the mine waste materials came from Site A (Chapter 2 of this dissertation, Table 3.2) and values and ranges of non-contaminated come from literature Kirkham (1979, 2008); Norrish, 1975; and Sauchelli, 1969, p.40.

To determine the level of crystallinity of the powder of the dust samples, X-ray diffraction (XRD) was employed using a PANalytical Empyrean Multi-Purpose X-Ray Diffractometer (PANalytical is part of the Spectris Company, Egham, Surrey, United Kingdom).

Dust samples were packed tightly into 27 mm sample holders and placed on a sample carriage for a batch analysis. All 14 samples were run using a robotic arm, so the XRD did not have to be continually opened to remove and replace new samples. We utilized programmable divergent slit (PDS) incident beam optics using a 0.04 radian Soller slit size (Soller slits are the collimator of the system) and a 15 mm mask as well as a 2 degree anti-scatter slit on a reflection transmission spinner sample stage and a Medipix3 PIXcel^{3D} detector (the readout) with 0.02 radian Soller slits on diffracted beam optics. The two theta ranges for each scan were 5 - 70° using the smallest step size available (0.006 degree) to yield the best resolution during the continuous scan. The total time for each of the scans was 17 minutes and 23 seconds.

To characterize the morphology and elemental composition of the dust samples, a scanning electron microscope (SEM) (Hitachi S-3500 N, Tokyo, Japan) in the Nanotechnology Innovation Center at Kansas State University was used. The dust samples were subjected to SEM coupled with energy dispersive X-ray spectrometry (EDX). Dust samples were mounted on an SEM stub using an adhesive carbon tape and analyzed for elemental composition using the SEM equipped with an Oxford energy dispersive X-ray detector (Oxford company, Abingdon, Oxfordshire, England, United Kingdom). The weight percentage (Atomic %) of elements were given by the EDX when measuring the dust samples.

In addition to the SEM technique, we used a Malvern Mastersizer 3000 with a Hydro EV adapter (Malvern instrument is part of the Ltd., Worcestershire, UK) to measure particle size of the dust samples. The Mastersizer 3000 uses the technique of laser diffraction to measure the size of particles through a wet dispersion unit after sonication to disperse any aggregates. It does this by measuring the intensity of light scattered as a laser beam passes through a dispersed particulate sample. The scattered laser light is registered on detectors. For the determination of

dust particle size, the Mastersizer uses two sources of light: red (wavelength 633 nm) and blue (wavelength 466 nm). The data are then analyzed to calculate the size of the particles that created the scattering pattern. The angle at which the beam is scattered is inversely proportional to the soil particle size. The measurement range of the apparatus is 10 nm to 3.5 mm. The software provided by the manufacturer recalculates the information from the detectors to give volumetric dust particle size. The median size of dust particles (Dx50) as well as the particle sizes of 90% of the volume (Dx90) and 10% of the volume (Dx10) were calculated.

4.4 Results and Discussion

The concentrations of the heavy metals in the 14 attic-dust samples were highly variable (Table 4.2), but the dust from the attic in the youngest building sampled, a house built in 1950 (Table 4.1), had the lowest concentrations of Pb and Zn, the two heavy metals mined in the mines of Galena, Kansas, starting in 1876 (Pope, 2005, p. 7). The highest concentrations of attic-dust Pb were in a house built in 1894, and the highest concentration of Zn occurred in attic dust of a store built in 1900. After 1955, mining activity declined (Johnson et al., 2016). The mines lasted until 1970 (Pope, 2005, p. 1). While the mines were active, the house built in 1950 had 20 years to collect dust, while the house built in 1894 and the store built in 1900 had 76 and 70 years, respectively to collect dust. Although based on only 14 samples, these results indicated that dust in buildings built since 1950 would have less Pb and Zn contamination than dust in buildings built before then.

The concentrations of the heavy metals in the 14 dust samples are given in Table 4.2. The concentrations of Cd, Cu, Ni, Pb, and Zn in the dust were higher than those in non-contaminated soils. The concentrations of the heavy metals in the dust were compared to the concentrations of the heavy metals in the mine waste materials from Site A, one of the two sites

sampled in Galena, KS, in November, 2014 (Chapter 2 of this dissertation). The data are given by Alghamdi et al., (in press, 2017, Table 15.2). The concentration in the dust was divided by the concentration in the mine waste materials (Table 4.3). For Cd, Pb, and Zn the ratio was roughly one, which showed that the dust was not enriched compared to the mine waste materials for these heavy metals. The heavy metals in the dust samples also were compared to heavy metal concentrations of soils in Cherokee County (Juracek, 2013). The analyses for Cd, Pb, and Zn using the spectroscopic method in Table 2 of Juracek (2013) were used for the comparison. Juracek (2013) gave seven analyses for Cd, Pb, and Zn, the only heavy metals presented in his work. The seven analyses were averaged together. For each dust sample the concentration of a heavy metal in the dust was divided by the average concentrations given by Juracek (2013). The ratios are shown in Table 4.4. They all were roughly one, which showed that the dust was coming from not only from the mine waste materials but also the surrounding soils and that the dust was not enriched in the concentrations of Cd, Pb, and Zn. The concentrations of Cd, Pb, and Zn found by Juracek (2013) in soils of the region were highly contaminated with Cd, Pb, and Zn compared to non- contaminated soils (Table 4.2).

However, the dust samples were highly elevated with Pb and Zn, as well as Cd, compared to average values found in non-contaminated soils (Table 4.2). I do not know the concentrations of heavy metals in dust from non- contaminated soils in Kansas, and, therefore, I cannot compare my results with dust found in buildings that are not near abandoned mines. Even though it is unrealistic to compare the highly contaminated mine waste materials to non-contaminated soils, it is interesting to note that Pb was almost 200 times more concentrated in the dust than the average value found in soils (1994.3 $\mu g\ g^{-1}$ Pb in the dust versus 10 $\mu g\ g^{-1}$ Pb in non-contaminated soils). Zinc was almost 100 times more concentrated in the dust than the average

value found in soils (4900.6 μg g^{-1} Zn in the dust versus 50 μg g^{-1} Zn in non-contaminated soils). Concentration of Cd in the dust was over 40 times more than the concentration of Cd found in non-contaminated soils (22.2 μg g^{-1} in the dust versus 0.5 μg g^{-1} for soils).

Others have also found that attic dust has a higher concentration of heavy metals than the surrounding soil. As noted in the introduction section of this chapter, Bačeva et al. (2011) studied attic dust near a ferronickel smelter plant in the Kavadarci region of Macedonia. The median value of nickel in samples of attic dust taken from the entire Kavadarci region was 220 mg kg^{-1} (220 μg g^{-1}), but the soil samples had a concentration of Ni as high as 1,200 mg kg^{-1}. In Slovenia, Gosar et al. (2006) found that the median Hg concentration of attic dust near a mercury mine exceeded the value in soils by three to six times, depending on the distance from the mine. In Greece, Pb in house dust near a sulphide ore mine was enriched two times compared to the concentration of Pb in the soil (Argyraki, 2014).

The concentrations of the heavy metals in the samples obtained by sweeping were not consistently greater or lesser than those in samples obtained by vacuuming (Table 4.2). These results suggest that either sweeping or vacuuming would be an acceptable method to obtain dust samples.

Regressions were made between Pb, Cd, and Zn and the age of the buildings (Figure 4.2). The regressions were done using SAS (9.3), and the outputs are shown in the appendix. The regressions showed a negative relationship, but it was only significant for Pb ($p=0.0176$). This indicates that the older buildings were more contaminated with heavy metals than the newer buildings.

Table 4.5 shows the results of the XRD analyses for the 14 different attic dust samples. Nine of the 14 samples contained at least one Pb-bearing mineral. Sample 1 and 10 had galena

(PbS), and Samples 5, 6, 7, 11, 12, 13, and 15 had anglesite [$Pb(SO_4)$]. Six of the 14 samples (Samples 1, 2, 4, 6, 12 and 15) had a mineral with Zn, and it was sphalerite (ZnS). All of the dust samples had quartz (SiO_2), and most of the 14 dust samples had calcite ($CaCO_3$), and aragonite ($CaCO_3$), which is a polymorph of calcite, differing slightly in structure. Seven of the 14 dust samples (samples 5, 6, 7, 11, 12, 13, and 15) contained muscovite [$KAl_3Si_3O_{10}(OH)_{1.8}F_{0.2}$]. Sample 2 had dolomite [$CaMg(CO_3)_2$] and samples 4, 6, and 7 had marcasite (FeS_2). Pyrite (FeS_2) was identified in sample 6 and Querol et al (2000) found pyrite as a primary mineral along with quartz and calcite. Baker et al (2014) studied the materials from an abandoned Pb/Zn smelter near Dearing, KS, and they identified galena as a major mineral. Pope (2005, p. 7) identified about 11 common minerals in the Tri-State area. Anglesite, calcite, cerussite ($PbCO_3$), chert (SiO_2 amorphous), dolomite, galena, hemimorphite [$Zn_4Si_2O_7(OH)_2.H_2O$], marcasite, quartz, smithsonite ($ZnCO_3$), and sphalertite were the most common minerals in the Tri-state area. Gill et al (2000) studied historic settled dusts in West Texas and they identified quartz, calcite, and muscovite in a dry powder. Other studies from former Pb/Zn mining sites in northern Tunisia have used XRD to identify minerals in tailing samples and < 2 μm, and they found galena, sphalerite, pyrite, cerussite, and anglesite (Boussen et al., 2010). In general, Pb and Zn ore occurred along with sulfide minerals (Pope, 2005, p. 5). Galena and sphalerite are the major minerals in the Tri-State area (Johnson et al., 2016, p. 1134).

Table 4.6 shows the particle size distribution of the 14 different attic dust samples, described in Table 4.1, as determined with the Malvern Mastersizer 3000. To interpret the table, we take, for example, the first sample. Sample 1 had three different values: 9.34 μm (Dx10), 64.8 μm (Dx50), and 173 μm (Dx90). This means that 10% of the sample had a size of 9.34 μm or smaller; 50% of the sample had a size of 64.8 μm or smaller; and 90% of the sample had a

size of 173 μm or smaller. For human health related concerns, observe the column in Table 4.6 for Dx(10), because it had two samples (Samples 1 and 5) smaller than 10 μm. As noted in the introduction of this chapter, dust particles that have a size less than 10 microns (10 μm), called PM_{10}, are of medical concern (Samet et al., 2000). Sample 1 also had the highest Zn and Ni concentration (Table 4.2). Sample 1 came from the sweeping sample in the attic of a store built in 1900. Sample 5 was the only basement sample, and it occurred in a school built in 1938. A dust sample falling within the definition of PM_{10} that is found in a school is of special concern, because this means that many children will be exposed to, not only dangerously small dust particles, but also the heavy metals associated with them; however, it is unlikely that children would frequent this school's basement. As for all the dust samples, Sample 5 had extremely high levels of Cd, Cu, Pb, Ni, and Zn compared to values in uncontaminated soils (Table 4.2). Except for Samples 7 and 15 with a Dx(10) values of 16.7 μm and 17.7 μm, the samples in the column for Dx(10) in Table 4.6 had values near 10 μm. If the dust from the attics and the basement sampled in Galena, KS, were breathed into the lungs, then there would be health problems, not only due to the size of the dust particles, but also because of the toxicity of these heavy metals. The particle size distribution of the 14 dust samples was similar to that observed by Davis and Gulson (2005) who investigated the particle size distribution of 38 attic dusts collected from houses in the city of Sydney, Australia, using Malvern laser particle size. The range ages of the houses from 4 to 106 years. They measured the dust sample that is < 250 μm as a volume percentage. They found 90%, 50%, 10% of the dust samples were smaller than 172.8 μm, 60.2 μm, 15.7 μm, respectively. In a study from Gill et al., (2000), they collected settled dust samples from houses in the southern Great Plains of Texas. They measured particle size using Malvern Mastersizer Laser. They found that the dust samples contain a fairly large proportion (>10%) of

PM_{10} size range. Even though most of the samples in Dx(10) column in Table 4.4 had values near PM_{10}, they represented only 10% of the total dust by mass.

Table 4.7 shows the particle size distribution (PM_{10} and $PM_{2.5}$) for all dust samples, as determined with the Malvern Mastersizer 3000. $PM_{2.5}$ is dust particles that have a size less than 2.5 microns. Note in Table 4.7 the values are in percent and they come from the raw data. About 10.13% of all dust samples had PM_{10} and 2.11% had $PM_{2.5}$.

Figures 4.3 - 4.6 show the surface morphology of the dust particles for samples 1, 2, 3, and 4 (see Table 4.1) from the area of interest (AOI) using secondary electron images (SE). The electron beam hits the sample surface to get SE images. SE images indicate the presence of particles containing elements with high atomic number. Inorganic materials such as hair are indicated in the darker areas. SE images are emitted by atoms near the surface of dust samples when their electrons become excited and have sufficient energy to escape the surface. Tables 4.8 - 4.11 show the elemental composition of dust samples using energy dispersive spectroscopy (EDX) at the AOI for samples 1, 2, 3, and 4. Comparison of SE images and EDX demonstrates that these dust particles contain C, O, Al, Si, S, Ca, Fe, and Zn and in addition sample 3 has one more element which is K. Lead was absent in dust particles because it was below the level of detection (0.1%). These data suggest that metals are immobilized in minerals with sulfide and silicates such as sphalerite, quartz, and marcasite.

Figures 4.7 - 4.16 show the surface morphology of the dust particles for samples 5, 6, 7, 9, 10, 11, 12, 13, 14, and 15 (see Table 4.1) from the particles of interest (POI) using back scattered electron (BSE) image. BSE images indicate the presence of POI containing an element of high atomic number which are the brighter particles. So, the BSE is sensitive to the atomic number. Tables 4.12 - 4.21 show the elemental composition of dust samples using EDX for the

POI for samples 5, 6, 7, 9, 10, 11, 12, 13, 14, and 15. Comparison of BSE images and EDX demonstrates that these POI contain C, O, Al, Si, S, Ca, Fe, Zn, Pb, K, Na, P, Mo, Ba, Cl, Pd, and Au. These results provide indirect evidence that minerals such as quartz, sphalerite, marcasite, anglesite, galena, alamosite, margarosanite, cerussite ($PbCO_3$), wulfenite ($PbMoO_4$), powellite ($CaMoO_4$), and massicot (PbO) are present. In general, EDX showed that about 64% of the dust samples had Pb and 100% of the dust samples had Zn.

4.5 Conclusion

The total concentrations of the heavy metals in the dust samples were highly variable. The dust samples were highly contaminated with Pb and Zn, and Cd, compared to average values found in uncontaminated soils. A significant correlation between the age of the building and the concentration existed for Pb but not Zn or Cd. About 10% of each dust sample had PM_{10}, which might potentially be a level that is high enough to be a health concern. The XRD showed that galena, sphalerite, anglesite, quartz, calcite, aragonite, pyrite, and cerussite minerals were in most of the dust samples. XRD observations agreed with the results of SEM-EDX.

4.6 References

Alghamdi, A. 2016. Rehabilitation of waste materials at abandoned lead and zinc mines in Galena, Kansas," PhD diss., Kansas State Univ., Manhattan (in preparation).

Alghamdi, A., M.B. Kirkham, D.R. Presley, G.M. Hettiarachchi, and L.Murray. 2017. Rehabilitation of an abandoned mine site with biosolids. In: N. Bolan, M.B. Kirkham, and Y.-S. Ok (Editors). Mine Site Rehabilitation and Revegetation, CRC Press, Taylor & Francis Group, Boca Raton, FL (in preparation).

Argyraki, A. 2014. Garden soil and house dust as exposure media for lead uptake in the mining village of Stratoni, Greece. Environ. Geochem. Health 36:677-692.

Bačeva Andonovska, K., T. Stafilov, and I. Karadjova. 2015. Assessment of trace elements bioavailability – ingestion of toxic elements from the attic dust collected from the vicinity of the ferro-nickel smelter plants. Macedonian Acad. Sci. Arts 36:93-104.

Bačeva, K., T. Stafilov, R. Šajn, C. Tănăselia, and S.I. Popov. 2011. Distribution of chemical elements in attic dust in the vicinity of a ferronickel smelter plant. Fresenius Environ. Bull. 20:2306-2314.

Baker, L. R., Pierzynski, G. M., Hettiarachchi, G. M., Scheckel, K. G., and Newville, M. 2014. Micro-X-ray fluorescence, micro-X-ray absorption spectroscopy, and micro-X-ray diffraction investigation of lead speciation after the addition of different phosphorus amendments to a smelter-contaminated soil. Journal of environmental quality, 43(2), 488-497.

Balabanova, B., T. Stifilov, R. Šajn, and K. Bačeva. 2011. Distribution of chemical elements in attic dust as reflection of their geogenic and anthropogenic sources in the vicinity of the copper mine and flotation plants. Arch. Environ. Contamination Toxicol. 61:173-184.

Boev, B., Stafilov, T., Bačeva, K., Šorša, A., and Boev, I. 2013. Influence of a nickel smelter plant on the mineralogical composition of attic dust in the Tikveš Valley, Republic of Macedonia. Environmental Science and Pollution Research, 20(6), 3781-3788.

Boussen, S., Sebei, A., Soubrand-Colin, M., Bril, H., Chaabani, F., and Abdeljaouad, S. 2010. Mobilization of lead-zinc rich particles from mine tailings in northern Tunisia by aeolian and run-off processes. Bulletin de la Société Géologique de France, 181(5), 459-471.

Brown, S.L., R.L. Chaney, and G.M. Hettiarachchi. 2015. Lead in urban soils: A real or perceived concern for urban agriculture? J. Environ. Quality (electronic journal only) doi:10.2134/jeq2015.07.0376. 11 pp.

Castillo, S., J.D. de la Rosa, A.M. Sánchez de la Campa, Y. González-Castanedo, J.C. Fernández-Caliani, I. Gonzalez, and A. Romero. 2013. Contribution of mine wastes to atmospheric metal deposition in the surrounding area of an abandoned heavily polluted mining district (Rio Tinto mines, Spain). Sci. Total Environ. 449:363-372.

Csavina, J., J. Field, M.P. Taylor, S. Gao, A. Landázuri, E.A. Betterton, and A.E. Sáez. 2012. A review on the importance of metals and metalloids in atmospheric dust and aerosol from mining operations. Sci. Total Environ. 433:58-73.

Cunningham, A.C., and J. Wallinga. 2009. Optically stimulated luminescence dating of young quartz using the fast component. Radiat. Measurements 44:423-428.

Gibson, A.M. 1972. *Wilderness Bonanza-The Tri-State District of Missouri, Kansas, and Oklahoma*. Norman, OK: University of Oklahoma Press, 362pp.

Gill, T.E., R.L. Reynolds, and T.M. Zobeck. 2000. Measurements of current and historic settled dusts in West Texas. Proceedings of the 93rd Air and Waste Management Association (AWMA) Annual Conference and Exhibition, AWMA Publication VIP-07 (ISBN 0-923204-34-2), Paper No. 0175. 15 pp.

Gosar, M., and Miler, M. (2011). Anthropogenic metal loads and their sources in stream sediments of the Meža River catchment area (NE Slovenia). Applied geochemistry, 26(11), 1855-1866.

Gosar, M., R. Šajn, and H. Biester. 2006. Binding of mercury in soils and attic dust in the Idrija mercury mine area (Slovenia). Sci. Total Environ. 369:150-162.

Grill, S. L. 2009. Dust Bowl days: a study of women's lives and experiences. College of William and Mary Undergraduate Honors Thesis. Paper 274.

Gurling, T. 2009. Luminescence Dating of Medieval and Early Modern Brickwork. Durham thesis, Durham University, Durham, United Kingdom. 336 pp.

Huertas, J.I., M.E. Huertas, and D.A. Solís. 2012. Characterization of airborne particles in an open pit mining region. Sci. Total Environ. 423:39-46.

Ilacqua, V., N.C.J. Freeman, J. Fagliano, and P.J. Lioy. 2003. The historical record of air pollution as defined by attic dust. Atmos. Environ. 37:2379-2389.

Johnson, A. W., Gutiérrez, M., Gouzie, D., and McAliley, L. R. 2016. State of remediation and metal toxicity in the Tri-State Mining District, USA. Chemosphere, 144, 1132-1141.

Juracek, K.E. 2013. Occurrence and variability of mining- related lead and zinc in the Spring River flood plain and tributary flood plains, Cherokee County, Kansas, 2009-11. Scientific Investigations Report 2013 – 5028. U.S. Department of the Interior, U.S. Geological Survey, Reston, VA. 70 p.

Kirkham, M.B. 1979. Trace elements, p. 571-575. In: R.W. Fairbridge and C.W. Finkl, Jr. (Editors). The Encyclopedia of Soil Science. Part 1. Physics, Chemistry, Biology, Fertility, and Technology. Dowden, Hutchinson, and Ross, Stroudsburg, PA.

Kirkham, M.B. 2008. Trace elements, p. 786-790. In: Chesworth, W. (Editor). Encyclopedia of Soil Science. Encyclopedia of Earth Sciences Series. Springer, Dordrecht, the Netherlands.

Kristof, N. 2016. America is Flint. The New York Times, 7 Feb. 2016, Sunday Review Section, p. 11. (Vol. 165, No. 57,135, p. SR11).

Lombi, E., and Susini, J. 2009. Synchrotron-based techniques for plant and soil science: opportunities, challenges and future perspectives. Plant and Soil, 320(1-2), 1-35.

Madsen, A.T., and A.S. Murray. 2009. Optically stimulated luminescence dating of young sediments: A review. Geomorphology 109:3-16.

Mejdahl, V. 1985. Thermoluminescence dating of partially bleached sediments. Nuclear Tracks Radiat. Measurements 10:711-715.

Moore, D. M., and Reynolds, R. C. 1989. X-ray Diffraction and the Identification and Analysis of Clay Minerals (Vol. 378). Oxford: Oxford university press.

Moral, R., Gilkes, R. J., and Jordán, M. M. 2005. Distribution of heavy metals in calcareous and non-calcareous soils in Spain. Water, Air, and Soil Pollution, 162(1-4), 127-142.

Neuberger, J.S., Mulhall, M., Pomatto, M.C., Sheverbush, J., Hassanein, R.S. (1990). Health problems in Galena, Kansas: A heavy metal mining superfund site. *Sci. Total Environ.* 94: 261-272.

Norrish, K. 1975. Geochemistry and mineralogy of trace elements, p. 55-81. In: D.J.D. Nicholas and A.R. Egan (Editors). Trace Elements in Soil-Plant-Animal Systems. Academic Press, New York.

Pope, L.M. 2005. Assessment of Contaminated Streambed Sediment in the Kansas Part of the Historic Tri-State Lead and Zinc Mining District, Cherokee County, 2004. USGS Scientific Investigations Report 2005-5251. U.S. Geological Survey, Reston, VA. 61 p.

Pope, L.M. 2005. Assessment of Contaminated Streambed Sediment in the Kansas Part of the Historic Tri-State Lead and Zinc Mining District, Cherokee County, 2004. USGS Scientific Investigations Report 2005-5251. Reston, VA: U.S. Geological Survey, 61pp.

Preusser, F., D. Degering, M. Fuchs, A. Hilgers, A. Kadereit, N. Klasen M. Krbetschek, D. Richter, and J.Q.G. Spencer. 2008. Luminescence dating: basics, methods and application. Quarternary Sci. J. 57:95-149.

Querol, X., Alastuey, A., Lopez-Soler, A., and Plana, F. 2000. Levels and chemistry of atmospheric particulates induced by a spill of heavy metal mining wastes in the Donana area, Southwest Spain. Atmospheric Environment, 34(2), 239-253.

Šajn, R. 2006. Factor analysis of soil and attic-dust to separate mining and metallurgy influence, Meza Valley, Slovenia. Math. Geol. 38:735-747.

Samet, J. M., Dominic, F., Curriero, F. C., Coursac, I., and ZeEger, S. L. 2000. Fine particulate air pollution and mortality in 20 US cities, 1987–1994.New England journal of medicine, 343(24), 1742-1749.

Sauchelli, V. 1969. Trace Elements in Agriculture. Van Nostrand Reinhodl, New York. 248 p.

Sposito, G., L.J. Lund, and A.C. Chang. 1982. Trace metal chemistry in arid-zonc field soils amended with sewage sludge: I. Fractionation of Ni, Cu, Zn, Cd, and Pb in solid phases. Soil Sci. Soc. Amer. 46:260.

Statistical Analysis System. 2013. *SAS Version 9.4*. Cary, NC: SAS Institute.

United States Environmental Protection Agency. 1995. Sampling house dust for lead. Basic concepts and literature review. Final Report. EPA 747-R-95-007. Technical Programs Branch, Chemical Management Division, Office of Pollution Prevention and Toxics, Office of Prevention, Pesticides, and Toxic Substances, U.S. Environmental Protection Agency, Washington, D.C. 98 pp.

Van Pelt, R.S., and T.M. Zobeck. 2007. Chemical constituents of fugitive dust. Environ. Monitoring Assessment 130:3-16.

Van Pelt, R.S., T.M. Zobeck, and T.E. Gill. 2002. Sediment deposition in an attic near a region of dust provenance: Implications for historic regional dust dispersion and deposition patterns. In: J.A. Lee and T.M. Zobeck, Eds. Proceedings of the ICAR5/GCTE-SEN

Joint Conference, International Center for Arid and Semiarid Lands Studies, Texas Tech University, Lubbock, Texas. Publication No. 02-2, p. 347-351.

Völgyesi, P., G. Jordan, D. Zacháry, C. Szabó, A. Bartha, and J. Matschullat. 2014. Attic dust reflects long-term airborne contamination of an industrial area: A case study from Ajka, Hungary. Appl. Geochem. 46:19-29.

von Suchodoletz, H., M. Fuchs, and L. Zöller. 2008. Dating Saharan dust deposits on Lanzarote (Canary Islands) by luminescence dating techniques and their implication for palaeoclimate reconstruction of NW Africa. Geochemistry, Geophysics, Geosystems G^3 (electronic journal only) Vol. 9, No. 3, doi:10.1029/2007GC001658. 19 pp.

Wu, C.D., P.E. Rosenfeld, R.C. Hesse, and J.J. Clark. 2008. Methods for collecting samples for assessing dioxins and other environmental contaminants in attic dust: A review. Organohalogen Compounds 70:527-530.

Yang, Q., H. Chen, and B. Li. 2015. Source identification and health risk assessment of metals in indoor dust in the vicinity of phosphorus mining, Guizhou Province, China. Arch. Environ. Contamination Toxicol. 68:20-30.

Figure 4.1 Locations of dust samples, using two methods, at 9 different sites in Galena, KS. Maps were made using ArcMap version (10.4.1).

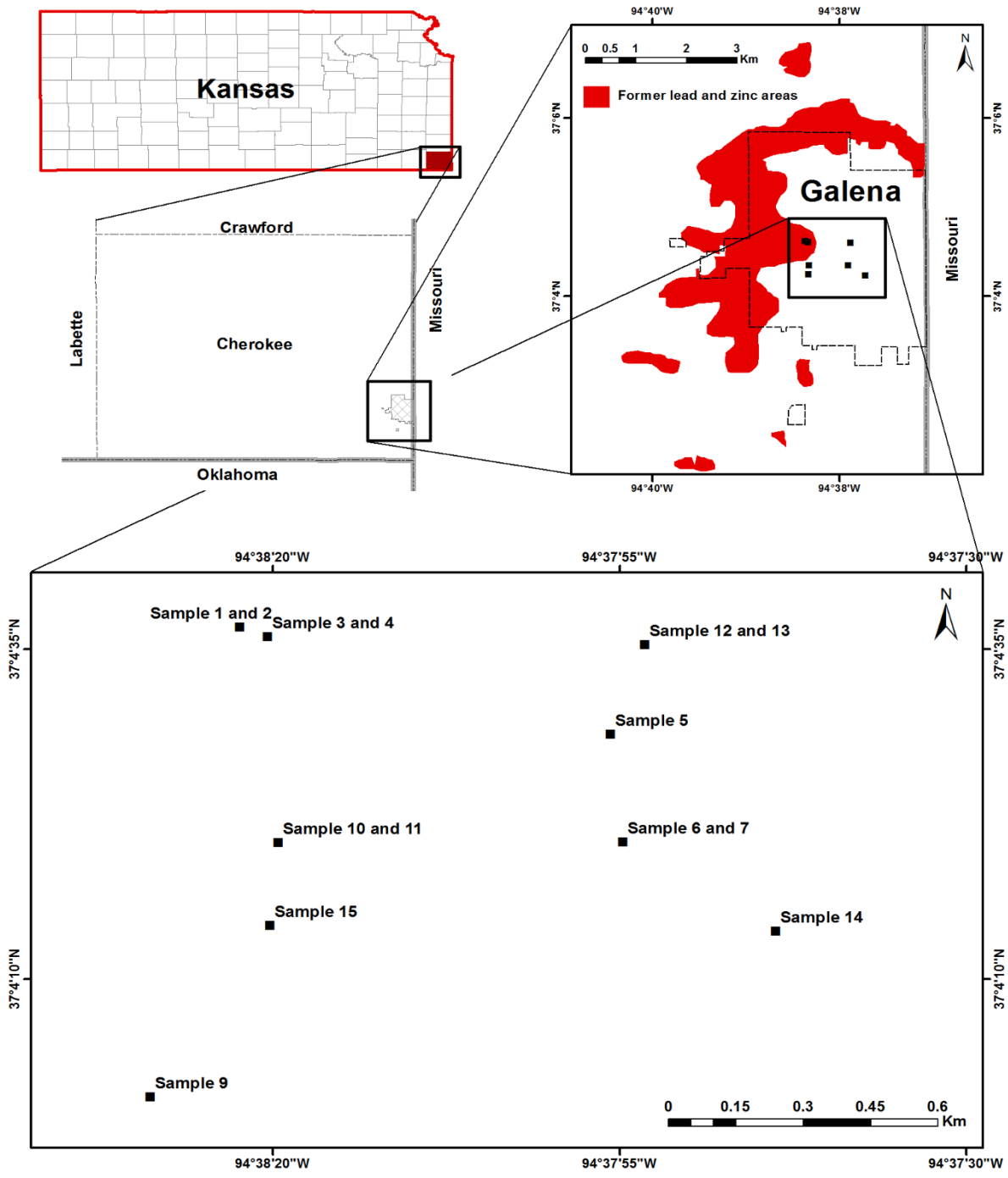

Figure 4.2 Relationship between year of construction and concentration of Pb, Cd, and Zn.

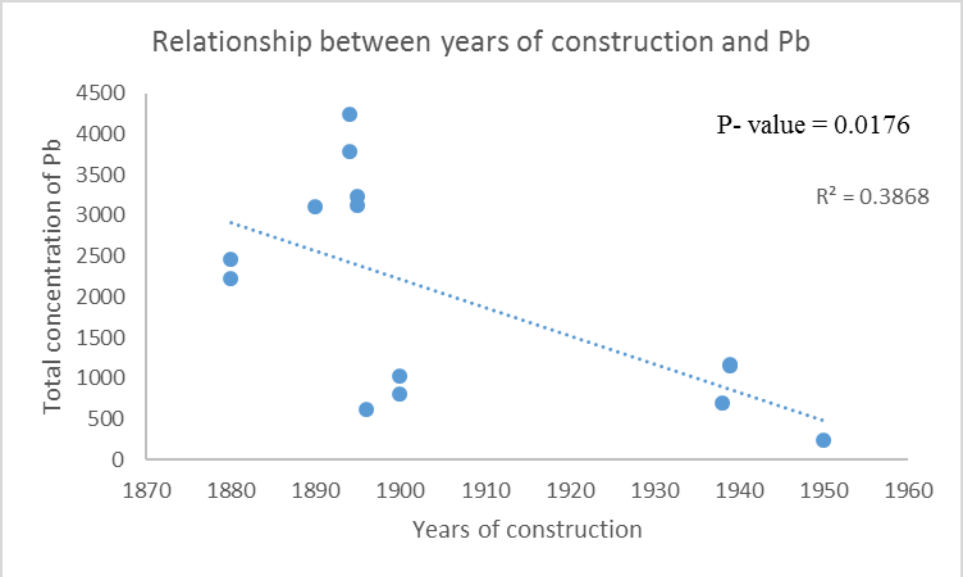

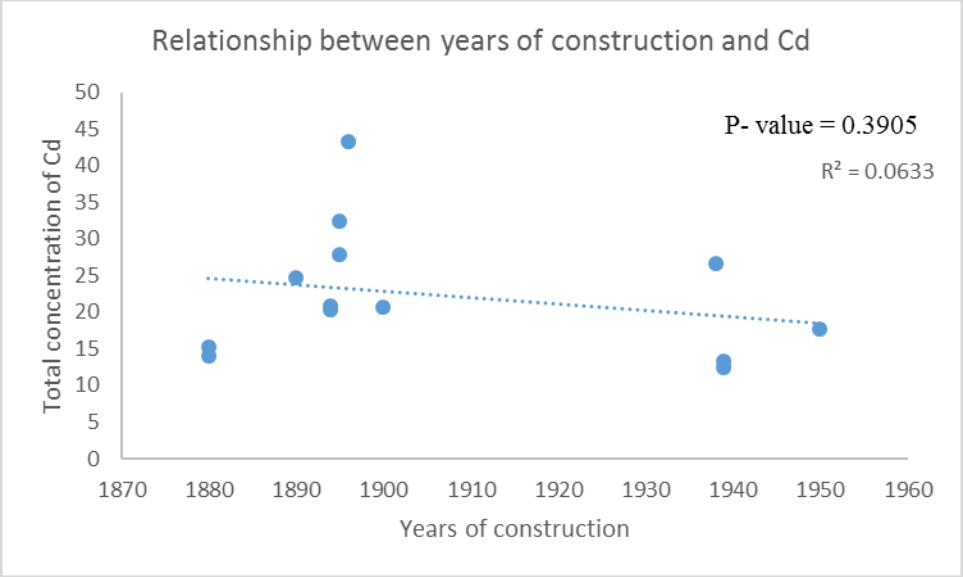

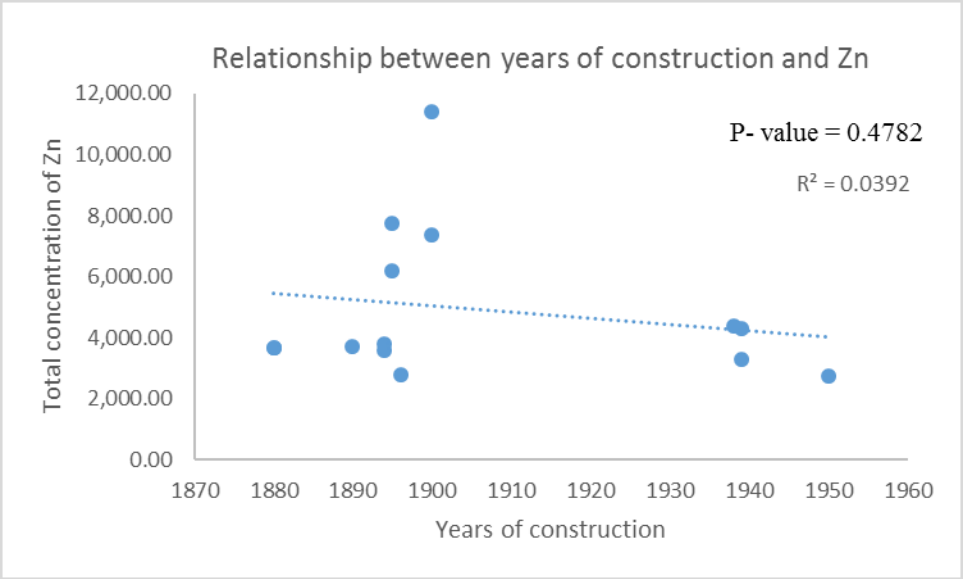
Relationship between years of construction and Zn
P- value = 0.4782
R² = 0.0392
Total concentration of Zn
12,000.00
10,000.00
8,000.00
6,000.00
4,000.00
2,000.00
0.00
1870
1880
1890
1900
1910
1920
1930
1940
1950
1960
Years of construction

Figure 4.3 Scanning electron microscopy (SEM) Secondary electron image (SE) shows the surface morphology from the area of interest (AOI) of dust sample 1, the image shows particles of different size, electron beam hit the sample then get SE image, the frame axis is 200 µm.

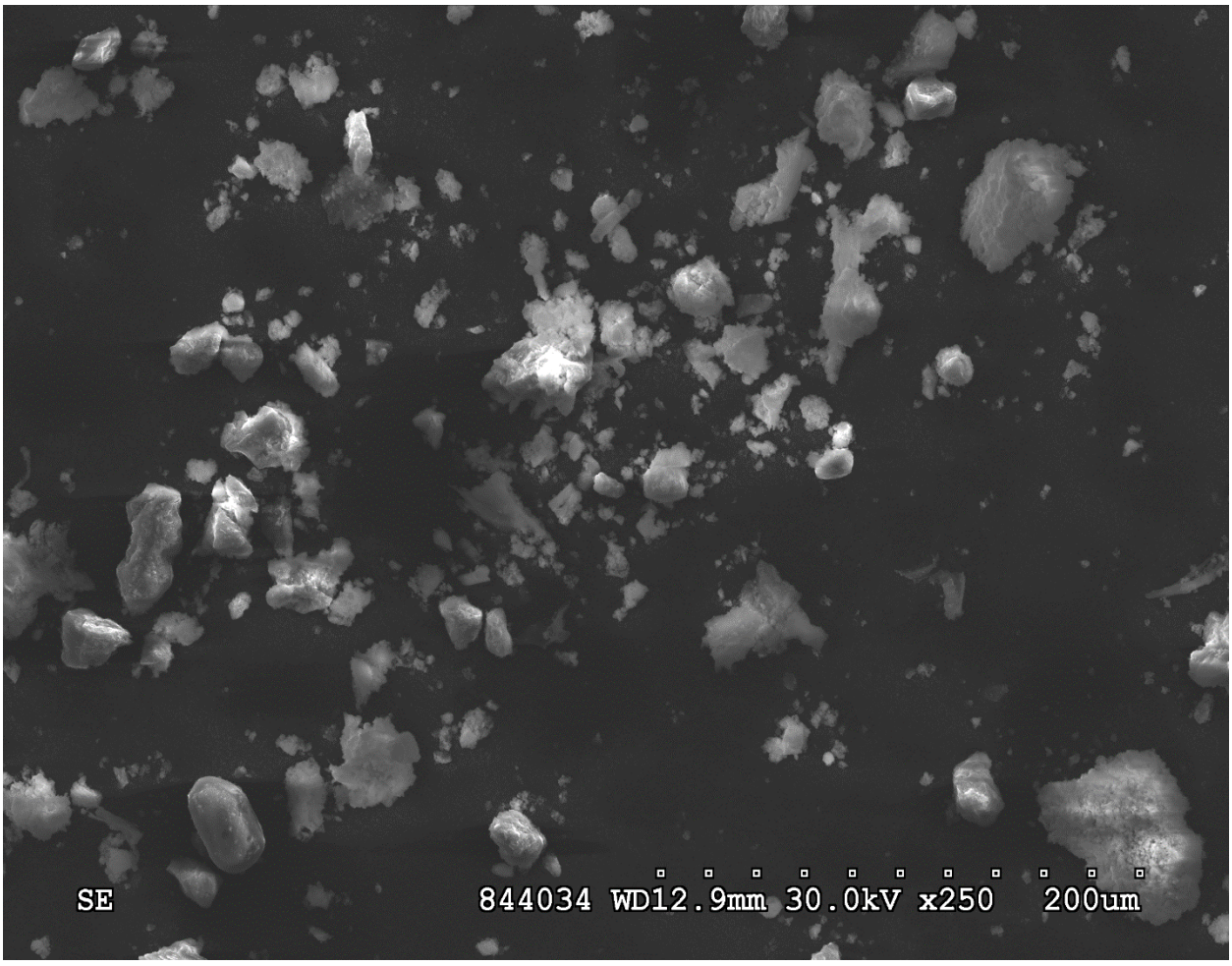

Figure 4.4 Scanning electron microscopy (SEM) Secondary electron image (SE) shows the surface morphology from the area of interest (AOI) of dust sample 2, the image shows particles of different size, electron beam hit the sample then get SE image, the frame axis is 1 mm.

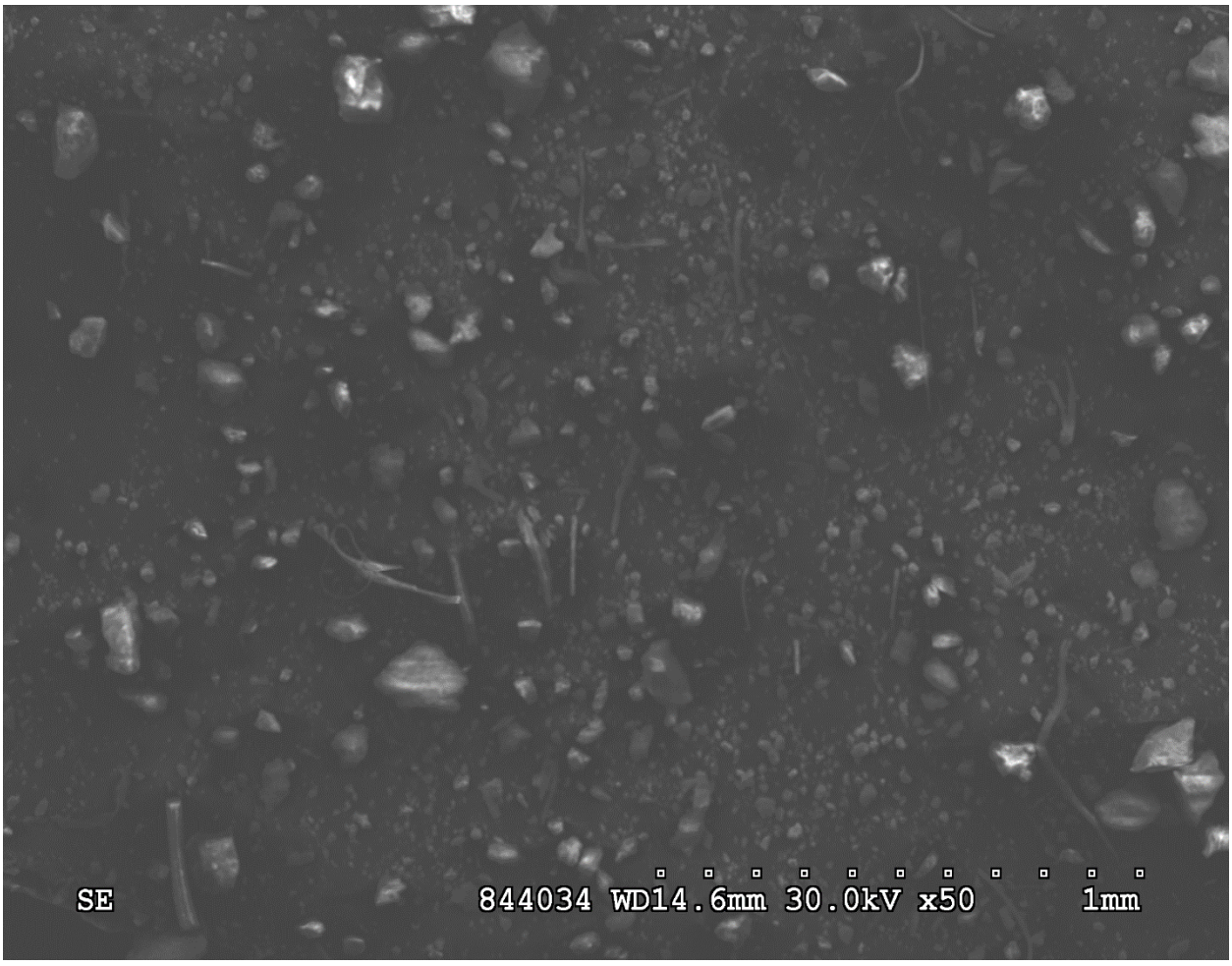

Figure 4.5 Scanning electron microscopy (SEM) Secondary electron image (SE) shows the surface morphology from the area of interest (AOI) of dust sample 3, the image shows particles of different size, electron beam hit the sample then get SE image, the frame axis is 500 µm.

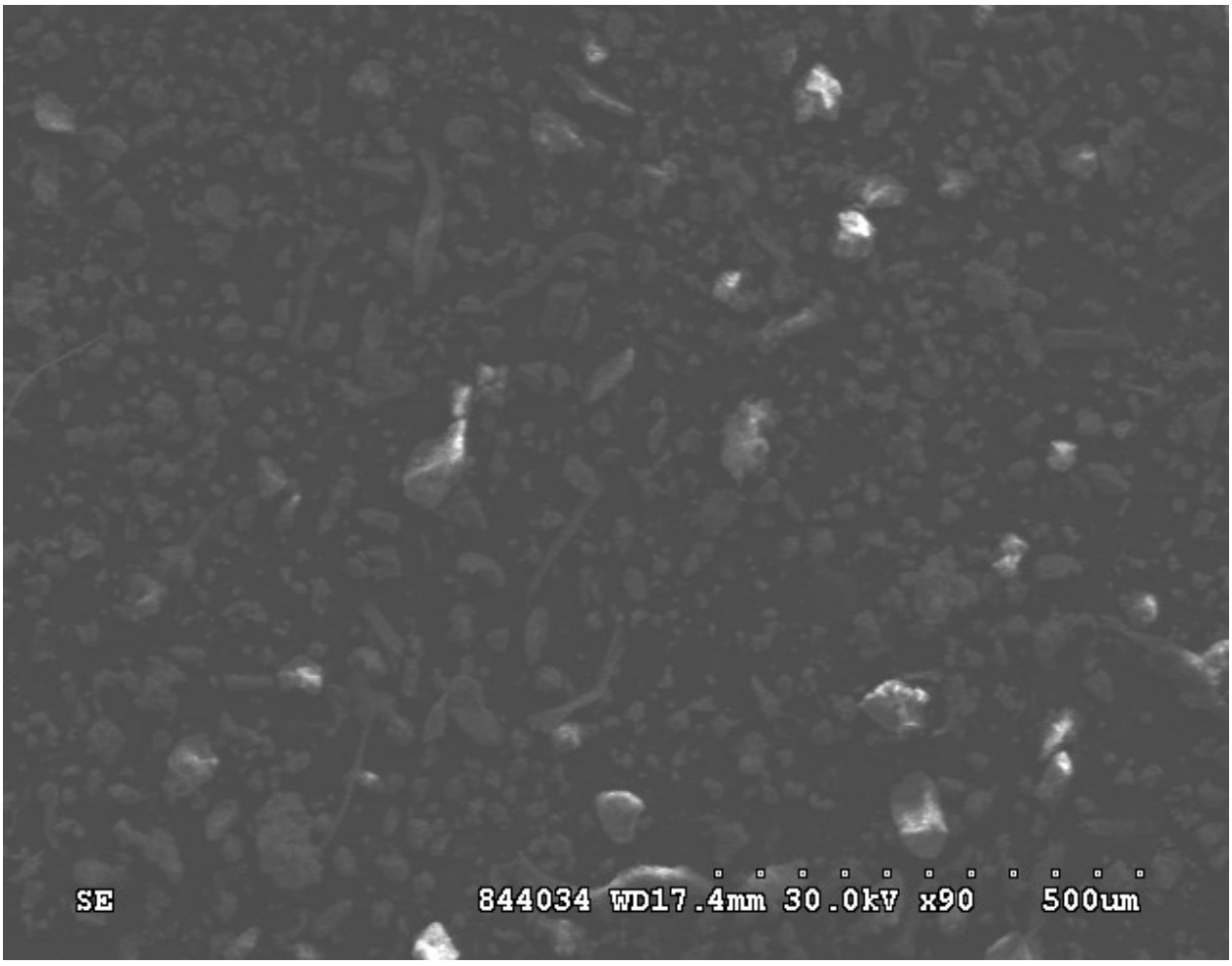

Figure 4.6 Scanning electron microscopy (SEM) Secondary electron image (SE) shows the surface morphology from the area of interest (AOI) of dust sample 4, the image shows particles of different size, electron beam hit the sample then get SE image, the frame axis is 1 mm.

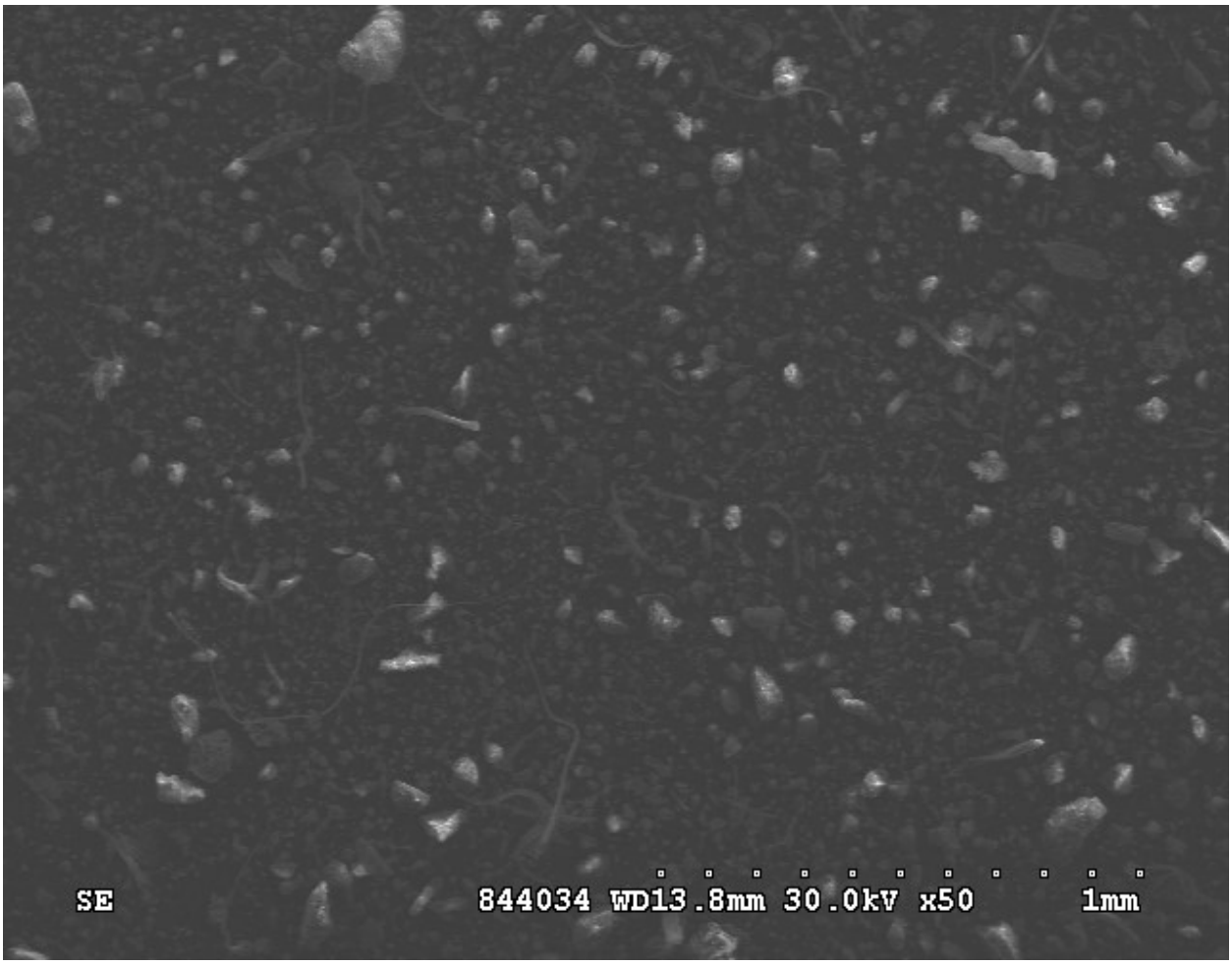

Figure 4.7 Scanning electron microscopy (SEM) back scattered electron (BSE) image shows the surface morphology of dust sample 5, the image shows particles of different size, electron beam hit the sample then get BSE image, selected brighter particles mean high atom number (high Z number), the frame axis is 300 µm.

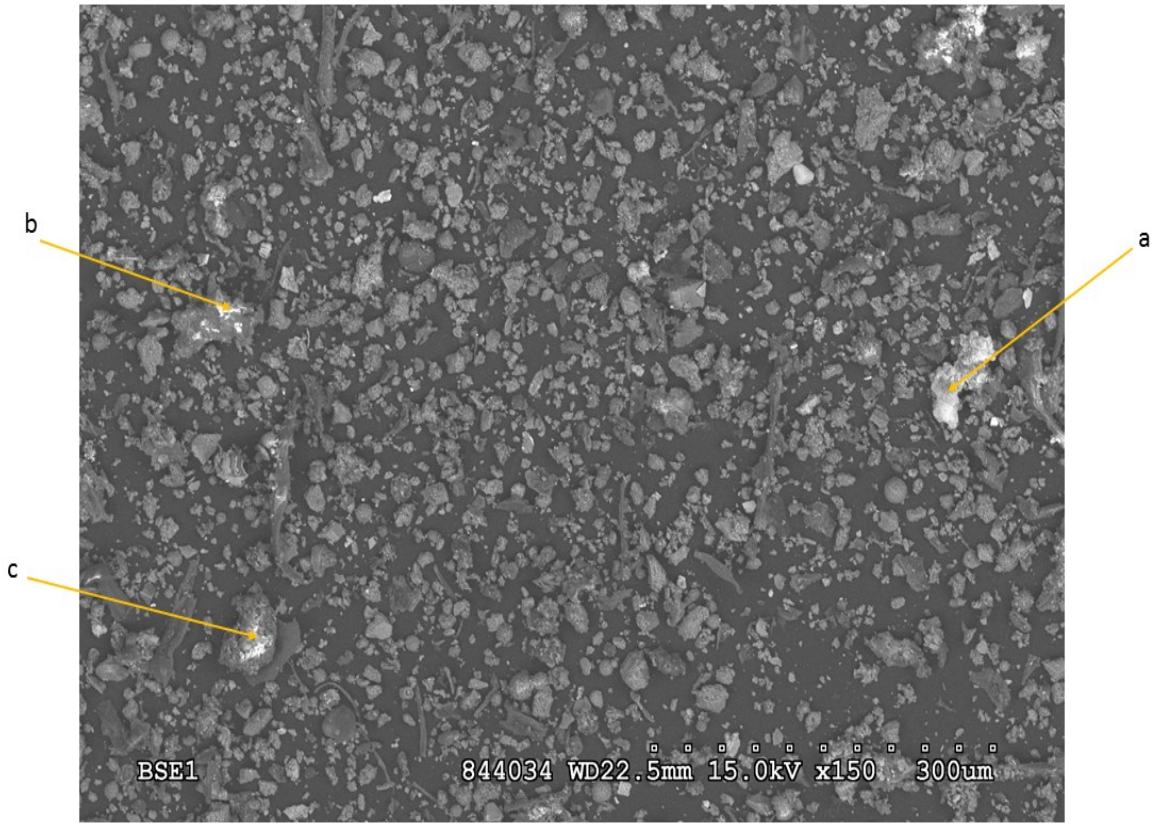

a, b, and c are the particles of interest (POI)

Figure 4.8 Scanning electron microscopy (SEM) back scattered electron (BSE) image shows the surface morphology of dust sample 6, the image shows particles of different size, electron beam hit the sample then get BSE image, selected brighter particles mean high atom number (high Z number), the frame axis is 300 µm.

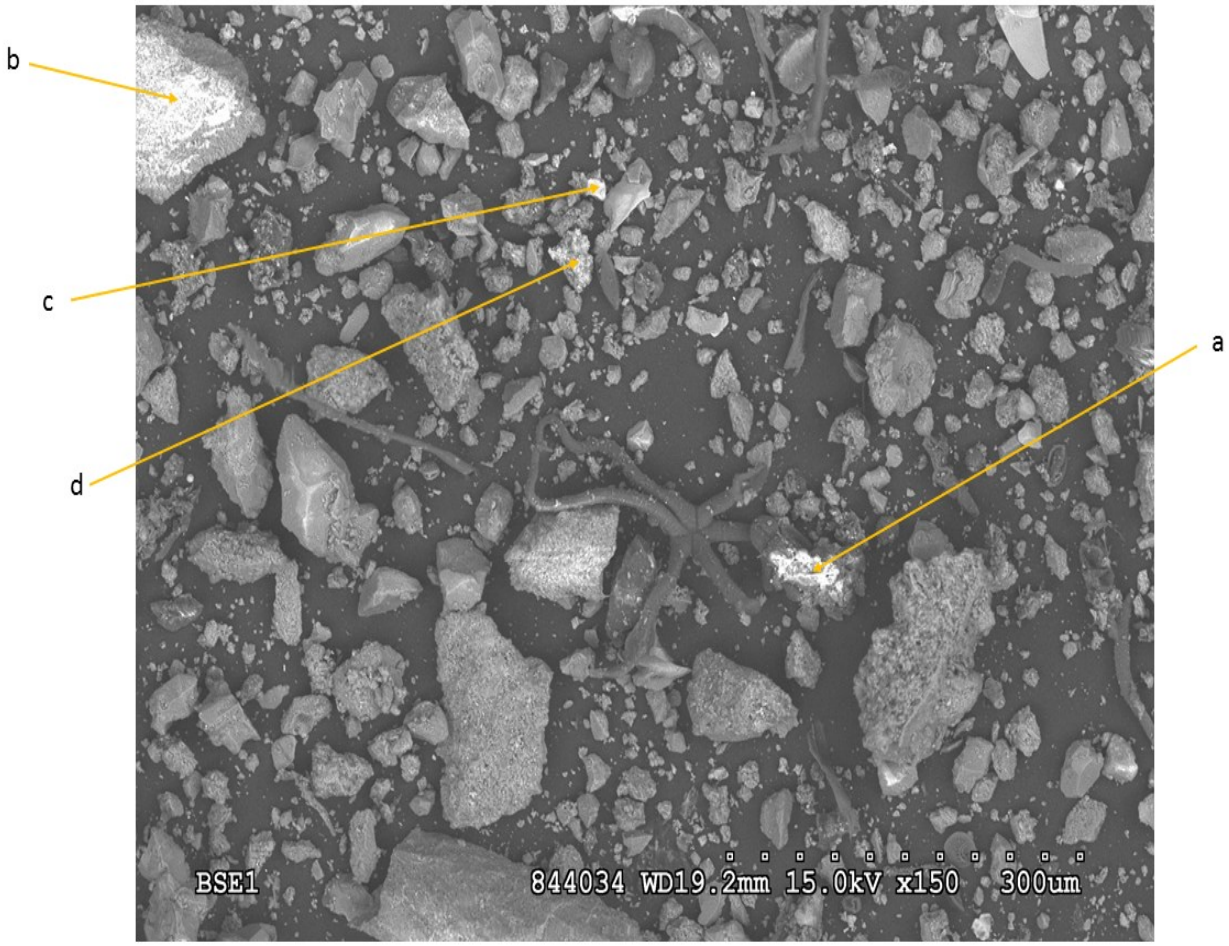

a, b, c, and d are the particles of interest (POI)

Figure 4.9 Scanning electron microscopy (SEM) back scattered electron (BSE) image shows the surface morphology of dust sample 7, the image shows particles of different size, electron beam hit the sample then get BSE image, selected brighter particles mean high atom number (high Z number), the frame axis is 300 µm.

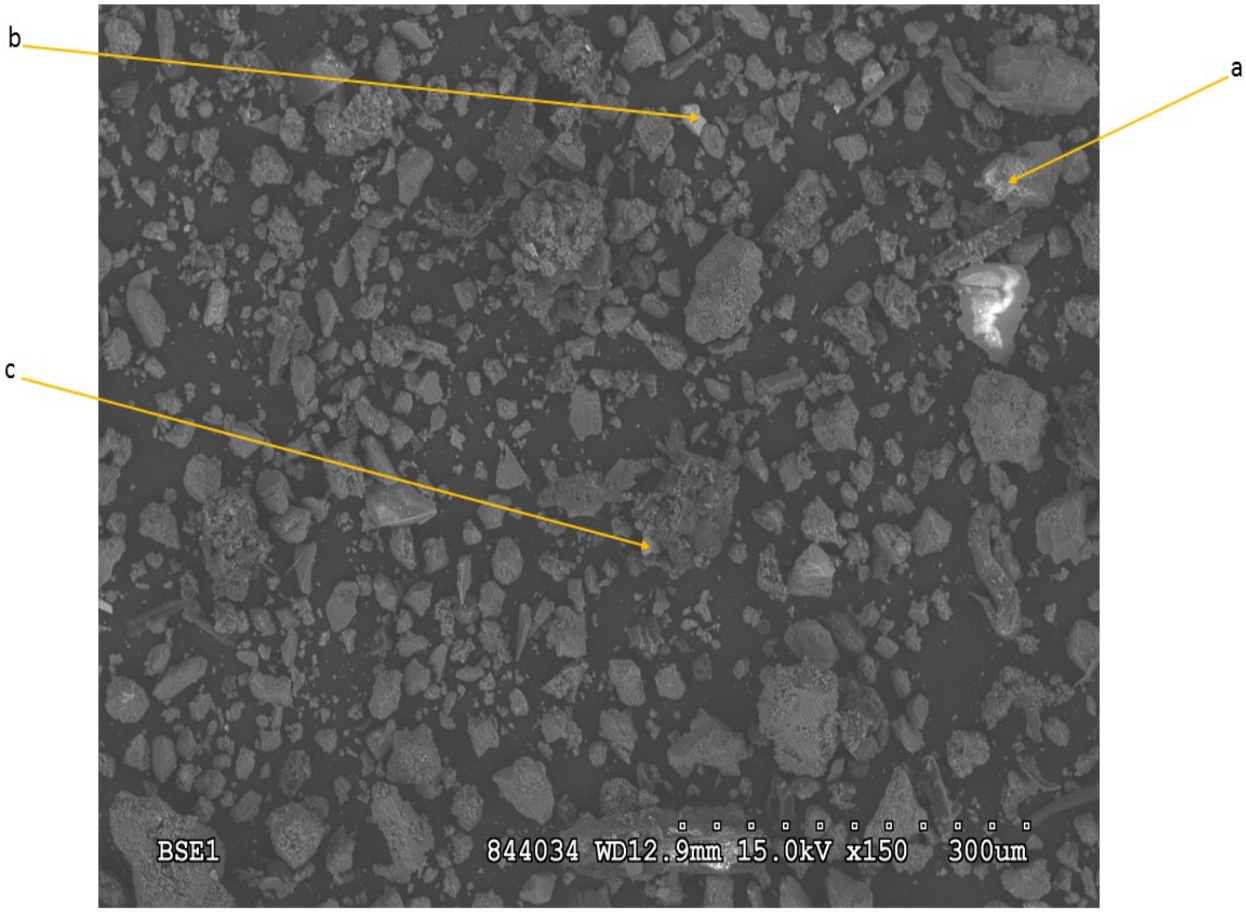

a, b, and c are the particles of interest (POI)

Figure 4.10 Scanning electron microscopy (SEM) back scattered electron (BSE) image shows the surface morphology of dust sample 9, the image shows particles of different size, electron beam hit the sample then get BSE image, selected brighter particles mean high atom number (high Z number), the frame axis is 300 µm.

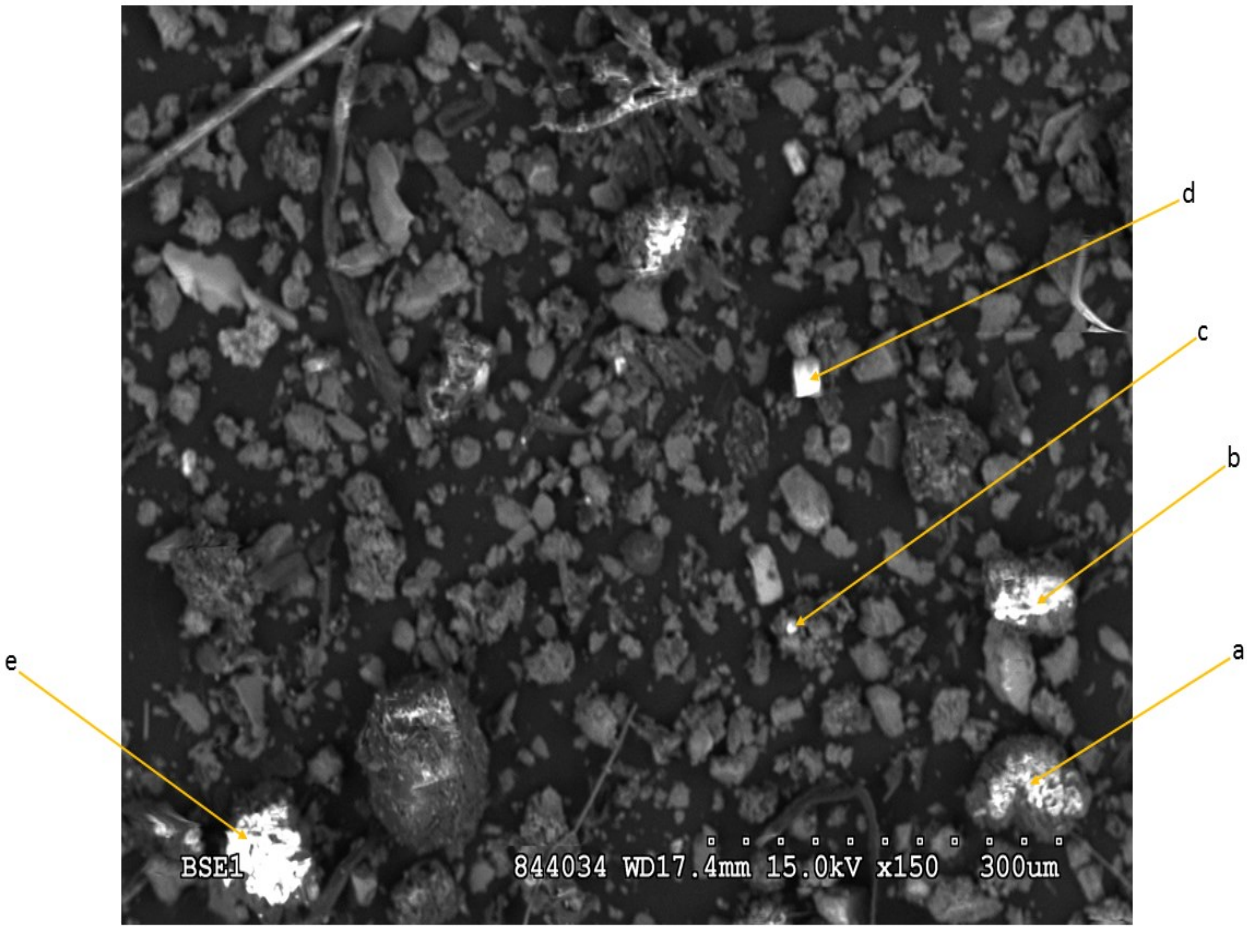

a, b, c, d, and e are the particles of interest (POI)

Figure 4.11 Scanning electron microscopy (SEM) back scattered electron (BSE) image shows the surface morphology of dust sample 10, the image shows particles of different size, electron beam hit the sample then get BSE image, selected brighter particles mean high atom number (high Z number), the frame axis is 300 µm.

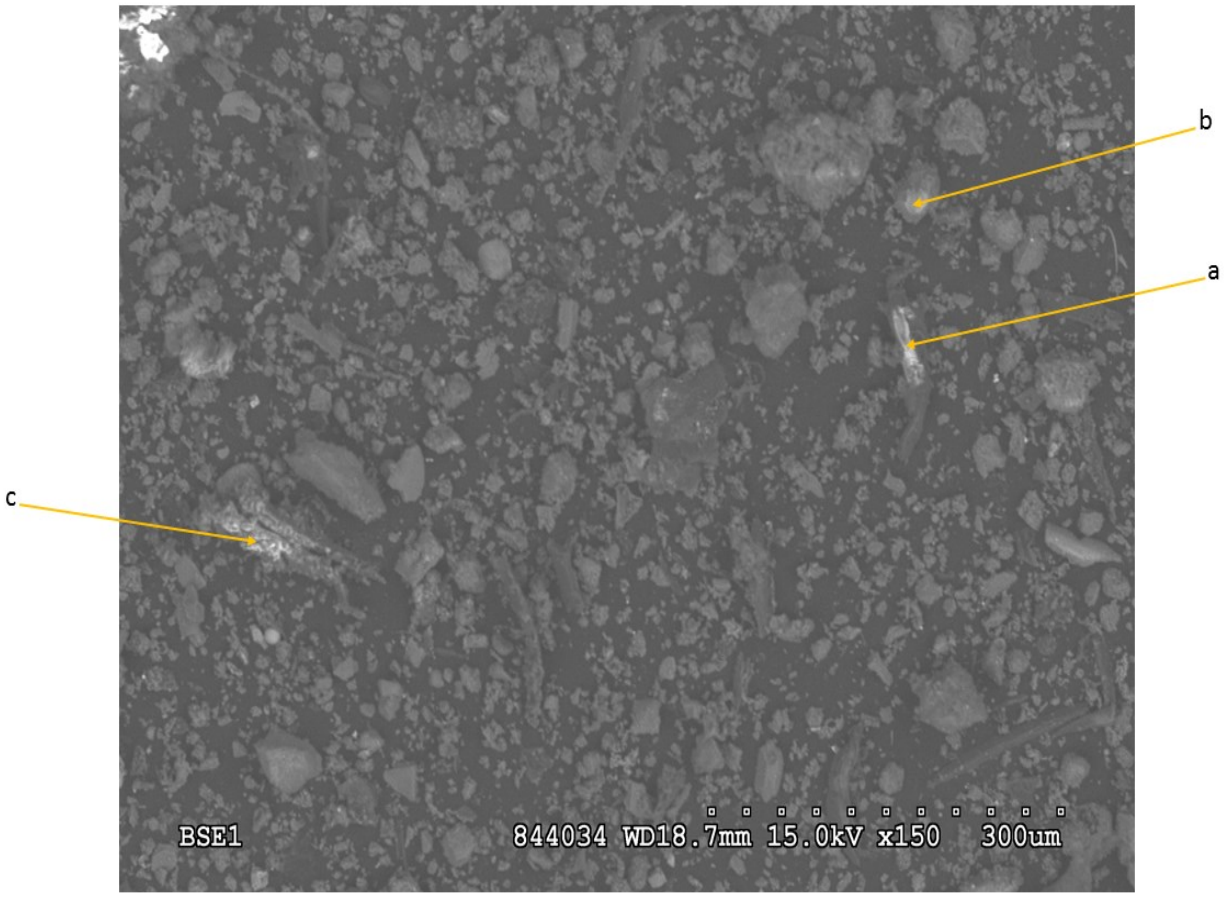

a, b, and c are the particles of interest (POI)

Figure 4.12 Scanning electron microscopy (SEM) back scattered electron (BSE) image shows the surface morphology of dust sample 11, the image shows particles of different size, electron beam hit the sample then get BSE image, selected brighter particles mean high atom number (high Z number), the frame axis is 30 µm.

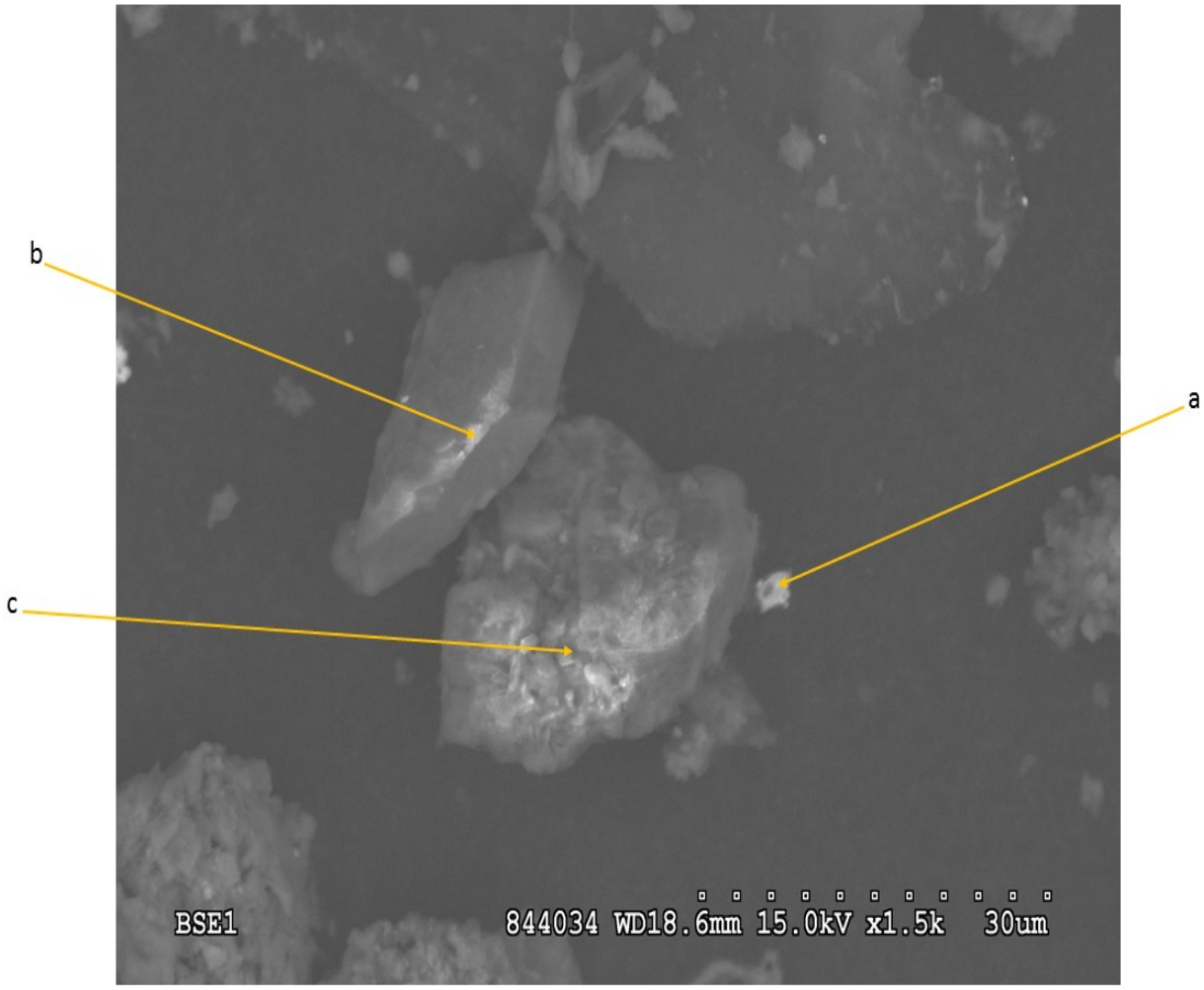

a, b, and c are the particles of interest (POI)

Figure 4.13 Scanning electron microscopy (SEM) back scattered electron (BSE) image shows the surface morphology of dust sample 12, the image shows particles of different size, electron beam hit the sample then get BSE image, selected brighter particles mean high atom number (high Z number), the frame axis is 300 µm.

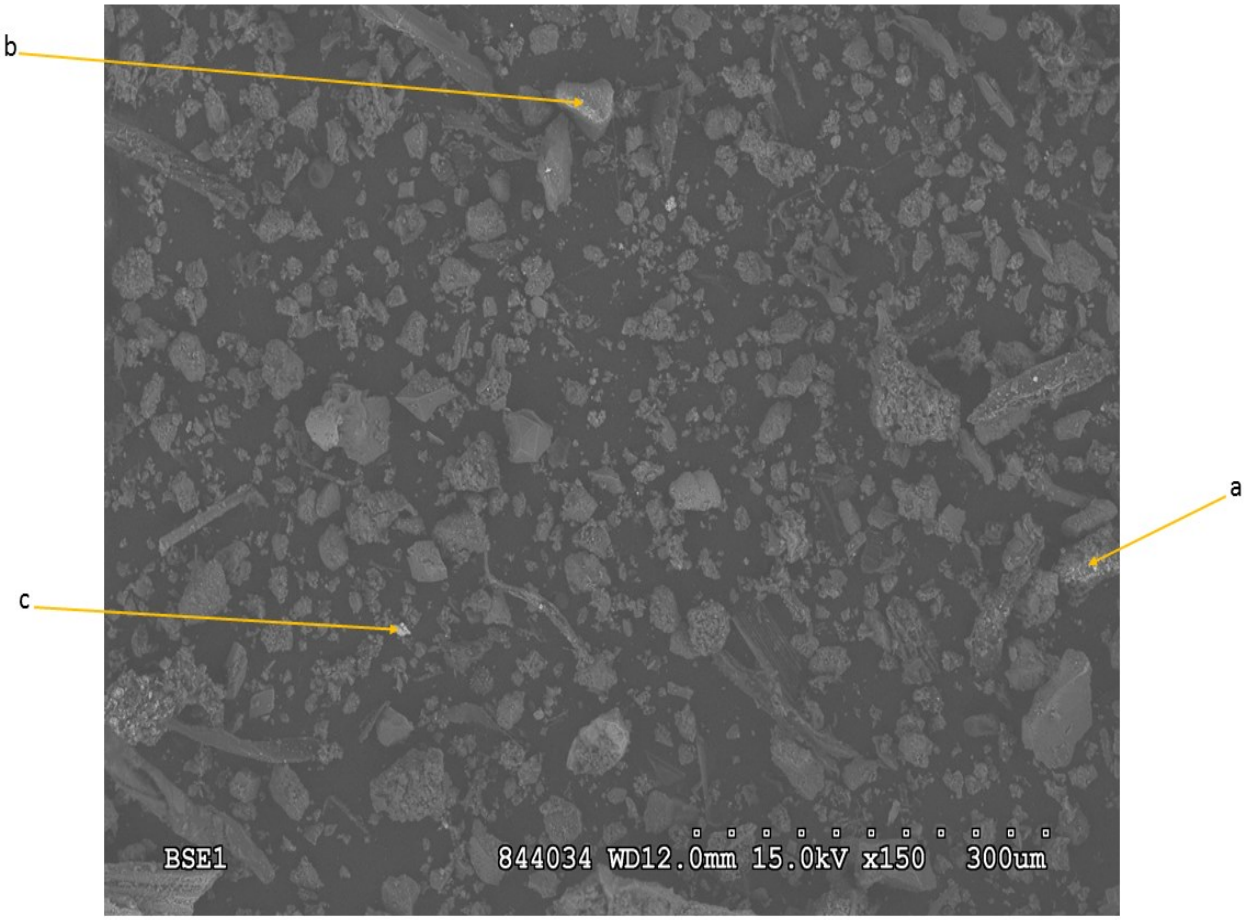

a, b, and c are the particles of interest (POI)

Figure 4.14 Scanning electron microscopy (SEM) back scattered electron (BSE) image shows the surface morphology of dust sample 13, the image shows particles of different size, electron beam hit the sample then get BSE image, selected brighter particles mean high atom number (high Z number), the frame axis is 30 µm.

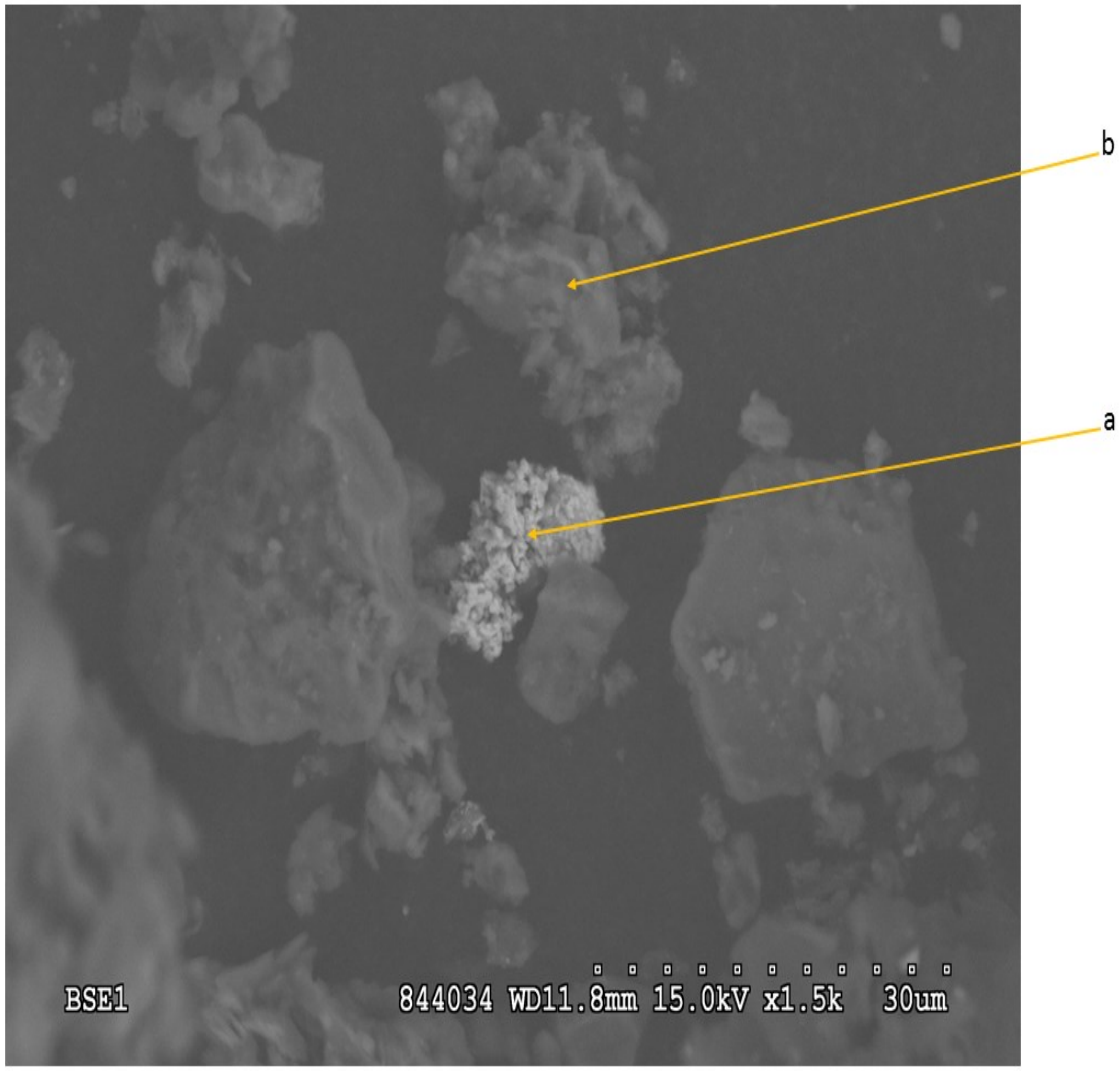

a and b are the particles of interest (POI)

Figure 4.15 Scanning electron microscopy (SEM) back scattered electron (BSE) image shows the surface morphology of dust sample 14, the image shows particles of different size, electron beam hit the sample then get BSE image, selected brighter particles mean high atom number (high Z number), the frame axis is 300 µm.

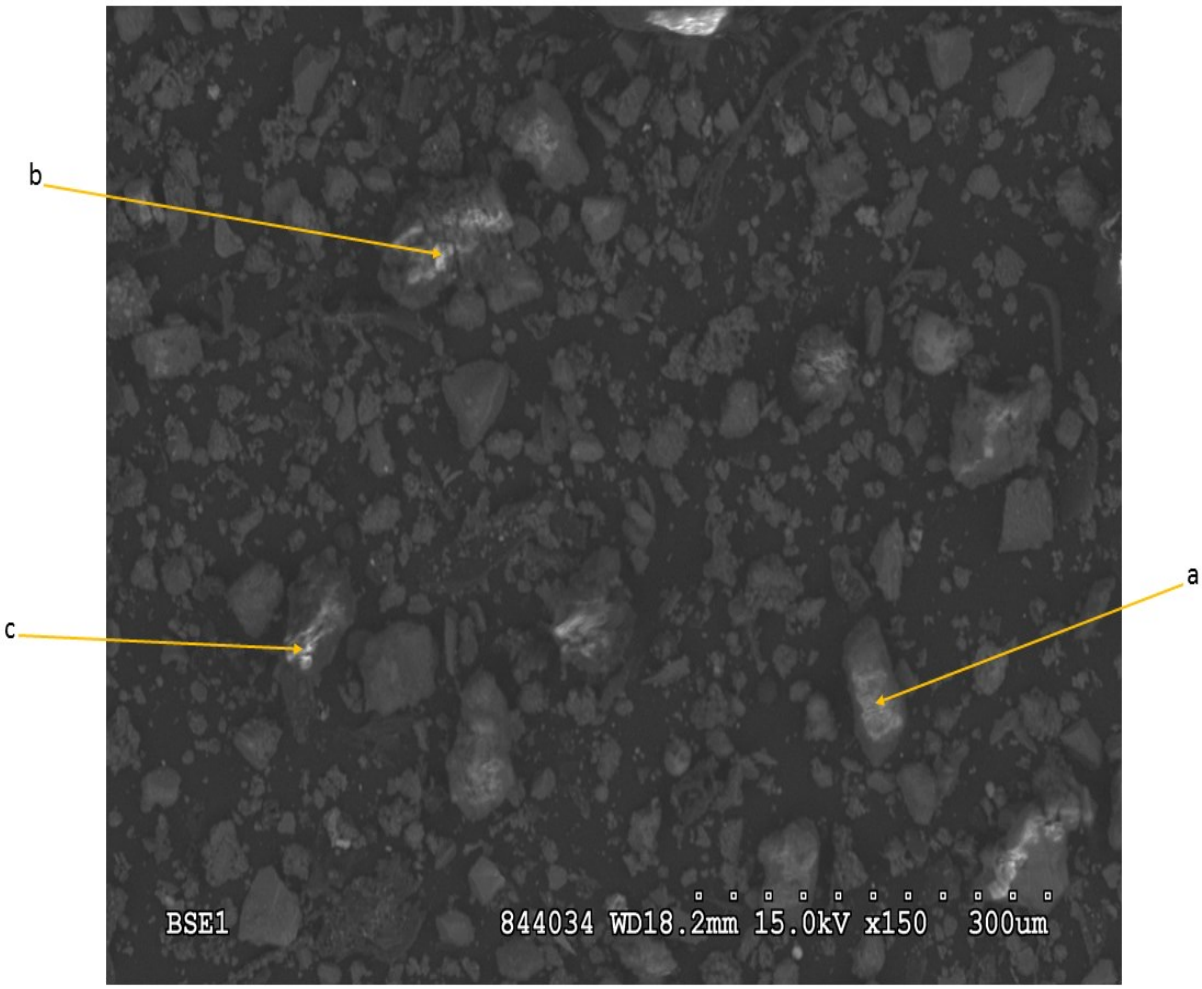

a, b, and c are the particles of interest (POI)

Figure 4.16 Scanning electron microscopy (SEM) back scattered electron (BSE) image shows the surface morphology of dust sample 15, the image shows particles of different size, electron beam hit the sample then get BSE image, selected brighter particles mean high atom number (high Z number), the frame axis is 30 and 20 µm.

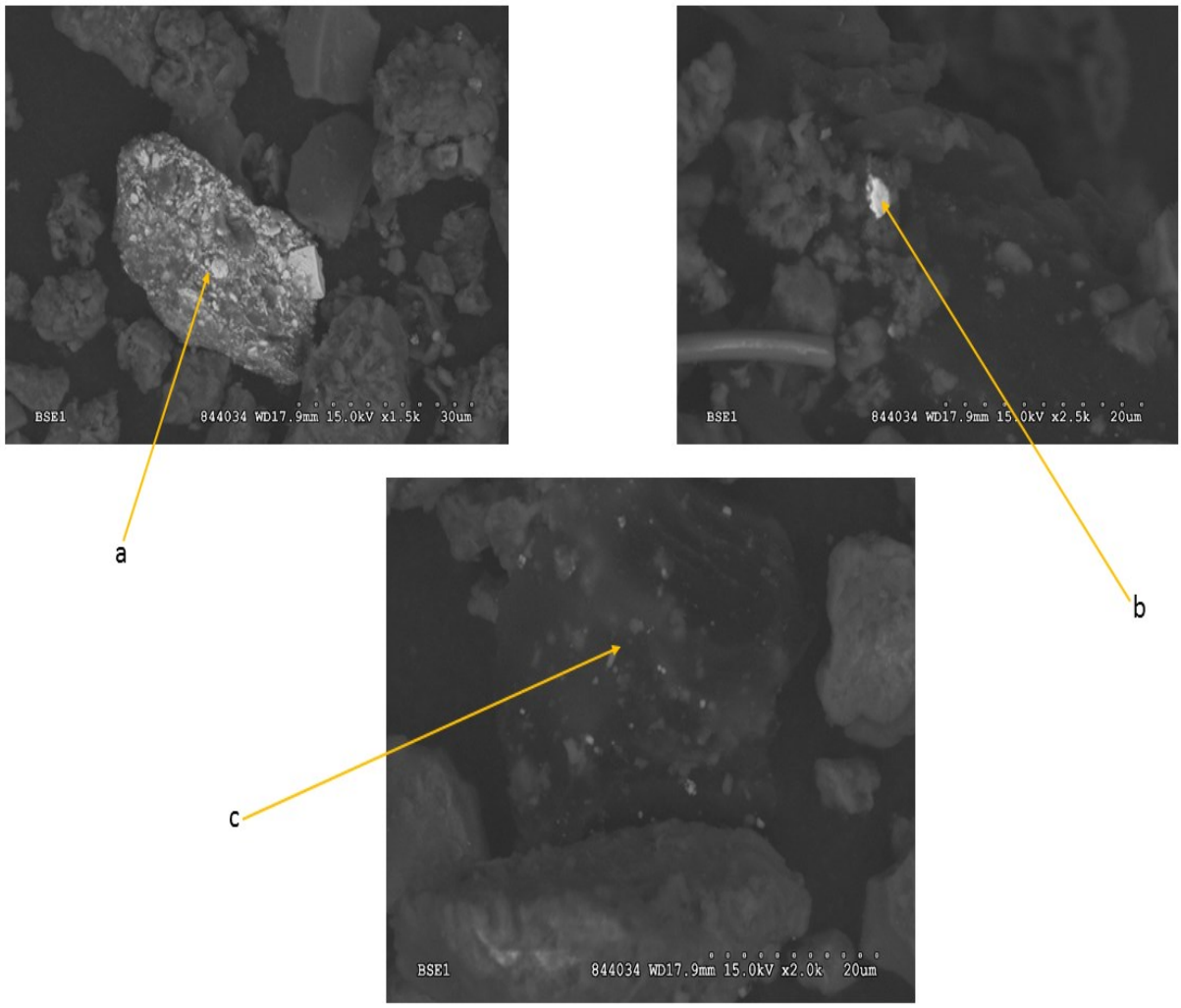

a, b, and c are the particles of interest (POI)

Table 4.1 Dust samples description

Dust Sample No	Date of Sampling	Methods	Type of Building	Floor of the Attics	Year of Construction	Building made out of	Area sampled (m^2)
1	8/20/2015	sweeping	Store	First	1900	Brick	1.83 X 1.83
2	8/20/2015	vacuuming	Store	First	1900	Brick	1.83 X 1.83
3	8/20/2015	sweeping	Store	Second	1895	Brick	1.23 X 1.23
4	8/20/2015	vacuuming	Store	Second	1895	Brick	1.23 X 1.23
5*	4/7/2016	sweeping	School	Basement	1938	Brick & Concrete	3.05 X 0.51
6	4/7/2016	sweeping	Galena Waterworks	First	1939	Brick & Concrete	1.07 X 1.07
7†	4/7/2016	vacuuming	Galena Waterworks	First	1939	Brick & Concrete	1.07 X 1.07
9†	4/7/2016	sweeping	House	Second	1950	Wood	2.44 X 0.61
10	4/8/2016	sweeping	Church	First	1880	Brick &Wood	1.22 X 0.91
11	4/8/2016	vacuuming	Church	First	1880	Brick &Wood	1.52 X 1.22
12	4/8/2016	sweeping	House	Second	1894	Wood	2.13 X 1.83
13	4/8/2016	vacuuming	House	Second	1894	Wood	1.52 X 1.07
14	4/8/2016	sweeping	House	Second	1890	Wood	1.37 X 1.37
15	4/8/2016	sweeping	House	Second	1896	Wood	0.76 X 0.76

*Not Attic.

†There was no Sample 8. When the sample was brought out of the attic into bright light, it was found that it was sawdust and not dust.

Table 4.2 Concentration of seven heavy metals in dust samples from Galena, Kansas, collected either by sweeping the floor or vacuuming the floor. Concentrations of the heavy metals in the mine waste materials also are given, along with the ratio of the concentration of the heavy metal in the dust sample divided by the concentration in the mine waste materials. Nine different buildings were sampled. Samples 1 and 2, 3 and 4, 6 and 7, 10 and 11, and 12 and 13 came from the same building, with one sample being swept and one sample being vacuumed. Each value is an individual measurement.

Dust sample[†]	Cd	Cu	Fe	Mn	Ni	Pb	Zn
	---------- $\mu g\ g^{-1}$ ----------						
1 (sweep)	21.6	224.9	9586.5	263.1	111.3	799.0	11,419.2
2 (vacuum)	20.7	232.9	5965.0	221.6	115.1	1021.8	7382.1
3 (sweep)	27.8	146.6	14,698.9	222.4	51.7	3239.3	7730.2
4 (vacuum)	32.5	148.0	15,074.3	188.8	64.6	3131.0	6200.5
5 (sweep)	26.6	3231.8	8151.9	341.6	20.8	703.5	4376.3
6 (sweep)	12.4	223.5	6951.0	183.1	71.7	1153.5	4287.7
7[‡] (vacuum)	13.4	337.7	8050.3	279.2	34.2	1167.2	3286.7
9[‡] (sweep)	17.7	83.4	6441.0	339.0	6.7	243.4	2738.8
10 (sweep)	15.3	73.6	9788.1	303.2	68.9	2467.9	3676.2
11 (vacuum)	14.0	65.4	9491.4	263.7	58.6	2227.6	3657.6
12 (sweep)	20.8	125.4	13,777.2	469.4	73.9	4250.2	3793.3
13 (vacuum)	20.4	149.6	10,313.7	418.2	60.2	3783.9	3600.4
14 (sweep)	24.7	282.9	9337.0	385.9	71.0	3113.0	3693.9
15 (sweep)	43.3	17.5	7786.8	716.2	13.5	619.5	2766.1
Aver. all samples	22.2	381.7	9672.4	328.2	58.7	1994.3	4900.6
Aver. Sweeping	23.4	490.0	8679.5	358.2	54.4	1843.3	4942.4
Aver. Vacuuming	20.2	186.7	9778.9	274.3	66.5	2266.3	4825.5
Mine waste materials	31.3b	44.1	3618.9	62.0	2.9	2643.0	3480.0
Non-contaminated soil[§]	0.5 (0.01-0.7)	20 (2-100)	30,000 (200-100,000)	850 (100-4000)	40 (0.2-5000)	10 (2-200)	50 (10-300)
	---------- Ratio of average value of dust to mine waste materials ----------						
Ratio (unitless)	0.7	8.7	2.7	5.3	20.2	0.8	1.4

[†] For a description of each sample, see Table 1.

[‡] There was no Sample 8. When the sample was brought out of the attic into bright light, it was found that it was sawdust and not dust.

[§] Average values and ranges come from Kirkham (1979), except for Ni, which comes from Kirkham (2008). Kirkham (1979, 2008) does not give values for Fe. The average value for Fe comes from Norrish (1975), and the range for Fe comes from Sauchelli (1969, p.40).

Table 4.3 Enrichment ratio (unitless) for each dust sample compared to mine waste materials from Site A.

Dust sample	Cd	Cu	Fe	Mn	Ni	Pb	Zn
	……..……Unitless……						
1	0.7	5.1	2.6	4.2	38.4	0.3	3.3
2	0.7	5.3	1.6	3.6	39.7	0.4	2.1
3	0.9	3.3	4.1	3.6	17.8	1.2	2.2
4	1.0	3.4	4.2	3.0	22.3	1.2	1.8
5	0.9	73.3	2.3	5.5	7.2	0.3	1.3
6	0.4	5.1	1.9	3.0	24.7	0.4	1.2
7	0.4	7.7	2.2	4.5	11.8	0.4	0.9
9	0.6	1.9	1.8	5.5	2.3	0.1	0.8
10	0.5	1.7	2.7	4.9	23.7	0.9	1.1
11	0.4	1.5	2.6	4.3	20.2	0.8	1.1
12	0.7	2.8	3.8	7.6	25.5	1.6	1.1
13	0.7	3.4	2.8	6.7	20.8	1.4	1.0
14	0.8	6.4	2.6	6.2	24.5	1.2	1.1
15	1.4	0.4	2.2	11.6	4.7	0.2	0.8
Average	0.7	8.7	2.7	5.3	20.3	0.8	1.4
Max	1.4	73.3	4.2	11.6	39.7	1.6	3.3
Min	0.4	0.4	1.6	3.0	2.3	0.1	0.8

The dust sample values given in table 4.2 were divided by the concentration of the heavy metals of the mine waste for the site A in $\mu g\ g^{-1}$ (Cd, 31.3; Cu, 44.1; Fe, 3618.9; Mn, 62.0; Ni, 2.9; Pb, 2643.0; Zn, 3480.0).

Table 4.4 Enrichment ratio (unitless) for each dust samples compare to different soils from Cherokee county.

Dust sample	Cd	Pb	Zn
	……..……..Unitless……..……		
1	0.9	0.5	2.4
2	0.8	0.6	1.5
3	1.1	1.9	1.6
4	1.3	1.9	1.3
5	1.1	0.4	0.9
6	0.5	0.7	0.9
7	0.5	0.7	0.7
9	0.7	0.1	0.6
10	0.6	1.5	0.8
11	0.6	1.3	0.8
12	0.8	2.5	0.8
13	0.8	2.3	0.7
14	1.0	1.9	0.8
15	1.8	0.4	0.6
Average	0.9	1.2	1.0
Max	1.8	2.5	2.4
Min	0.5	0.1	0.6

The dust sample values given in table 4.2 were divided by the average concentration of the heavy metals of soils in Cherokee county in $\mu g\ g^{-1}$ (Cd, 24.6; Pb, 1670.1; Zn, 4828.3) **(**Juracek, 2013).

Table 4.5 Major minerals that occur in dust using x-ray diffraction (XRD) of the <150 µm from 9 different sites at Galena, KS. The order that the minerals listed in do not reflect the abundance.

Sample number	Minerals	Formula
1	Quartz	SiO_2
	Riebeckite	$Na_2Fe_3Fe_2(Si_8O_{22})(OH)_2$
	Calcite	$CaCO_3$
	Cerium ammonium nitrate	$(NH_4)_2Ce(NO_3)_6$
	Galena	PbS
	Aragonite	$CaCO_3$
	Sphalerite	ZnS
2	Calcite	$CaCO_3$
	Quartz	SiO_2
	Dolomite	$CaMg(CO_3)_2$
	Aragonite	$Ca(CO_3)$
	Iron aluminum	AlFe
	Sphalerite	ZnS
3	Quartz	SiO_2
	Goethite	FeO(OH)
	Calcite	$CaCO_3$
	Aragonite	$CaCO_3$
	Iron aluminum	AlFe
4	Quartz	SiO_2
	Jarosite	$KFe_3(SO_4)_2(OH)_6$
	Goethite	FeO(OH)
	Aragonite	$CaCO_3$
	Sphalerite	ZnS
	Marcasite	FeS_2
5	Anglesite	$Pb(SO_4)$
	Microcline	$KAlSi_3O_8$
	Muscovite	$KAl_3Si_3O_{10}(OH)_{1.8}F_{0.2}$
	Goethite	FeO(OH)
	Calcite	$CaCO_3$
	Quartz	SiO_2

	Hematite	Fe_2O_3
	Rutile	TiO_2
6	Anglesite	$Pb(SO_4)$
	Muscovite	$KAl_3Si_3O_{10}(OH)_{1.8}F_{0.2}$
	Goethite	$FeO(OH)$
	Calcite	$CaCO_3$
	Aragonite	$CaCO_3$
	Marcasite	FeS_2
	Aluminum Iron	$AlFe$
	Sphalerite	ZnS
	Pyrite	FeS_2
	Quartz	SiO_2
7	Anglesite	$Pb(SO_4)$
	Calcite	$CaCO_3$
	Goethite	$FeO(OH)$
	Cerium ammonium nitrate	$(NH_4)_2Ce(NO_3)_6$
	Aragonite	$CaCO_3$
	Marcasite	FeS_2
	Quartz	SiO_2
	Iron aluminum	$AlFe$
	Muscovite	$KAl_3Si_3O_{10}(OH)_{1.8}F_{0.2}$
9	Goethite	$Fe^{3+}O(OH)$
	Iron aluminum	$AlFe$
	Quartz	SiO_2
	Calcite	$CaCO_3$
10	Wavellite	$Al_3(PO_4)_2(OH)_3F_{0.5}•5(H_2O)$
	Goethite	$FeO(OH)$
	Calcite	$CaCO_3$
	Aragonite	$CaCO_3$
	Galena	PbS
	Quartz	SiO_2
	Iron aluminum	$AlFe$
11	Anglesite	$Pb(SO_4)$

	Goethite	$FeO(OH)$
	Calcite	$CaCO_3$
	Muscovite	$KAl_3Si_3O_{10}(OH)_{1.8}F_{0.2}$
	Aragonite	$CaCO_3$
	Quartz	SiO_2
12	Anglesite	$Pb(SO_4)$
	Goethite	$FeO(OH)$
	Calcite	$CaCO_3$
	Sphalerite	ZnS
	Muscovite	$KAl_3Si_3O_{10}(OH)_{1.8}F_{0.2}$
	Aragonite	$CaCO_3$
	Quartz	SiO_2
	Iron aluminum	$AlFe$
13	Anglesite	$Pb(SO_4)$
	Muscovite	$KAl_3Si_3O_{10}(OH)_{1.8}F_{0.2}$
	Goethite	$FeO(OH)$
	Calcite	$CaCO_3$
	Aragonite	$CaCO_3$
	Quartz	SiO_2
	Iron aluminum	$AlFe$
14	Microcline	$KAlSi_3O_8$
	Orthoclase	$KAlSi_3O_8$
	Quartz	SiO_2
	Calcite	$CaCO_3$
15	Anglesite	$Pb(SO_4)$
	Goethite	$FeO(OH)$
	Cerium ammonium nitrate	$(NH_4)_2Ce(NO_3)_6$
	Muscovite	$KAl_3Si_3O_{10}(OH)_{1.8}F_{0.2}$
	Aragonite	$CaCO_3$
	Quartz	SiO_2
	Sphalerite	ZnS
	Iron aluminum	$AlFe$

Table 4.6 Particle size distribution by volume of dust samples using a Malvern Mastersizer 3000. Each value is the average of three replicates for each sample.

Dust #	Dx (10)	Dx (50)	Dx (90)
	----------µm----------		
1	9.3	64.8	173
2	10.3	73.8	189
3	11.2	42.1	149
4	11.0	45.7	156
5	5.9	23.9	98
6	13.1	65.8	186
7	16.7	61.1	179
9	12.6	49.9	156
10	10.2	42.9	139
11	11.4	51.5	169
12	12.6	54.4	173
13	10.1	38.3	141
14	13.1	53.5	160
15	17.7	69.8	174

Dx (10), Dx (50), and Dx (90) are the 10%, 50% (median), and 90% of dust sample particle diameter, respectively.

Table 4.7 Particle size distribution (PM10 and PM2.5) by volume of dust samples using a Malvern Mastersizer 3000.

Dust #	% of sample < 2.5 μm	% of sample < 10 μm
1	3.07	11.51
2	2.76	10.70
3	2.02	10.02
4	1.84	10.22
5	4.25	22.76
6	2.01	8.28
7	1.46	5.50
9	1.54	8.40
10	2.12	11.24
11	1.77	9.72
12	1.49	8.36
13	2.14	11.57
14	1.49	8.08
15	1.51	5.40
Max	4.25	22.76
Min	1.46	5.40
Average	2.11	10.13

Table 4.8 Scanning electron microscopy (SEM) energy dispersive X-ray (EDX) data shows the elemental composition (C, O, Al, Si, S, Ca, Fe, and Zn) that appear in area of interest (AOI) in sample 1 (see Figure 4.2) .

Element	Atomic %
C	65.87
O	27.20
Al	0.33
Si	2.26
S	0.52
Ca	2.97
Fe	0.45
Zn	0.40

Table 4.9 Scanning electron microscopy (SEM) energy dispersive X-ray (EDX) data shows the elemental composition (C, O, Si, S, Ca, Fe, and Zn) that appear in area of interest (AOI) in sample 2 (see Figure 4.3).

Element	Atomic %
C	65.46
O	28.35
Si	2.08
S	0.43
Ca	3.06
Fe	0.20
Zn	0.42

Table 4.10 Scanning electron microscopy (SEM) energy dispersive X-ray (EDX) data shows the elemental composition (C, O, Al, Si, S, K, Ca, Fe, and Zn) that appear in area of interest (AOI) in sample 3 (see Figure 4.4).

Element	Atomic %
C	63.35
O	29.44
Al	0.48
Si	5.18
S	0.36
K	0.11
Ca	0.40
Fe	0.47
Zn	0.21

Table 4.11 Scanning electron microscopy (SEM) energy dispersive X-ray (EDX) data shows the elemental composition (C, O, Al, Si, S, Ca, Fe, and Zn) that appear in area of interest (AOI) in sample 4 (see Figure 4.5).

Element	Atomic %
C	64.11
O	27.83
Al	0.44
Si	5.11
S	0.69
Ca	0.39
Fe	0.61
Zn	0.82

Table 4.12 Scanning electron microscopy (SEM) energy dispersive X-ray (EDX) data shows the elemental composition (C, O, Al, Si, S, Ca, Ti, Fe, Zn, and K) that appear in three particles of interest (POI) in sample 5 (see Figure 4.6).

Element	Atomic %		
	a	b	c
C	60.21	ND	34.4
O	36.45	91.46	55.1
Al	0.26	5.73	2.6
Si	1.90	16.58	9.7
S	0.24	0.34	0.30
Ca	0.58	1.09	0.85
Ti	0.14	ND	ND
Fe	0.09	0.44	0.15
Zn	0.12	0.01	0.08
K	ND	1.73	ND

ND- not detected.

Table 4.13 Scanning electron microscopy (SEM) energy dispersive X-ray (EDX) data shows the elemental composition (C, O, Al, Si, S, K, Ca, Fe, Zn, Pb, and Na) that appear in four particles of interest (POI) in sample 6 (see Figure 4.7).

Element	Atomic %			
	a	b	c	d
C	42.58	18.11	ND	45.78
O	49.50	95.08	76.82	45.36
Al	0.69	2.84	ND	0.52
Si	5.45	14.87	11.08	6.32
S	0.26	ND	ND	0.16
K	0.08	0.53	ND	ND
Ca	1.11	3.97	ND	1.14
Fe	0.26	0.68	ND	0.40
Zn	0.06	0.13	ND	ND
Pb	ND	ND	12.11	ND
Na	ND	ND	ND	0.32

ND- not detected.

Table 4.14 Scanning electron microscopy (SEM) energy dispersive X-ray (EDX) data shows the elemental composition (C, O, Al, Si, S, K, Ca, Fe, Zn, and Pb) that appear in three particles of interest (POI) in sample 7 (see Figure 4.8).

Element	Atomic %		
	a	b	C
C	42.58	ND	ND
O	49.50	73.87	80.03
Al	0.69	ND	1.11
Si	5.45	18.68	12.13
S	0.26	ND	1.14
K	0.08	ND	0.32
Ca	1.11	5.03	4.90
Fe	0.26	ND	0.40
Zn	0.06	ND	0.02
Pb	ND	2.42	ND

ND- not detected.

Table 4.15 Scanning electron microscopy (SEM) energy dispersive X-ray (EDX) data shows the elemental composition (C, O, Mg, Al, Si, S, Ca, Fe, Zn, Pb, P, Cl, and K) that appear in five particles of interest (POI) in sample 9 (see Figure 4.9).

Element	Atomic %				
	a	b	c	D	e
C	59.90	61.23	55.07	58.4	62.91
O	35.84	34.72	43.40	36.1	35.23
Mg	ND	0.54	ND	ND	0.38
Al	0.45	0.36	ND	0.25	0.14
Si	2.69	2.53	0.61	1.05	0.74
S	0.27	0.11	ND	ND	0.13
Ca	0.78	0.32	0.61	0.54	0.32
Fe	ND	0.14	ND	ND	ND
Zn	ND	0.05	ND	ND	0.01
Pb	ND	ND	0.31	0.26	ND
P	ND	ND	ND	ND	0.07
Cl	ND	ND	ND	ND	0.05
K	0.08	ND	ND	ND	0.04

ND- not detected.

Table 4.16 Scanning electron microscopy (SEM) energy dispersive X-ray (EDX) data shows the elemental composition (B, C, O, Al, Si, S, K, Ca, Fe, Zn, Pb, Mo, and P) that appear in three particles of interest (POI) in sample 10 (see Figure 4.10).

Element	Atomic %		
	a	b	c
B	ND	ND	62.19
C	73.43	45.77	ND
O	24.42	45.98	32.94
Al	ND	ND	0.42
Si	1.06	3.85	3.42
S	ND	ND	0.38
K	ND	ND	0.08
Ca	0.18	1.32	0.39
Fe	ND	1.12	0.14
Zn	ND	ND	0.05
Pb	0.48	0.54	ND
Mo	0.43	ND	ND
P	ND	1.42	ND

ND- not detected.

Table 4.17 Scanning electron microscopy (SEM) energy dispersive X-ray (EDX) data shows the elemental composition (C, O, Na, Al, Si, S, K, Ca, Fe, Zn, and Pb) that appear in three particles of interest (POI) in sample 11 (see Figure 4.11).

Element	Atomic %		
	a	b	c
C	72.86	ND	61.72
O	ND	74.92	34.04
Na	ND	2.34	ND
Al	ND	5.36	0.28
Si	8.61	15.34	2.63
S	10.92	ND	0.75
K	ND	1.77	ND
Ca	ND	ND	0.48
Fe	ND	ND	0.07
Zn	ND	0.26	0.02
Pb	7.61	ND	ND

ND- not detected.

Table 4.18 Scanning electron microscopy (SEM) energy dispersive X-ray (EDX) data shows the elemental composition (C, O, Al, Si, S, K, Ca, Fe, Zn, Pb, and Mo) that appear in three particles of interest (POI) in sample 12 (see Figure 4.12).

Element	Atomic %		
	a	b	c
C	56.63	ND	ND
O	39.12	62.17	85.03
Al	0.43	5.87	ND
Si	2.80	16.34	ND
S	0.41	2.24	ND
K	ND	2.07	ND
Ca	0.30	5.32	3.35
Fe	0.21	2.38	ND
Zn	0.10	3.61	ND
Pb	ND	ND	5.77
Mo	ND	ND	5.85

ND- not detected.

Table 4.19 Scanning electron microscopy (SEM) energy dispersive X-ray (EDX) data shows the elemental composition (O, Al, Si, S, Ca, Zn, and Pb) that appear in two particles of interest (POI) in sample 13 (see Figure 4.13).

Element	Atomic %	
	a	b
O	86.45	85.35
Al	ND	0.75
Si	ND	1.09
S	ND	6.94
Ca	ND	5.79
Zn	ND	0.08
Pb	13.55	ND

ND- not detected.

Table 4.20 Scanning electron microscopy (SEM) energy dispersive X-ray (EDX) data shows the elemental composition (C, O, Al, Si, S, K, Ca, Fe, Zn, and Pb) that appear in three particles of interest (POI) in sample 14 (see Figure 4.14).

Element	Atomic %		
	a	b	c
C	58.78	35.85	69.66
O	37.06	52.29	27.40
Al	0.39	1.26	0.41
Si	2.86	7.14	1.13
S	0.28	1.30	0.62
K	0.16	0.17	ND
Ca	0.19	1.01	0.40
Fe	0.16	0.39	ND
Zn	0.11	0.29	ND
Pb	ND	ND	0.37

ND- not detected.

Table 4.21 Scanning electron microscopy (SEM) energy dispersive X-ray (EDX) data shows the elemental composition (C, O, Al, Si, S, K, Ca, Fe, Zn, Pb, Mo, Ba, Cl, Pd, and Au) that appear in three particles of interest (POI) in sample 15 (see Figure 4.15).

Element	Atomic %		
	a	b	c
C	47.13	76.55	61.43
O	44.55	ND	34.16
Al	0.73	2.20	0.67
Si	4.83	7.96	3.04
S	ND	ND	0.25
K	ND	0.61	ND
Ca	0.11	7.73	0.26
Fe	0.37	1.05	0.13
Zn	0.28	0.25	0.06
Pb	1.03	ND	ND
Mo	0.65	ND	ND
Ba	0.32	ND	ND
Cl	ND	0.96	ND
Pd	ND	0.99	ND
Au	ND	1.71	ND

ND- not detected.

Chapter 5 - Conclusions and Future Research

Abandoned mine sites have left a legacy of contamination. The lead (Pb) and zinc (Zn) mines in the Tri-State Mining District of southeast Kansas, southwest Missouri, and northeast Oklahoma are such mines. Galena, Kansas, located in the District, had operational mines between 1876 and 1970. Mine waste materials surround Galena's abandoned mines, and they are highly polluted, not only with Pb and Zn, but also cadmium (Cd) which co-occurs geologically with Zn. The mine wastes support almost no growth of vegetation. Because limited information about the mine waste materials in Galena exists, three studies were done.

The first study characterized the physical properties of the mine waste materials. Measurements of hydraulic conductivity, bulk density, water content, aggregate stability, and particle size were taken in November 2014 on plots established in May 2006, which had been amended with different amounts of compost, lime, and bentonite. The physical characteristics of the mine waste materials were highly variable, and the amendments added 8.5 years earlier had no effect on them, except the wind erodible fraction (fraction <0.84 mm in diameter). It was low on treatments that contained bentonite. The results suggested that bentonite reduced the wind erodible fraction. Future studies should follow up on this observation to determine if amendments of clay last a long time (i.e., 8 years or more) and could be used to reduce wind erosion from mine waste materials.

Because no studies had been done to see if biosolids could be used to remediate the mine waste materials, an experiment was conducted in a greenhouse at Kansas State University with the mine waste materials from Galena. For 110 days, sudex, a sorghum-sudan grass hybrid, was grown in pots with the mine waste materials and half the pots received biosolids. Only the sudex grown with biosolids produced heads with grain. The plants grown without biosolids were

stunted and showed severe heavy metal toxicity. The biosolids reduced the uptake of Pb, Zn, and Cd from the mine waste materials. Even though large amounts of Pb, Zn, and Cd accumulated in the roots, their transfer to the heads was limited. Concentrations of Pb and Zn in the heads were normal. These results showed that transfer of heavy metals through sudex is limited, and, even though high concentrations of a heavy metal are in the roots, the grain can have normal concentrations. The increased growth of the plants grown with biosolids appeared to be due to the organic carbon and phosphorus that the biosolids added to the mine waste materials. The use of bioslids may be a promising method to reduce availability of heavy metals at mine sites. Because no studies have been done at Galena with biosolids, a field study should be carried out to determine if they can revegetate the degraded land.

Dust is a public health concern if it contains particulate matter (PM) called PM_{10}. Particles of this size are less than 10 microns in diameter. Many studies have shown the importance of attic dust in documenting heavy metal pollution from a mine. However, the dust in attics in Galena, Kansas, had never been studied. Therefore, in the third study reported in this dissertation 14 attic dust samples from buildings in Galena, including shops and houses, were collected and characterized by measuring their concentrations of heavy metals, mineralogy, and particle size. Concentrations of the heavy metals in the dust samples were variable, but they all were were highly contaminated with Pb, Zn, and Cd compared to average values found in uncontaminated soils. Galena, sphalerite, anglesite, quartz, calcite, aragonite, pyrite, and cerussite minerals were identified in most of the dust samples. Approximately 10% of the dust samples had the size of medical importance, PM_{10}. Dust of this size, found in a school in Galena, is of major concern, because this means that children will be exposed to dangerously small dust particles contaminated with heavy metals. If a child is exposed to Pb-contaminated

dust, or sucks a finger that has touched the dust, that child may suffer lifelong brain damage. Future studies need to analyze the dust from many buildings in Galena to assess the danger from the dust. Residents of Galena have a higher incidence of kidney disease, heart disease, skin cancer, and anemia compared to residents in control towns, and the dust that the citizens breathe in Galena may be partially responsible for these diseases.

Appendix A - Physical Properties of Mine Waste Materials at an Abandoned Mine in Central USA

Figure A.1 Appendix: Average hydraulic conductivity of each plots at Site A.

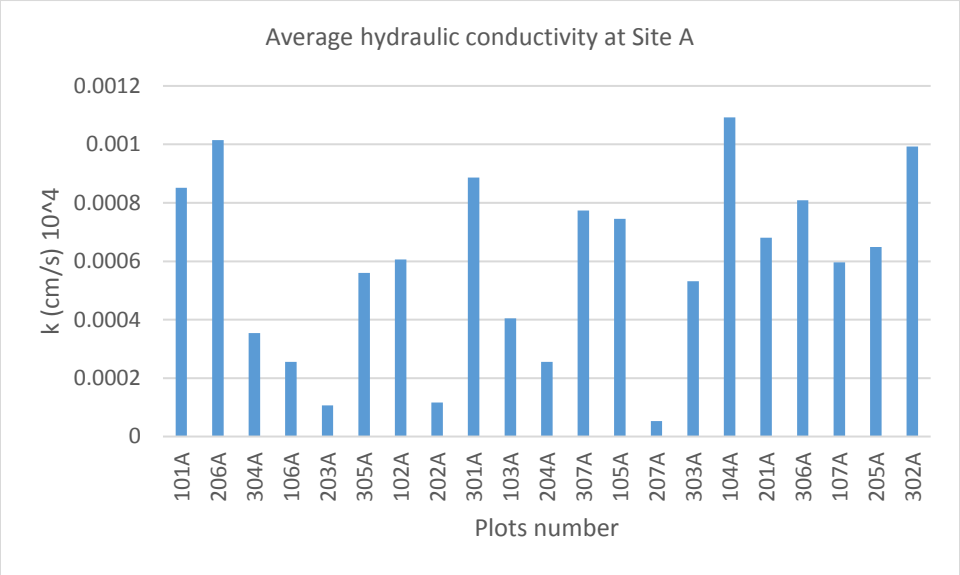

Where:

101, 206, and 304 are control;

106, 203, and 305 are low compost;

102, 202, and 301are high compost;

103, 204, and 307 are low compost plus lime;

105, 207, and 303 are high compost plus lime;

104, 201, and 306 are low compost plus lime plus bentonite;

107, 205, and 302 are high compost plus lime plus bentonite;

Figure A.2 Appendix: Average hydraulic conductivity of each plots at Site B.

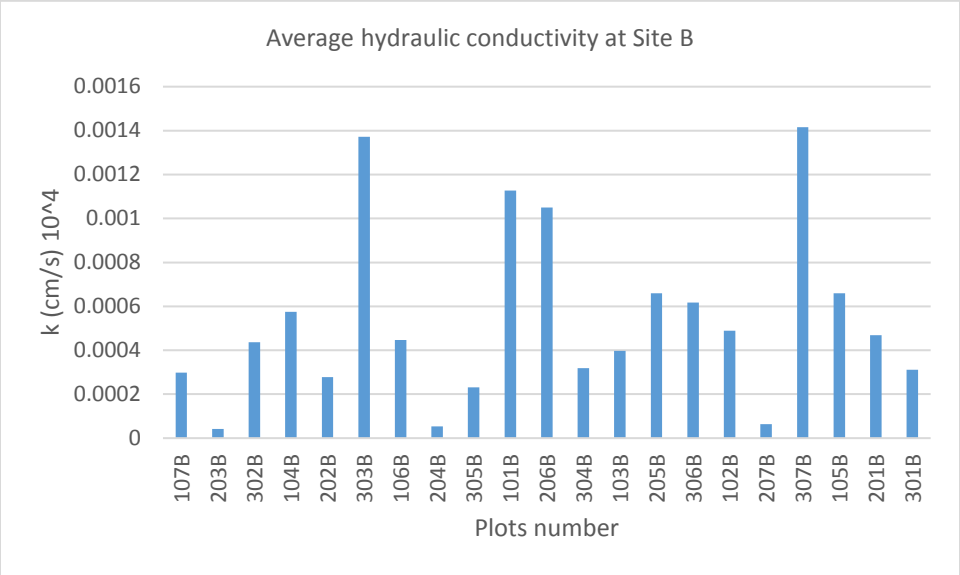

Where:

107, 203, and 302 are control

104, 202, and 303 are low compost

106, 204, and 305 are high compost

101, 206, and 304 are low compost plus lime

103, 205, and 306 are high compost plus lime

102, 207, and 307 are low compost plus lime plus bentonite

105, 201, and 301 are high compost plus lime plus bentonite

Figure A.3 Appendix: Cumulative Infiltration for each plots at Site A. (a), (b), and (c) are control treatment.

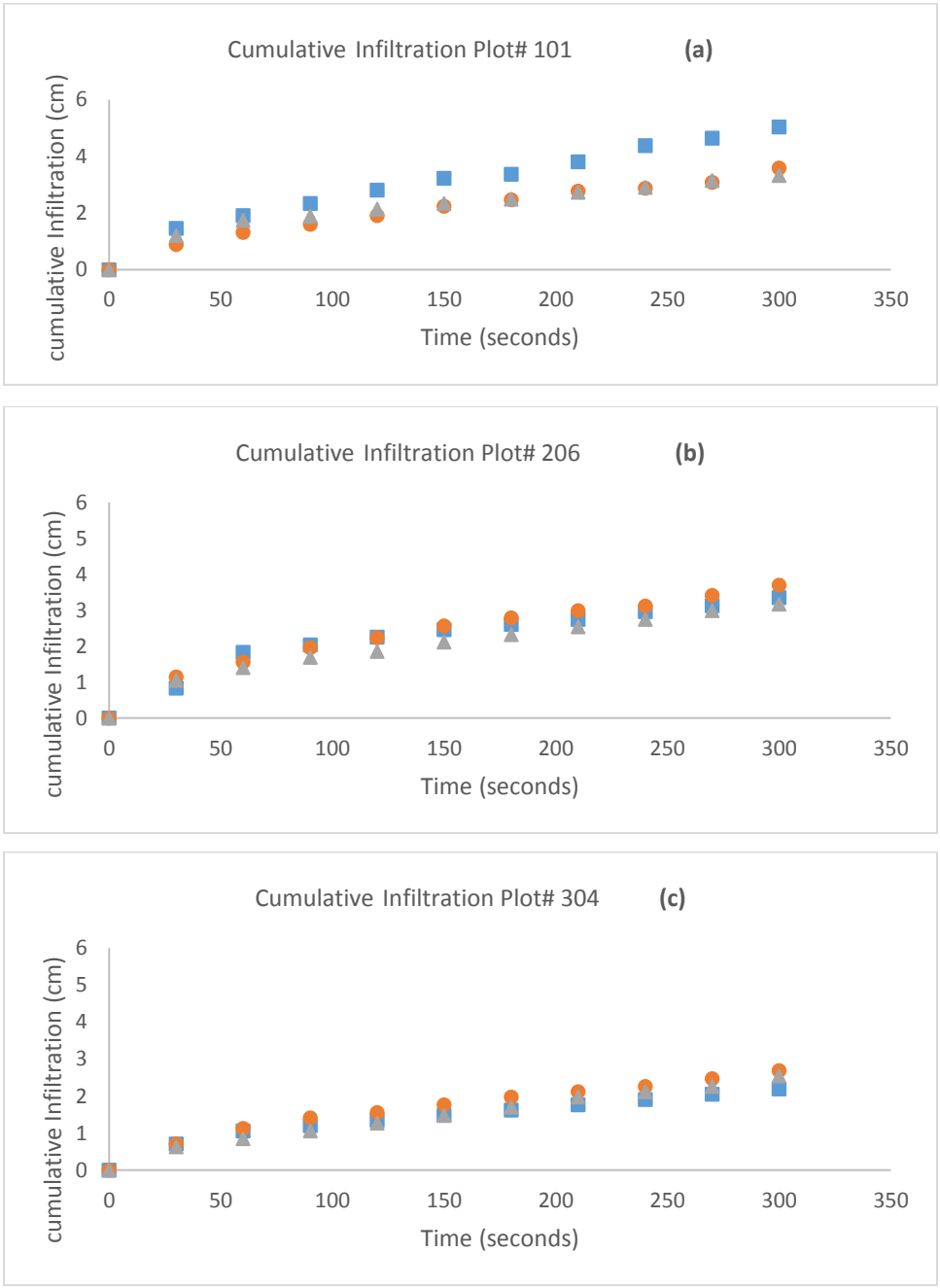

Figure A.4 Appendix: Cumulative infiltration for each plots at Site A. (d), (e), and (f) are low compost treatment.

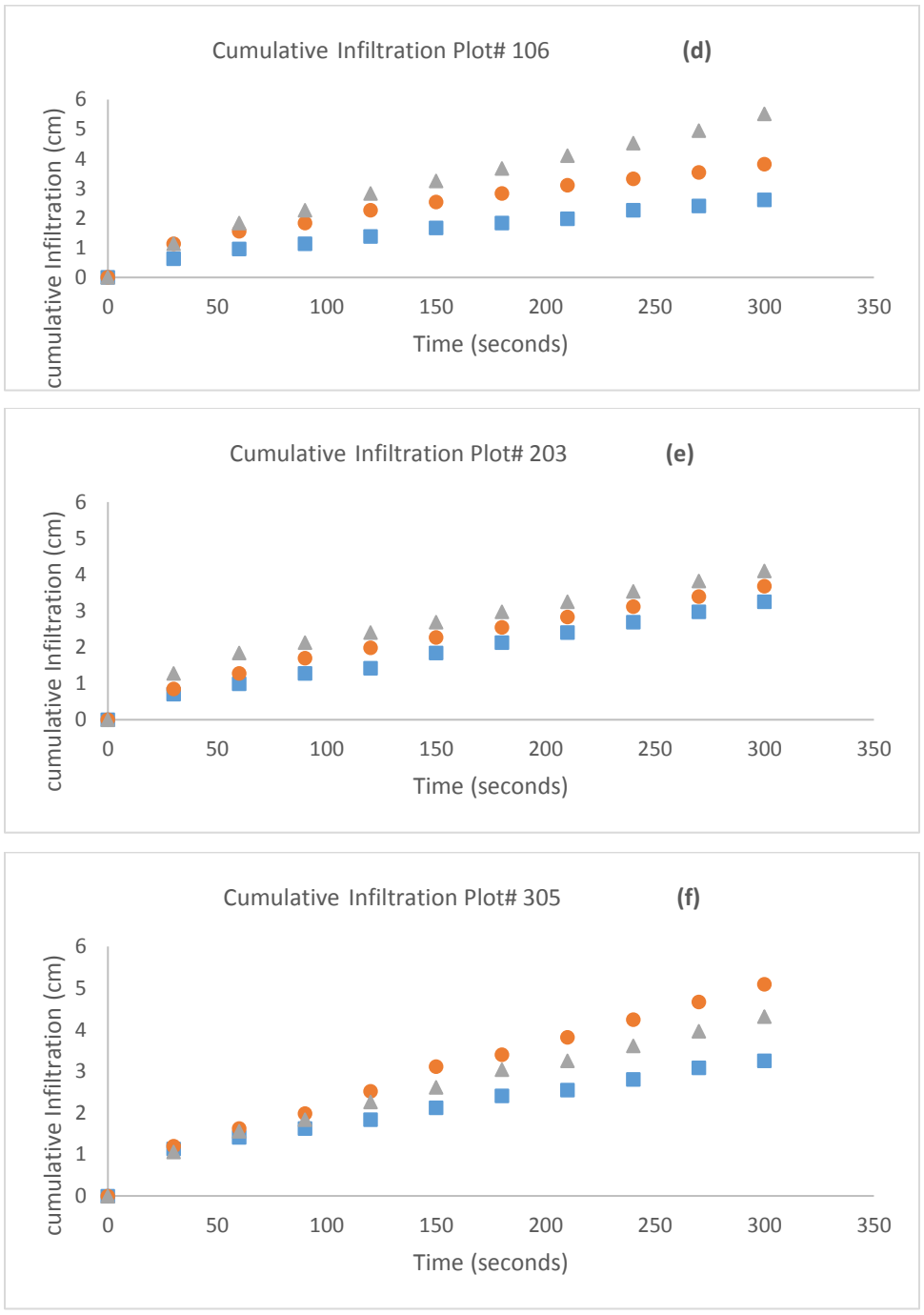

Figure A.5 Appendix: Cumulative infiltration for each plots at Site A. (g), (h), and (i) are high compost treatment.

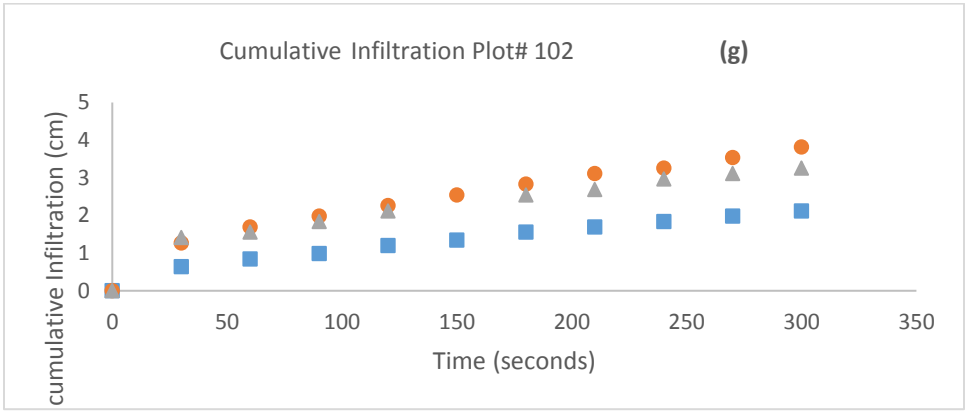

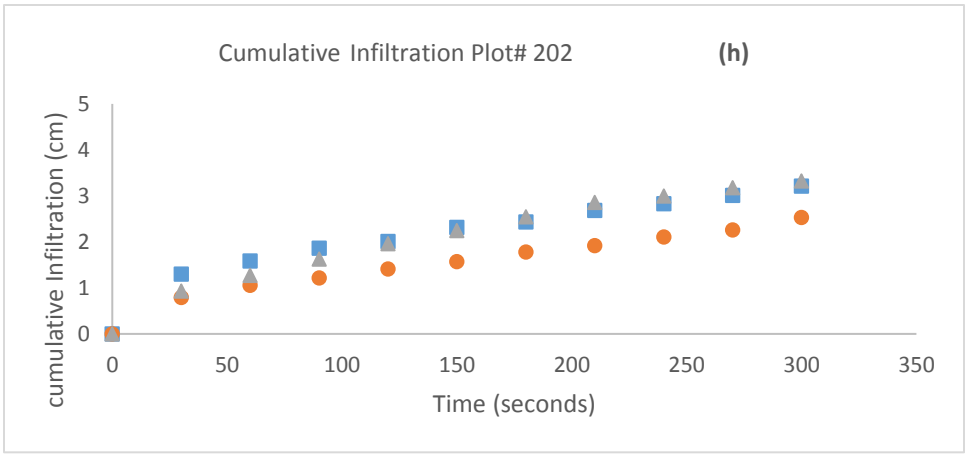

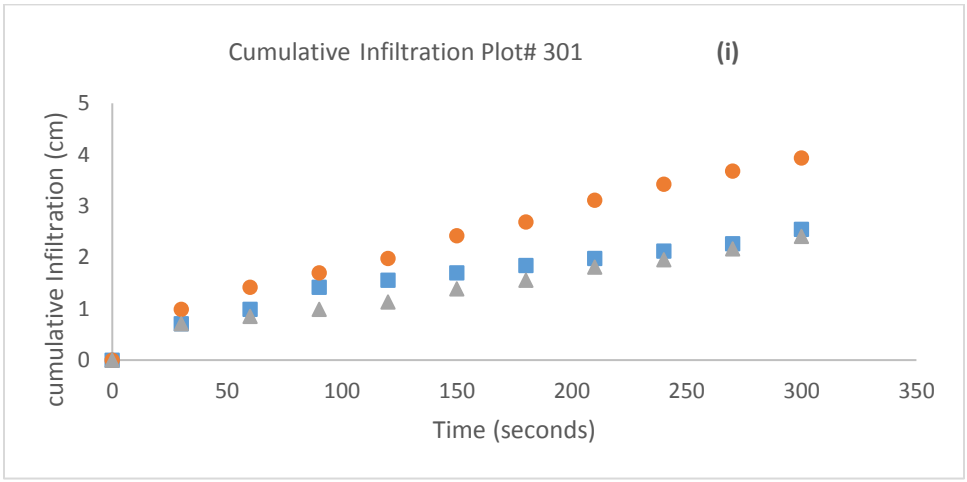

Figure A.6 Appendix: Cumulative infiltration for each plots at Site A. (j), (k), and (l) are low compost plus lime treatment.

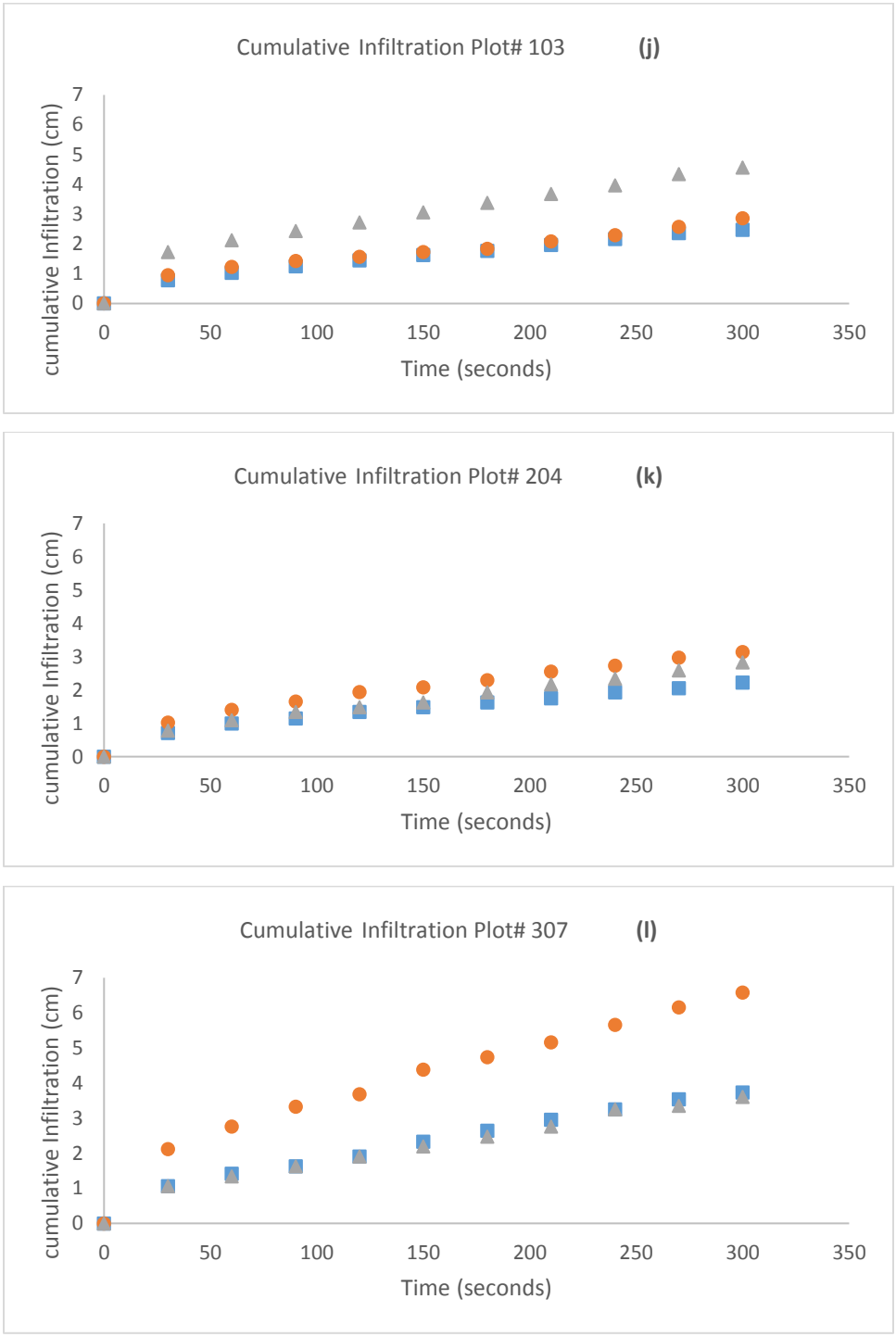

Figure A.7 Appendix: Cumulative infiltration for each plots at Site A. (m), (n), and (o) are high compost plus lime plus lime treatment.

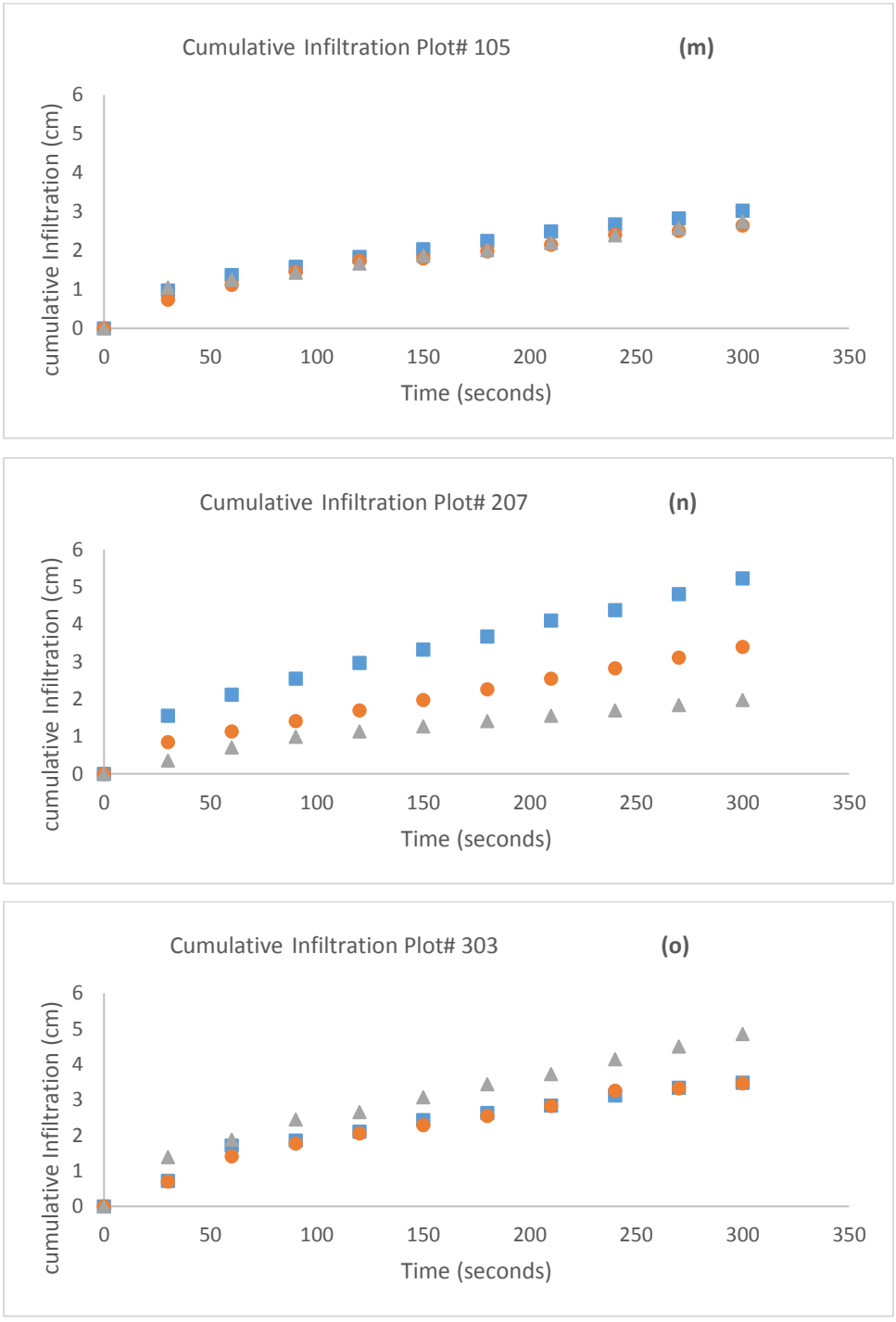

Figure A.8 Appendix: Cumulative infiltration for each plots at Site A. (p), (q), and (r) are low compost plus lime plus bentonite treatment.

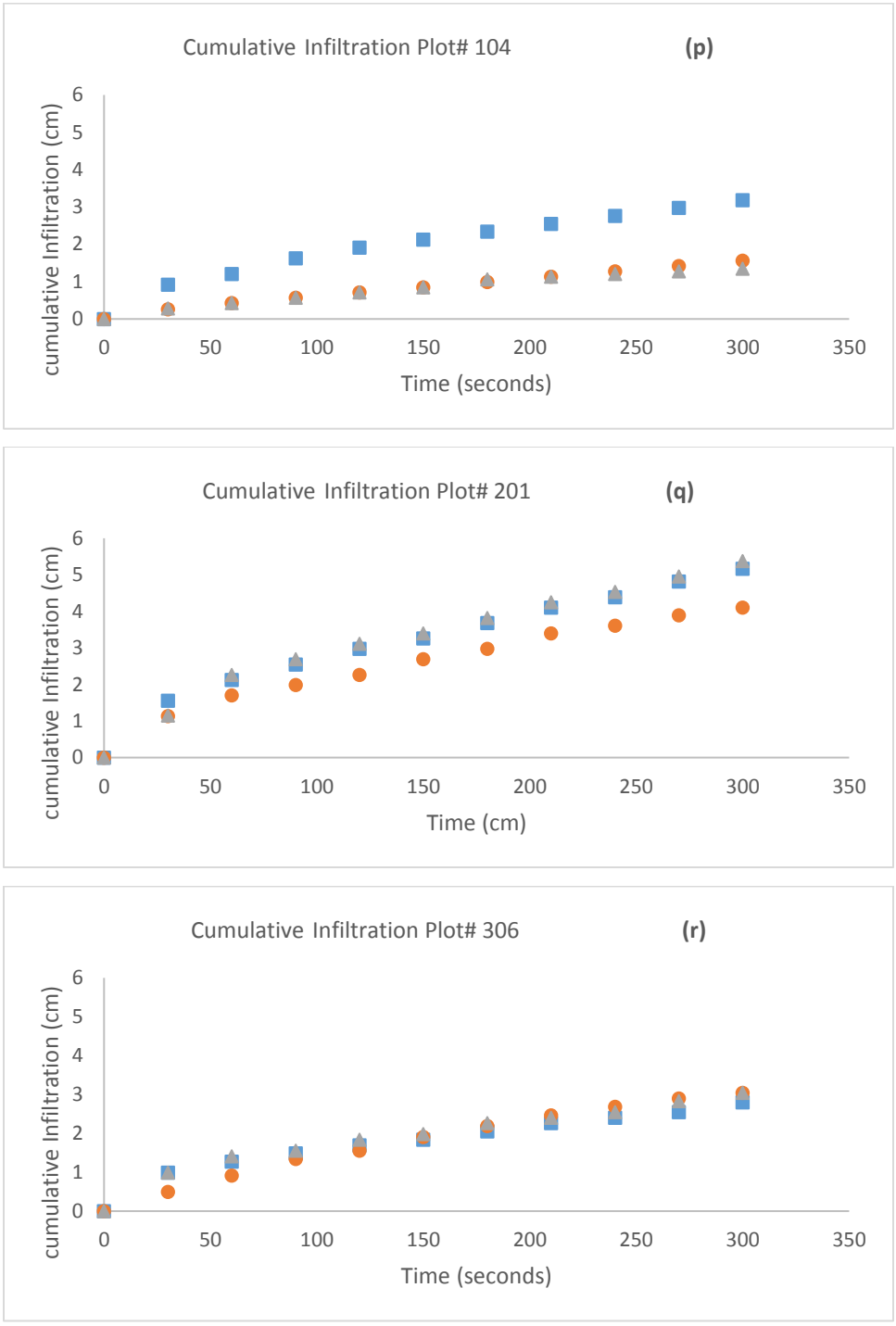

Figure A.9 Appendix: Cumulative infiltration for each plots at Site A. (s), (t), and (u) are high compost plus lime plus bentonite treatment.

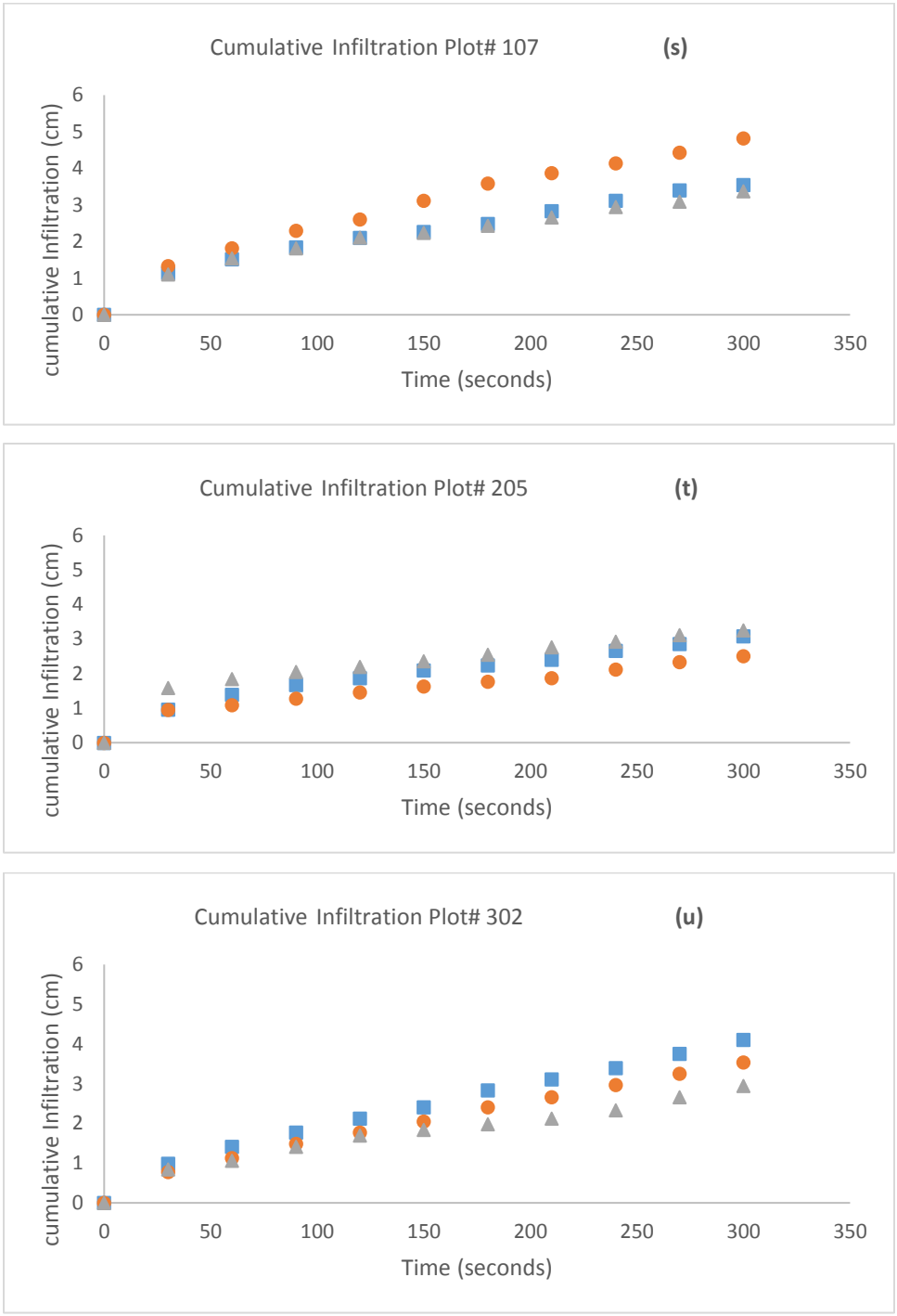

Figure A.10 Appendix: Cumulative infiltration for each plots at Site B. (a), (b), and (c) are control treatment.

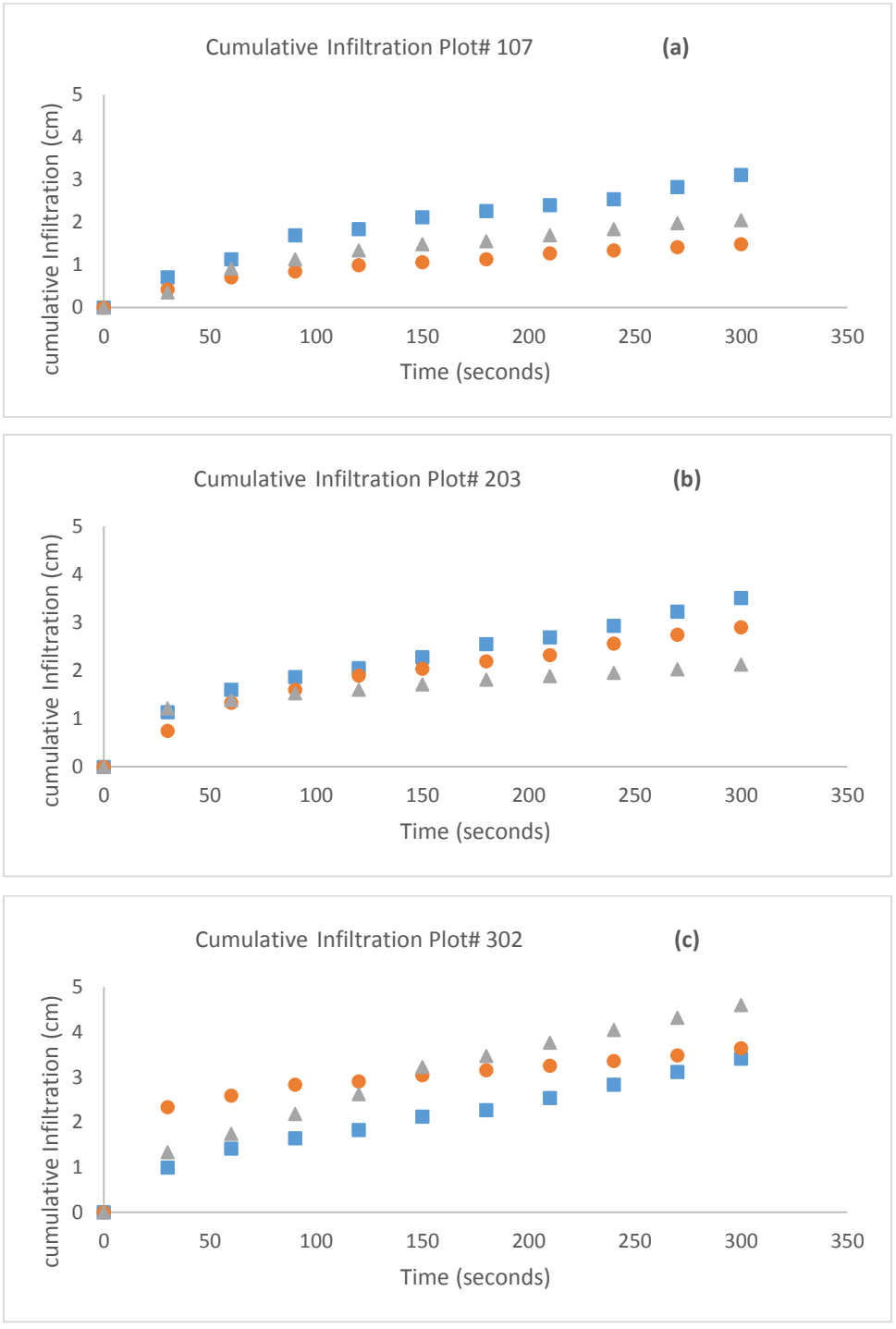

Figure A.11 Appendix: Cumulative infiltration for each plots at Site B. (d), (e), and (f) are low compost treatment.

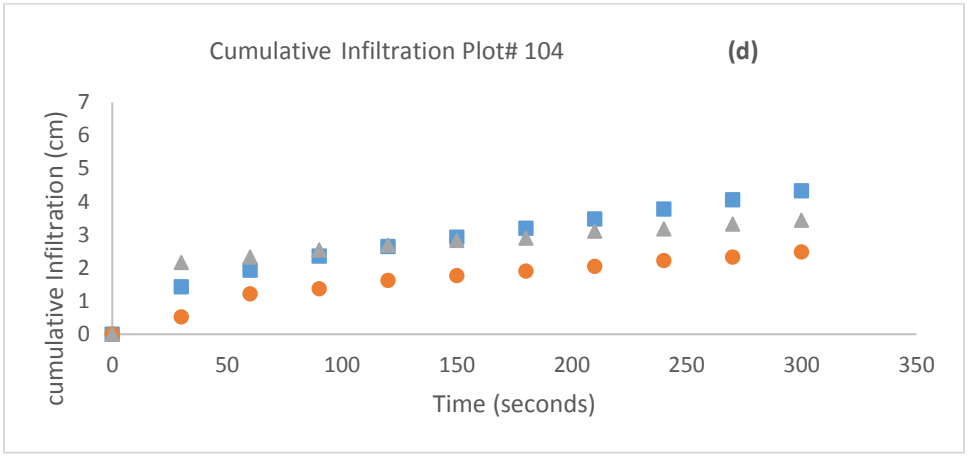

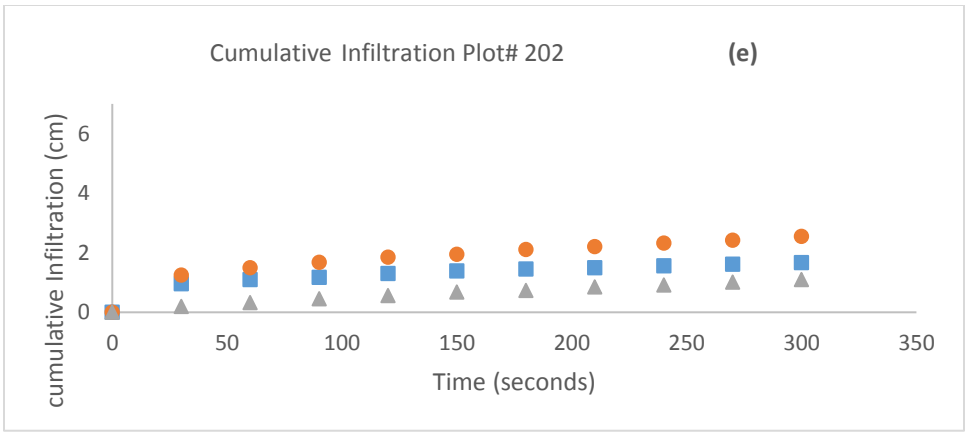

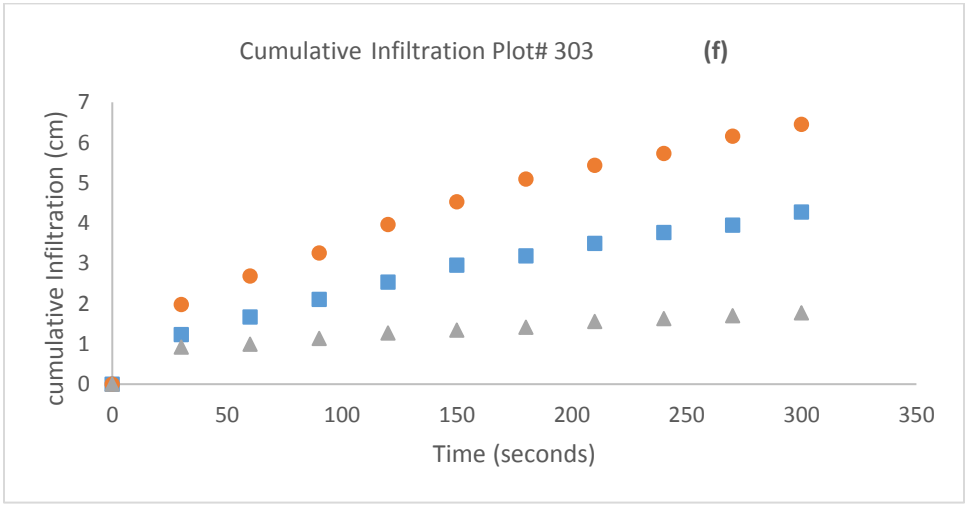

Figure A.12 Appendix: Cumulative infiltration for each plots at Site B. (g), (h), and (i) are high compost treatment.

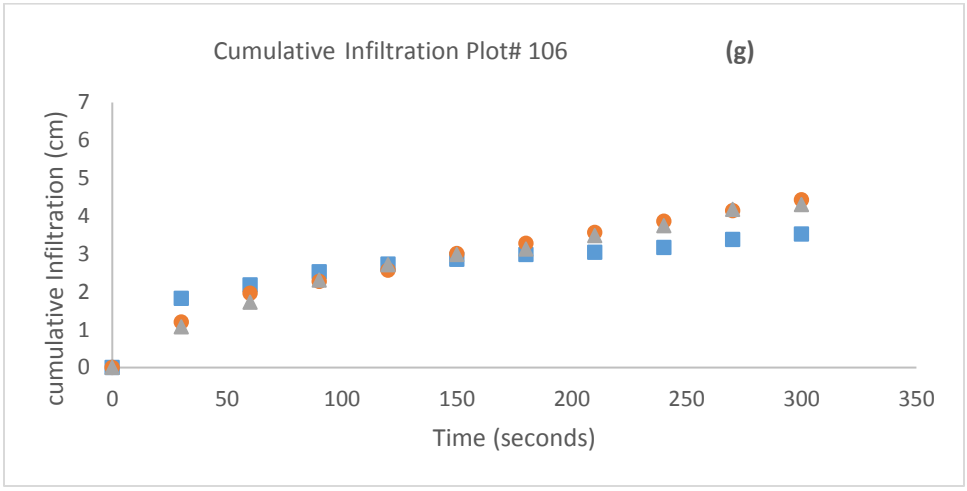

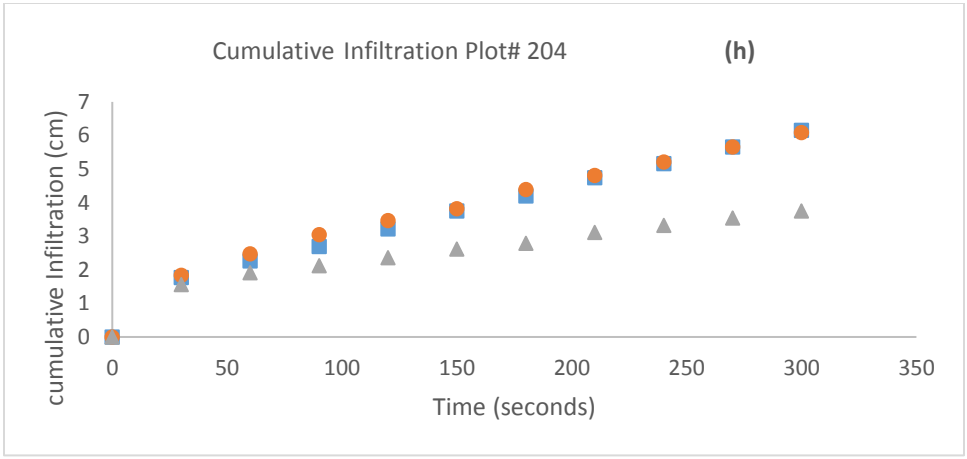

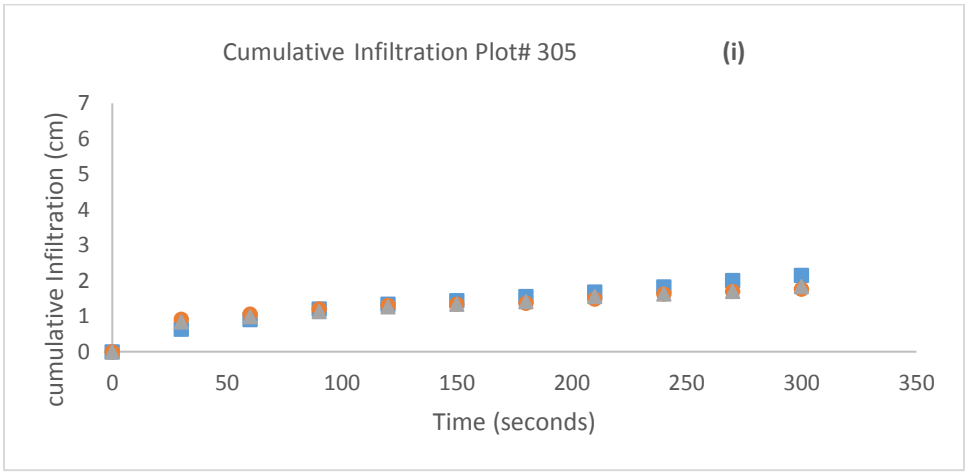

Figure A.13 Appendix: Cumulative infiltration for each plots at Site B. (j), (k), and (l) are low compost plus lime treatment.

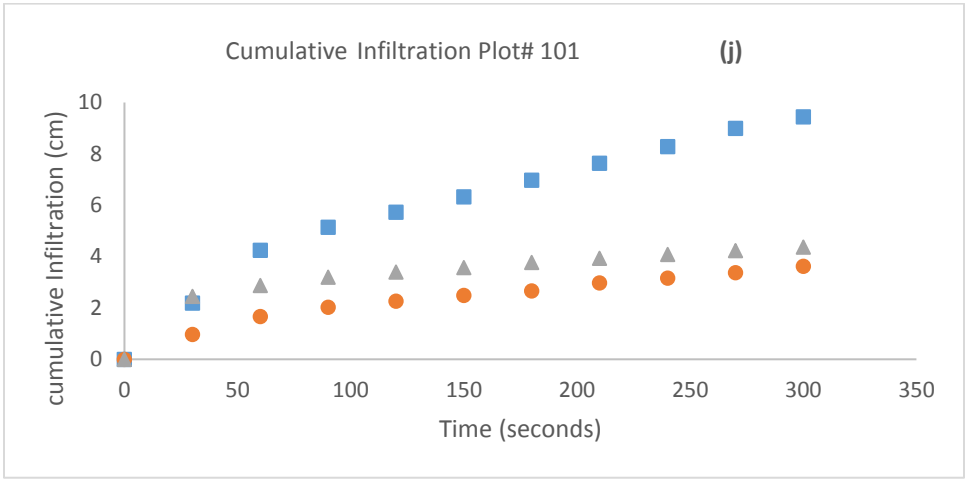

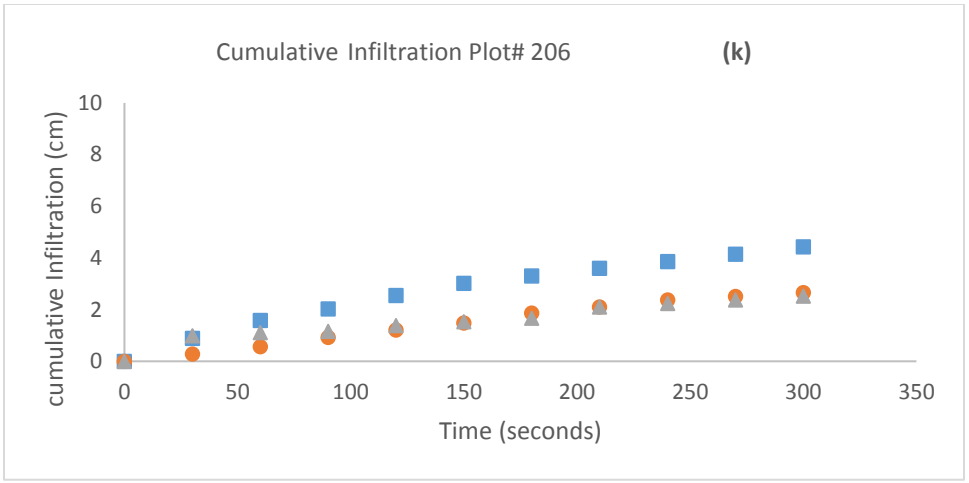

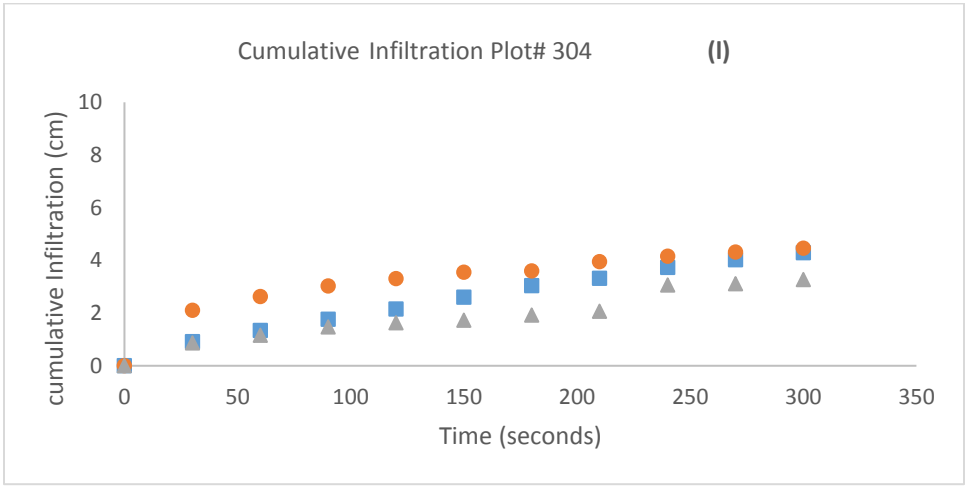

Figure A.14 Appendix: Cumulative infiltration for each plots at Site B. (m), (n), and (o) are high compost plus lime treatment.

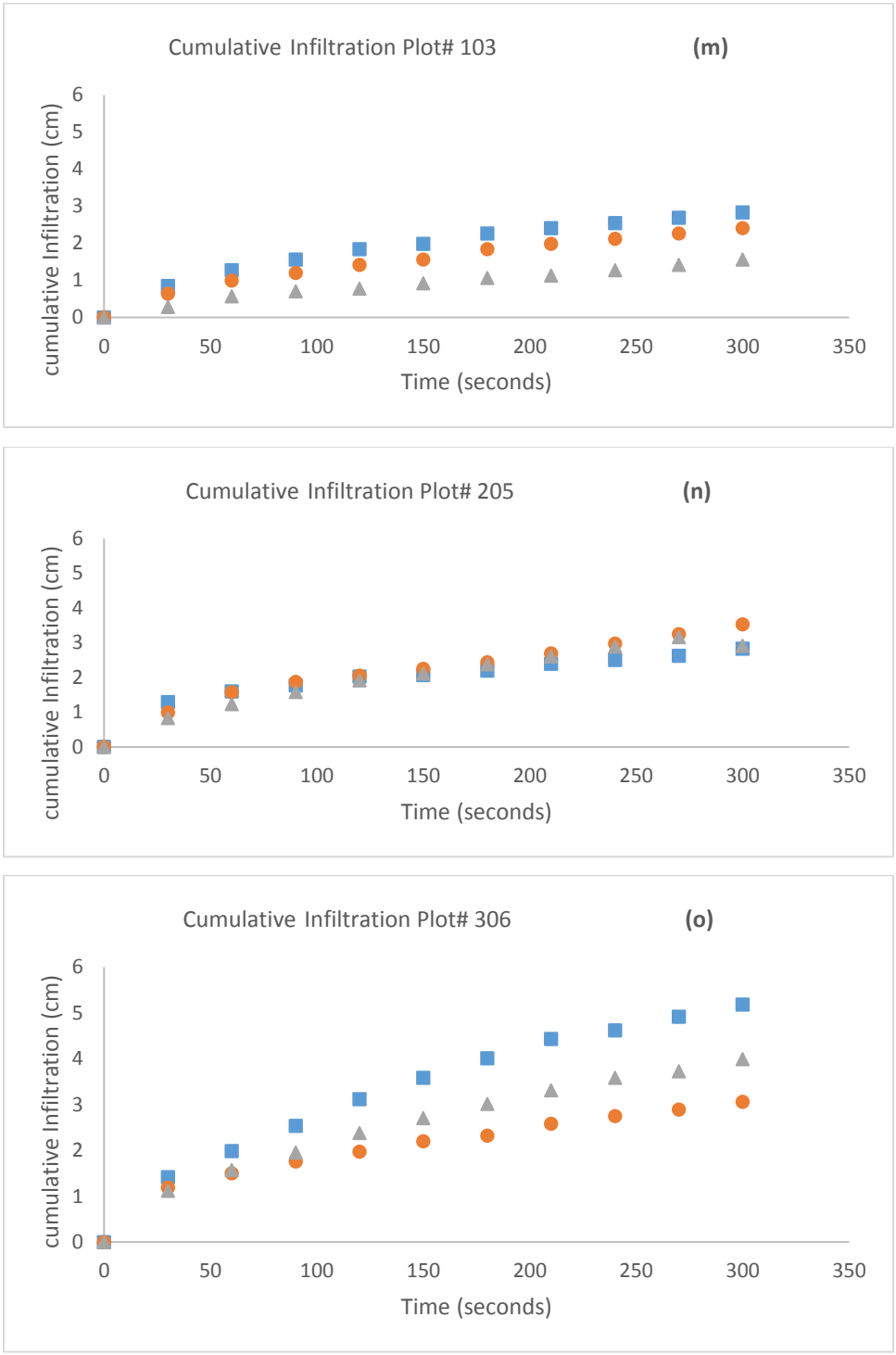

Figure A.15 Appendix: Cumulative infiltration for each plots at Site B. (p), (q), and (r) are low compost plus lime plus bentonite treatment.

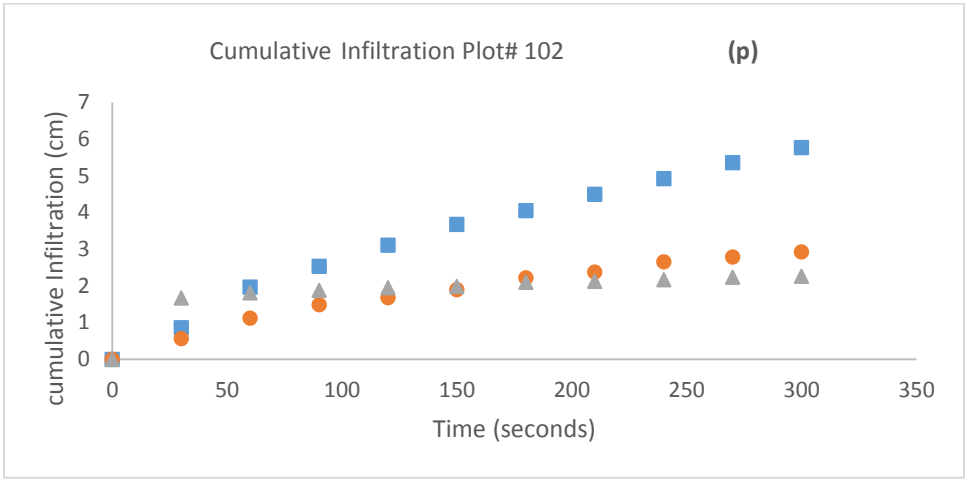

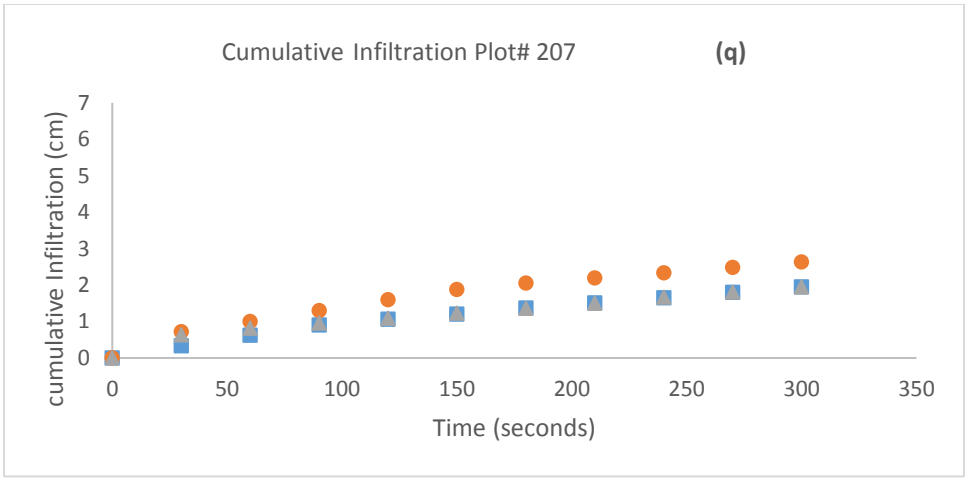

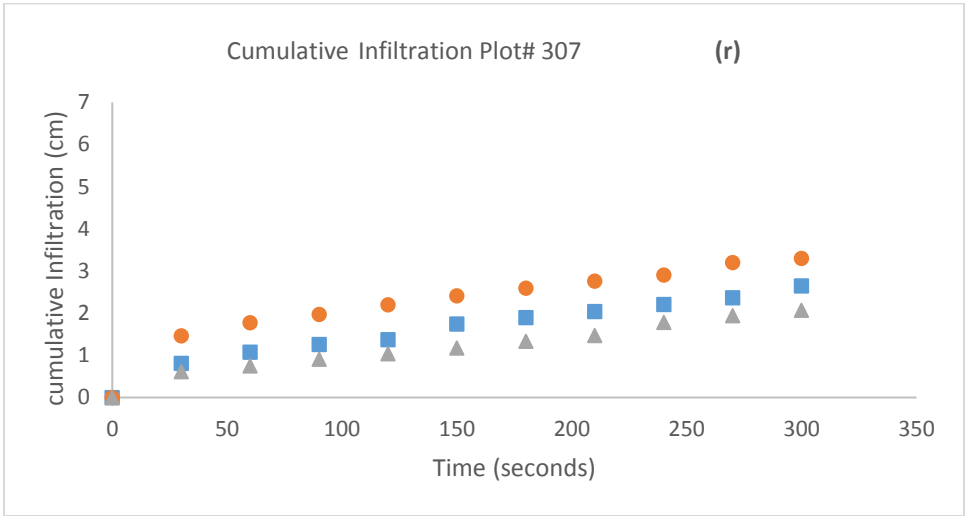

Figure A.16 Appendix: Cumulative infiltration for each plots at Site B. (s), (t), and (u) are high compost plus lime plus bentonite treatment.

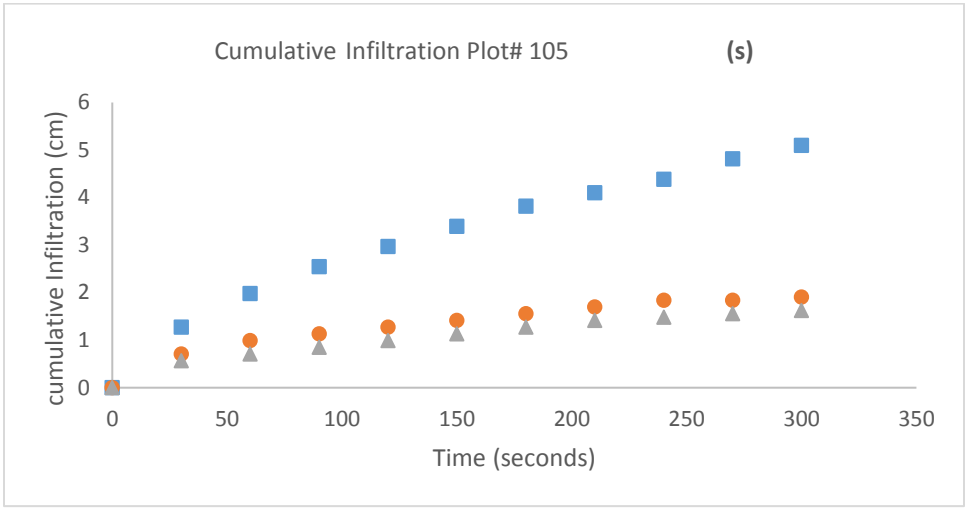

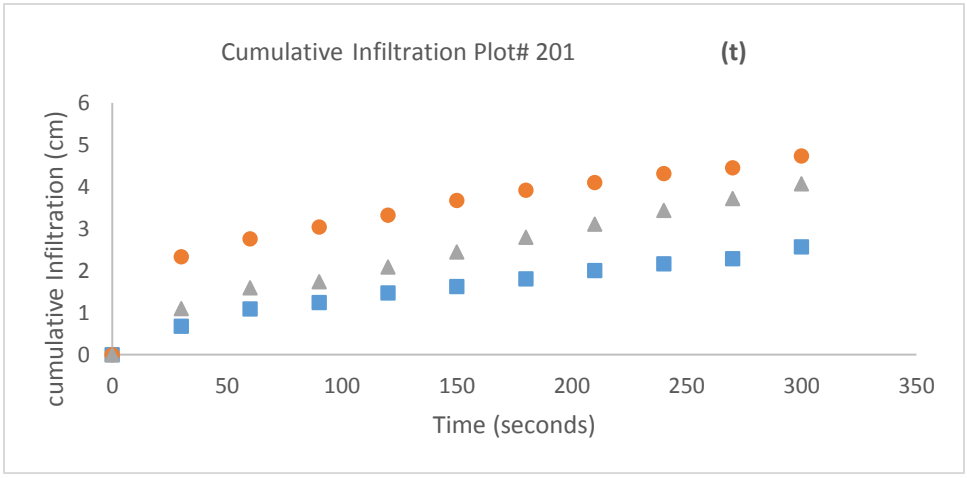

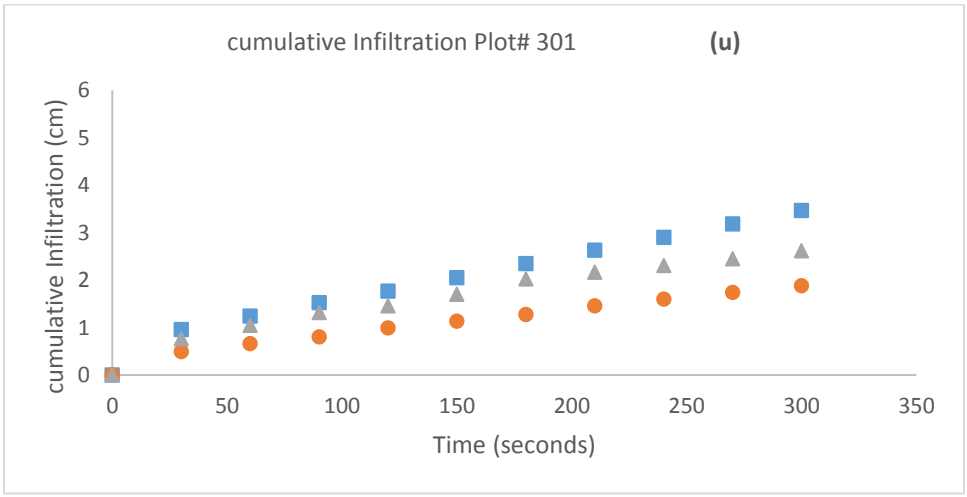

Appendix B - Rehabilitation of an Abandoned Mine Site with Biosolids

Figure B.1 Appendix: 42 soil buckets from Site A and B.

Figure B.2 Appendix: Air dried the mine waste materials for Site A and B.

Figure B.3 Appendix: Sieving the mine waste materials from Site A and B.

Figure B.4 Appendix: Biosolids from Manhattan Kansas Wastewater Treatment Plant.

Figure B.5 Appendix: Planting seeds of Sudex, a sorghum-sudangrass hybrid.

Figure B.6 Appendix: Pan Evaporation.

Figure B.7 Appendix: Symptoms of heavy metal toxicity for plants grown without biosolids.

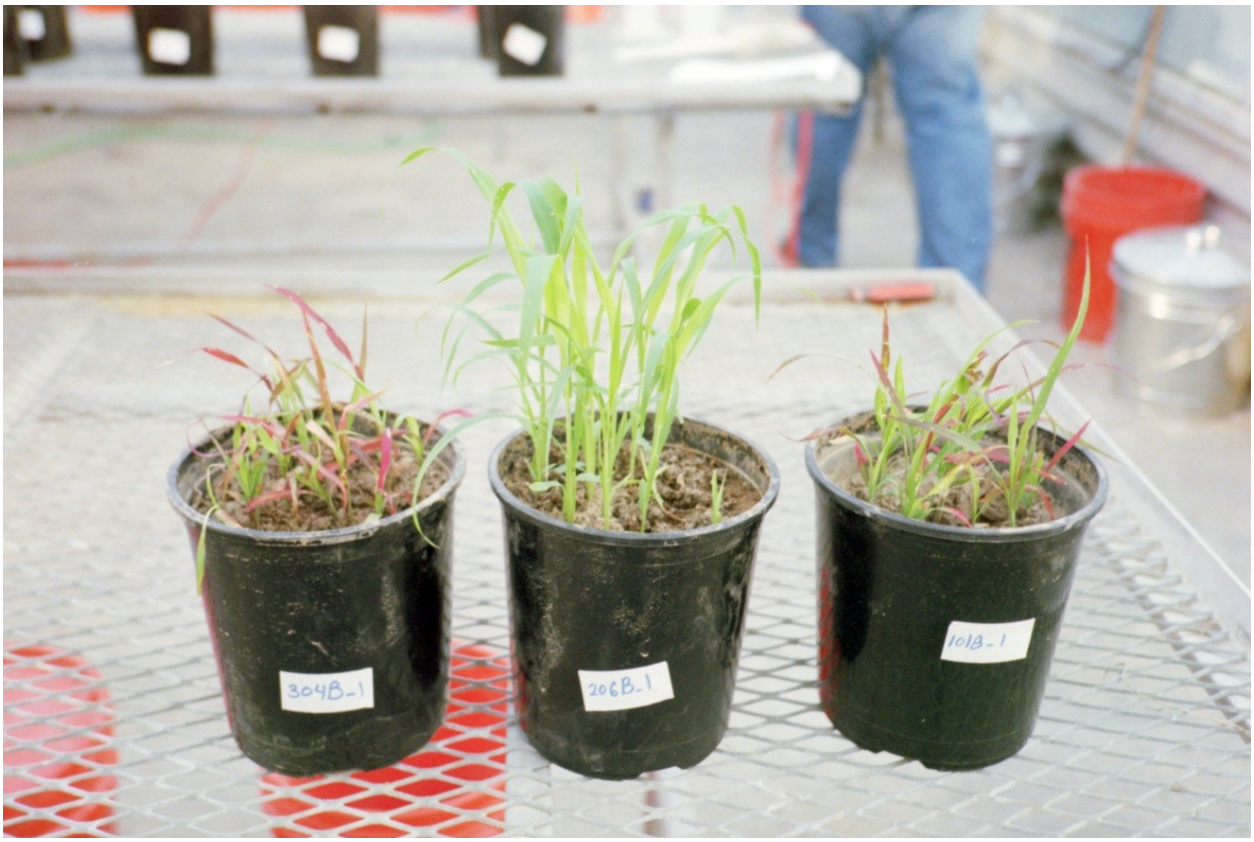

Figure B.8 Appendix: Sudex 44 days after planting. Plants in back row grown with biosolids

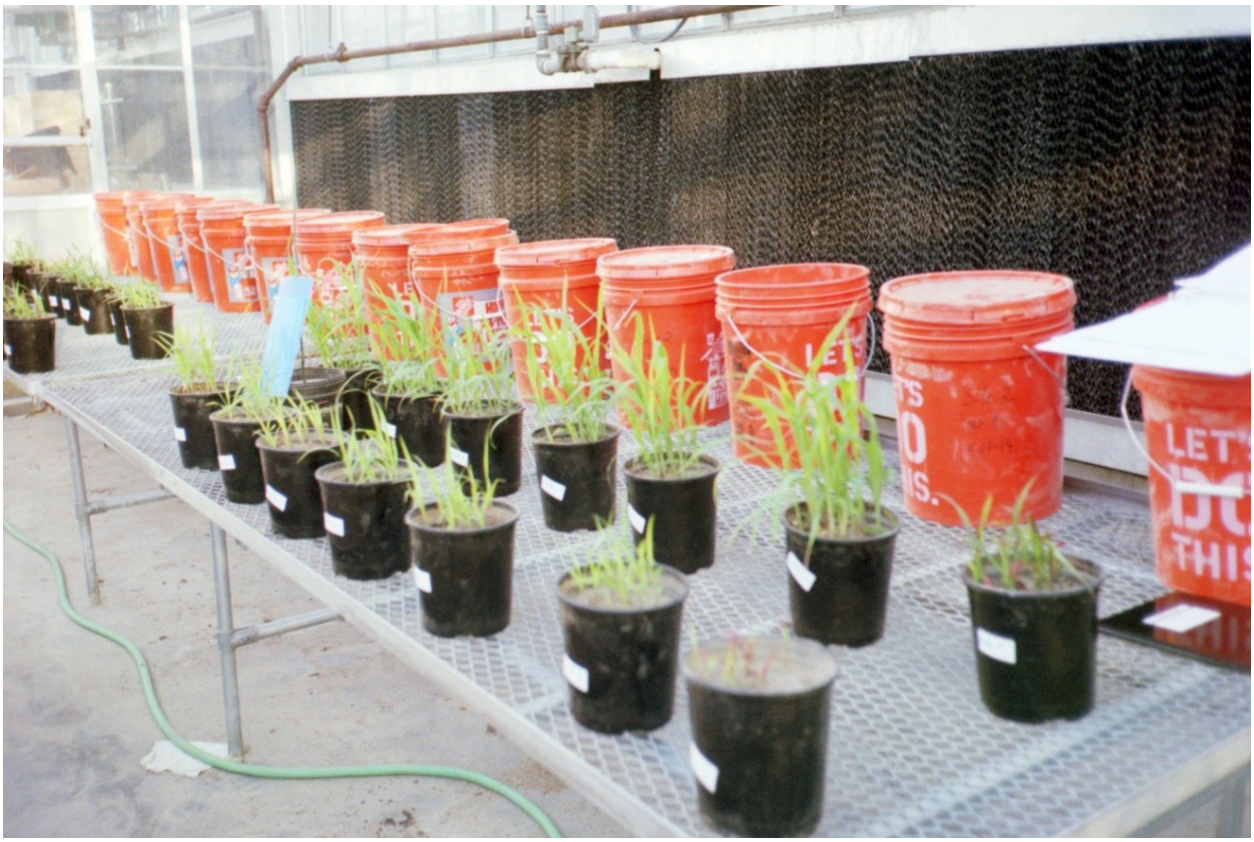

Figure B.9 Appendix: Plants grown with biosolids are on right, and they were the only ones to produce heads.

Table B.1 Appendix to table B.37 Appendix shows the statistical analysis of the seven treatments using LSMEANS at 0.05 level. Statistical analyses were performed using PROC GLIM of SAS Version 9.4 (Statistical Analysis System, 2013).

Table B.1 Appendix: Mine waste materials test for logarithm of hydrogen ion (pH), electrical conductivity (EC), cation exchange capacity (CEC), and organic matter (OM) at Site A and B. Means followed by the same letter are not statistically different at 0.05.

Treatment	pH		EC		CEC		OM	
			ms cm^{-1}		meq $100g^{-1}$		%	
	Site A	Site B	Site A	Site B	Site A	Site B	Site A	Site B
Control (CO)	6.93 b	6.37 ab	0.24 a	0.19 a	5.14 ab	5.95 ab	1.92 abc	1.19 abc
Low compost (LC)	7.19 ab	6.69 ab	0.23 a	0.39 a	7.35 a	7.21 a	2.38 a	2.32 a
High compost (HC)	7.02 ab	6.32 ab	0.25 a	0.41 a	3.35 b	4.71 b	1.23 abc	1.33 bc
Low compost + lime (LCL)	7.26 a	5.88 b	0.17 a	0.18 a	3.55 b	4.51 b	1.06 bc	1.33 bc
High compost + lime (HCL)	7.27 a	7.18 a	0.24 a	0.41 a	5.56 ab	6.29 ab	2.37 a	2.11 ab
Low compost + lime + bentonite (LCLB)	7.25 a	7.23 a	0.20 a	0.37 a	4.72 b	5.77 ab	2.24 ab	1.45 bc
High compost + lime + bentonite (HCLB)	7.23 a	5.41 b	0.17 a	0.29 a	3.56 b	5.50 ab	0.93 c	1.22 c

Table B.2 Appendix: Mine waste materials test for total nitrogen (T N), total carbon (T C), and total organic carbon (T O C) at Site A and B. Means followed by the same letter are not statistically different at 0.05.

Treatment	T N		T C		T O C	
	%					
	Site A	Site B	Site A	Site B	Site A	Site B
Control (CO)	0.14 abc	0.11 abc	1.37 ab	1.14 ab	1.26 ab	1.13 ab
Low compost (LC)	0.17 a	0.15 a	1.69 a	1.53 a	1.45 a	1.43 a
High compost (HC)	0.09 bc	0.09 abc	0.85 b	0.83 b	0.72 b	0.79 b
Low compost + lime (LCL)	0.09 c	0.08 c	0.75 b	0.71 b	0.69 b	0.72 b
High compost + lime (HCL)	0.16 ab	0.13 ab	1.63 a	1.33 ab	1.44 a	1.21 ab
Low compost + lime + bentonite (LCLB)	0.14 abc	0.09 abc	1.35 ab	0.94 ab	1.28 ab	0.89 ab
High compost + lime + bentonite (HCLB)	0.09 c	0.09 bc	0.71 b	0.73 b	0.70 b	0.71 b

Table B.3 Appendix: Mine waste materials test for phosphorus (P) and total phosphorus (T P) at Site A and B. Means followed by the same letter are not statistically different at 0.05.

Treatment	P		T P	
	mg kg^{-1}			
	Site A	Site B	Site A	Site B
Control (CO)	283.0 a	162.3 ab	758.7 a	685.7 abc
Low compost (LC)	370.3 a	361.6 ab	873.3 a	1020.3 ab
High compost (HC)	197.0 a	127.4 ab	630.3 a	638.3 abc
Low compost + lime (LCL)	116.5 a	25.2 b	457.3 a	479.0 c
High compost + lime (HCL)	383.9 a	420.6 a	879.7 a	1039.7 a
Low compost + lime + bentonite (LCLB)	290.9 a	88.0 ab	689.3 a	610.3 abc
High compost + lime + bentonite (HCLB)	128.1 a	37.7 b	518.3 a	546.0 bc

Table B.4 Appendix: Extractable concentration (mg kg^{-1}) of copper (Cu), iron (Fe), and manganese (Mn) in mine waste materials at Site A and B. Means followed by the same letter are not statistically different at 0.05.

Treatment	Cu		Fe		Mn	
	mg kg^{-1}					
	Site A	Site B	Site A	Site B	Site A	Site B
Control (CO)	2.73 a	10.3 ab	1.13 a	42.23 ab	0.27 a	2.70 a
Low compost (LC)	1.30 a	8.17 ab	0.73 a	37.80 ab	0.13 a	1.97 a
High compost (HC)	4.47 a	6.03 ab	1.17 a	29.57 bc	0.10 a	1.60 a
Low compost + lime (LCL)	4.40 a	6.83 ab	1.18 a	33.07 abc	0.13 a	2.70 a
High compost + lime (HCL)	3.13 a	5.70 b	1.13 a	26.20 bc	0.07 a	1.80 a
Low compost + lime + bentonite (LCLB)	3.17 a	5.33 b	5.47 a	17.40 c	0.40 a	3.93 a
High compost + lime + bentonite (HCLB)	4.40 a	14.43 a	5.33 a	48.40 a	0.30 a	1.87 a

Table B.5 Appendix: Extractable concentration (mg kg^{-1}) of zinc (Zn), lead (Pb), nickel (Ni), and cadmium (Cd) in mine waste materials at Site A and B. Means followed by the same letter are not statistically different at 0.05.

Treatment	Zn		Pb		Ni		Cd	
	mg kg^{-1}							
	Site A	Site B	Site A	Site B	Site A	Site B	Site A	Site B
Control (CO)	324.7 ab	154.9 a	83.8 a	65.5 ab	0.33 a	0.10 a	9.17 a	1.63 ab
Low compost (LC)	326.8 a	113.4 a	21.8 a	59.1 ab	0.37 a	0.10 a	8.87 a	0.80 b
High compost (HC)	300.9 bc	145.1 a	273.6 a	57.8 ab	0.18 b	0.10 a	5.20 b	1.23 b
Low compost + lime (LCL)	303.9 abc	126.5 a	216.6 a	77.8 ab	0.17 b	0.10 a	5.77 b	1.17 b
High compost + lime (HCL)	310.4 abc	124.2 a	101.1 a	57.2 ab	0.27 ab	0.10 a	5.93 b	0.83 b
Low compost + lime + bentonite (LCLB)	298.2 c	148.9 a	231.5 a	112.8 a	0.27 ab	0.13 a	5.40 b	1.80 ab
High compost + lime + bentonite (HCLB)	301.2 abc	189.3 a	211.2 a	39.9 b	0.13 b	0.13 a	5.90 b	3.03 a

Table B.6 Appendix: Total concentration (mg kg^{-1}) of copper (Cu), iron (Fe), and manganese (Mn) in mine waste materials at Site A and B. Means followed by the same letter are not statistically different at 0.05.

Treatment	Cu		Fe		Mn	
	mg kg^{-1}					
	Site A	Site B	Site A	Site B	Site A	Site B
Control (CO)	53.78 a	45.4 a	4023.1 a	8564 a	70.57 a	234.1 a
Low compost (LC)	41.60 a	44.33 a	3464.0 ab	5893 a	72.55 a	163.2 a
High compost (HC)	44.38 a	34.99 a	3468.0 ab	8520 a	39.12 a	126.3 a
Low compost + lime (LCL)	40.35 a	33.77 a	3310.7 b	9842 a	48.81 a	234.0 a
High compost + lime (HCL)	45.37 a	37.11 a	3674.2 ab	8415 a	78.84 a	141.2 a
Low compost + lime + bentonite (LCLB)	41.39 a	36.34 a	3958.5 a	10347 a	80.33 a	356.7 a
High compost + lime + bentonite (HCLB)	41.57 a	54.10 a	3434.0 ab	9119 a	43.77 a	231.4 a

Table B.7 Appendix: Total concentration (mg kg^{-1}) of zinc (Zn), lead (Pb), nickel (Ni), and cadmium (Cd) in mine waste materials at Site A and B. Means followed by the same letter are not statistically different at 0.05.

Treatment	Zn		Pb		Ni		Cd	
	mg kg^{-1}							
	Site A	Site B	Site A	Site B	Site A	Site B	Site A	Site B
Control (CO)	3625.3 a	4057.2 a	3129.0 a	1142.0 a	3.40 a	3.43 a	38.82 a	89.31 a
Low compost (LC)	3569.0 a	2542.9 b	1875.0 a	1125.6 a	3.02 abc	3.42 a	40.55 a	22.81 b
High compost (HC)	3354.9 a	3275.9 ab	4022.0 a	1102.3 a	2.54 bc	2.71 a	22.24 a	39.79 b
Low compost + lime (LCL)	3381.1 a	2802.1 ab	2485.0 a	1053.8 a	2.39 c	2.97 a	26.97 a	30.96 b
High compost + lime (HCL)	3422.1 a	2633.5 b	2286.0 a	1015.5 a	3.40 a	3.73 a	24.71 a	30.96 b
Low compost + lime + bentonite (LCLB)	3622.7 a	3114.0 ab	2191.0 a	1194.0 a	3.15 ab	4.14 a	37.57 a	37.56 b
High compost + lime + bentonite (HCLB)	3386.6 a	3068.1 ab	2511.0 a	1252.6 a	2.33 c	3.87 a	28.29 a	32.82 b

Table B..8 Appendix: Mine waste materials with biosolids, for logarithm of hydrogen ion (pH), electrical conductivity (EC), cation exchange capacity (CEC), and organic matter (OM) at Site A and B. Means followed by the same letter are not statistically different at 0.05.

Treatment	pH		EC ms cm^{-1}		CEC meq $100g^{-1}$		OM %	
	Site A	Site B	Site A	Site B	Site A	Site B	Site A	Site B
Control (CO)	6.47 a	6.35 ab	1.13 ab	1.39 ab	5.9 ab	8.37 a	2.04 b	2.73 ab
Low compost (LC)	6.80 a	6.50 ab	0.90 b	1.35 ab	8.27 ab	8.23 a	3.32 ab	2.83 a
High compost (HC)	6.61 a	6.55 ab	1.04 ab	1.15 ab	5.20 b	7.20 a	1.99 b	2.06 ab
Low compost + lime (LCL)	6.46 a	5.75 ab	1.06 ab	0.85 b	4.13 b	7.07 a	1.83 b	1.82 ab
High compost + lime (HCL)	7.05 a	7.034 a	1.37 a	1.69 a	10.20 a	8.63 a	4.59 a	2.44 ab
Low compost + lime + bentonite (LCLB)	6.86 a	7.10 a	1.03 ab	1.29 ab	7.73 ab	6.60 a	3.33 ab	2.03 ab
High compost + lime + bentonite (HCLB)	6.61 a	5.14 b	0.99 ab	1.03 b	6.87 ab	7.10 a	2.05 b	1.77 b

Table B.9 Appendix: Mine waste materials with biosolids, total nitrogen (T N), total carbon (T C), and total organic carbon (T O C) at Site A and B. Means followed by the same letter are not statistically different at 0.05.

Treatment	T N		T C		T O C	
	%					
	Site A	Site B	Site A	Site B	Site A	Site B
Control (CO)	0.12 b	0.12 a	1.97 b	1.42 a	1.17 b	1.32 a
Low compost (LC)	0.16 ab	0.12 a	1.90 ab	1.45 a	1.58 b	1.35 a
High compost (HC)	0.12 b	0.11 a	1.04 b	1.13 a	0.85 b	1.09 a
Low compost + lime (LCL)	0.11 b	0.09 a	1.02 b	0.86 a	0.97 b	0.80 a
High compost + lime (HCL)	0.24 a	0.13 a	2.78 a	1.37 a	2.58 a	1.27 a
Low compost + lime + bentonite (LCLB)	0.17 ab	0.10 a	2.01 ab	0.99 a	1.74 ab	0.91 a
High compost + lime + bentonite (HCLB)	0.12 b	0.09 a	1.27 b	0.85 a	1.17 b	0.82 a

Table B.10 Appendix: Mine waste materials with biosolids, phosphorus (P) and total phosphorus (T P) at Site A and B. Means followed by the same letter are not statistically different at 0.05.

Treatment	P		T P	
	mg kg^{-1}			
	Site A	Site B	Site A	Site B
Control (CO)	499.0 a	351.3 a	1039.0 ab	944.0 a
Low compost (LC)	665.3 a	437.7 a	1253.7 ab	1040.3 a
High compost (HC)	457.0 a	376.0 a	935.0 ab	948.0 a
Low compost + lime (LCL)	400.0 a	272.9 a	788.7 b	814.0 a
High compost + lime (HCL)	731.0 a	382.7 a	1561.0 a	986.0 a
Low compost + lime + bentonite (LCLB)	569.3 a	198.0 a	1143.3 ab	777.7 a
High compost + lime + bentonite (HCLB)	533.0 a	157.0 a	1020.3 ab	696.3 a

Table B.11 Appendix: Extractable concentration (mg kg^{-1}) of copper (Cu), iron (Fe), and manganese (Mn) in mine waste materials with biosolids, at Site A and B. Means followed by the same letter are not statistically different at 0.05.

Treatment	Cu		Fe		Mn	
	mg kg^{-1}					
	Site A	Site B	Site A	Site B	Site A	Site B
Control (CO)	3.93 a	11.47 a	1.23 a	47.47 ab	0.10 a	4.40 a
Low compost (LC)	1.40 a	9.50 a	1.70 a	39.20 ab	0.03 a	3.30 a
High compost (HC)	4.43 a	7.17 a	2.30 a	31.47 ab	0.33 a	2.93 a
Low compost + lime (LCL)	5.17 a	7.80 a	4.20 a	41.37 ab	0.93 a	4.77 a
High compost + lime (HCL)	1.20 a	6.63 a	2.80 a	24.40 b	0.27 a	2.97 a
Low compost + lime + bentonite (LCLB)	3.87 a	5.30 a	5.10 a	17.77 b	0.97 a	5.23 a
High compost + lime + bentonite (HCLB)	3.57 a	12.63 a	7.50 a	59.87 a	1.03 a	4.03 a

Table B.12 Appendix: Extractable concentration (mg kg-1) of zinc (Zn), lead (Pb), nickel (Ni), and cadmium (Cd) in mine waste materials with biosolids, at Site A and B. Means followed by the same letter are not statistically different at 0.05.

Treatment	Zn		Pb		Ni		Cd	
	mg kg^{-1}							
	Site A	Site B	Site A	Site B	Site A	Site B	Site A	Site B
Control (CO)	330.23 ab	161.27 a	83.20 a	64.80 a	0.37 ab	0.10 a	8.60 a	1.70 ab
Low compost (LC)	333.47 a	98.30 a	20.40 a	57.37 a	0.47 a	0.10 a	9.37 a	0.80 b
High compost (HC)	312.07 ab	98.63 a	186.90 a	57.40 a	0.23 b	0.067 a	5.03 b	0.80 b
Low compost + lime (LCL)	311.53 ab	87.10 a	168.70 a	74.57 a	0.27 ab	0.10 a	5.17 b	0.70 b
High compost + lime (HCL)	325.10 ab	108.77 a	23.90 a	48.70 a	0.47 a	0.067 a	7.00 ab	0.80 b
Low compost + lime + bentonite (LCLB)	309.57 b	121.10 a	182.80 a	62.63 a	0.43 ab	0.067 a	4.77 b	1.27 ab
High compost + lime + bentonite (HCLB)	314.03 ab	155.17 a	125.90 a	54.43 a	0.27 b	0.10 a	6.13 ab	2.00 a

Table B.13 Appendix: Total concentration (mg kg^{-1}) OF copper (Cu), iron (Fe), and manganese (Mn) IN mine waste materials with biosolids, at Site A and B. Means followed by the same letter are not statistically different at 0.05.

Treatment	Cu		Fe		Mn	
	mg kg^{-1}					
	Site A	Site B	Site A	Site B	Site A	Site B
Control (CO)	64.3 a	53.4 a	3894.1 a	7821.0 a	57.77 b	256.70 a
Low compost (LC)	76.97 a	54.63 a	4309.6 a	9957.0 a	93.07 ab	154.30 a
High compost (HC)	54.73 a	45.83 a	3473.7 a	7797.0 a	65.20 b	148.20 a
Low compost + lime (LCL)	55.0 a	45.97 a	3851.2 a	9895.0 a	56.50 b	238.40 a
High compost + lime (HCL)	53.87 a	44.27 a	3927.2 a	7335.0 a	126.10 a	164.90 a
Low compost + lime + bentonite (LCLB)	51.50 a	39.07 a	4084.2 a	9441.0 a	105.93 ab	307.00 a
High compost + lime + bentonite (HCLB)	50.30 a	51.70 a	3978.8 a	10155.0 a	75.50 ab	115.40 a

Table B.14 Appendix: Total concentration (mg kg^{-1}) of zinc (Zn), lead (Pb), nickel (Ni), and cadmium (Cd) in mine waste materials with biosolids, for at Site A and B. Means followed by the same letter are not statistically different at 0.05.

Treatment	Zn		Pb		Ni		Cd	
	mg kg^{-1}							
	Site A	Site B	Site A	Site B	Site A	Site B	Site A	Site B
Control (CO)	4108.7 a	5304.0 a	4249.0 a	1256.3 a	3.53 ab	4.27 a	44.13 ab	32.57 a
Low compost (LC)	4107.3 a	2665.0 a	5554.0 a	1438.8 a	4.07 ab	2.33 b	47.40 a	24.83 a
High compost (HC)	4103.8 a	5935.0 a	4717.0 a	1187.1 a	3.13 b	2.57 ab	29.30 ab	54.53 a
Low compost + lime (LCL)	3934.2 a	5365.0 a	2725.0 a	1351.5 a	3.17 b	2.87 ab	33.40 ab	53.0 a
High compost + lime (HCL)	4113.4 a	4769.0 a	2092.0 a	1134.8 a	4.77 a	2.70 ab	28.53 ab	24.3 a
Low compost + lime + bentonite (LCLB)	4150.8 a	4671.0 a	2546.0 a	1202.6 a	4.30 ab	3.47 ab	25.10 b	32.57 a
High compost + lime + bentonite (HCLB)	3858.5 a	3197.0 a	1962.0 a	1450.0 a	3.67 ab	1.93 b	36.80 ab	36.30 a

Table B.15 Appendix: Mine waste materials without biosolids, for logarithm of hydrogen ion (pH), electrical conductivity (EC), cation exchange capacity (CEC), and organic matter (OM) at Site A and B. Means followed by the same letter are not statistically different at 0.05.

Treatment	pH		EC		CEC		OM	
			ms cm^{-1}		meq $100g^{-1}$		%	
	Site A	Site B	Site A	Site B	Site A	Site B	Site A	Site B
Control (CO)	7.31 a	6.84 ab	0.88 a	0.88 ab	3.87 b	8.83 ab	1.39 b	2.52 a
Low compost (LC)	7.46 a	6.75 ab	0.79 a	1.28 a	6.77 ab	11.33 a	2.97 ab	2.53 a
High compost (HC)	7.41 a	6.89 ab	0.73 a	0.88 ab	4.47 b	6.63 b	1.66 b	1.99 ab
Low compost + lime (LCL)	7.53 a	5.99 ab	0.98 a	0.81 ab	4.03 b	5.80 b	1.42 b	1.48 b
High compost + lime (HCL)	7.53 a	7.64 a	1.11 a	1.18 a	12.10 a	7.67 ab	3.89 a	2.26 ab
Low compost + lime + bentonite (LCLB)	7.56 a	7.54 ab	0.92 a	1.14 ab	6.13 ab	7.17 ab	2.54 ab	1.77 ab
High compost + lime + bentonite (HCLB)	7.36 a	5.60 b	0.79 a	0.61 b	4.47 b	6.67 b	1.92 b	1.48 b

Table B.16 Appendix: Mine waste materials without biosolids, total nitrogen (T N), total carbon (T C), and total organic carbon (T O C) at Site A and B. Means followed by the same letter are not statistically different at 0.05.

Treatment	T N		T C		T O C	
	%					
	Site A	Site B	Site A	Site B	Site A	Site B
Control (CO)	0.09 c	0.13 a	0.78 bc	1.44 a	0.67 b	1.29 a
Low compost (LC)	0.17 ab	0.11 a	1.85 ab	1.26 a	1.59 ab	1.19 ab
High compost (HC)	0.10 bc	0.10 a	1.12 bc	0.99 a	0.98 b	0.89 ab
Low compost + lime (LCL)	0.09 c	0.09 a	0.75 c	0.80 a	0.73 b	0.69 b
High compost + lime (HCL)	0.21 a	0.11 a	2.47 a	1.30 a	2.19 a	1.18 ab
Low compost + lime + bentonite (LCLB)	0.15 abc	0.09 a	1.47 abc	0.58 a	1.48 ab	0.76 ab
High compost + lime + bentonite (HCLB)	0.10 bc	0.09 a	1.08 bc	0.71 a	1.04 b	0.73 ab

Table B.17 Appendix: Mine waste materials without biosolids, phosphorus (P) and total phosphorus (T P) at Site A and B. Means followed by the same letter are not statistically different at 0.05.

Treatment	P		T P	
	mg kg^{-1}		%	
	Site A	Site B	Site A	Site B
Control (CO)	195.7 ab	284.7 a	546.3 b	756.3 a
Low compost (LC)	462.3 ab	323.1 a	959.0 ab	871.3 a
High compost (HC)	285.4 ab	274.7 a	740.7 ab	735.3 a
Low compost + lime (LCL)	140.2 b	180.0 a	435.7 b	663.0 a
High compost + lime (HCL)	622.3 a	241.0 a	1271.3 a	807.3 a
Low compost + lime + bentonite (LCLB)	390.4 ab	111.9 a	778.3 ab	589.3 a
High compost + lime + bentonite (HCLB)	343.7 ab	38.1 a	705.3 ab	512.7 a

Table B.18 Appendix: Extractable concentration (mg kg^{-1}) of copper (Cu), iron (Fe), and manganese (Mn) in mine waste materials without biosolids, at Site A and B. Means followed by the same letter are not statistically different at 0.05.

Treatment	Cu		Fe		Mn	
	mg kg^{-1}					
	Site A	Site B	Site A	Site B	Site A	Site B
Control (CO)	3.33 a	11.70 ab	0.63 a	39.33 ab	0.00 a	2.97 a
Low compost (LC)	1.07 a	9.13 ab	0.50 a	35.73 ab	0.00 a	2.57 a
High compost (HC)	3.80 a	6.43 ab	2.13 a	27.13 ab	0.00 a	2.03 a
Low compost + lime (LCL)	4.03 a	7.07 ab	4.10 a	32.53 ab	0.47 a	2.73 a
High compost + lime (HCL)	1.03 a	5.43 ab	1.27 a	20.27 b	0.10 a	1.93 a
Low compost + lime + bentonite (LCLB)	3.03 a	4.73 b	5.67 a	14.37 b	0.33 a	2.60 a
High compost + lime + bentonite (HCLB)	2.87 a	14.30 a	6.13 a	50.23 a	0.27 a	2.90 a

Table B.19 Appendix: Extractable concentration (mg kg^{-1}) of zinc (Zn), lead (Pb), nickel (Ni), and cadmium (Cd) in mine waste materials without biosolids, at Site A and B. Means followed by the same letter are not statistically different at 0.05.

Treatment	Zn		Pb		Ni		Cd	
	mg kg^{-1}							
	Site A	Site B	Site A	Site B	Site A	Site B	Site A	Site B
Control (CO)	320.10 a	156.07 a	152.00 a	67.93 a	0.17 a	0.10 a	8.63 ab	1.80 ab
Low compost (LC)	329.10 a	98.80 a	27.80 a	58.00 a	0.33 a	0.07 ab	9.47 a	0.87 ab
High compost (HC)	308.27 a	100.87 a	237.80 a	59.07 a	0.20 a	0.03 ab	6.07 ab	0.90 ab
Low compost + lime (LCL)	300.67 a	88.20 a	266.00 a	70.50 a	0.17 a	0.00 b	5.90 ab	0.73 b
High compost + lime (HCL)	317.60 a	96.93 a	35.40 a	48.23 a	0.33 a	0.03 ab	7.10 ab	0.77 b
Low compost + lime + bentonite (LCLB)	294.07 a	117.47 a	253.90 a	64.37 a	0.27 a	0.03 ab	4.80 b	1.37 ab
High compost + lime + bentonite (HCLB)	307.40 a	162.33 a	181.10 a	58.43 a	0.17 a	0.07 ab	6.57 ab	2.43 a

Table B.20 Appendix: Total concentration (mg kg^{-1}) of copper (Cu), iron (Fe), and manganese (Mn) in mine waste materials without biosolids, at Site A and B. Means followed by the same letter are not statistically different at 0.05.

Treatment	Cu		Fe		Mn	
	mg kg^{-1}					
	Site A	Site B	Site A	Site B	Site A	Site B
Control (CO)	55.7 a	55.5 a	3620.7 a	7652.0 abc	51.10 b	214.60 a
Low compost (LC)	50.23 a	52.57 a	3967.6 a	6949.0 c	93.30 ab	221.80 a
High compost (HC)	48.20 a	43.37 a	3493.8 a	7563.0 abc	63.23 ab	191.8 a
Low compost + lime (LCL)	46.73 a	42.87 a	3867.6 a	9793.0 a	55.47 b	262.60 a
High compost + lime (HCL)	46.67 a	41.43 a	3735.3 a	8249.0 abc	113.60 a	175.50 a
Low compost + lime + bentonite (LCLB)	46.17 a	36.3 a	3983.2 a	9421.0 ab	100.00 ab	328.90 a
High compost + lime + bentonite (HCLB)	42.53 a	52.33 a	3604.2 a	7042.0 bc	95.37 ab	150.80 a

Table B.21 Appendix: Total concentration (mg kg^{-1}) of zinc (Zn), lead (Pb), nickel (Ni), and cadmium (Cd) in mine waste materials without biosolids, at Site A and B. Means followed by the same letter are not statistically different at 0.05.

Treatment	Zn		Pb		Ni		Cd	
	mg kg^{-1}							
	Site A	Site B	Site A	Site B	Site A	Site B	Site A	Site B
Control (CO)	4010.0 a	5483.1 ab	3300.4 a	1260.8 a	3.17 a	3.27 a	39.10 ab	32.57 a
Low compost (LC)	4172.8 a	5198.8 ab	2093.6 a	1271.1 a	4.07 a	2.97 a	49.60 a	23.90 a
High compost (HC)	3794.8 a	5616.3 ab	3366.1 a	1192.9 a	3.03 a	2.60 a	27.77 b	41.10 a
Low compost + lime (LCL)	3836.9 a	4818.1 b	2623.9 a	1316.5 a	3.17 a	3.17 a	28.50 b	36.23 a
High compost + lime (HCL)	4131.9 a	4827.8 b	1939.2 a	1122 a	4.27 a	2.63 a	25.97 b	26.97 a
Low compost + lime + bentonite (LCLB)	4354.8 a	5324.5 ab	2436.1 a	1103.1 a	4.07 a	3.43 a	31.17 b	35.03 a
High compost + lime + bentonite (HCLB)	3567.7 a	6288.6 a	1736.9 a	1335.8 a	3.07 a	2.73 a	31.77 b	44.30 a

Table B.22 Appendix: Concentration (%) of phosphorus (P), potassium (k), calcium (Ca), magnesium (Mg), and total nitrogen (T N) of shoots grown in mine waste materials with biosolids, at Site A and B. Means followed by the same letter are not statistically different at 0.05.

Treatment	P		K		Ca		Mg		T N	
	%									
	Site A	Site B	Site A	Site B	Site A	Site B	Site A	Site B	Site A	Site B
Control (CO)	0.34 a	0.31 b	1.36 a	1.29 a	1.04 a	0.58 abc	0.37 a	0.41 a	2.24 a	1.16 ab
Low compost (LC)	0.26 a	0.31 b	1.19 ab	1.21 a	0.98 ab	0.55 bc	0.29 c	0.42 a	1.34 b	1.05 b
High compost (HC)	0.36 a	0.32 b	1.24 ab	1.26 a	0.99 ab	0.57 bc	0.35 ab	0.41 a	1.83 ab	1.25 ab
Low compost + lime (LCL)	0.39 a	0.33 ab	1.17 ab	1.40 a	0.83 c	0.53 bc	0.33 abc	0.39 a	1.68 ab	1.63 ab
High compost + lime (HCL)	0.29 a	0.29 b	1.08 b	1.17 a	0.88 bc	0.67 ab	0.31 bc	0.44 a	1.08 b	1.01 b
Low compost + lime + bentonite (LCLB)	0.28 a	0.29 b	1.15 ab	1.27 a	0.93 abc	0.72 a	0.29 c	0.41 a	1.18 b	1.18 ab
High compost + lime + bentonite (HCLB)	0.36 a	0.47 a	1.16 ab	1.57 a	0.95 ab	0.51 c	0.32 abc	0.34 a	1.63 ab	1.89 a

Table B.23 Appendix: Concentration (mg kg^{-1}) of copper (Cu), iron (Fe), manganese (Mn), and zinc (Zn) of shoots grown in mine waste materials with biosolids, at Site A and B. Means followed by the same letter are not statistically different at 0.05.

Treatment	Cu		Fe		Mn		Zn	
	mg kg^{-1}							
	Site A	Site B	Site A	Site B	Site A	Site B	Site A	Site B
Control (CO)	8.90 a	6.47 b	1308.6 a	109.60 b	75.57 a	36.77 a	4647.0 a	418.9 b
Low compost (LC)	2.37 a	6.70 b	105.7 a	101.60 b	39.77 a	49.93 a	1375.0 b	232.8 b
High compost (HC)	7.63 a	8.97 ab	487.6 a	138.10 b	47.67 a	53.00 a	2856.0 ab	516.7 b
Low compost + lime (LCL)	7.87 a	11.8 ab	500.8 a	181.80 b	57.47 a	101.73 a	2889.0 ab	1044.5 ab
High compost + lime (HCL)	2.47 a	4.97 b	65.50 a	129.40 b	25.13 a	20.50 a	643.0 b	115.3 b
Low compost + lime + bentonite (LCLB)	3.13 a	5.67 b	73.70 a	197.60 b	36.60 a	45.53 a	872.0 b	565.8 b
High compost + lime + bentonite (HCLB)	5.97 a	17.60 a	559.90 a	431.60 a	71.80 a	93.43 a	2870.0 ab	2083.6 a

Table B.24 Appendix: Concentration (mg kg^{-1}) of lead (Pb), nickel (Ni), and cadmium (Cd) of shoots grown in mine waste materials with biosolids, at Site A and B. Means followed by the same letter are not statistically different at 0.05.

Treatment	Pb		Ni		Cd	
	mg kg^{-1}					
	Site A	Site B	Site A	Site B	Site A	Site B
Control (CO)	159.07 a	8.17 b	2.47 a	1.17 ab	26.23 a	5.07 b
Low compost (LC)	13.90 b	10.40 b	0.57 b	0.87 ab	7.87 b	3.03 b
High compost (HC)	79.63 ab	20.03 ab	2.30 a	1.03 ab	12.97 ab	5.40 b
Low compost + lime (LCL)	71.40 ab	33.77 ab	2.33 a	1.40 ab	12.97 ab	7.47 b
High compost + lime (HCL)	10.27 b	6.77 b	0.53 a	0.30 b	4.47 b	2.13 b
Low compost + lime + bentonite (LCLB)	28.07 ab	12.7 ab	0.93 a	1.00 ab	6.07 b	4.37 b
High compost + lime + bentonite (HCLB)	55.27 ab	63.53 a	1.90 a	1.67 a	14.0 ab	19.0 a

Table B.25 Appendix: Concentration (%) of phosphorus (P), potassium (k), calcium (Ca), magnesium (Mg), and total nitrogen (T N) of shoots grown in mine waste materials without biosolids, at Site A and B. Means followed by the same letter are not statistically different at 0.05.

Treatment	P		K		Ca		Mg		TN	
	%									
	Site A	Site B	Site A	Site B	Site A	Site B	Site A	Site B	Site A	Site B
Control (CO)	0.14 a	0.30 a	1.09 b	1.90 a	1.21 a	0.88 ab	0.43 a	0.30 a	1.08 a	0.87 a
Low compost (LC)	0.25 a	0.27 a	1.27 ab	1.85 a	1.65 a	0.70 b	0.34 abc	0.29 a	0.98 a	0.94 a
High compost (HC)	0.18 a	0.25 a	1.25 ab	1.74 a	1.27 a	0.78 ab	0.34 bc	0.31 a	1.10 a	1.07 a
Low compost + lime (LCL)	0.14 a	0.16 a	1.27 ab	1.36 a	1.33 a	0.71 b	0.38 abc	0.35 a	1.20 a	0.71 a
High compost + lime (HCL)	0.34 a	0.36 a	1.47 a	2.01 a	1.64 a	0.92 ab	0.31 bc	0.29 a	0.90 a	0.90 a
Low compost + lime + bentonite (LCLB)	0.25 a	0.24 a	1.46 a	1.89 a	1.54 a	1.14 a	0.29 c	0.27 a	1.02 a	0.96 a
High compost + lime + bentonite (HCLB)	0.20 a	0.24 a	1.31 ab	1.53 a	1.32 a	0.89 ab	0.40 ab	0.38 a	1.07 a	1.06 a

Table B.26 Appendix: Concentration (mg kg^{-1}) of copper (Cu), iron (Fe), manganese (Mn), and zinc (Zn) of shoots grown in mine waste materials without biosolids, at Site A and B. Means followed by the same letter are not statistically different at 0.05.

Treatment	Cu		Fe		Mn		Zn	
	mg kg^{-1}							
	Site A	Site B	Site A	Site B	Site A	Site B	Site A	Site B
Control (CO)	9.50 a	10.00 ab	1696.0 a	155.0 a	36.70 a	24.60 a	2584.0 a	847.0 ab
Low compost (LC)	3.53 a	14.73 ab	252.0 b	1602.0 a	18.70 b	57.87 a	1561.0 bc	872.0 ab
High compost (HC)	7.60 a	13.53 ab	527.0 ab	1186.0 a	21.20 ab	53.97 a	1629.0 bc	895.0 ab
Low compost + lime (LCL)	8.17 a	24.50 ab	330.0 b	4495.0 a	19.30 b	135.87 a	1883.0 abc	1846.0 ab
High compost + lime (HCL)	5.13 a	7.97 b	327.0 b	180.0 a	31.60 ab	21.17 a	1512.0 bc	137.0 b
Low compost + lime + bentonite (LCLB)	4.50 a	8.47 ab	193.0 b	502.0 a	24.40 ab	38.60 a	1213.0 c	714.0 ab
High compost + lime + bentonite (HCLB)	5.57 a	26.10 a	601.0 ab	5647.0 a	24.50 ab	126.60 a	2095.0 ab	2510.0 a

Table B.27 Appendix: Concentration (mg kg^{-1}) of lead (Pb), nickel (Ni), and cadmium (Cd) of shoots grown in mine waste materials without biosolids, at Site A and B. Means followed by the same letter are not statistically different at 0.05.

Treatment	Pb		Ni		Cd	
	mg kg^{-1}					
	Site A	Site B	Site A	Site B	Site A	Site B
Control (CO)	274.10 a	18.80 a	2.60 a	0.50 a	30.80 a	9.03 ab
Low compost (LC)	68.50 a	105.00 a	0.95 a	1.70 a	20.73 a	7.80 ab
High compost (HC)	249.90 a	114.90 a	1.13 a	2.57 a	20.27 a	9.33 ab
Low compost + lime (LCL)	212.30 a	317.40 a	1.50 a	7.50 a	27.47 a	14.70 ab
High compost + lime (HCL)	72.80 a	19.00 a	0.90 a	0.67 a	14.43 a	2.90 b
Low compost + lime + bentonite (LCLB)	100.30 a	23.60 a	0.90 a	0.55 a	14.70 a	8.80 ab
High compost + lime + bentonite (HCLB)	163.10 a	284.50 a	2.00 a	6.40 a	26.20 a	20.90 a

Table B.28 Appendix: Concentration (%) of nitrogen (N) phosphorus (P), potassium (k), calcium (Ca), and magnesium (Mg) of roots grown in mine waste materials with biosolids, at Site A and B. Means followed by the same letter are not statistically different at 0.05.

Treatment	N		P		K		Ca		Mg	
	%									
	Site A	Site B	Site A	Site B	Site A	Site B	Site A	Site B	Site A	Site B
Control (CO)	1.39 a	0.73 a	0.33 a	0.14 a	0.93 a	0.53 a	0.53 a	0.23 a	0.35 a	0.16 a
Low compost (LC)	1.04 a	0.75 a	0.24 a	0.17 a	0.71 a	0.49 a	0.55 a	0.32 a	0.26 bc	0.17 a
High compost (HC)	1.34 a	0.80 a	0.34 a	0.16 a	0.97 a	0.52 a	0.51 a	0.32 a	0.32 ab	0.19 a
Low compost + lime (LCL)	1.17 a	0.98 a	0.39 a	0.19 a	0.87 a	0.62 a	0.43 a	0.22 a	0.31 abc	0.20 a
High compost + lime (HCL)	1.01 a	0.75 a	0.20 a	0.14 a	0.55 a	0.53 a	0.51 a	0.31 a	0.23 c	0.18 a
Low compost + lime + bentonite (LCLB)	1.05 a	0.74 a	0.22 a	0.14 a	0.58 a	0.53 a	0.51 a	0.29 a	0.25 bc	0.17 a
High compost + lime + bentonite (HCLB)	1.06 a	0.72 a	0.35 a	0.27 a	0.85 a	0.80 a	0.47 a	0.20 a	0.29 abc	0.23 a

Table B.29 Appendix: Concentration (mg kg^{-1}) of copper (Cu), iron (Fe), manganese (Mn), and zinc (Zn) of roots grown in mine waste materials with biosolids, at Site A and B. Means followed by the same letter are not statistically different at 0.05.

Treatment	Cu		Fe		Mn		Zn	
	mg kg^{-1}							
	Site A	Site B	Site A	Site B	Site A	Site B	Site A	Site B
Control (CO)	79.10 a	43.97 b	5566.0 a	9008.0 ab	75.60 a	140.80 a	10397.0 a	2053.0 b
Low compost (LC)	36.33 a	45.23 b	2542.0 a	6782.0 ab	59.57 a	85.60 a	6516.0 a	1329.0 b
High compost (HC)	76.87 a	39.90 b	7526.0 a	5913.0 b	89.97 a	55.17 a	10839.0 a	2888.0 ab
Low compost + lime (LCL)	80.27 a	56.03 ab	5984.0 a	8403.0 ab	70.07 a	135.40 a	11673.0 a	3431.0 ab
High compost + lime (HCL)	28.87 a	37.40 b	2477.0 a	6918.0 ab	55.53 a	153.60 a	4001.0 a	3272.0 ab
Low compost + lime + bentonite (LCLB)	53.93 a	34.63 b	3965.0 a	7749.0 ab	70.43 a	150.27 a	5324.0 a	2543.0 ab
High compost + lime + bentonite (HCLB)	74.37 a	91.03 a	5839.0 a	11100.0 a	84.03 a	93.27 a	10651.0 a	5862.0 a

Table B.30 Appendix: Concentration (mg kg^{-1}) of lead (Pb), nickel (Ni), and cadmium (Cd) of roots grown in mine waste materials with biosolids, at Site A and B. Means followed by the same letter are not statistically different at 0.05.

Treatment	Pb		Ni		Cd	
	mg kg^{-1}					
	Site A	Site B	Site A	Site B	Site A	Site B
Control (CO)	1070.6 a	554.4 ab	10.45 a	5.13 ab	59.80 a	12.70 ab
Low compost (LC)	944.9 a	561.5 ab	3.67 a	4.20 b	38.53 a	7.90 b
High compost (HC)	1771.2 a	502.6 b	10.53 a	3.93 b	52.13 a	15.23 ab
Low compost + lime (LCL)	1400.1 a	651.9 ab	12.37 a	7.00 ab	48.73 a	25.77 ab
High compost + lime (HCL)	674.7 a	541.4 b	3.03 a	4.73 b	16.43 a	23.20 ab
Low compost + lime + bentonite (LCLB)	1352.4 a	494.0 b	5.03 a	6.40 ab	27.60 a	14.43 ab
High compost + lime + bentonite (HCLB)	1163.8 a	789.5 a	10.87 a	16.70 a	54.87 a	31.80 a

Table B.31 Appendix: Concentration (%) of nitrogen (N) phosphorus (P), potassium (k), calcium (Ca), and magnesium (Mg) of roots grown in mine waste materials without biosolids, at Site A and B. Means followed by the same letter are not statistically different at 0.05.

Treatment	N		P		K		Ca		Mg	
	%									
	Site A	Site B	Site A	Site B	Site A	Site B	Site A	Site B	Site A	Site B
Control (CO)	0.89 ab	0.60 a	0.15 a	0.14 a	1.01 a	0.79 a	0.36 b	0.30 a	0.27 a	0.27 a
Low compost (LC)	0.85 ab	0.60 a	0.14 a	0.14 a	0.83 a	0.80 a	0.42 ab	0.41 a	0.27 a	0.25 a
High compost (HC)	0.84 ab	0.55 a	0.13 a	0.15 a	0.87 a	0.92 a	0.40 b	0.45 a	0.26 a	0.27 a
Low compost + lime (LCL)	0.91 a	0.63 a	0.11 a	0.15 a	0.89 a	0.99 a	0.36 b	0.26 a	0.27 a	0.24 a
High compost + lime (HCL)	0.73 b	0.62 a	0.17 a	0.16 a	0.81 a	0.85 a	0.57 a	0.43 a	0.29 a	0.30 a
Low compost + lime + bentonite (LCLB)	0.73 b	0.57 a	0.13 a	0.12 a	0.82 a	0.86 a	0.42 ab	0.40 a	0.26 a	0.27 a
High compost + lime + bentonite (HCLB)	0.77 ab	0.56 a	0.14 a	0.12 a	0.94 a	0.69 a	0.38 b	0.25 a	0.29 a	0.23 a

Table B.32 Appendix: Concentration (mg kg^{-1}) of copper (Cu), iron (Fe), manganese (Mn), and zinc (Zn) of roots grown in mine waste materials without biosolids, at Site A and B. Means followed by the same letter are not statistically different at 0.05.

Treatment	Cu		Fe		Mn		Zn	
	mg kg^{-1}							
	Site A	Site B	Site A	Site B	Site A	Site B	Site A	Site B
Control (CO)	52.60 a	58.97 a	8832.1 a	10978.0 a	51.15 ab	131.60 a	7703.0 a	3728.0 b
Low compost (LC)	26.53 a	62.00 a	5047.0 a	14064.0 a	45.93 b	128.10 a	6242.0 ab	3588.0 b
High compost (HC)	57.67 a	63.43 a	7222.0 a	12623.0 a	55.23 ab	111.70 a	6688.0 ab	3907.0 b
Low compost + lime (LCL)	48.03 a	71.07 a	7500.0 a	18260.0 a	51.87 ab	154.80 a	5967.0 ab	3332.0 b
High compost + lime (HCL)	29.10 a	51.30 a	5501.0 a	9094.0 a	67.27 a	93.30 a	5523.0 ab	3107.0 b
Low compost + lime + bentonite (LCLB)	36.63 a	47.73 a	5321.0 a	11335.0 a	50.77 ab	142.90 a	4882.0 b	4642.0 b
High compost + lime + bentonite (HCLB)	38.87 a	69.80 a	5838.0 a	15119.0 a	44.60 b	159.00 a	6219.0 ab	13016.0 a

Table B.33 Appendix: Concentration (mg kg^{-1}) of lead (Pb), nickel (Ni), and cadmium (Cd) of roots grown in mine waste materials without biosolids, at Site A and B. Means followed by the same letter are not statistically different at 0.05.

Treatment	Pb		Ni		Cd	
	mg kg^{-1}					
	Site A	Site B	Site A	Site B	Site A	Site B
Control (CO)	1994.0 a	651.6 a	10.25 a	9.23 a	76.55 a	28.23 b
Low compost (LC)	927.2 a	723.6 a	5.43 a	14.37 a	48.03 a	22.40 b
High compost (HC)	2359.0 a	716.8 a	7.87 a	12.57 a	61.77 a	28.20 b
Low compost + lime (LCL)	1508.0 a	903.2 a	9.23 a	20.77 a	67.83 a	19.83 b
High compost + lime (HCL)	1022.0 a	533.0 a	6.10 a	9.10 a	36.10 a	24.73 b
Low compost + lime + bentonite (LCLB)	1429.0 a	673.6 a	6.00 a	8.83 a	37.77 a	39.43 b
High compost + lime + bentonite (HCLB)	1291.0 a	803.8 a	8.80 a	11.70 a	67.00 a	131.00 a

Table B.34 Appendix: Concentration (%) of phosphorus (P), potassium (k), calcium (Ca), and magnesium (Mg) of grains grown in mine waste materials with biosolids, at Site A and B. Means followed by the same letter are not statistically different at 0.05.

Treatment	P		K		Ca		Mg	
	%							
	Site A	Site B	Site A	Site B	Site A	Site B	Site A	Site B
Control (CO)	NA	0.28 a	NA	0.82 a	NA	0.13 a	NA	0.27 a
Low compost (LC)	0.27 a	0.24 ab	0.82 b	0.70 a	0.16 a	0.15 a	0.20 a	0.27 a
High compost (HC)	NA	0.25 ab	NA	0.77 a	NA	0.15 a	NA	0.27 a
Low compost + lime (LCL)	0.22 b	0.23 b	0.67 c	0.68 a	0.17 a	0.10 a	0.22 a	0.23 a
High compost + lime (HCL)	0.28 a	0.24 ab	0.96 a	0.71 a	0.15 a	0.15 a	0.23 a	0.27 a
Low compost + lime + bentonite (LCLB)	0.21 b	0.24 ab	0.58 d	0.80 a	0.19 a	0.14 a	0.22 a	0.25 a
High compost + lime + bentonite (HCLB)	0.27 a	0.27 ab	0.88 b	0.91 a	0.14 a	0.12 a	0.22 a	0.24 a

Table B.35 Appendix: Concentration (mg kg^{-1}) of copper (Cu), iron (Fe), manganese (Mn), and zinc (Zn) of grains grown in mine waste materials with biosolids, at Site A and B. Means followed by the same letter are not statistically different at 0.05.

Treatment	Cu		Fe		Mn		Zn	
	mg kg^{-1}							
	Site A	Site B	Site A	Site B	Site A	Site B	Site A	Site B
Control (CO)	NA	12.30 a	NA	179.75 ab	NA	24.70 a	NA	66.25 ab
Low compost (LC)	4.00 a	12.05 a	453.60 a	138.90 b	19.30 a	33.35 a	141.90 a	65.40 a
High compost (HC)	NA	11.05 a	NA	127.45 b	NA	20.75 a	NA	54.45 ab
Low compost + lime (LCL)	7.70 a	8.30 b	230.20 a	121.00 b	21.10 a	15.80 a	114.40 a	46.60 b
High compost + lime (HCL)	5.95 a	11.17 a	259.60 a	118.07 b	12.20 a	18.50 a	86.70 a	52.17 ab
Low compost + lime + bentonite (LCLB)	6.35 a	11.30 a	455.20 a	155.00 ab	19.30 a	12.70 a	138.30 a	47.10 b
High compost + lime + bentonite (HCLB)	5.30 a	11.00 ab	185.00 a	279.40 a	14.10 a	24.00 a	100.90 a	67.20 a

Table B.36 Appendix: Concentration (mg kg^{-1}) of lead (Pb), nickel (Ni), and cadmium (Cd) of grains grown in mine waste materials with biosolids, at Site A and B. Means followed by the same letter are not statistically different at 0.05.

Treatment	Pb		Ni		Cd	
	mg kg^{-1}					
	Site A	Site B	Site A	Site B	Site A	Site B
Control (CO)	NA	2.50 a	NA	0.45 a	NA	0.90 a
Low compost (LC)	3.70 a	2.20 a	1.42 a	1.00 a	2.35 a	1.40 a
High compost (HC)	NA	1.15 a	NA	0.40 a	NA	0.25 a
Low compost + lime (LCL)	0.90 a	0.50 a	1.36 a	NA	1.80 a	NA
High compost + lime (HCL)	2.40 a	1.05 a	1.84 a	0.60 a	2.15 a	0.433 a
Low compost + lime + bentonite (LCLB)	8.65 a	2.10 a	1.27 a	NA	2.60 a	0.30 a
High compost + lime + bentonite (HCLB)	3.50 a	3.80 a	1.35 a	1.00 a	2.00 a	1.40 a

NA= no data

Table B.37 Appendix: Concentration (%) of total nitrogen (TN) and total carbon (TC) of grains grown in mine waste materials with biosolids, at Site A and B. Means followed by the same letter are not statistically different at 0.05.

Treatment	TN		TC	
	%			
	Site A	Site B	Site A	Site B
Control (CO)	NA	1.57 a	NA	45.19 ab
Low compost (LC)	1.42 a	1.38 ab	44.16 a	45.60 a
High compost (HC)	NA	1.35 b	NA	45.35 ab
Low compost + lime (LCL)	1.36 a	1.36 b	45.96 a	45.41 ab
High compost + lime (HCL)	1.84 a	1.42 ab	41.63 a	45.41 ab
Low compost + lime + bentonite (LCLB)	1.27 a	1.32 b	44.67 a	45.39 ab
High compost + lime + bentonite (HCLB)	1.35 a	1.42 ab	44.63 a	44.53 b

NA= no data

Appendix C - Characterization of Interior Building Dust at an Abandoned Lead and Zinc Mining Area

Figure C.1 through C.21 have been prepared the following way. Maps were made using ArcMap version (10.4.1). Quantile classification method to make the maps. Quantile distributes a set of values into group that contain an equal number of values.

Figure C.1 Appendix: Classification of Mn in dust samples, using sweeping method at 9 different sites in Galena, KS.

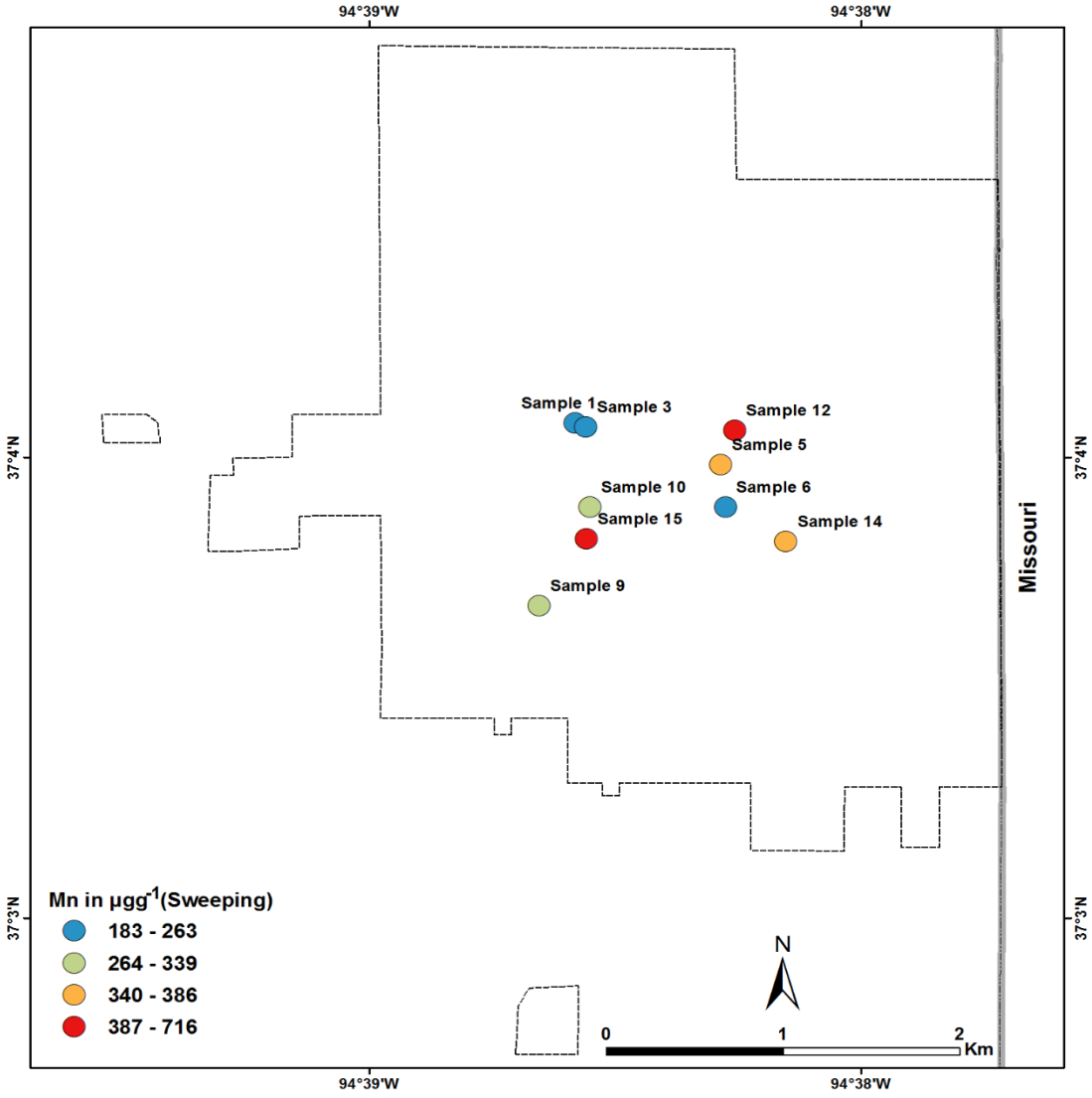

Figure C.2 Appendix: Classification of Ni in dust samples, using sweeping method at 9 different sites in Galena, KS.

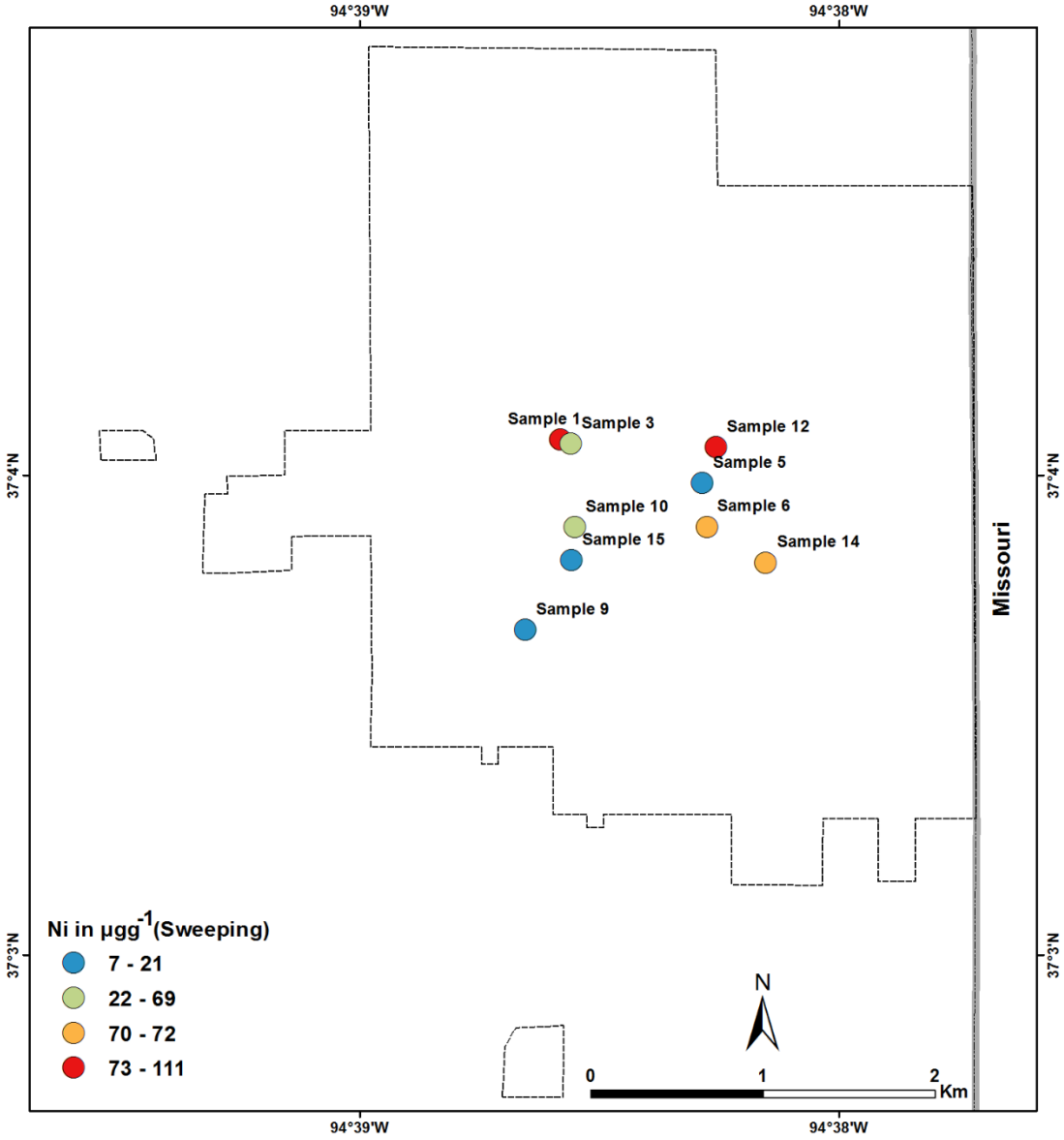

Figure C.3 Appendix: Classification of Cu in dust samples, using sweeping method at 9 different sites in Galena, KS.

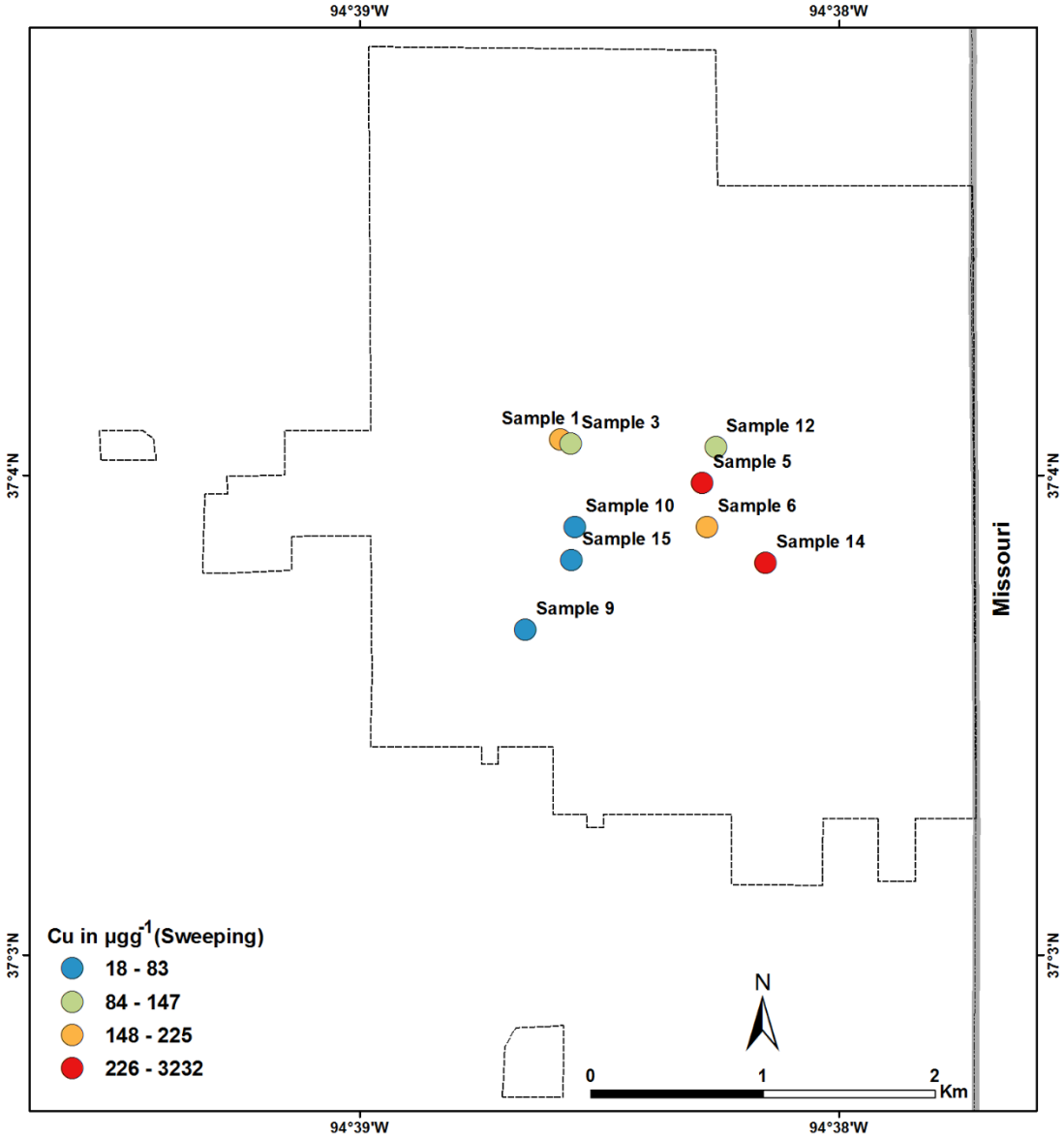

Figure C.4 Appendix: Classification of Fe in dust samples, using sweeping method at 9 different sites in Galena, KS.

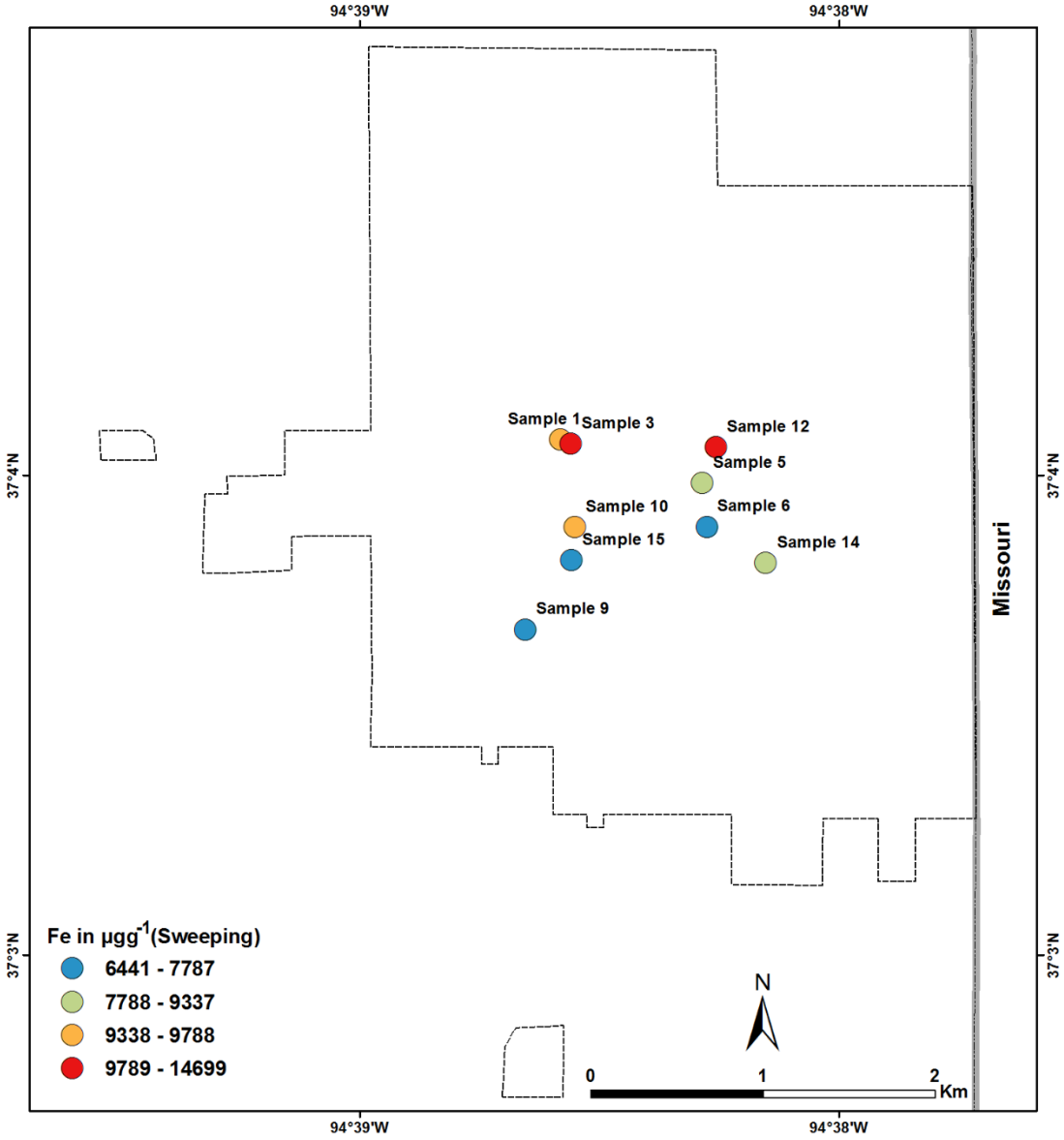

Figure C.5 Appendix: Classification of Pb in dust samples, using sweeping method at 9 different sites in Galena, KS.

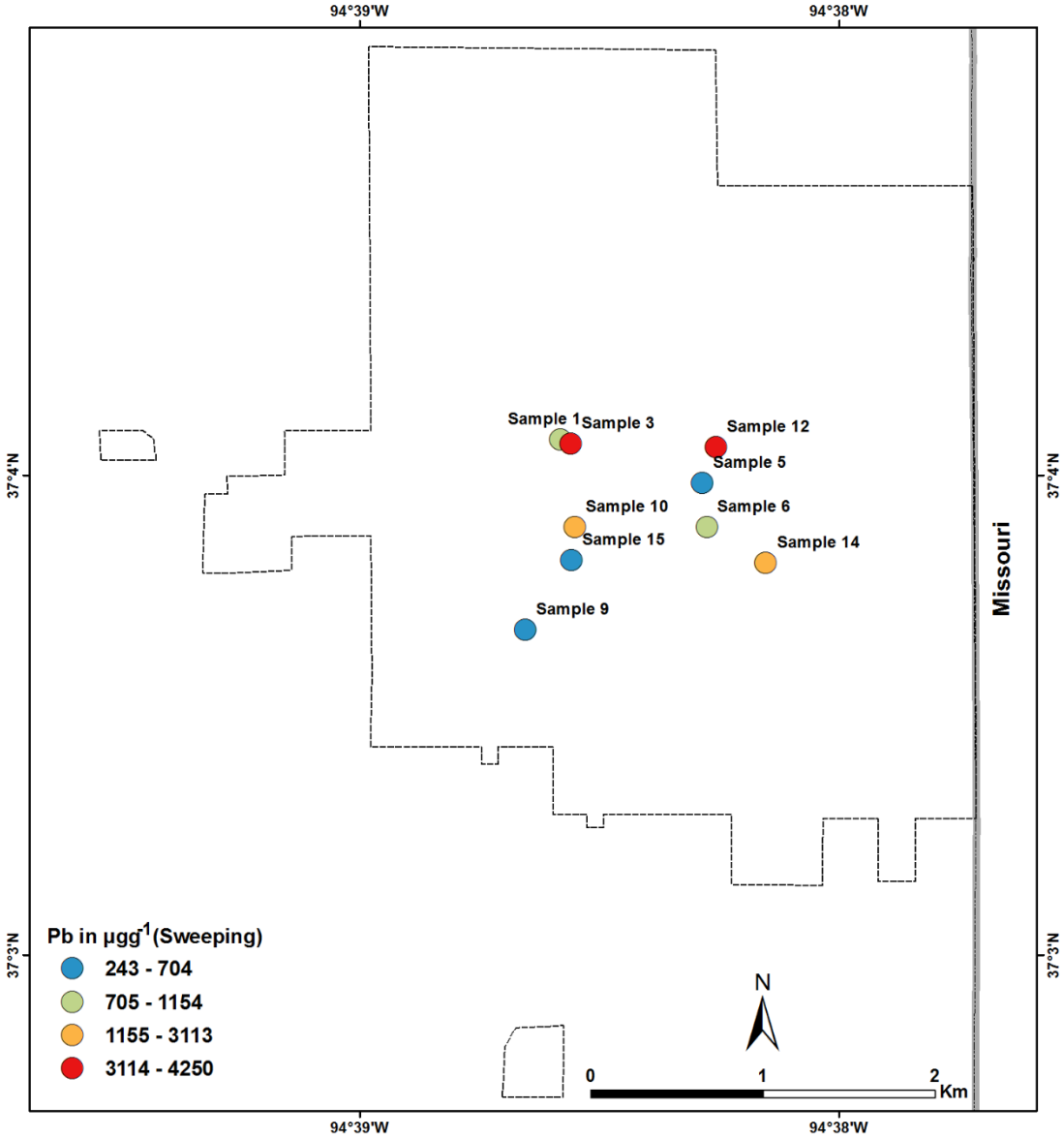

Figure C.6 Appendix: Classification of Zn in dust samples, using sweeping method at 9 different sites in Galena, KS.

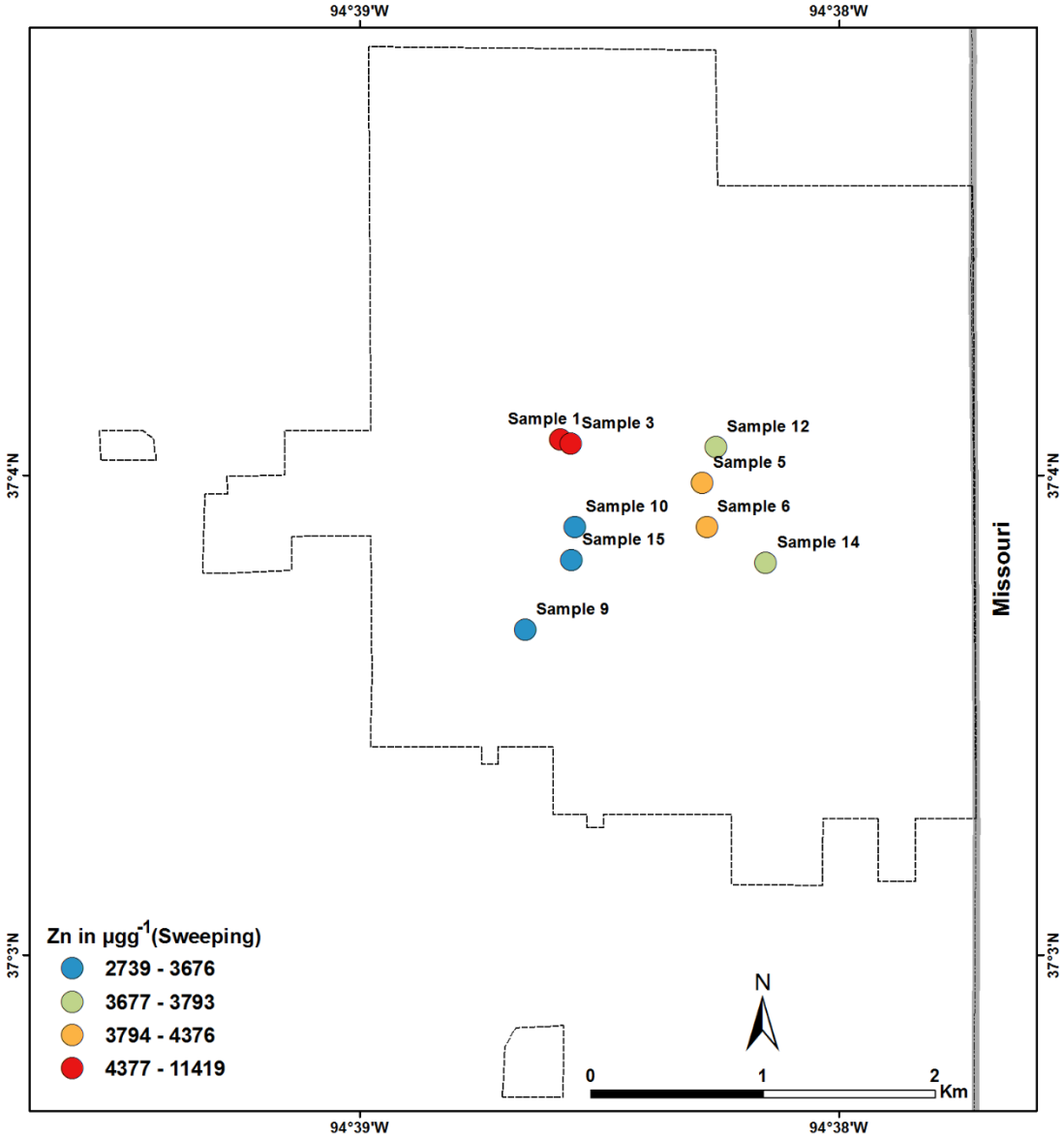

Figure C.7 Appendix: Classification of Cd in dust samples, using sweeping method at 9 different sites in Galena, KS.

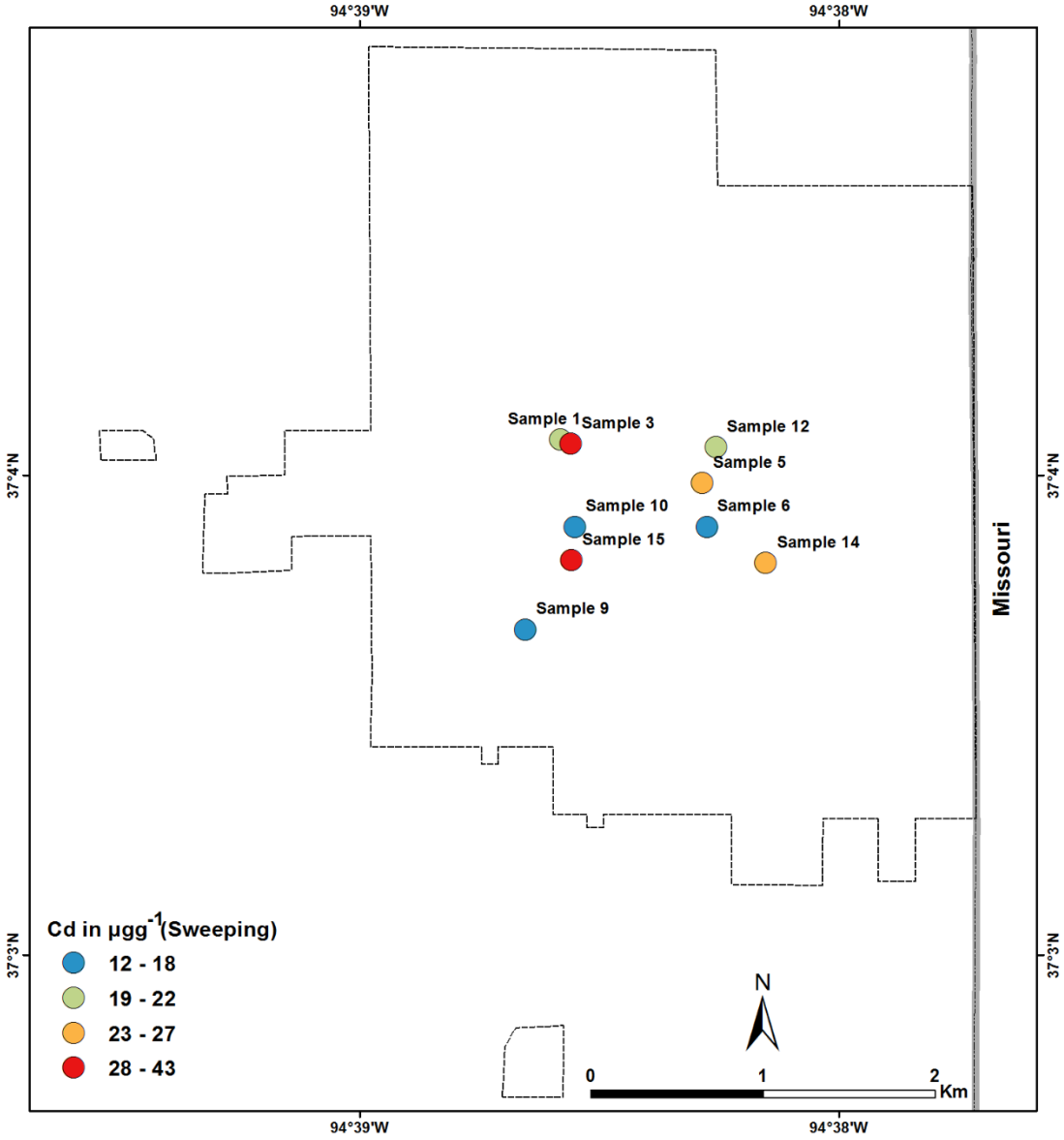

Figure C.8 Appendix: Classification of Mn in dust samples, using vacuuming method at 5 different sites in Galena, KS.

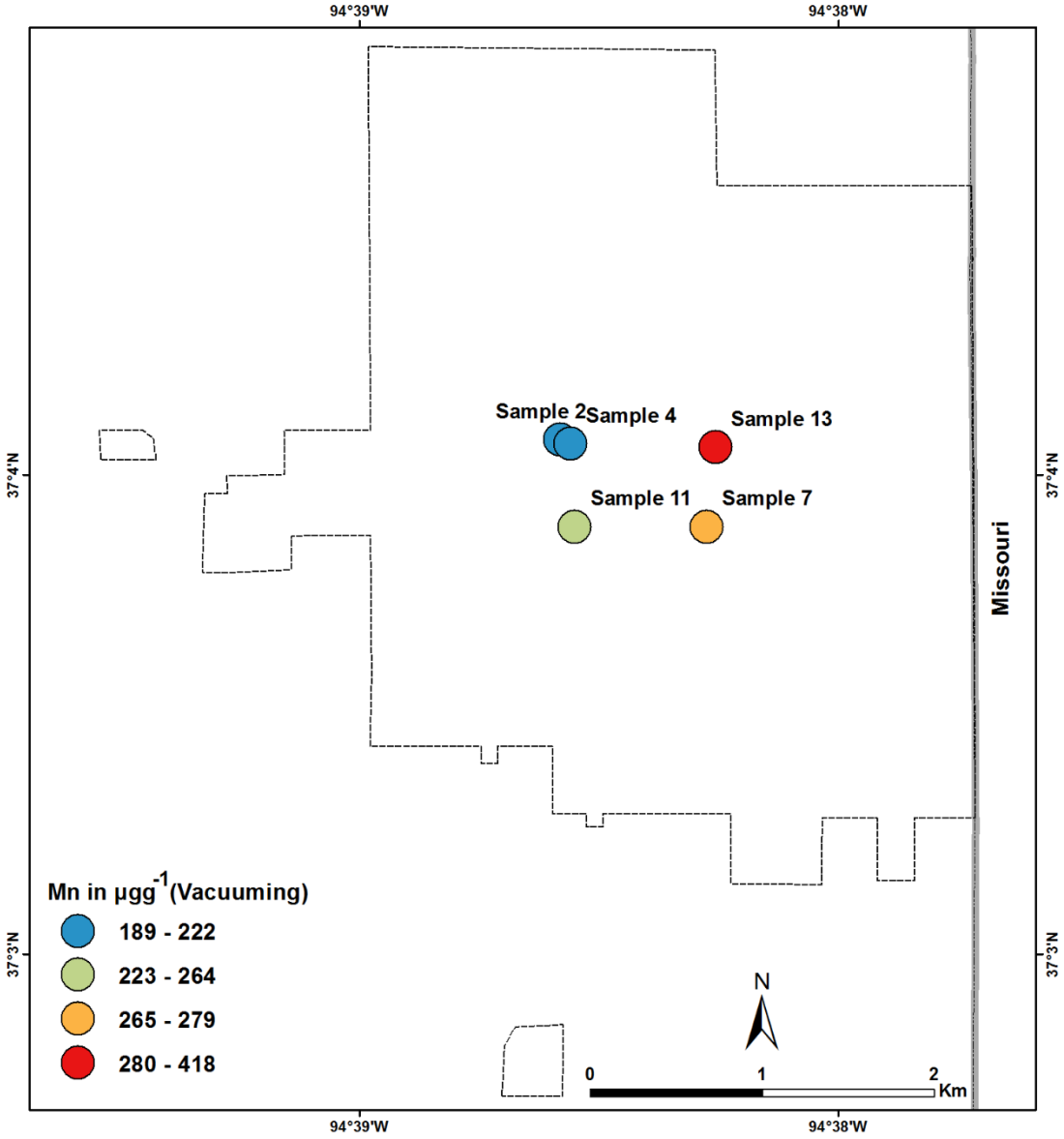

Figure C.9 Appendix: Classification of Ni in dust samples, using vacuuming method at 5 different sites in Galena, KS.

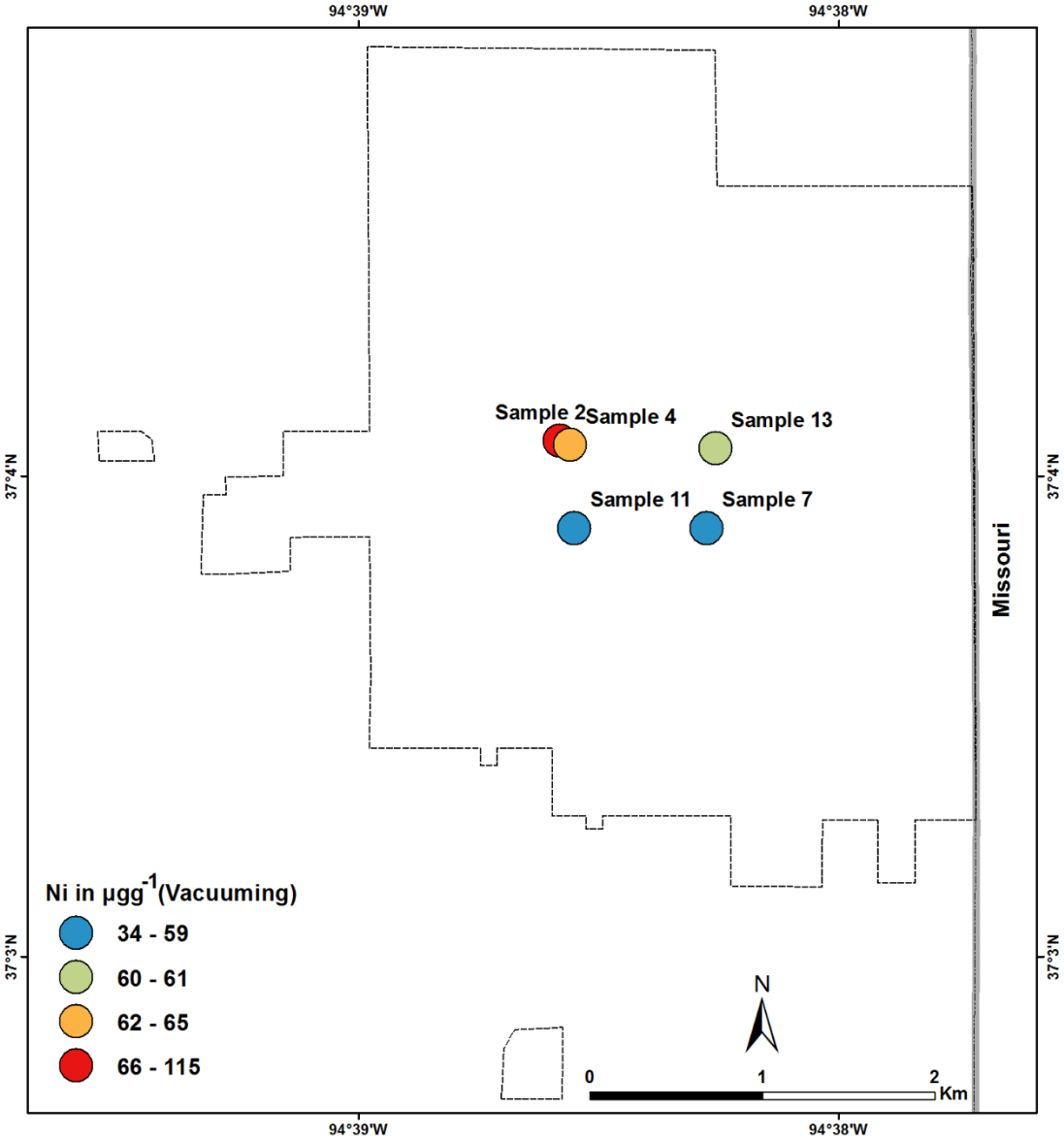

Figure C.10 Appendix: Classification of Cu in dust samples, using vacuuming method at 5 different sites in Galena, KS.

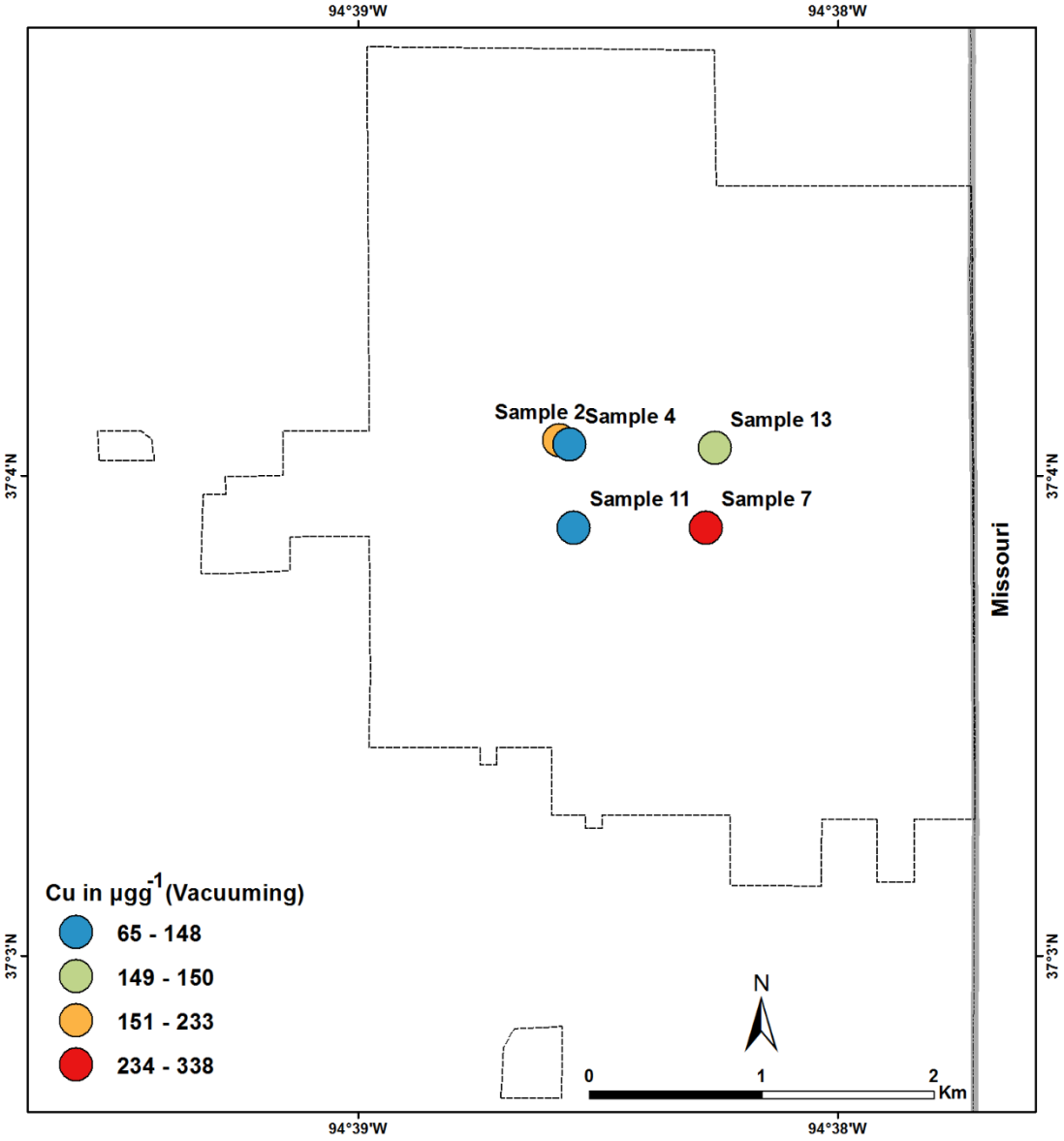

Figure C.11 Appendix: Classification of Fe in dust samples, using vacuuming method at 5 different sites in Galena, KS.

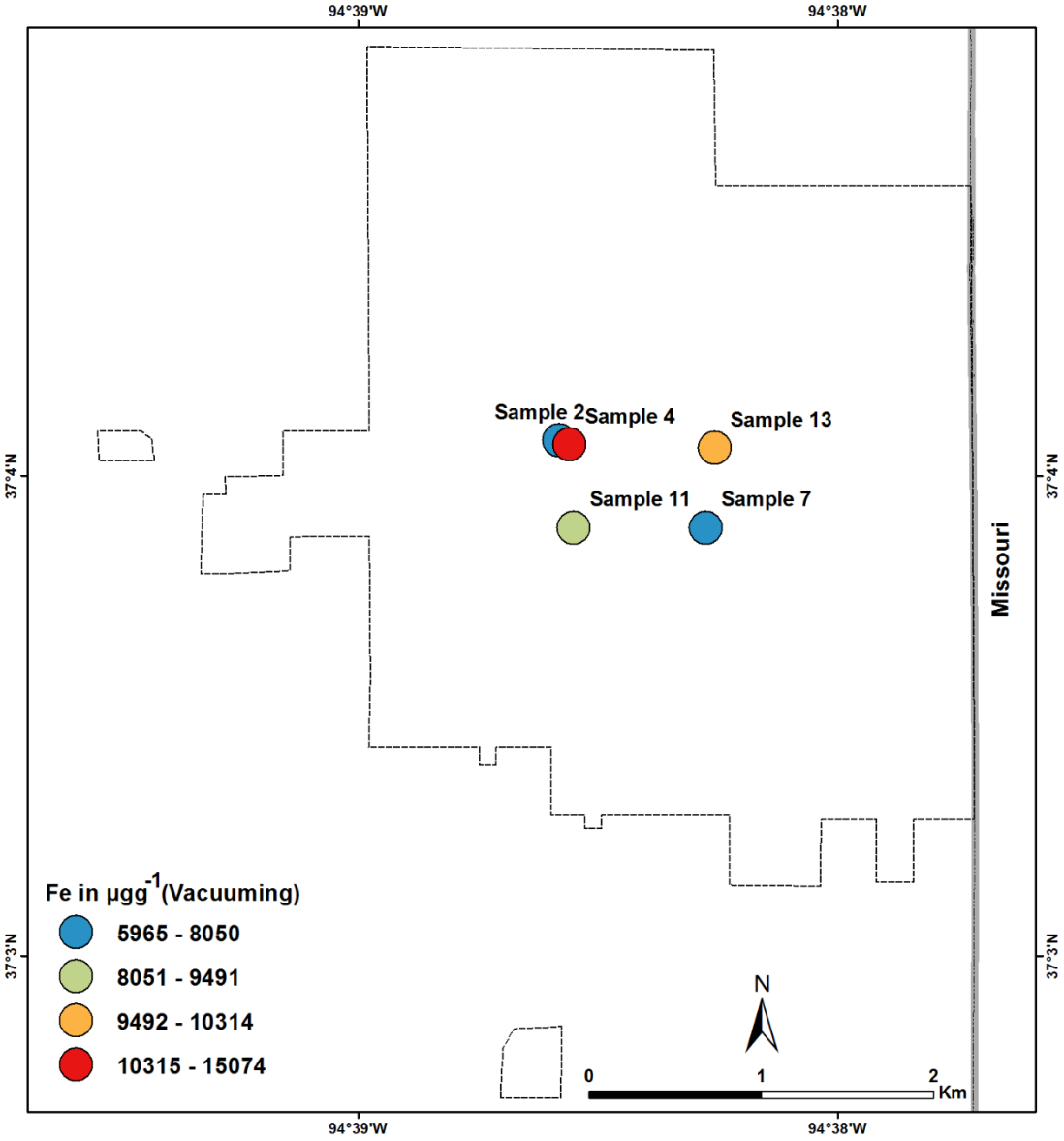

Figure C.12 Appendix: Classification of Pb in dust samples, using vacuuming method at 5 different sites in Galena, KS.

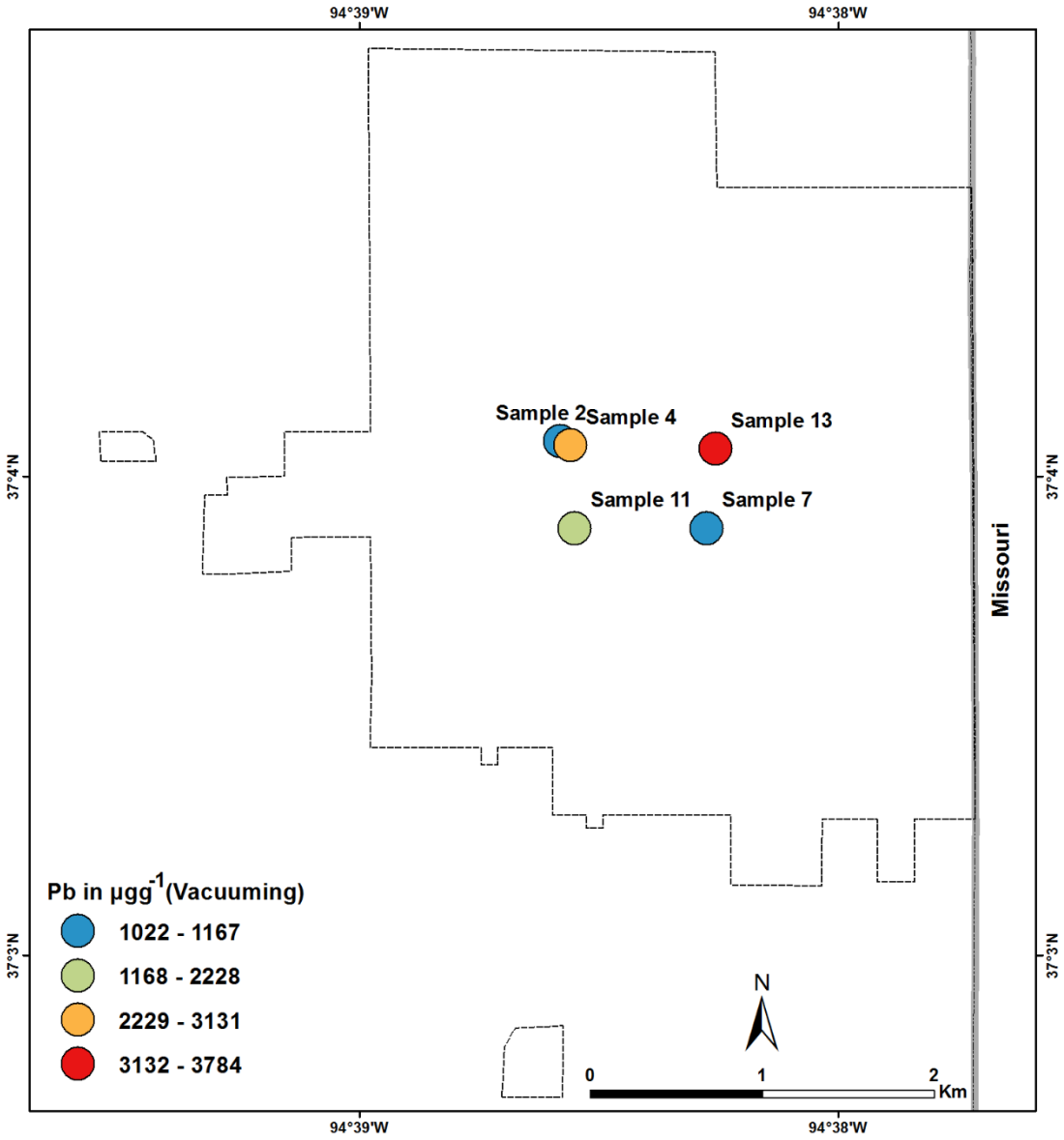

Figure C.13 Appendix: Classification of Zn in dust samples, using vacuuming method at 5 different sites in Galena, KS.

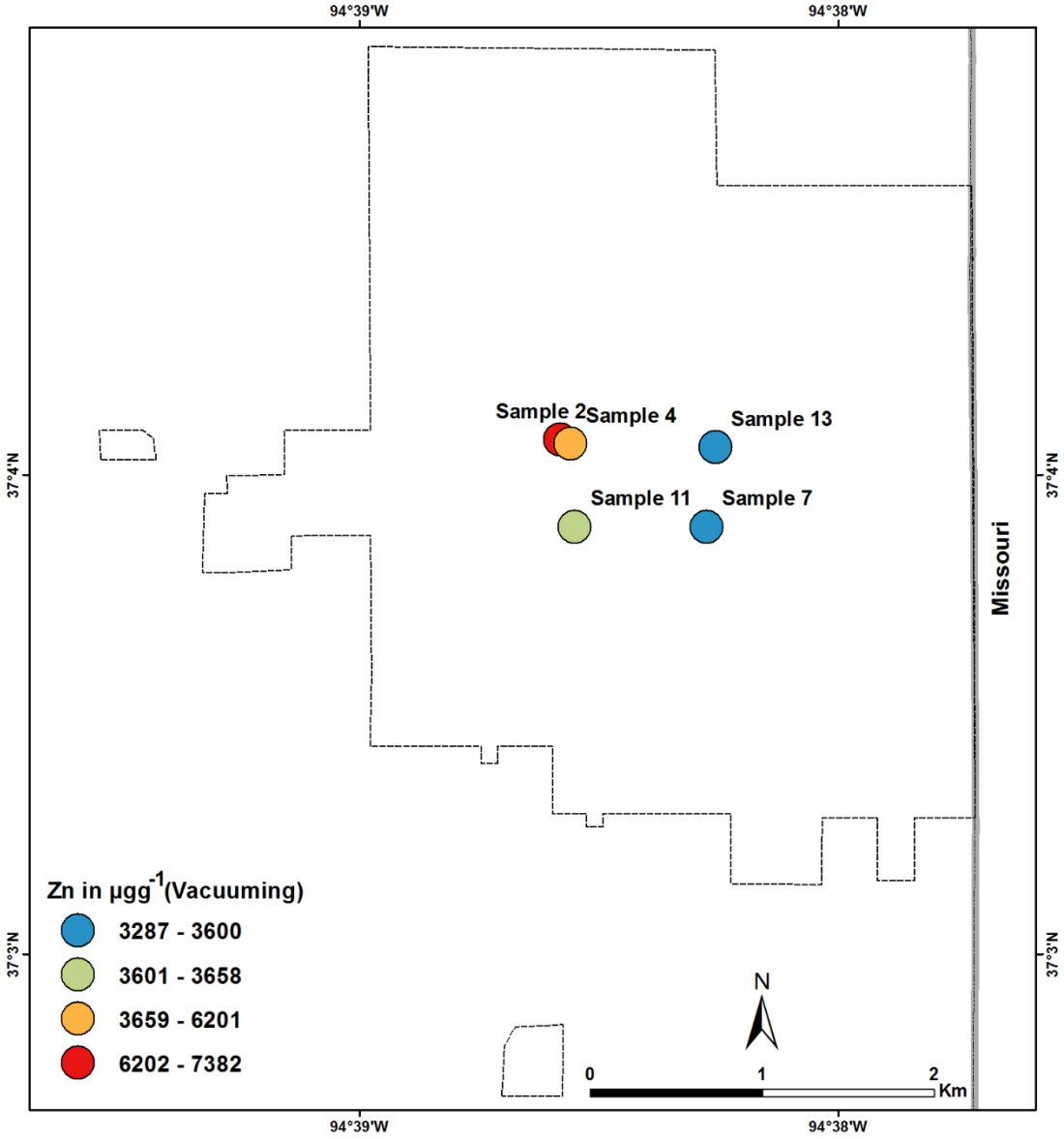

Figure C.14 Appendix: Classification of Cd in dust samples, using vacuuming method at 5 different sites in Galena, KS.

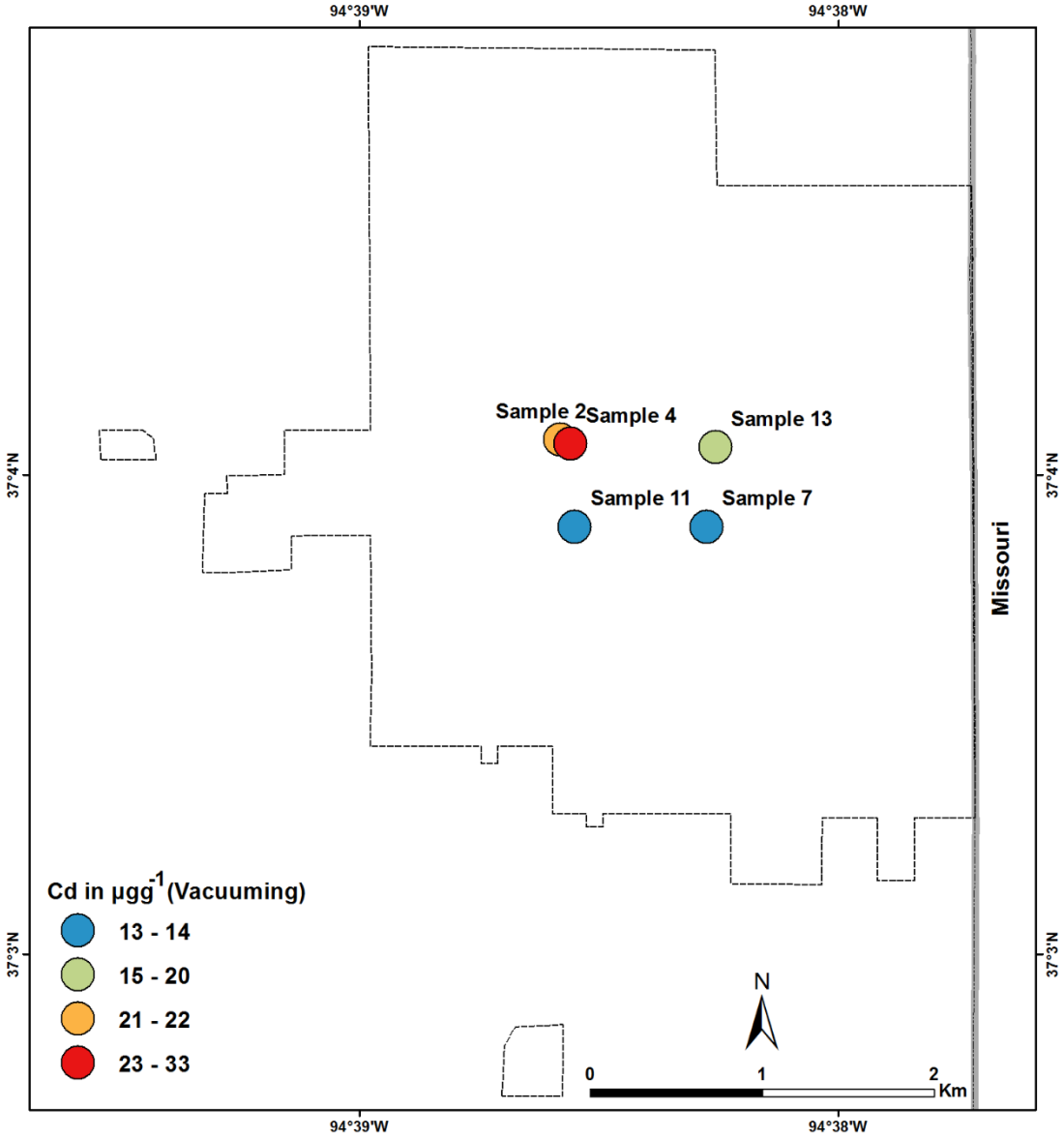

Figure C.15 Appendix: Classification of Mn in all 14 different dust samples, in Galena, KS.

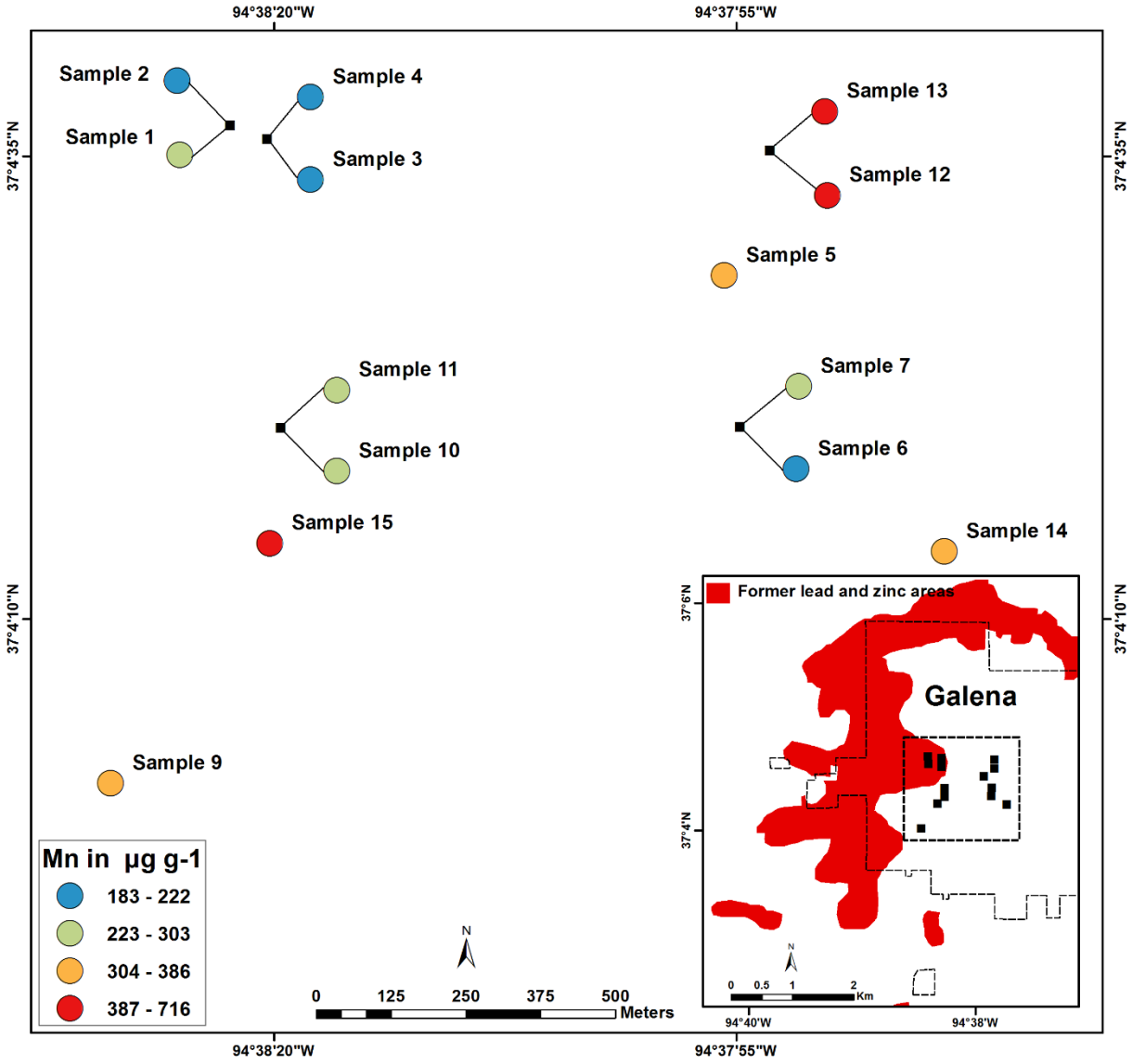

Figure C.16 Appendix: Classification of Ni in all 14 different dust samples, in Galena, KS.

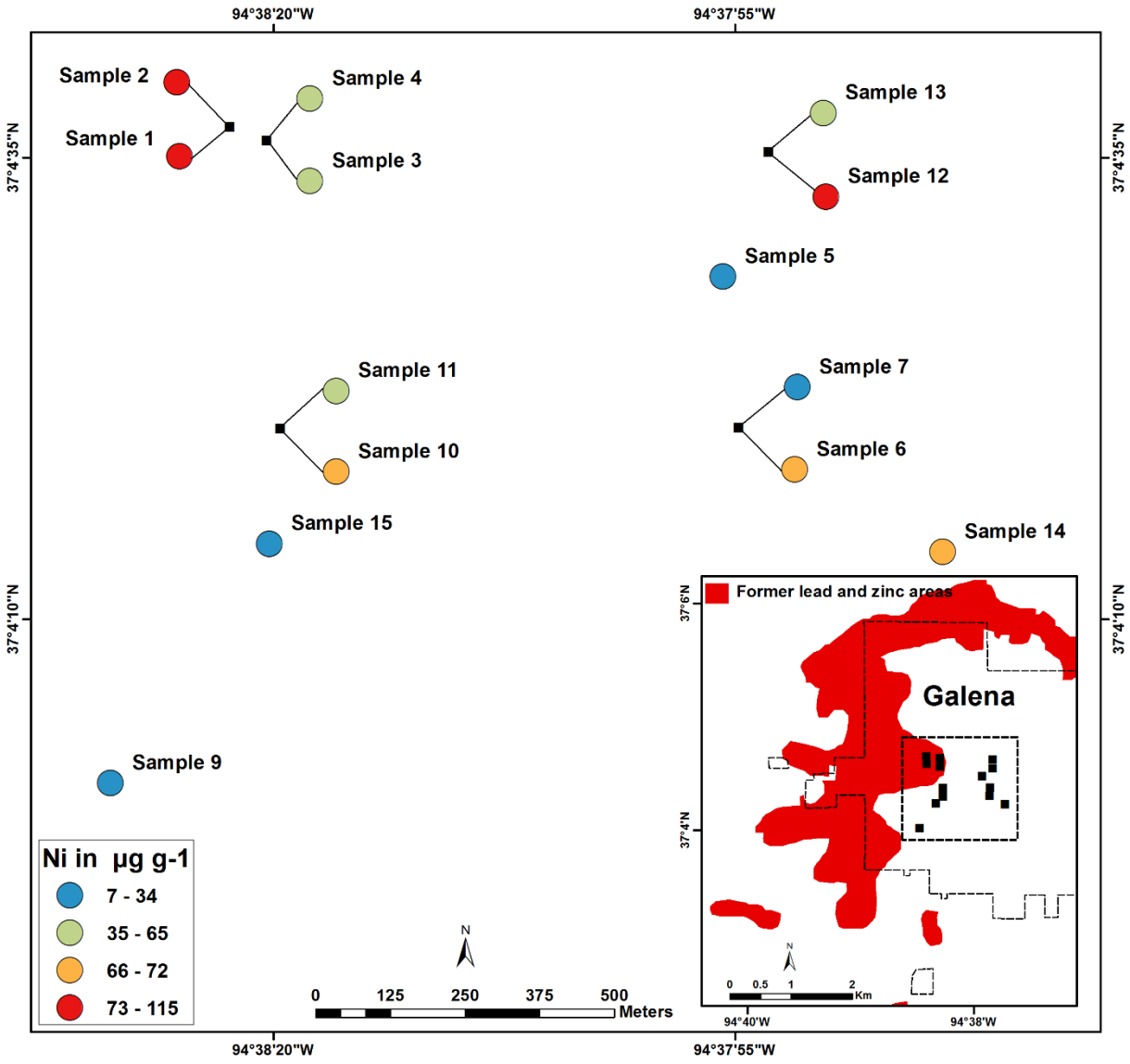

Figure C.17 Appendix: Classification of Cu in all 14 different dust samples, in Galena, KS.

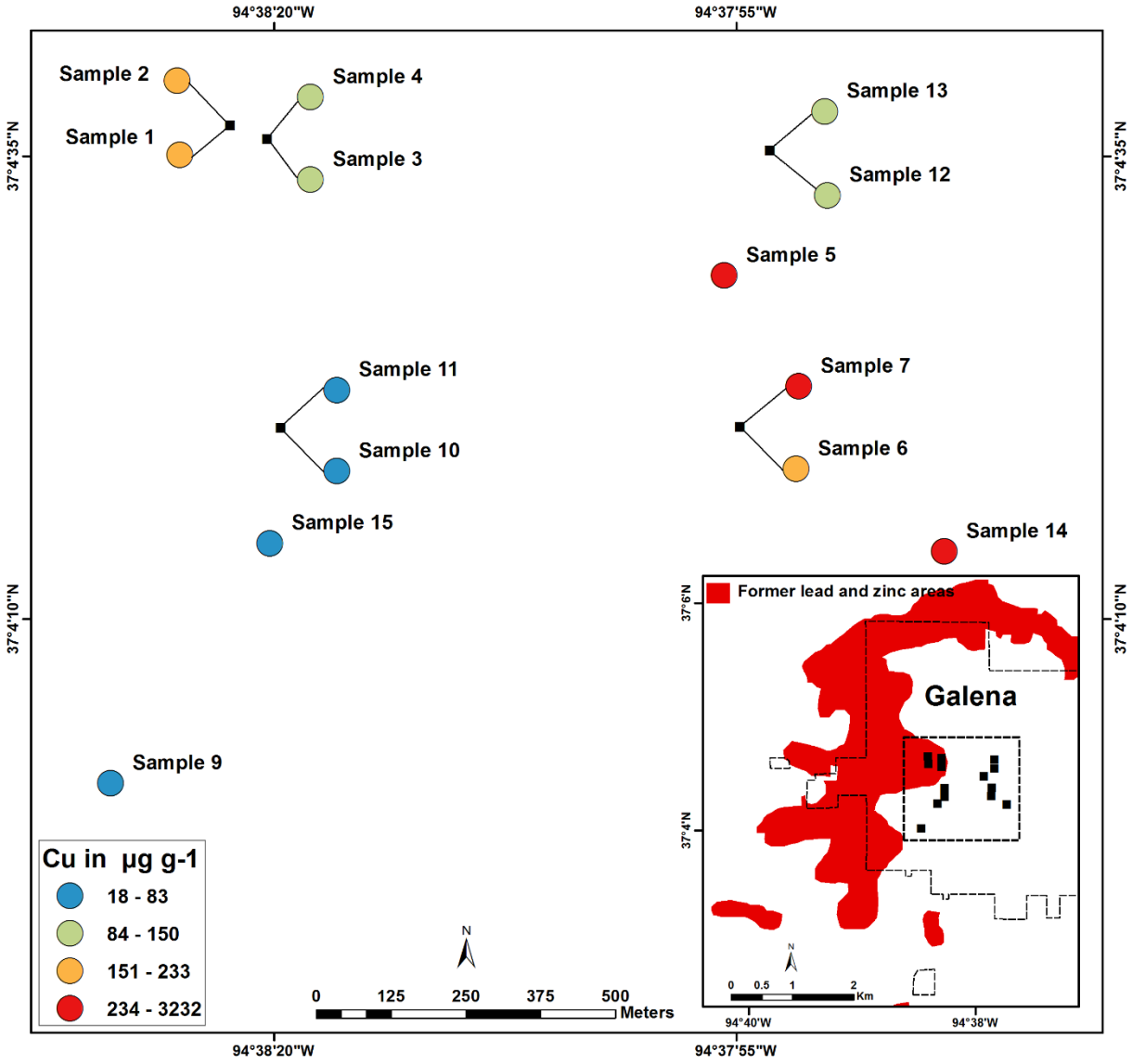

Figure C.18 Appendix: Classification of Fe in all 14 different dust samples, in Galena, KS.

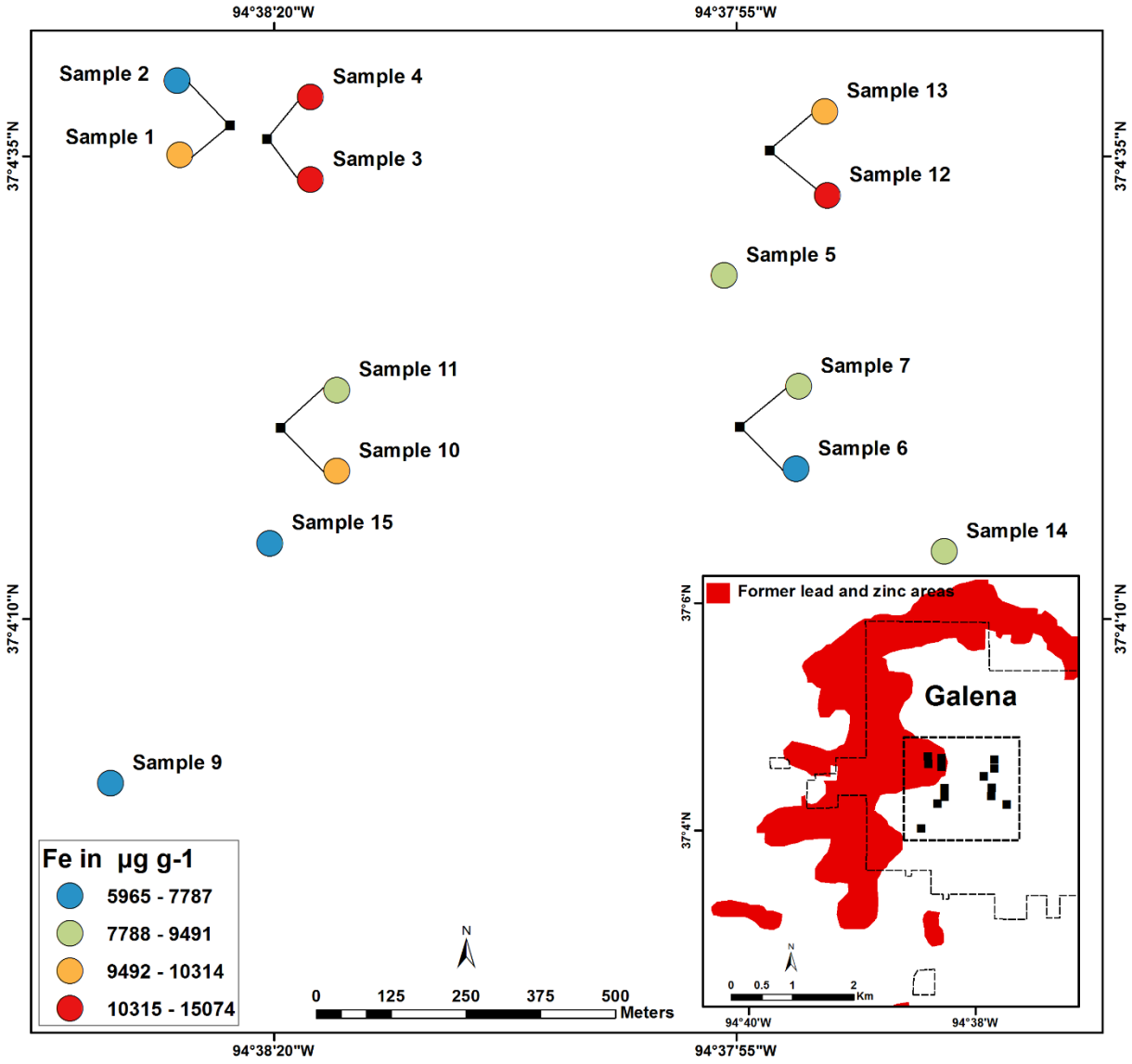

Figure C.19 Appendix: Classification of Pb in all 14 different dust samples, in Galena, KS.

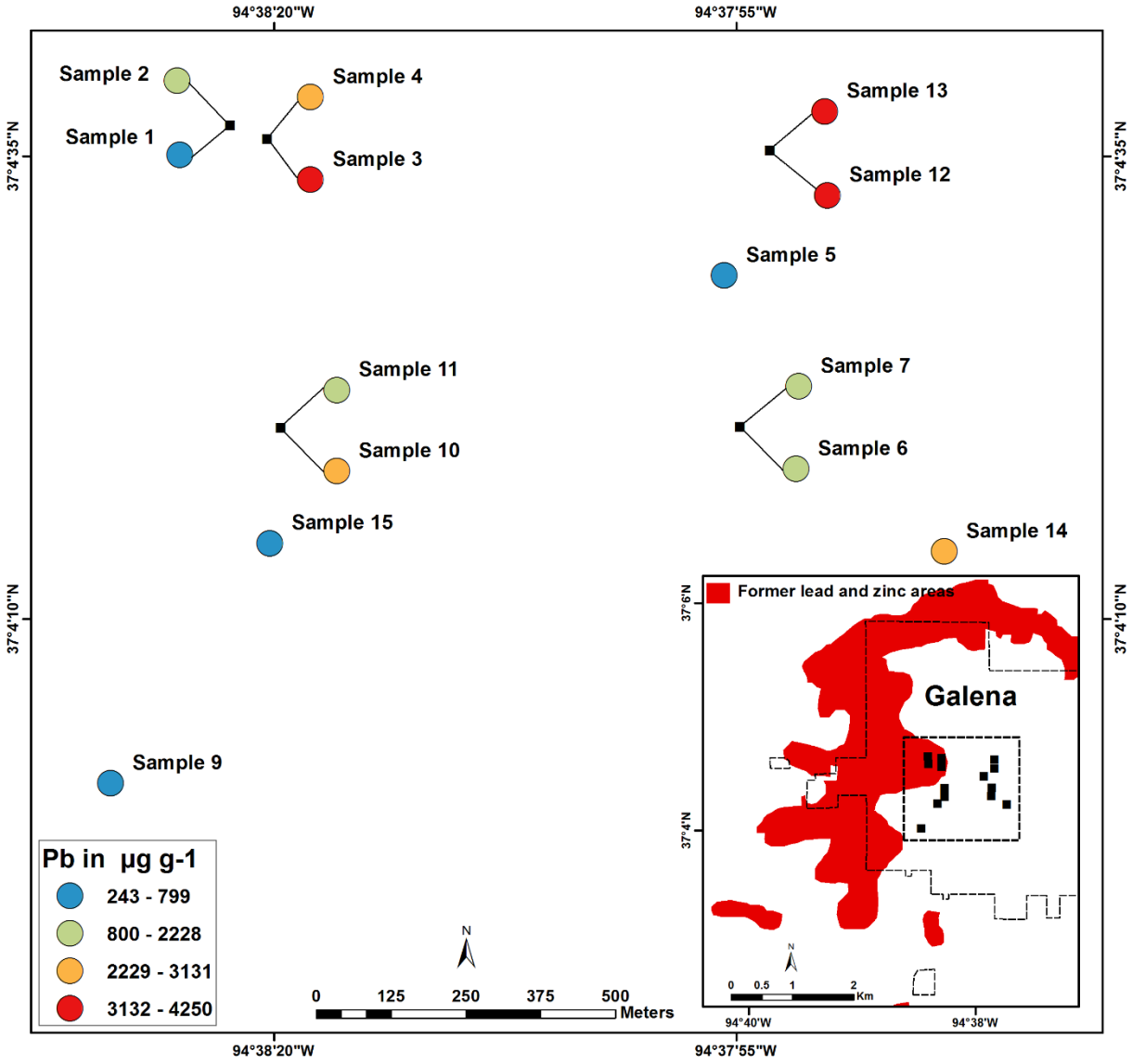

Figure C.20 Appendix: Classification of Zn in all 14 different dust samples, in Galena, KS.

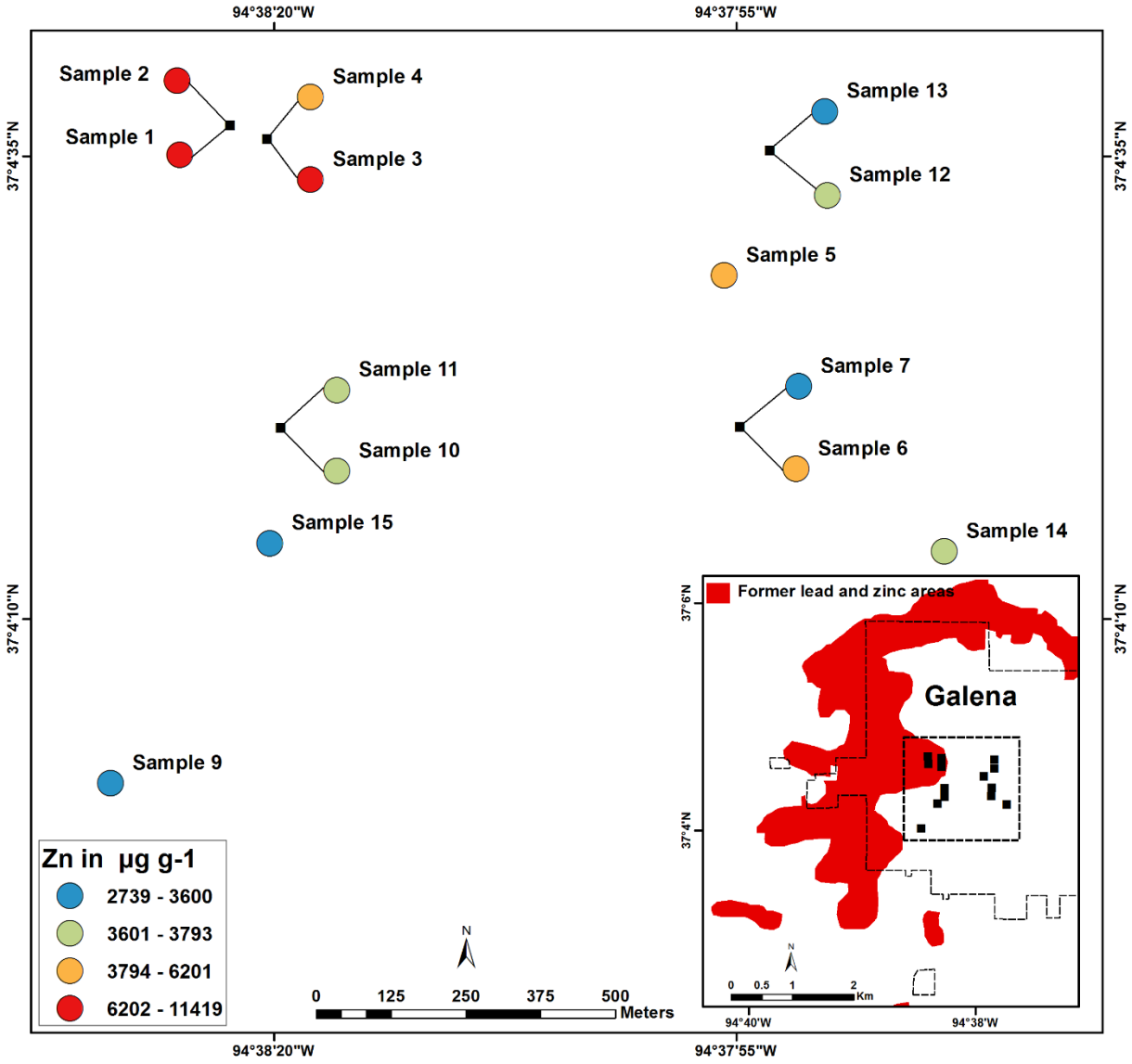

Figure C.21 Appendix: Classification of Cd in all 14 different dust samples, in Galena, KS.

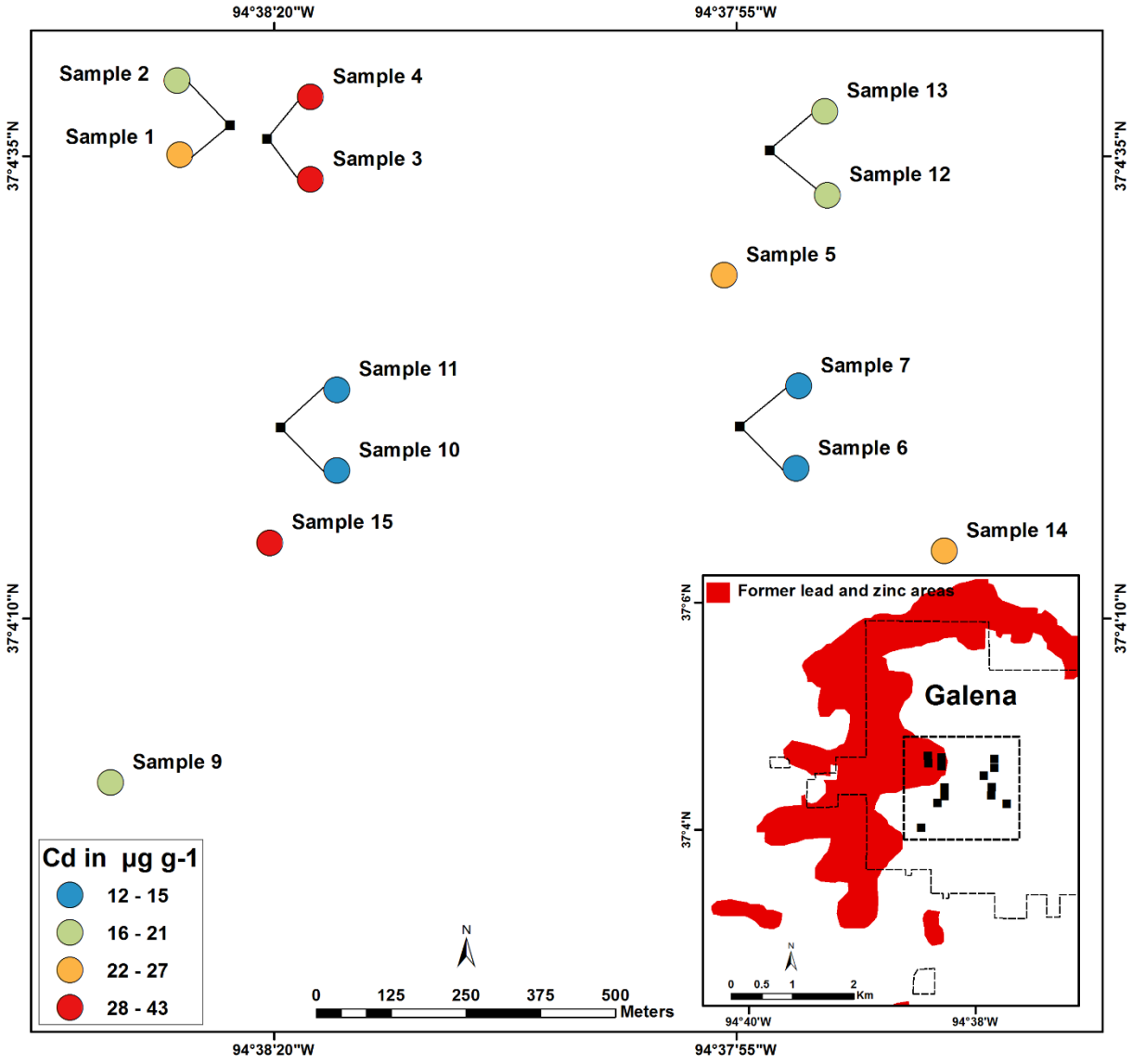

Figure C.22 Appendix: Attic dust samples.

Table C.1 Appendix: SAS output for regression of Pb Vs age of buildings.

Simple Linear Regression

The REG Procedure

Model: MODEL1

Dependent Variable: year

Number of Observations Read 14

Number of Observations Used 14

Analysis of Variance

Source	DF	Sum of Squares	Mean Square	F Value	Pr > F
Model	1	2879.89496	2879.89496	7.57	0.0176
Error	12	4565.53362	380.46113		
Corrected Total	13	7445.42857			

Root MSE	19.50541	**R-Square**	0.3868
Dependent Mean	1906.42857	**Adj R-Sq**	0.3357
Coeff Var	1.02314		

Parameter Estimates

Variable	DF	Parameter Estimate	Standard Error	t Value	Pr > |t|
Intercept	**1**	1928.72003	9.63443	200.19	<.0001
conc	**1**	-0.01118	0.00406	-2.75	0.0176

Table C.2 Appendix: SAS output for regression of Cd Vs age of buildings.

Simple Linear Regression

The REG Procedure

Model: MODEL1

Dependent Variable: year

Number of Observations Read 14

Number of Observations Used 14

Analysis of Variance

Source	DF	Sum of Squares	Mean Square	F Value	Pr > F
Model	1	461.82401	461.82401	0.79	0.3905
Error	12	6983.60456	581.96705		
Corrected Total	13	7445.42857			

Root MSE	24.12399	**R-Square**	0.0620
Dependent Mean	1906.42857	**Adj R-Sq**	-0.0161
Coeff Var	1.26540		

Parameter Estimates

Variable	DF	Parameter Estimate	Standard Error	t Value	Pr > |t|
Intercept	**1**	1922.13804	18.77653	102.37	<.0001
conc	**1**	-0.70672	0.79334	-0.89	0.3905

Table C.3 Appendix: SAS output for regression of Zn Vs age of buildings.

Simple Linear Regression

The REG Procedure

Model: MODEL1

Dependent Variable: year

Number of Observations Read	14
Number of Observations Used	13
Number of Observations with Missing Values	1

Analysis of Variance

Source	DF	Sum of Squares	Mean Square	F Value	Pr > F
Model	1	345.74476	345.74476	0.54	0.4782
Error	11	7055.17832	641.37985		
Corrected Total	12	7400.92308			

Root MSE	25.32548	**R-Square**	0.0467
Dependent Mean	1906.92308	**Adj R-Sq**	-0.0399
Coeff Var	1.32808		

Parameter Estimates

Variable	DF	Parameter Estimate	Standard Error	t Value	Pr > |t|
Intercept	**1**	1921.27442	20.77038	92.50	<.0001
conc	**1**	-0.00326	0.00444	-0.73	0.4782

Table C.4 Appendix: Major d-spacing and intensity of some minerals that occur in dust using XRD of the <150 µm from 9 different sites at Galena, KS. D-spacing is interatomic spacing in angstroms and intensity is peaks intensity. References for d-spacing and intensity are given in the table.

Minerals	Major d-spacing (Å)	Intensity (%)	Reference
Quartz	4.257	22	Mindat.org
	3.342	100	
	2.457	8	
	2.282	8	
	1.8179	14	
	1.5418	9	
	1.3718	8	
	3.342	1	Webmineral.com
	4.257	22	
	1.8179	14	
	3.34	‡	Harris and White., 2008
	4.26	‡	
	1.82	‡	
Calcite	3.86	12	Mindat.org
	3.035	100	
	2.495	14	
	2.285	18	
	2.095	18	
	1.913	17	
	1.875	17	
	1.604	10	
	3.035	100	Webmineral.com
	2.095	18	
	2.285	18	
	3.03	‡	Harris and White., 2008
	1.87	‡	

	3.85	‡	
Galena	2.969	100	Webmineral.com
	3.429	84	
	2.099	57	
Aragonite	3.40	‡	Harris and White., 2008
	1.98	‡	
	3.27	‡	
Dolomite	2.886	100	Mindat.org
	2.192	30	
	1.787	30	
	1.804	20	
	2.015	15	
	3.7	10	
	2.405	10	
	2.670	10	
	2.883	100	Webmineral.com
	1.785	60	
	2.191	50	
	2.88	‡	Harris and White., 2008
	2.19	‡	
	1.80	‡	
Sphalerite	3.123	100	Webmineral.com
	1.912	51	
	1.633	30	
Goethite	4.18	‡	Harris and White., 2008
	2.45	‡	
	2.70	‡	
Anglesite	3.001	100	Webmineral.com
	4.26	87	
	3.333	86	

Marcasite	2.69	100	Mindat.org
	3.43	70	
	1.75	50	
	2.41	40	
	2.71	30	
	2.31	40	
	1.91	30	
	1.59	20	
	2.71	100	Webmineral.com
	1.76	63	
	3.44	40	
	2.69	‡	Harris and White., 2008
	3.43	‡	
	1.75	‡	
Pyrite	1.63	‡	Harris and White., 2008
	2.71	‡	
	2.43	‡	
Muscovite	10.0	‡	Harris and White., 2008
	3.33	‡	
	5.0	‡	
Aragonite	3.40	‡	Harris and White., 2008
	1.98	‡	
	3.27	‡	
Hematite	2.69	‡	Harris and White., 2008
	2.59	‡	
	1.69	‡	
Rutile	3.26	‡	Harris and White., 2008
	1.69	‡	
	2.49	‡	
Microcline	3.24	‡	Harris and White., 2008

	3.29	‡	
	4.22	‡	
Orthoclase	3.31	‡	Harris and White., 2008
	3.77	‡	
	4.22	‡	
Iron aluminum	2.048	100	Morris et al., 1981
	1.1820	24	
	1.4472	13	
	2.899	8	
	0.9157	9	
Cerium ammonium nitrate	3.676	27	Morris et al., 1981
	3.408	26	
	3.116	23	
	3.068	28	
	2.946	15	
	2.447	23	
	2.441	21	
	2.421	23	
	2.364	23	
	2.343	15	
	2.248	15	
Jarosite	3.08	‡	Harris and White., 2008
	3.11	‡	
	5.09	‡	

‡ no data.